AD/A-005 831

AMORPHOUS SEMICONDUCTORS

James C. Thompson

Texas University at Austin

Prepared for:

Advanced Research Projects Agency

September 1974

070120

Final Technical Report

1 April 1973--30 September 1974

ARPA Order Number 1562

Program Code Number 0D10

University of Texas at Austin--Grantee

Effective Date: 1 April 1973

Expiration Date: 30 September 1974

Amount of Grant: $29,296.00

Grant Number DA-ARO-D-31-124-73-G81

James C. Thompson 512/471-5926

James C. Thompson 512/471-5926

Amorphous Semiconductors

Sponsored by

Advanced Research Projects Agency

ARPA Order No. 1562

The views and conclusions contained in this document
are those of the
as necessarily re
either expressed
Projects Agency

Appro
di

1. Introduction

Four years ago a proposal was submitted for ARO review which concerned the effect of pressure on the properties of amorphous semiconductors. The work was funded, and this is the final report. While there had been a few papers[1] dealing with pressure effects prior to that time, relatively little was known, and the interpretation of available data on related properties (e.g., the temperature coefficient [1,2] of any given parameter A contains a term dependent on dA/dP) was restricted thereby.

It was hoped that measurements could be made on a wide variety of chalcogenide-based alloys over the pressure range 0-16 kbar and over a temperature range possibly reaching 1000°C.

Two events have severely restricted performance under this grant. First, was the death of Professor D. S. Hughes who was the source of high-pressure expertise in the project. Second, was the delay, by many months, in delivery of a high pressure bomb. These events, together with the attendant changes in plans, priorities, and capabilities resulted in considerable start-up delays and loss of mid-term productivity.

Improved understanding of the nature of amorphous semiconductors[2-5] has resulted in far fewer samples being required to yield a meaningful survey of alloy properties, as will be seen in subsequent sections of this report. Nevertheless several important questions remain to be settled.

While the original proposal suggested that sound-speed measurements be primarily used for location of the glass transition, it has turned out that measurements of the speed of compressional and shear

waves made in searches for a glass transition have also been used in equation-of-state studies. This data provides compressibilities (or, shear and bulk moduli) over the available pressure and temperature range and is the first such characterization of these materials.

The following sections provide details of our work on sample preparation and other experimental procedures (Sect. 2); together with results on equation-of-state (Sect. 3); the glass-transition phenomenon (Sect. 4); and dc and ac conductivity (Sect. 5). Other sections concern publications and personnel.

2. Experimental

2A. Sample Preparation

This work has been based entirely on studies of bulk semiconducting alloy glasses. By using bulk glass, problems of sample reproducibility have been avoided and materials production facilities have been reduced. There is a disadvantage in our inability to produce as wide a range of compositions as in thin film work. Sample production has followed standard procedures.

Known amounts of the desired constitutients (five 9's pure) are crushed then weighed out on a Mettler balance* in glove box* with an inert gas atmosphere. Typical samples weighed 20-30 gm . They are then placed in a quartz ampoule, sealed off under fore-pump vacuum, and placed in a rocking tube furnace*. Heating cycles depend on the material used but generally involved temperatures near 800°C and periods of approximately one day. Samples were dropped from the furnace to an air or water quench.

The sample is then removed from the ampoule by means of a diamond wheel connected to a high speed pneumatic drill motor. Once the glass ingot is removed from the ampoule it is cut into suitable lengths with an S. S. White airbrasive cutter. Some of the experiments with these glasses require that the ends of the cylindrical

*bought with funds provided by this grant.

samples cut from the ingot be flat and parallel. The parallelism and flatness of the ends of the sample is produced by polishing on a rotating optical flat supplied by Buehler. The sample is placed in a "V-block" and ground down with alumina powder (.05 micron) to the required specifications of the experiment.

Over 70 different kinds of samples were made, with more than 150 different quenches carried out. Table I lists the kinds of samples, while Table II describes the fate of individual samples.

TABLE I

Sample Number	Composition in per cent	Sample Number	Composition in per cent
5	Te 72 Ge 9 As 19	26	As 40 Se 45 Te 15
6	Te 72 Ge 11 As 17	27	As 40 Se 30 Te 30
7	Te 72 Ge 13 As 15	28	As 40 Se 15 Te 45
8	Te 72 Ge 15 As 13	29	As 40 Te 60
9	Te 72 Ge 17 As 11	18-6-a	#18-6 with Gd. doping
10	Te 75 Ge 15 As 10	18-7	#18 with Yt. doping
11	Te 78 Ge 9 As 13	18-2-a	#18-2 with ~ 10% Mn doping
12	Te 70 Ge 13 As 17	18-8	#18 with mn doping
13	Te 67 Ge 14 As 19	30	As 40 Se 12 Te 48
14	Te 65 Ge 15 As 20	31	As 40 Se 48 Te 12
15	Se 60 Ge 20 As 20	BA 1	Te 80 Ge 8 As 12
16	Te 12.5, Tl 25, As 25, Se 37.5	BA 2	Te 75 Ge 10 As 15
17	Te 75 Ge 15 As 10	BA 3	Te 70 Ge 12 As 18
10a	#10 with 1% Na doping	18-12	#18 with .5% doping of #18-8
18	As 40 Se 60	32	Te 75 Ge 5 As 20
19	Ge 10 As 65 Te 25	18-12a	#18-12 with .5% doping of #18-8
20	Ge 5 As 65 Te 30	18-4	#18-4 with .1% Cr doping
21	Ge 10 As 60 Te 30	BA 4	Te 80 Ge 10 As 10
22	Ge 5 As 60 Te 35	BA 5	Te 75 Ge 12 As 13
23	Ge 10 As 55 Te 35	BA 6	Te 70 Ge 14 As 16
24	Ge 5 As 55 Te 40	BA 7	Te 80 Ge 6 As 14
		BA 8	Te 75 Ge 13 As 12

TABLE I

Sample Number	Composition in per cent	Sample Number	Composition in per cent
BA 9	Te 70 Ge 10 As 20	PA 17	#33 with 2% Ag doping
33	As 40 S 60	Pa 18	#33 with 3% Ag doping
Cu	Cu 25 As 25 Se 50	PA 19	#33 with 4% Ag doping
PA	As 25 Te 50 Si 25	PA 20	#18 with 1.5% Ag doping
K1	Cd 30 Ge 15 As 55	PA 21	#18 with 2% Ag doping
K2	As 40 Se 40 Te 20	N 1	#18 with 1% Cr doping
K3	As 40 Se 30 Te 30	PA 22	#33 with 1% Ag doping
K4	Ge 33 , As 33 , Se 16 , Te 16	PA 23	#33 with 5% Au doping
PA 6 A	As 40, Te 60 (#29)	PA 24,25	#33 with 1% Au doping
PA 6	#33 with .1% Ag doping	N 2	#33 with ½% Cr doping
PA 7	#33 with .2% Ag doping	BEN	Cd 25 Ge 25 As 50
PA 8	#33 with .5% Ag doping		
PA 9	#33 with 1.0% Ag doping		
PA 10	#18 with .1% Ag doping		
PA 11	#18 with .2% Ag doping		
PA 12	#18 with .5% Ag doping		
PA 13	#18 with 1.0% Ag doping		
PA 14,15	Same as PA 6 A		
K 5	Ge 33 Se 20 Te 46		
K 6	Ge 33 Se 33 Te 33		
K 7	Ge 33 Se 66		
PA 16	#33 with 1.5% Ag doping		

TABLE II

ple que ber	Date Weighed	Who Weighed It	Temp. Cooked At (°C)	Crystal or Amorph.	Sample Unique Number	Date Weighed	Who Weighed It	Temp. Cooked At (°C)	Crystal or Amorph.
2	10-7-71			A	12-2a				
3	10-12-71	J. Smith		C	12-2b			860	A
1	10-12-71				10 test			500, 860	C
1	10-14-71	J. Smith			10-9	3-14-72	(refired)	860	
1	10-20-71	J. Black	800		10-9	3-16-72	(refired)		C
1	10-21-71	J. Smith	800		6-2	3-16-72	J. Smith		C
2			800		10-10	3-19-72		860	C
-1	11-21-71	J. Smith	600		17-1	4-4-72			
-2	12-16-71	J. Smith	800	C	10-10	4-4-72	(refired)	900	
-4	1-14-72	J. Smith			6-2	4-18-72	(refired)	700	C
-3	1-13-72	(refired)	800, 500		10-11	4-20-72	J. Smith	860	C
-4	1-18-72	(refired)	800		10-11a	4-27-72	10-11 (refired)	950	A
-5	1-18-72	J. Black			17-2	4-27-72	J. Smith	350, 900	A
-4	1-19-72	(refired)	800		6-2	5-23-72	(refired)	360	
-6	2-3-72	J. Black	800		18-2	5-31-72	J. Smith		
-7	2-11-72	J. Smith	800	C	19-1	6-5-72	D. Nance	400, 590, 800	
-2	2-24-72		870	C	18-3	6-7-72	J. Black		
-8	3-2-72				18-5	6-12-72	D. Nance	600	
-6	3-3-72	(refired)	860		21-1	6-13-72	D. Nance		
-9	3-7-72	J. Black		C	22-1	6-13-72	D. Nance		
2a				C	23-1	6-13-72	D. Nance		
-1	3-9-72		600		24-1	6-13-72	D. Nance		

TABLE II

Sample Unique Number	Date Weighed	Who Weighed It	Temp. Cooked At (°C)	Crystal or Amorph.	Sample Unique Number	Date Weighed	Who Weighed It	Temp. Cooked At (°C)	Crystal or Amorph.
19-2	6-14-72	D. Nance			29-1	11-10-72	D. Nance	470, 600, 800	C
10-12	6-19-72	D. Nance	860	A	30-1	11-17-72	D. Nance		
18-4	6-19-72	D. Nance			31-1	11-17-72	D. Nance		
17-3	6-20-72	D. Nance	500, 800	A	5-4	12-1-72	D. Nance	800	A
5-3	6-21-72	D. Nance			17-5	12-4-72	D. Nance	800	A
13-2	6-26-72	D. Nance			18-9	12-8-72	D. Nance	400, 600, 630	
18-6	6-28-72	D. Nance	500, 700		BA 1.01	1-17-73	D. Nance	820	A
18-6-a	8-16-72	D. Nance			BA 3.01	1-17-73	D. Nance	820	A
18-7	8-21-72	D. Nance			18-10	1-17-73	D. Nance	600	A
10-13	9-8-72	D. Nance	860	A	BA 2.01	1-19-73	D. Nance	820	A
17-4	9-11-72	D. Nance	860	A	18-11	1-19-73	D. Nance	400	A
10-14	9-25-72	D. Nance	860	A	10-19	1-22-73	D. Nance		
18-2-a	10-16-72	D. Nance	500		10-20	1-22-73	D. Nance	860	metal co A
25-1	10-16-72	D. Nance	470, 600	A	18-12	2-6-73	D. Nance	400	A
10-15	10-20-72	D. Nance	860	A	17-6	2-6-73	D. Nance	800	A
10-16	10-20-72	D. Nance	860	A	18-12	2-9-73	(refired)		
18-8	10-27-72	D. Nance	600	A	BA 1.02	2-13-72	D. Nance	820	A
10-17	10-30-72	D. Nance	860	A	17-7	2-13-73	D. Nance	800	A
26-1	10-30-72	D. Nance	470, 600, 800	A	32-1	2-20-73	D. Nance		
27-1	11-6-72	D. Nance	470	A	10-11			820	A
10-18	11-6-72	D. Nance	800	A	BA 2.02	2-27-73	D. Nance	820	A
28-1	11-10-72	D. Nance	470, 620 800	A	BA 2.02	3-5-73	(refired)		A

TABLE II

ple que ber	Date Weighed	Who Weighed It	Temp. Cooked At (°C)	Crystal or Amorph.	Sample Unique Number	Date Weighed	Who Weighed It	Temp. Cooked At (°C)	Crystal or Amorph.
2-b	3-6-73	D. Nance	400, 650		6-3	8-7-73	D. Nance	800	
.03	3-13-73	D. Nance	820	A	10-21	8-8-73	D. Nance		
.04	3-13-73	D. Nance	820		13-3	8-8-73	D. Nance	800	
.05	3-13-73	D. Nance	820		14-2	8-8-73	D. Nance	800	
.06	3-20-73	D. Nance	820	A	17-8	8-8-73	D. Nance		
-13	4-16-73	D. Nance	400, 600		Cu-1	9-20-73	J. Siegrist	400, 620, 800	
-4	4-21-73	D. Nance	400, 600		33-2	10-5-73	D. Nance	400, 600	
.01	6-5-73	J. Siegrist	820	metal core A	33-3	10-17-73	D. Nance		
.01	6-5-73	J. Siegrist	800	A	29-2	10-17-73	J. Siegrist		
.01	6-11-73	D. Nance	820	A	17-9	1-9-74	J. Siegrist	800	
.01	6-12-73	D. Nance	820	C	18-20	1-9-74	J. Siegrist	400, 600	
.01	6-13-73	D. Nance	820	A	18-21	1-9-74	J. Siegrist	400	
.01	6-14-73	D. Nance	820		PA-2	1-9-74	J. Siegrist		
-15	6-15-73	J. Siegrist	400, 620		PA-3	1-9-74	J. Siegrist		
-16	6-15-73	J. Siegrist	400		PA-4	1-17-74	J. Siegrist		
-16	6-29-73	(refired)	400, 680	A	PA-5	1-17-74	J. Siegrist		
-1	7-18-73	D. Nance		A	K 1	1-22-74	J. Siegrist	800	
-17	7-18-73	D. Nance	400	A	K 2	1-22-74	J. Siegrist	600	
-18	7-23-73	J. Siegrist	400, 620	A	K 3	1-22-74	J. Siegrist	600	
-2			800	C	K 4	1-29-74	J. Siegrist	600	
-19	8-2-73	D. Nance	450, 600		PA-6A	1-29-74	J. Siegrist		
-20	8-3-73	D. Nance			PA 6	2-7-74	J. Siegrist		

TABLE II

Sample Unique Number	Date Weighed	Who Weighed It	Temp. Cooked At (°C)	Crystal or Amorph.	Sample Unique Number	Date Weighed	Who Weighed It	Temp. Cooked At (°C)	Crystal or Amorph.
PA 7	2-7-74	J. Siegrist			33-6	3-26-74	J. Siegrist		
PA 8	2-7-74	J. Siegrist			18-4	3-26-74	J. Siegrist		
PA 9	2-7-74	J. Siegrist			17-10	3-26-74	J. Siegrist	800	
PA 10	2-12-74	J. Siegrist			17-11	5-29-74	J. Siegrist		
PA 11	2-12-74	J. Siegrist			17-12	5-29-74	J. Siegrist		
PA 12	2-12-74	J. Siegrist			PA 22	5-29-74	J. Siegrist		
PA 13	2-12-74	J. Siegrist			PA 23	6-5-74	J. Siegrist		
K 5	2-19-74	J. Siegrist	600		PA 24	6-5-74	J. Siegrist		
K 6	2-19-74	J. Siegrist	600		PA 25	6-5-74	J. Siegrist	600	
K 7	2-19-74	J. Siegrist			N 2	6-13-74	J. Siegrist		
PA 14	2-19-74	J. Siegrist			BEN-1	6-13-74	J. Siegrist		
PA 15	2-19-74	J. Siegrist			BEN-2	6-13-74	J. Siegrist		
K 1			600		Cu-2	6-18-74	J. Siegrist		
PA 16	3-12-74	J. Siegrist							
PA 17	3-12-74	J. Siegrist							
PA 18	3-12-74	J. Siegrist							
N-1	3-74	J. Siegrist							
PA 19	3-14-74	J. Siegrist							
PA 20	3-14-74	J. Siegrist							
PA 21	3-14-74	J. Siegrist							
33-4	3-26-74	J. Siegrist							
33-5	3-26-74	J. Siegrist							

2B. High Pressure Apparatus and Techniques

The high pressure apparatus with which this project was begun had been designed for the purpose of creating an environment equivalent to that in the earth's crust. Specifically it was designed[6] for temperatures from room temperature to 1000°C and for pressures up to either 10 kbar or 30 kbar depending on which of two available modifications was employed. As detailed knowledge of the capabilities and limitations of the high pressure equipment was acquired in preliminary experiments it became clear that alterations would be desirable.

First, however, a description of the operation of the apparatus is in order. The pressure medium is N_2 gas which is obtained at 2000 psi from standard bottled gas cylinders. It is then compressed in two stages by hydraulic pumps and gas-oil separators to 30,000 psi. During this compression the gas enters a compound steel cylinder through a very small (0.005 in.) port just below the initial position of the piston, Fig. 1 and 2. The upper hydraulic ram forces the piston past this part and then compresses the gas to the final pressure. Pressures in excess of 18 kbar have been achieved[6] in a compound steel cylinder with a 3/4 in. diameter bore and to 10 kbar in a 1-1/4 in. diameter cylinder. Only the larger, lower pressure system has been used in this research. The lower hydraulic ram serves to hold everything together within the massive steel frame, and, for the small, higher pressure system, to provide a prestressing force for the cone-in-cone type compound steel cylinders.

Since the amorphous materials turned out to be easily compressible it was decided at an early stage to limit the pressure range below

10 kbar. The procedures and apparatus for this range are substantially simpler, bur nevertheless required modification.

The accuracy required in the measurements of the variation of the d.c. conductivity with temperature and pressure for amorphous semiconductors was found to exceed the precision of measurement of temperature and pressure with the pressure apparatus in its original configuration. This lack of precision also adversely affected the measurement of glass transition temperatures at high pressures. Preliminary measurements also indicated that it would be necessary with some amorphous semiconducting materials to go to temperatures somewhat below room temperature to observe any frequency dependent conductivity.

The factor limiting the precision of temperature measurement was the use of platinum vs. platinum 13% rhodium thermocouples (ANS/type R) in the original configuration. A number of users have noted that there is a strong pressure effect on the emf of platinum alloy thermocouple combinations which also depends on the exact experimental configuration (i.e. the temperature of the pressure feed-throughs, and the composition of the feed-throughs).[7] The error could possibly be as great as $10^{o}C$ for our measurements. This amount of error was totally unacceptable for the conductivity measurements and was of the same order as the expected pressure shift of the glass transition temperatures of the amorphous semiconductors.

For these reasons, the platimum alloy thermocouples were replaced by chromel vs. alumel thermocouples (ANS/type K). This thermocouple shows the lowest pressure effect on thermal emf of any common alloy

combination; however, it was not used in the original apparatus as it was intended for use to temperatures in excess of 1000°C at elevated pressures with a nitrogen pressure medium. Robertson et.al.[7] noted a problem with deterioration of this thermocouple combination at temperatures above 900°C in a high pressure nitrogen atmosphere. As it did not appear desirable in any of the amorphous semiconductors investigations to make measurements at temperatures approaching 900°C, no problems with chromel vs. alumel thermocouples were contemplated.

Limitations in the temperature range and in the precision of the pressure measurements were not so simply resolved as the improvement of temperature measurement. In the pressure apparatus, the sample temperature was controlled by means of a resistance wire furnace surrounding the sample in the sample holder. The minimum temperature was thus limited to room temperature. The only practical way to reduce the lower temperature limit for this apparatus is to immerse it in a cooled temperature controlled bath. This technique is at best quite limited, by the brittle transitions of the steels used in the construction of the apparatus, by the freezing temperature of the hydraulic oil at high pressures, and by failure of the moving seals at low temperatures.

The problem of the precision of pressure measurements was also related to the temperature control problem. The pressure gauge consists of a coil of manganin wire with approximately 100 Ω resistance.

This coil is incorporated into the lower closure of the pressure apparatus. As the pressure changes, the resistance of the manganin coil changes by a very small amount. This resistance change is very nearly linear with pressure and can be measured by means of a Wheatstone bridge. There is, however, in addition to the pressure coefficient of resistance also a temperature coefficient which creates problems. When measurements are being made at elevated temperature using the internal furnace, the temperature of the manganin coil is at some unknown temperature between the sample temperature and room temperature. As the resultant error was a function of temperature, pressure, and sample cell configuration, there was no effective method of correcting for it.

In order to circumvent these experimental difficulties, it was decided to modify the apparatus so that pressures could be generated in one pressure vessel or intensifier and transmitted from the intensifier to an experimental pressure vessel through high pressure tubing. In this manner, the manganin gauge could be incorporated into the system in such a place that it could be held at room temperature and could be corrected by a compensating coil at atmospheric pressure but in thermal contact with the active coil. The intensifier in such a system can be kept at room temperature thus eliminating any possible problems with the freezing of hydraulic oil or with moving seals at low or high temperatures. The problem of experimental temperature range can be solved through a proper choice of materials for the construction of the experimental pressure vessel.

A diagram of the modified system is shown in Fig. 3. No modifications were made in the equipment which compressed the nitrogen to a pressure of 30,000 PSI. At this pressure the nitrogen is introduced through a valve (not shown in Fig. 3) into the intensifier. The intensifier consists of the original 10 kbar press as shown in Fig. 1 and 2 with the modifications shown in Fig. 4. The lower hydraulic ram was replaced by the lower spacer, the compound steel cylinder and lower closure of the press were replaced by a somewhat different compound steel cylinder, and the piston and piston support block of the press were replaced by a modified piston support block and piston with an improved moving seal.

In operation, the nitrogen enters through the bottom seal through a piece of high pressure tubing, thus eliminating the port in the side of the cylinder which tended to adversely affect the life of the upper (moving) seal in the original configuration. This and the unsupported area design seal have combined to greatly extend the seal life. The compound steel cylinder itself was modified from the construction of the previous cylinder only in the elimination of the top extension of the inner cylinder which served as the gas inlet and modification from a bored through construction to a blind bore to approximately half the length of the cylinder with a smaller hole bored on through for the gas inlet tubing.

The alloys used in the construction of the cylinder and piston and piston support block for the intensifier modification are the same as those which were used in the construction of the original 10 kbar press. The inner cylinder is of Carpenter tool steel #883 hardened to 43-45 Rc, the outer cylinder is A.I.S.I. 4340 steel hardened to 32-35 Rc. The piston support block is of Carpenter Vega steel hardened to Rc 44-48, and the piston and steel parts of the pressure seal are of Carpenter 610 steel hardened to Rc 44-48. The rough machining was done in the departmental shop. The parts for the cylinder were then shipped to Houston where they were heat treated, finish ground and polished, and assembled in commercial heat treating and grinding establishments. The remaining parts were finished in the engineering labs at this university.

As shown in Fig. 3, the manganin gauge is separate from both the intensifier and the experimental pressure vessel. In this manner it is not affected by the temperature of the experimental vessel.

Two experimental pressure vessels are being used in this research, one which was produced here, and one which was purchased from a commercial firm. These were both originally planned to have coaxially shielded electrical leads using a technique first introduced by Cornish and Ruoff[8]. In this technique, a type of coaxial cable which is made by swaging a solid metallic sheath onto a powdered dielectric containing the inner conductor or conductors. It was originally desired to isolate the coaxial shield from the

pressure vessel so that they could be separately grounded, the sheath through the instruments being used for measurements and the pressure vessel through the pressure tubing. It was desired in this manner to eliminate the possibility of ground loop emfs which could give erroneous measurements. Leads made using a triaxial variety of the sheathed cable have been reported to have an impedance of greater than $10^{13}\ \Omega$[9] and other investigators have reported its use for high frequency a.c. measurements to frequencies as high as 300 MHz[10,11]. Several investigators have reported the successful use of these leads with gas systems to high pressures at both low and high temperatures[11,12]. It was further believed that the absence of any signal-reflecting interfaces between the sample and the a.c. conductivity bridge would be an improvement over any other high pressure leads.

For these reasons, an attempt was made both here and at Harwood Engineering to build a high pressure vessel for use with a gas atmosphere which would incorporate the sheathed cable for leads. However, in contrast to the results reported by Schirber and Shanfeldt, it was found to be impossible to obtain a seal for a gas pressure medium which could be cycled more than once to any appreciable pressure without leaking. For this reason, Harwood Engineering redesigned the pressure vessel they were building to have 7 unshielded leads with steel-cone-in-boron-nitride-cone type pressure leadins. For a sketch of the Harwood pressure vessel see Drawing 5. The vessel is of compound steel construction, the inner cylinder being of aircraft quality E-4340 steel hardened to 38-40 Rc. The outer cylinder is of

mild steel and is an interference fit on the inner cylinder. The gas enters the pressure vessel through the hemishperical end of the 6 inch long experimental area, whereas the electrical leads enter through the pressure head at the other end. There are five copper leads and a chromel-alumel thermocouple pair.

The vessel from Harwood was designed primarily for measurements above room temperature with the extreme temperature limits being -70°C (imposed by the brittle transition of the F-4340 steel used in its construction) and 400°C (imposed by the softening or decrease in tensile strength and yield strength of the F-4340 steel) for use to the designed pressure of 150,000 PSI. This vessel was ordered on 30 August 1972 and delivered in October 1973. Delays were ascribed to a shop fire, a move to a new shop, difficulties with the coaxial seals, lost air freight, cracked cones, etc., etc., etc. Since the original apparatus failed early in 1973 (a crack appeared at the gas-inlet hole) there were several months when the pressure range was limited, when no apparatus was functional, or when only the Berylco apparatus was available.

To satisfy the requirement of a lower temperature capability for the conductivity studies, a pressure vessel was designed and constructed which could be used to a temperature limit imposed only by the freezing point of the pressure transmitting fluid. This pressure vessel is shown in Drawing 6. It, too, is of compound construction, the inner cylinder being constructed of Berylco 25 alloy (2% beryllium, .3% cobalt, balance copper) heat treated to

a hardness of approximately 40Rc. Due to the possible health hazard involved in working with beryllium and its alloys, care was observed in the machining processes to avoid heat build up in the alloy material and to capture and properly dispose of all of the machining scrap and dust. The outer cylinder is an interference-fit jacket composed of annealed copper. The purpose of this jacket is to absorb fragments from the inner cylinder in the case of rupture at high pressures. Annealed copper was chosen for this purpose because of its high ductility. As the remaining parts are primarily under compressive loads rather than tensile loads, they were made of steel rather than Berylco 25.

The machine work for this cylinder and the necessary heat treating were all done in university facilities. The steel parts of the pressure heads, seals, and gland nuts are made of Carpenter Vega steel hardened to 42-44 Rc.

The original pressure head had two leads made from the sheathed cable described earlier. Measurements of a.c. conductivity and d.c. conductivity were made for temperatures down to -85^{o}C with a nitrogen atmosphere at pressures up to 2 kbar. The d.c. conductivity results were quite acceptable; however, the a.c. results were not. As noted previously, problems with leakage through the dielectric were not solved with the consequence that measurements above 2 kbar were impossible with a gas system. For this reason, a second pressure head with steel-cone-in-pipestone-cone seals has been made and is

presently being used for a.c. measurements and measurements at pressures above 2 kbar with a gas pressure medium.

In use this pressure vessel is immersed in a liquid temperature-controlled bath and the temperature is monitored with a thermocouple attached to the outside of the pressure vessel. One is thus limited to fairly low heating or cooling rates as an internal furnace cannot be used.

In addition to the nitrogen pressure-generating system, we have been making measurements in the beryllium-copper pressure vessel at room temperature and above and to pressures of 100,000 PSI using a liquid medium pressure generating system (Aminco) using Dow Corning DC 200 silicone oil with a viscosity of 3 centistakes. Due to the freezing point of this fluid, it is not possible to go to temperatures below room temperature.

2C. Acoustic Techniques

Acoustic measurements have been used in both equation-of-state and glass transition studies. In most cases it is the speed of the ultrasonic wave which is the observed parameter in the pulse-echo technique which is now described. The actual experimental parameter in this work is the transit time of a short duration burst of 10 MHz sound waves traveling in a cylindrical sample. The sample is usually about 1 cm in length and 1 cm in diameter with the end faces perpendicular to the cylindrical axis. The end faces must be flat and parallel to each other. A 10 MHz, gold plated, quartz piezoelectric transducer is bonded to one face of the sample. The sample is placed in an especially designed holder which provides electrical corrections for an internal heater and thermocouple as well as connections to the transducer.

One problem that is particularly manifest in this type of experiment is that of bonding the quartz piezoelectric transducer to the sample. It is the nature of the experiment itself that presents the difficulty, that is, the hostile environment in which the sample is placed. The bonding material must be capable of supporting both shear and longitudinal acoustic waves under conditions of extreme pressure and elevated temperatures. Several materials were used with only limited success. For example, glyptol was used because it formed a solid bond between transducer and sample and withstood elevated temperatures. But, under hydrostatic pressure of a few kilobars the glyptol bond developed non-uniform stresses which caused it to break away from the sample, causing loss of data. Diffusion pump oil was also used as a bonding agent and it produced quite satisfactory

results under pressure. However, as the temperature was raised, the viscosity of the oil became so low as to only marginally support shear waves. Finally, an excellent bonding material was found. It is Permatex-2, manufactured by the Permatex Company, Brooklyn, New York. This material is readily soluble in isopropanol and remains soft under pressure and elevated temperatures, yet supports shear waves well above 100°C. The use of Permatex-2 has served to considerably ease the experimental process.

At the heart of any measurement lies some sort of stable reference to which the measurement can be compared. This reference is provided by the very stable, Time Mark Generator which triggers the Arenburg oscillator and the oscilloscope. The oscillator sends a 1 μsec boost of 10 MHz sine waves to the transducer which converts the electrical energy into mechanical vibrations of the same frequency. These sound waves are transmitted to the sample via the sample-transducer bond and propagated through the sample. Reflections from the opposite face of the sample are received at the transducer and converted to electrical energy for detection. In this manner a series of reflected pulses are sent to the tuned pre-amp and amplifier. Diode limiting circuits are provided to protect the preamplifier from saturation since the amplitudes of the reflected pulses are far less than the initial pulse from

the oscillator. The amplified, reflected wave packets are displayed on one sweep of the oscilloscope and compared with timing pulses (on another sweep) which are in phase with the initiating trigger. In this manner, the time duration between reflections of sound waves in the sample is easily determined. Fig.(7a) shows the presentation on the face of the oscilloscope CRT as displayed on an x-y Recorder using a high speed sampling unit. Fig (7b) shows an expanded view of a single wave packet and the time-mark reference pulses to which it is compared. Comparison is made by measuring the time between the peaks of each successive wave packet. Time measurements of 10 to 20 wave packets are made to obtain the average time duration between wave packets. As the experimental parameters are changed, e.g., temperature or pressure, the wave packet will move in time with respect to the reference time-mark pulses. This motion of the wave packet, or the change in transit time, can be measured with a high degree of accuracy by further expanding the oscilloscope sweep to display only a single sine wave peak to be compared to the reference time-mark pulses, Fig. (8).

With the transition time known, the speed of ultrasound in the sample is calculated from $C_s = \frac{2\ell_o}{t}$, where C_s = sound speed, ℓ_o = length of the sample at zero pressure (1 atm), and t is the measured transit time. However, as the sample undergoes hydrostatic compression, the sample length is no longer equal to ℓ_o. Rather the length is then $\frac{\ell_o}{y(p)}$ where $\ell(p)$, the length under pressure, is related to the original length ℓ_o by the function

$y(p)$; $y(p) \geq 1$. The function $y(p)$ is calculated using the method of Cook[13], described below. Assuming equal compressibility in all directions, as expected for a glass, K_T, the isothermal compressibility is related to the adiabatic compressibility, Ks, by

$$K_T \equiv \frac{-3}{\ell} \frac{\partial \ell}{\partial P}\Big)_T = \gamma K_s \equiv \frac{-3\gamma}{\ell} \frac{\partial \ell}{\partial P}\Big)_s \tag{1}$$

where γ is the ratio of specific heats.

If the initial density is

$$\rho_o = \frac{M}{V_o} = \frac{M}{\ell_o^3}$$

then $\rho(P) = \rho_o\, y(P)^3$.

Now the sound speed for longitudinal waves is given by

$$v_\ell^2(P) = \frac{1}{\rho(P)} \left(\frac{1}{K_s} + \frac{4}{3}\mu_s\right) = \frac{\ell_o^2}{y(P)^2 t_\ell(P)^2} \tag{2}$$

where μ_s is the shear modular and $t_\ell(P)$ is the measured transit time of longitudinal waves in the sample as a function of pressure and

$$v_s^2 = \frac{1}{\rho(P)}\,\mu_s = \frac{\ell_o^2}{y(P)^2 t_s^2(P)} \tag{3}$$

where $t_s(P)$ is the measured transit time of shear waves in the sample as a function of pressure .

Equations 1, 2, and 3 can be combined to give

$$\int_o^P dy(P)dP = \frac{\gamma}{3\rho_o \ell_o^2} \int_o^P \left[\frac{1}{t_\ell(P)^2} - \frac{4}{3}\frac{1}{t_s(P)^2}\right]^{-1} dP$$

hence

$$y(P) = 1 + \frac{\gamma}{3\rho_o \ell_o^2} \int_o^P \left[\frac{1}{t_\ell(P)^2} - \frac{4}{3}\frac{1}{t_s(P)^2}\right]^{-1} dP \quad .$$

The function y(P) can then be calculated from the measured transit times for both shear and longitudinal sound waves. And, in turn, the isothermal and adiabatic compressibilities as well as several other properties may be determined, with only γ as an assumed parameter.

2D. Compressibility

As a complement to the acoustical measurements of the equation of state, separate direct measurements of the compressibility and thermal expansion were undertaken.

Since glass is an isotropic solid, it is sufficient to measure the change in length of the solid under pressure to calculate the compressibility. There are a variety of techniques. Bridgman, in the majority of his measurements at lower pressures, used a linear potentiometer technique[14]. Strain gauge techniques have have also been used[15]. Recently differential transformer techniques[16-21] have been used to measure linear dilation because the instrumentation is somewhat less complicated.

A linear variable differential transformer[22] (LVDT) was used to measure the change in length of the glass under hydrostatic pressure. The LVDT and sample holder, as shown in Fig. 9, were placed inside a 10 kbar pressure apparatus of the Bridgman design using nitrogen gas as the pressure medium. The springloaded copper plunger directly followed the relative change in length of the sample as compared to the iron sample holder. The plunger was connected to the magnetic core of the LVDT. As the sample length decreased, relative to the linear compression of the sample holder, the LVDT core moved and the output from the LVDT was changed. The screw section at the bottom of the sample holder allowed different size samples to be measured. With the exception of the NaCl calibration

sample, the samples used in this investigation were 2 cm long. The spring at the top of the sample holder held the LVDT in place.

Primary excitation of the LVDT at 2.5 kHz and amplification and detection of the output was provided by a standard Schaevitz Engineering Model No. CAS 2500 signal conditioner. The output from the signal conditioner and from the manganin pressure gauge were simultaneously displayed on an x-y recorder.

The apparatus was calibrated by measuring the linear dilation of NaCl, CKl, KBr, and KI single crystals. The compressibilities of the chalcogenide glasses were then calculated by interpolation.

The thermal expansion was measured in an analogous method to the measurement of compressibility. The LVDT was directly calibrated with a micrometer. Since the change in length for a temperature shift of $10^{o}C$ is much less than the change in length for a pressure change of 1 kbar, the measurement was considerably less satisfactory.

The sample was placed inside a quartz sample holder with a quartz plunger connected to the LVDT. One end of the quartz sample holder was in an oil bath, the other with the LVDT was at room temperature. Using this technique the thermal expansion of As_2Se_3 was measured on the heating cycle to be $1.9\pm0.2 \times 10^{-5}\ {}^{o}C^{-1}$. The thermal expansion of $Te_{15}Ge_3As_2$ was measured to be $1.6\pm0.2 \times 10^{-5}\ {}^{o}C^{-1}$. S. F. Chistov, et. al.[23] measured the thermal exapnsion of As_2Se_3 to be $2.2 \times 10^{-5}\ {}^{o}C^{-1}$.

2E. Glass Transition Experiments

The glass transition temperature[24-27], T_g, is generally observed by changes in a wide variety of properties: viscosity, thermal expansion coefficient, heat capacity (DTA)[28], compressibility[29], dielectric properties[30], Mössbauer line width[31], NMR[32] and sound speed[20]. The procedures near the end of the list tend to give a higher T_g than the others because of the well-known restriction[25] that T_g varies according to the duration of the experiment--and the duration is essentially the period of the high frequency signal used, say, in dielectric constant or acoustic experiments in contrast to DTA measurements which require several minutes. However, there are indications of the "dc" transition even in megaHertz acoustic measurements as close inspection of the data of Litovitz and coworkers[20] will reveal. Furthermore, the higher T_g obtained in short duration experiments shifts with composition, pressure, etc., parallel with the conventional, low-frequency transition temperature[33]. It therefore seems possible to use the high-frequency techniques for the determination of T_g as reliably as any other. One must also expect T_g to vary when the thermal history of the sample varies.

We describe here a technique for the determination of T_g using an acoustic signal but avoiding any measure of the sound speed. Instead, the reflection coefficient R, at a quartz-sample interface, is observed[34].

The sound speed, c, for an isotropic, fluid medium is given by

$$c = \sqrt{1/\rho K_s},$$

while the acoustic impedance, Z, is

$$Z = \sqrt{\rho/K_s},$$

where ρ is the density and K_s the adiabatic compressibility. Changes in density and compressibility at T_g cause the changes in c reported by Litovitz[6]. Clearly, changes must also occur in Z. Sound speed measurements[35] require knowledge of the sample dimensions, sample size sufficient for a measurable delay, as well as flat parallel ends so that precise measurements in the neighborhood of a phase change are often difficult. Relative impedance measurements, on the other hand, require only one flat face, and a significantly smaller sample.

The amplitude reflection coefficient R is given by

$$R = (Z_1 - Z_2)/(Z_1 + Z_2),$$

where Z_1 is the impedance of the material in which the signal is transmitted and Z_2 the impedance of the sample from which the signal is reflected. Since Z_1 and any bonding effects are all chosen to be smooth, slow functions of temperature any variation in R must be due to changes in the sample at T_g.

In a glass there are, of course, contributions to c and Z from the shear modulus[35] but the essential observability of T_g remains.

Fig. 10 shows a sketch of the apparatus. The sample, at A, is an irregular chip (when solid) polished only at the face which

is sealed to the quartz or Al delay line C by some bonding material (e.g., silicone oil) at B. With those glasses for which the liquid state is easily accessible, such as glycerol, a tube is sealed on top of the quartz and the sample poured in. No bond at B is required and a slight tilt of the whole apparatus prevents reflections at the upper surface of the liquid from interfering with reflections at B. The transducer E is sealed onto the quartz at D. A block diagram of the apparatus is shown in Fig. 11a. The high frequency signal is generated by the Ahrenberg pulsed oscillator. The longitudinal sound wave is generated at the transducer, traverses the quartz rod, is reflected at the quartz-sample interface and returns to the transducer for detection. The pulse is amplified and detected. The pulse due to the transmitted pulse is gated out, and the maximum amplitude of the reflected pulse is peak detected. A dc voltage proportional to the amplitude of the reflected pulse is applied to the xy recorder and plotted against the sample temperature measured by a thermocouple. The quartz delay line and sample are temperature controlled with equipment appropriate to the substances being studied. For the high pressure work, the quartz delay line is mounted inside a heater wound on a soapstone cylinder and insulated by another soapstone cylinder.

As another approach to the desire to measure the glass transition with experimental times of ultrasonic frequencies (eg 10^{-10} sec.), an apparatus was built to enable measurement of sound velocity of the glasses in their melts. The apparatus is shown in Fig. 11b. It is constructed from fused quartz. It is basically the same delay line configuration as in the reflection experiments except there is a reflector opposite the end of the delay line. The ultrasonic wave should be generated at the ultrasonic transducer, propagate through the delay line, into the sample, be reflected off the other piece of quartz, travel both through the sample and delay line, and be detected by the tranducer. Unfortunately, this experiment has not yielded any data as yet. The molten glasses refuse to wet the end of the quartz rod sufficiently well to propagate a signal through the sample material.

2F. AC and DC Conductivity

Among the measurements to be made in this experimental program is the conductivity as a function of pressure, temperature, frequency, and sample composition.

As the conductivities displayed by these materials are fairly low, one major problem encountered is due to sample conductances being exceeded by leakage conductances in leads where the leads are taken in a broad sense to mean the whole conductive path between the sample and measuring instrument.

The samples have been made in a sandwich type geometry where the dimensions have varied somewhat with sample conductivity. Thus, the samples are effectively lossy capacitors. For samples with high conductivity, the samples were ground to a long thin shape approximately 1 cm long and with a surface area of approximately 10^{-1} cm^2 and the contacts were applied to the small surfaces on the ends of the sample. For lower conductivity materials, the samples were ground to a wafer shape with a thickness ranging from0.06 to 0.08 cm and a surface area of from 0.60 to 0.80 cm. The contacts here were applied to the large surfaces on either side of the sample. In several instances measurements were made on a long sample and a wafer shaped sample having the same composition. In these cases, the calculated conductivities agreed within a very few per cent.

A number of different types of contacts have been tried, primarily silver conductive compounds such as are sometimes used

in screen painting of printed circuit boards. In addition, some measurements were attempted using a carbon composition; however, the data obtained from this sample did not conform to that obtained from the samples using silver composition and the dc data also indicated rectifying behavior at the contacts. Upon examination of the sample after cycling to pressure, these carbon contacts were found to be only loosely attached and easily flaked off. A number of the silver compounds did not adhere too well to the sample surfaces after curing and gave results which weren't repeatable when cycled in pressure. The compound which we finally settled on is manufactured by Acheson Collids Company under the trade name of Electrodag 415. This particular material gave repeatable results in most cases, and the few occasions on which problems were encountered were probably due to improper cleaning of the sample before application of the contact.

In addition to the silver and carbon conductive compounds, evaporation of silver onto the samples under vacuum was tried; however, the results did not differ from those obtained with Electrodag 415 and therefore, due to the difficulty of this procedure, it was abandoned.

It should be noted at this point that the original reason for attempting to use carbon electrodes was the observation by a number of investigators that some contact materials tended to diffuse into the samples causing changes in the electrical properties with time. Among the offending materials were silver and gold.

Primarily these problems were noted in thin film investigations. In this lab, however, measurements over several weeks with samples having silver electrodes have shown no changes with time even when taken to temperatures fairly close to the softening point. In one set of measurements where the temperature was taken very close to the softening temperature, small changes were observed; however, they are believed to have been due to partial crystallization of the sample on the surface.

The dc conductivity was measured by standard techniques. The ac conductivity was measured by two different systems. For frequencies between 10 and 10^5 Hz, a Wavetek model 114 signal generator was used to apply a voltage across the sample and a known resistance in series. A P.A.R. model 128 lock-in amplifier was then used to determine the voltage across the sample which was in phase with a known voltage across known resistances. Then the voltage across the resistor:

$$\vec{V}_R = V_o e^{iwt} = I_R R \; ; \quad I_R = \frac{V_o}{R}$$

however, the current through the sample:

$$I_S = I_R, \text{ but}$$

$$\vec{V}_S = I_S \vec{Z}_S \; ; \; \vec{Z}_S = \frac{\vec{V}_S}{I_S} = \frac{\vec{V}_S}{I_R} \text{ , thus}$$

$$R_S = \mathrm{Re}\vec{Z}_S = \frac{\mathrm{Re}\vec{V}_S}{I_R} = \frac{R\ \mathrm{Re}\vec{V}_S}{V_o}$$

where the vector signs indicate complex quantities.

If it is also desired that the sample capacitance be known, the quadrature phase for $\vec{V}_S$ may be measured to obtain:

$$X_S = \frac{1}{\omega C} = \mathrm{Im}\vec{Z}_S = \frac{R\,\mathrm{Im}\vec{V}_S}{V_o} \quad .$$

For frequencies from 10^5 to 10^7 Hz, a Wayne Kerr model B 602 Universal RF bridge was used to measure sample capacitance and conductance.

A comment about a possible source of error in the high pressure measurement of conductivity and capacitance is in order here. In making a measurement of the impedance or resistance of a sample in a high pressure vessel, the leads from the instrumentation to the sample must pass through the massive metallic wall of the pressure vessel in some manner so as not to be extruded by the internal pressure. This is accomplished by supporting the electrical lead against the high pressure with some dielectric material which is impermiable to the pressure medium. The ideal material electrically would be a perfectly lossless material with a very low dielectric constant; however, the necessary mechanical properties impose a number of constraints. The materials most often used are boron nitride and a naturally occuring material called pipestone (catlinite). For this research, pipestone has been used exclusively for the electrical measurements because although its electrical properties are unknown, it is superior

mechanically in our experience to boron nitride and matches boron nitride electrically in use. The two electrical feedthroughs for the leads to the sample act as two impedances in series shunting the sample impedance. Care must thus be observed to see that the complex conductances of these feedthroughs are negligible with respect to that of the sample or that measurements from each of the leads to ground are measured so that calculated corrections may be made.

For the dc conductivity measurements, the resistance of the leads was of the order of 10^{12} Ω or better whereas the sample resistance was of the order of 10^{8} Ω at room temperature. The effect of temperature and pressure on the leads was negligible except in the case of total failure due to the eventual extrusion of the dielectric. It was thus necessary only to check before and after each run to determine that the feedthroughs were in good order. For the low frequency ac measurements, the real conductance of the feedthroughs was far below that of the sample conductance on all measurements made. Due to the failure to observe any frequency dependent conductivity in the early measurements, and since frequency dependent conductivity is more easily observed the higher the frequency, it was decided to abandon the low frequency technique until the measurements with the Wayne-Kerr bridge should indicate the probability of observing some frequency dependence in a sample at the lower frequencies.

With the Wayne Kerr bridge, the shunting effect of the pressure feedthroughs is corrected through the technique known as three-terminal measurements which provides for the mathematical correction of the instrument measurements to account for impedances which shunt the measurement terminals to the neutral terminal. This neutral terminal is attached through the cable shields to the pressure vessel. At this point, a description of the limitations of the Wayne Kerr bridge and the correction methods which are used to correct the instrument readings is in order.

The Wayne Kerr bridge with its wide frequency range is to some extent a compromise. It is a transformer ratio-arm bridge which has three internal standards, a conductance standard, a capacitance standard and an inductance standard. In measuring a reactive component, one has the choice between the capacitance or the inductance standard. In a transformer ratio-arm bridge such as the Wayne Kerr bridge, ac signals are sent from a source to detector through the standards and through the unknown. The signals from the source are coupled by transformers through the three paths (unknown, conductance standard, and reactance standard) so that they cancel one another out at the detector when the bridge is balanced.

In the Wayne Kerr bridge, there are three means of changing this transformer coupling. The first is determined by the manner in which the unknown is connected to the bridge; there are two modes, one in which unknowns with high impedances are measured directly as described above--the other in which the shunting effect

of the unknown in a T-network with two known resistors is determined. This second mode is for very low impedances and is of no interest in the present investigation. In the standard direct measurement mode (called the parallel bridge mode because the unknown conductance and reactance are determined as if the unknown was a parallel combination of a perfect resistor and a perfect capacitor or inductor), there are five possible ways to connect the sample to three pairs of terminals, each having a different order of magnitude of coupling. For each of the standards (the conductive and the reactive), there are two means of varying the transformer coupling. A set of five switches provides for discrete changes in the coupling as well as the choice between the capacitive and the inductive reactance standards. For each of the two standards being used there is one switch which provides for normal or reversed coupling and one which provides for a choice between a coupling factor of 1 or 10. In addition to this discrete coupling variation for the standards, the coupling of each may be changed in a continuously variable manner by a device called a magnetic potentiometer. The magnitudes of the sample conductance and capacitance or inductance are determined from the terminals the unknown is connected to and the positions of the five switches, and the exact values are determined from scales on the two magnetic potentiometers when the bridge is balanced. Although, at the inception of this program a very high ac conductivity was expected, it was soon observed to be extremely small. For this reason, the ability to measure very small dissipation factors or loss tangents

became very important. This is true because the solution for a current distribution problem is the same mathematically as that for the analogous electrostatic potential distribution problem except that conductivity, σ, is substituted for dielectric constant, ε. This means that, for a given ratio of σ/ε regardless of sample geometry, we will have a given ratio of sample conductance to sample capacitance , i.e. a given loss tangent.

Thus to calculate the minimum level of ac conductivity observable with the Wayne Kerr bridge, it is necessary to calculate the ratio of minimum conductance standard coupling to maximum capacitance standard coupling for the bridge. The minimum level of conductance standard coupling is obtained by use of the X10 position of the conductance multiplier switch (this divides conductance indications by a factor of 10) and by a minimum reading on the conductance magnetic potentiometer. The least count is 1% of full scale and although interpolation to 1/10 of a least count is possible, the least count may be considered the minimum useful reading. We thus obtain a coupling of 10^{-3} as the smallest for the conductance standard. The maximum coupling for the capacitance standard is obtained by use of the X1 position of the capacitance multiplier switch and by a full scale reading on the capacitance magnetic potentiometer. This gives a coupling factor of 1 for the capacitance standard. The ratio of conductance standard to capicitance standard in the Wayne Kerr bridge is 10μU/1pF. Thus the minimum measurable ratio of sample conductance to sample capacitance is 10^{4}U/F.
Since the dissipation factor is given by:

$$D = \frac{Xc}{R} = \frac{G}{WC} \quad ,$$

the minimum dissipation factor is frequency dependent and ranges from $1.59.10^{-2}$ at 10^{5}Hz to $1.59.10^{-4}$ at 10^{7}Hz.

In addition to this basic limitation, a number of other experimental problems have been encountered in the use of the Wayne Kerr bridge which have only recently been understood well enough to approach this measurement limit. Due to the very small values of conductivity which are to be measured, anything affecting the conductivity measurement at all will constitute an unacceptable amount of error.

The bridge was primarily designed to make measurements of devices or circuits attached with very short leads to the bridge. Due to the hazards involved in high pressure investigations, this was not acceptable in this program. The literature which was supplied by Wayne Kerr with the bridge did not provide any information concerning the use of cables between the bridge and the element to be measured other than a development of the three terminal correction method. When this correction alone was applied to data taken with cables, it improved the data, but did not fully correct the errors. Upon inquiry concerning the use of cables with the bridge, the manufacturer's service representative suggested measurements of samples at the bridge and at the ends of the cables and correlations of the results by means of a graph or chart. He further noted that this would be necessary with each sample being measured since there would be both

conductive and reactive components. Due to the expected and observed variations due to temperature and pressure, this procedure would be inapplicable for many of the measurements to be made. It thus appeared that to follow this recommendation would necessitate measurements of a tremendous number of capacitor and resistor combinations to cover the range of possible sample measurements under experimental conditions.

In order to better understand the errors involved and try to develop some systematic correction calculation which would not require the infinity of characterization measurements, calculations were made of the effect of cables on signals passing through them. These calculations showed that with perfectly lossless cables and with a perfect mismatch between the cable impedance and sample impedance, the signal reflections from the cable sample interfaces would cause a magnitude error. This magnitude error is approximately equal to the product of the secants of ϕ_e and ϕ_i where:

$$\phi_e = \frac{2\pi\nu\ell_e}{v} \quad \text{and} \quad \phi_i = \frac{2\pi\nu\ell_i}{v}$$

where ℓ_e and ℓ_i are the lengths of the two cables, ν is the signal frequency, and v is the propogation velocity in the cable. This magnitude error thus increases with cable length and frequency and is less for cables with higher wave propagation velocities. If the imperfect reflection at the sample-cable interfaces is taken into account, there will be slight phase shifts from one end of the cables to the other. This phase shift will cause a pure capacitance to appear to the bridge as a capacitance shunted by a conductance, and the magnitude of the spurious conductance indicated by the bridge will be approximately a linear function of frequency for fairly

short cables. By means of a computer program the three terminal correction, correction of the magnitude shift due to reflections at sample-cable interfaces, and a correction for the spurious conductance due to phase shifts caused by the imperfect reflections at the sample-cable interface were computed. These corrections made a great deal of improvement in the data, and it was believed for a while that they were sufficient; however, it was discovered that there was a further phase shift due to losses in the cables. The losses which cause this phase shift are so small that it would be impossible to measure them to the accuracy required for a good correction of the data.

A number of other sources of error have been observed which would be of little or no consequence in measuring larger dissipation factors. It has been observed that when a capacitor is measured, the bridge indicates a negative conductance component. As this result is obviously unacceptable, a determination has been made of the apparent conductance-capacitance relation for a variety of ceramic capacitors at a variety of frequencies. Points were fairly closely grouped for any given capacitance for a given frequency and bridge range and they followed a fairly simple, although not linear, curve. For low frequencies there is almost no deviation from zero for these curves; however, at the two highest frequencies used (4.65MHz and 10MHz), there is a rather marked deviation from zero and, especially at 10MHz, there is a great deal of curvature. The deviation from zero indicates that for these frequencies the standards in the bridge are not perfectly trimmed. This is not unexpected as there are only two trim controls for each standard with which to get the best trim compromise for the large frequency range that is covered. The curvature of the

G vs. C plot however is an indication that some of the transformers are saturating and the effective coupling is changing slightly. This would explain the earlier problems encountered in the attempts to determine the series resistances and stray inductances of the matching transformers.

The measurements of the conductance versus capacitance of the capacitors was made with the cables and pressure head. Since it was known at this time that any observed frequency dependent conductivity would be very small, it was decided to return to the original suggestion of the manufacturer's representative and use a graph to correct the results. The number of graphs required would only depend on the number of different frequencies and different bridge ranges used and would not depend on the sample conductance. Further the number of bridge ranges could be limited very much by arranging to make the samples with a given capacitance. For this correction purpose, it was decided to use capacitors as standards. The G vs. C points were plotted on the range to be used for sample data taking. Lines were then drawn very close to these points just on the low loss side. This line was then used as the zero conductivity line to be subtracted from sample conductance readings taken with the bridge. In this manner, the capacitors are being used and considered as a perfect capacitance standard. As the same time, the three terminal correction and corrections for phase shifts (all at atmospheric pressure and room temperature) are being made automatically.

There is a small but noticeable shift of the G vs. C values with pressure. This (and any similar shift for temperature changes) must be taken into account separately. It has been found possible

to make a pressure run with a capacitor and observe the shift of the G vs. C calibration curve with pressure. There is a negligible shift in capacitance for these capacitors with pressure and it is believed that there should be no change in the conductivity either. Thus, any change in the measured conductivity of a capacitor should be due to changes in the three terminal errors or to changes in the pressure transmitting fluid with pressure. As the capacitor leads do not present as much surface area for interaction with the pressure fluid as do the samples, measurements are planned to investigate this possibility. Presently measurements are being made to look for any shift in the G vs. C calibration curve with temperature.

Correction of sample data by means of the G vs. C calibration curve for the same conditions of temperature and pressure corrects for all known errors except for the magnitude error which is due to the reflections at the sample-cable interfaces. This correction has been determined by making measurements of a capacitor (with approximately the same impedance as a sample) at the bridge and then at the ends of the cables and determining the ratio for each frequency of the two measured impedances. This ratio should not be too sensitive to pressure or temperature for a given set of cables if the sample impedance does not change too much.

It is believed that, with these corrections in hand, the accuracy of measurements for all experimental conditions in the present apparatus with low loss samples will approach the accuracy which could be expected of measurements with the bridge alone.

Despite the obvious difficulties in determining and applying the corrections described above reliable data can be (and is being) obtained.

3. Acoustic Results

The techniques described in Sec. 2.C. were used to obtain transit times which were then analysed as described in that section. Calculations made using measured values of the transit times are tabulated in Table II. In all cases of chalcogenide glasses studied, the transit times for both shear and longitudinal waves displayed quadratic behavior over the range of pressure from 0-8 Kbar. The columns in Table II are the following, from left to right. L/L_o is the ratio of the length under pressure to the original length (i.e. $1/y(P)$). V/V_o is the ratio of the volume under pressure to the original volume. V/V_{OM} is V/V_o as calculated using the Muruaghan equation[36].

$$V/V_{OM} = [(1 + \frac{\partial B}{\partial P})_T P \kappa_T]^{[-1/\frac{\partial B}{\partial P})_T]}$$

where $\frac{\partial B}{\partial P})_T$ is the pressure derivative of the Bulk Modulus evaluated at P=0. The Muruaghan Eq. has been used successfully to predict V/V_o at higher pressures based on measurements taken at modest pressures. DBDP in Table II is the value of $\partial B/\partial P)_T$ evaluated at P = 0 Kappa is κ_T. Pressure is written in Bars. VL and VS are longitudinal and shear velocities respectively. Y-Mod is Youngs Modulus, Shear-Mod is the shear modulus. Theta is the Debye temperature in degrees Kelvin. The Debye temperature was calculated from[37]

$$\Theta_D = \frac{h}{K_B} \left(\frac{3QA\rho}{12\rho 566M} \right)^{1/3} v_{ave}$$

where h is Planks constant; K_B = Boltzman constant; A = Avogadros number; Q = number of atoms per molecule; ρ = density; M = molecular

3.1a

L/LO	V/VO	V/VOM	DBDP	KAPPA	PRESSURE	VL	VS	Y-MOD	SHEAR-MOD	THETA
1.0000E+00	1.0000E+00	1.0000E+00	1.0000E+00	8.3428E-12	0.	2.518E+05	1.356E+05	1.468E+11	5.663E+10	1.512E+02
9.9972E-01	9.9917E-01	9.9917E-01	5.7814E+00	8.3028E-12	1.00E+02	2.523E+05	1.357E+05	1.472E+11	5.678E+10	1.514E+02
9.9945E-01	9.9834E-01	9.9836E-01	5.7814E+00	8.2631E-12	2.00E+02	2.528E+05	1.359E+05	1.476E+11	5.692E+10	1.516E+02
9.9917E-01	9.9752E-01	9.9755E-01	5.7814E+00	8.2237E-12	3.00E+02	2.533E+05	1.361E+05	1.480E+11	5.706E+10	1.518E+02
9.9890E-01	9.9671E-01	9.9676E-01	5.7814E+00	8.1847E-12	4.00E+02	2.538E+05	1.362E+05	1.485E+11	5.721E+10	1.520E+02
9.9863E-01	9.9590E-01	9.9598E-01	5.7814E+00	8.1461E-12	5.00E+02	2.542E+05	1.364E+05	1.489E+11	5.735E+10	1.522E+02
9.9796E-01	9.9389E-01	9.9408E-01	5.7814E+00	8.0510E-12	7.50E+02	2.555E+05	1.368E+05	1.499E+11	5.771E+10	1.527E+02
9.9730E-01	9.9192E-01	9.9225E-01	5.7814E+00	7.9580E-12	1.00E+03	2.567E+05	1.373E+05	1.509E+11	5.806E+10	1.532E+02
9.9665E-01	9.8998E-01	9.9048E-01	5.7814E+00	7.8671E-12	1.25E+03	2.579E+05	1.377E+05	1.520E+11	5.841E+10	1.536E+02
9.9601E-01	9.8806E-01	9.8877E-01	5.7814E+00	7.7784E-12	1.50E+03	2.591E+05	1.381E+05	1.530E+11	5.876E+10	1.541E+02
9.9537E-01	9.8618E-01	9.8712E-01	5.7814E+00	7.6917E-12	1.75E+03	2.603E+05	1.385E+05	1.540E+11	5.911E+10	1.546E+02
9.9475E-01	9.8432E-01	9.8552E-01	5.7814E+00	7.6070E-12	2.00E+03	2.615E+05	1.389E+05	1.550E+11	5.945E+10	1.551E+02
9.9413E-01	9.8249E-01	9.8398E-01	5.7814E+00	7.5243E-12	2.25E+03	2.627E+05	1.393E+05	1.560E+11	5.979E+10	1.555E+02
9.9352E-01	9.8069E-01	9.8248E-01	5.7814E+00	7.4437E-12	2.50E+03	2.638E+05	1.397E+05	1.570E+11	6.013E+10	1.560E+02
9.9292E-01	9.7891E-01	9.8103E-01	5.7814E+00	7.3650E-12	2.75E+03	2.650E+05	1.401E+05	1.579E+11	6.046E+10	1.564E+02
9.9233E-01	9.7716E-01	9.7962E-01	5.7814E+00	7.2883E-12	3.00E+03	2.661E+05	1.404E+05	1.589E+11	6.079E+10	1.569E+02
9.9174E-01	9.7543E-01	9.7825E-01	5.7814E+00	7.2135E-12	3.25E+03	2.672E+05	1.408E+05	1.599E+11	6.111E+10	1.573E+02
9.9117E-01	9.7373E-01	9.7693E-01	5.7814E+00	7.1406E-12	3.50E+03	2.684E+05	1.412E+05	1.608E+11	6.143E+10	1.577E+02
9.9059E-01	9.7205E-01	9.7564E-01	5.7814E+00	7.0696E-12	3.75E+03	2.695E+05	1.415E+05	1.617E+11	6.175E+10	1.581E+02
9.9003E-01	9.7039E-01	9.7438E-01	5.7814E+00	7.0004E-12	4.00E+03	2.706E+05	1.419E+05	1.626E+11	6.206E+10	1.586E+02
9.8947E-01	9.6875E-01	9.7316E-01	5.7814E+00	6.9331E-12	4.25E+03	2.716E+05	1.423E+05	1.635E+11	6.237E+10	1.590E+02
9.8892E-01	9.6714E-01	9.7197E-01	5.7814E+00	6.8676E-12	4.50E+03	2.727E+05	1.426E+05	1.644E+11	6.267E+10	1.594E+02
9.8838E-01	9.6554E-01	9.7080E-01	5.7814E+00	6.8040E-12	4.75E+03	2.737E+05	1.429E+05	1.653E+11	6.297E+10	1.598E+02
9.8784E-01	9.6396E-01	9.6967E-01	5.7814E+00	6.7421E-12	5.00E+03	2.748E+05	1.433E+05	1.662E+11	6.327E+10	1.601E+02
9.8731E-01	9.6241E-01	9.6856E-01	5.7814E+00	6.6819E-12	5.25E+03	2.758E+05	1.436E+05	1.670E+11	6.355E+10	1.605E+02
9.8678E-01	9.6087E-01	9.6748E-01	5.7814E+00	6.6235E-12	5.50E+03	2.768E+05	1.439E+05	1.678E+11	6.384E+10	1.609E+02
9.8626E-01	9.5935E-01	9.6642E-01	5.7814E+00	6.5669E-12	5.75E+03	2.778E+05	1.442E+05	1.687E+11	6.411E+10	1.613E+02
9.8575E-01	9.5785E-01	9.6539E-01	5.7814E+00	6.5119E-12	6.00E+03	2.787E+05	1.445E+05	1.695E+11	6.438E+10	1.616E+02
9.8524E-01	9.5636E-01	9.6437E-01	5.7814E+00	6.4587E-12	6.25E+03	2.797E+05	1.448E+05	1.702E+11	6.465E+10	1.620E+02
9.8473E-01	9.5489E-01	9.6337E-01	5.7814E+00	6.4071E-12	6.50E+03	2.806E+05	1.451E+05	1.710E+11	6.491E+10	1.623E+02
9.8423E-01	9.5344E-01	9.6239E-01	5.7814E+00	6.3572E-12	6.75E+03	2.815E+05	1.454E+05	1.718E+11	6.516E+10	1.626E+02
9.8374E-01	9.5200E-01	9.6143E-01	5.7814E+00	6.3089E-12	7.00E+03	2.824E+05	1.457E+05	1.725E+11	6.540E+10	1.629E+02
9.8325E-01	9.5058E-01	9.6049E-01	5.7814E+00	6.2623E-12	7.25E+03	2.832E+05	1.459E+05	1.732E+11	6.564E+10	1.633E+02
9.8276E-01	9.4917E-01	9.5956E-01	5.7814E+00	6.2172E-12	7.50E+03	2.841E+05	1.462E+05	1.739E+11	6.588E+10	1.636E+02
9.8228E-01	9.4778E-01	9.5864E-01	5.7814E+00	6.1738E-12	7.75E+03	2.849E+05	1.464E+05	1.746E+11	6.610E+10	1.639E+02
9.8180E-01	9.4640E-01	9.5773E-01	5.7814E+00	6.1319E-12	8.00E+03	2.857E+05	1.467E+05	1.752E+11	6.632E+10	1.641E+02
9.8133E-01	9.4503E-01	9.5684E-01	5.7814E+00	6.0916E-12	8.25E+03	2.864E+05	1.469E+05	1.758E+11	6.653E+10	1.644E+02
9.8086E-01	9.4368E-01	9.5596E-01	5.7814E+00	6.0529E-12	8.50E+03	2.872E+05	1.471E+05	1.764E+11	6.673E+10	1.647E+02

Material: As_2S_3 Temperature: 25°C $\delta = 1$

L/LO	V/VO	V/VoM	DBDP	KAPPA	PRESSURE	VL	VS	Y-MOD	SHEAR-MOD	THETA
1.0000E+00	1.0000E+00	1.0000E+00	1.0000E+00	8.4586E-12	0.	2.498E+05	1.342E+05	1.440E+11	5.553E+10	1.497E+02
9.9972E-01	9.9916E-01	9.9916E-01	5.9232E+00	8.4165E-12	1.00E+02	2.503E+05	1.344E+05	1.445E+11	5.568E+10	1.499E+02
9.9944E-01	9.9832E-01	9.9833E-01	5.9232E+00	8.3747E-12	2.00E+02	2.508E+05	1.346E+05	1.449E+11	5.583E+10	1.501E+02
9.9916E-01	9.9749E-01	9.9752E-01	5.9232E+00	8.3333E-12	3.00E+02	2.513E+05	1.348E+05	1.453E+11	5.598E+10	1.504E+02
9.9889E-01	9.9666E-01	9.9672E-01	5.9232E+00	8.2923E-12	4.00E+02	2.518E+05	1.350E+05	1.458E+11	5.613E+10	1.506E+02
9.9861E-01	9.9584E-01	9.9593E-01	5.9232E+00	8.2517E-12	5.00E+02	2.523E+05	1.351E+05	1.462E+11	5.628E+10	1.508E+02
9.9793E-01	9.9381E-01	9.9401E-01	5.9232E+00	8.1518E-12	7.50E+02	2.536E+05	1.356E+05	1.473E+11	5.666E+10	1.513E+02
9.9726E-01	9.9181E-01	9.9216E-01	5.9232E+00	8.0542E-12	1.00E+03	2.549E+05	1.360E+05	1.484E+11	5.703E+10	1.518E+02
9.9660E-01	9.8985E-01	9.9038E-01	5.9232E+00	7.9590E-12	1.25E+03	2.561E+05	1.365E+05	1.494E+11	5.739E+10	1.523E+02
9.9596E-01	9.8791E-01	9.8866E-01	5.9232E+00	7.8661E-12	1.50E+03	2.574E+05	1.369E+05	1.505E+11	5.776E+10	1.528E+02
9.9531E-01	9.8601E-01	9.8700E-01	5.9232E+00	7.7754E-12	1.75E+03	2.586E+05	1.373E+05	1.515E+11	5.812E+10	1.533E+02
9.9468E-01	9.8413E-01	9.8539E-01	5.9232E+00	7.6870E-12	2.00E+03	2.598E+05	1.377E+05	1.526E+11	5.848E+10	1.538E+02
9.9406E-01	9.8229E-01	9.8384E-01	5.9232E+00	7.6008E-12	2.25E+03	2.610E+05	1.382E+05	1.536E+11	5.883E+10	1.543E+02
9.9345E-01	9.8047E-01	9.8234E-01	5.9232E+00	7.5168E-12	2.50E+03	2.622E+05	1.386E+05	1.546E+11	5.918E+10	1.548E+02
9.9284E-01	9.7867E-01	9.8089E-01	5.9232E+00	7.4349E-12	2.75E+03	2.634E+05	1.390E+05	1.556E+11	5.953E+10	1.552E+02
9.9224E-01	9.7691E-01	9.7948E-01	5.9232E+00	7.3552E-12	3.00E+03	2.646E+05	1.394E+05	1.566E+11	5.987E+10	1.557E+02
9.9165E-01	9.7516E-01	9.7811E-01	5.9232E+00	7.2777E-12	3.25E+03	2.658E+05	1.398E+05	1.576E+11	6.021E+10	1.561E+02
9.9107E-01	9.7345E-01	9.7678E-01	5.9232E+00	7.2022E-12	3.50E+03	2.669E+05	1.402E+05	1.586E+11	6.054E+10	1.566E+02
9.9049E-01	9.7175E-01	9.7549E-01	5.9232E+00	7.1288E-12	3.75E+03	2.680E+05	1.405E+05	1.595E+11	6.087E+10	1.570E+02
9.8993E-01	9.7008E-01	9.7423E-01	5.9232E+00	7.0574E-12	4.00E+03	2.692E+05	1.409E+05	1.605E+11	6.120E+10	1.575E+02
9.8936E-01	9.6843E-01	9.7301E-01	5.9232E+00	6.9880E-12	4.25E+03	2.703E+05	1.413E+05	1.614E+11	6.151E+10	1.579E+02
9.8881E-01	9.6680E-01	9.7182E-01	5.9232E+00	6.9207E-12	4.50E+03	2.714E+05	1.416E+05	1.623E+11	6.183E+10	1.583E+02
9.8826E-01	9.6520E-01	9.7066E-01	5.9232E+00	6.8553E-12	4.75E+03	2.724E+05	1.420E+05	1.632E+11	6.213E+10	1.587E+02
9.8772E-01	9.6361E-01	9.6953E-01	5.9232E+00	6.7919E-12	5.00E+03	2.735E+05	1.423E+05	1.641E+11	6.243E+10	1.591E+02
9.8718E-01	9.6204E-01	9.6843E-01	5.9232E+00	6.7304E-12	5.25E+03	2.745E+05	1.427E+05	1.650E+11	6.273E+10	1.595E+02
9.8665E-01	9.6049E-01	9.6734E-01	5.9232E+00	6.6708E-12	5.50E+03	2.755E+05	1.430E+05	1.658E+11	6.302E+10	1.599E+02
9.8613E-01	9.5897E-01	9.6629E-01	5.9232E+00	6.6131E-12	5.75E+03	2.765E+05	1.433E+05	1.666E+11	6.330E+10	1.603E+02
9.8561E-01	9.5745E-01	9.6525E-01	5.9232E+00	6.5573E-12	6.00E+03	2.775E+05	1.436E+05	1.675E+11	6.358E+10	1.606E+02
9.8510E-01	9.5596E-01	9.6424E-01	5.9232E+00	6.5033E-12	6.25E+03	2.784E+05	1.439E+05	1.682E+11	6.384E+10	1.610E+02
9.8459E-01	9.5448E-01	9.6324E-01	5.9232E+00	6.4512E-12	6.50E+03	2.793E+05	1.442E+05	1.690E+11	6.411E+10	1.613E+02
9.8409E-01	9.5302E-01	9.6226E-01	5.9232E+00	6.4009E-12	6.75E+03	2.802E+05	1.445E+05	1.698E+11	6.436E+10	1.616E+02
9.8359E-01	9.5158E-01	9.6130E-01	5.9232E+00	6.3524E-12	7.00E+03	2.811E+05	1.448E+05	1.705E+11	6.461E+10	1.620E+02
9.8310E-01	9.5014E-01	9.6035E-01	5.9232E+00	6.3056E-12	7.25E+03	2.820E+05	1.451E+05	1.712E+11	6.485E+10	1.623E+02
9.8261E-01	9.4873E-01	9.5942E-01	5.9232E+00	6.2607E-12	7.50E+03	2.828E+05	1.453E+05	1.719E+11	6.508E+10	1.626E+02
9.8212E-01	9.4733E-01	9.5850E-01	5.9232E+00	6.2174E-12	7.75E+03	2.836E+05	1.456E+05	1.726E+11	6.530E+10	1.629E+02
9.8164E-01	9.4594E-01	9.5759E-01	5.9232E+00	6.1760E-12	8.00E+03	2.844E+05	1.458E+05	1.732E+11	6.552E+10	1.632E+02
9.8117E-01	9.4456E-01	9.5669E-01	5.9232E+00	6.1362E-12	8.25E+03	2.852E+05	1.460E+05	1.738E+11	6.572E+10	1.634E+02
9.8070E-01	9.4320E-01	9.5580E-01	5.9232E+00	6.0981E-12	8.50E+03	2.859E+05	1.463E+05	1.744E+11	6.592E+10	1.637E+02

Material: As_2S_3 Temperature: 60°C Y =1

L/LO	V/VO	V/VOM	DBDP	KAPPA	PRESSURE	VL	VS	Y-MOD	SHEAR-MOD	THETA
1.0000E+00	1.0000E+00	1.0000E+00	1.0000E+00	8.5392E-12	0.	2.485E+05	1.335E+05	1.424E+11	5.490E+10	1.489E+02
9.9972E-01	9.9915E-01	9.9915E-01	6.0266E+00	8.4955E-12	1.00E+02	2.490E+05	1.336E+05	1.429E+11	5.505E+10	1.491E+02
9.9943E-01	9.9830E-01	9.9832E-01	6.0266E+00	8.4522E-12	2.00E+02	2.495E+05	1.338E+05	1.433E+11	5.520E+10	1.493E+02
9.9915E-01	9.9746E-01	9.9750E-01	6.0266E+00	8.4093E-12	3.00E+02	2.501E+05	1.340E+05	1.437E+11	5.535E+10	1.495E+02
9.9888E-01	9.9663E-01	9.9669E-01	6.0266E+00	8.3669E-12	4.00E+02	2.506E+05	1.342E+05	1.442E+11	5.550E+10	1.497E+02
9.9860E-01	9.9580E-01	9.9590E-01	6.0266E+00	8.3249E-12	5.00E+02	2.511E+05	1.344E+05	1.446E+11	5.565E+10	1.499E+02
9.9791E-01	9.9376E-01	9.9396E-01	6.0266E+00	8.2217E-12	7.50E+02	2.524E+05	1.348E+05	1.457E+11	5.602E+10	1.504E+02
9.9724E-01	9.9174E-01	9.9210E-01	6.0266E+00	8.1211E-12	1.00E+03	2.537E+05	1.353E+05	1.468E+11	5.638E+10	1.510E+02
9.9658E-01	9.8976E-01	9.9031E-01	6.0266E+00	8.0231E-12	1.25E+03	2.549E+05	1.357E+05	1.478E+11	5.675E+10	1.515E+02
9.9592E-01	9.8781E-01	9.8858E-01	6.0266E+00	7.9276E-12	1.50E+03	2.562E+05	1.361E+05	1.489E+11	5.711E+10	1.520E+02
9.9528E-01	9.8589E-01	9.8691E-01	6.0266E+00	7.8346E-12	1.75E+03	2.574E+05	1.366E+05	1.499E+11	5.747E+10	1.525E+02
9.9464E-01	9.8400E-01	9.8530E-01	6.0266E+00	7.7440E-12	2.00E+03	2.587E+05	1.370E+05	1.509E+11	5.783E+10	1.530E+02
9.9401E-01	9.8214E-01	9.8374E-01	6.0266E+00	7.6559E-12	2.25E+03	2.599E+05	1.374E+05	1.520E+11	5.819E+10	1.534E+02
9.9339E-01	9.8031E-01	9.8224E-01	6.0266E+00	7.5702E-12	2.50E+03	2.611E+05	1.378E+05	1.530E+11	5.854E+10	1.539E+02
9.9278E-01	9.7851E-01	9.8078E-01	6.0266E+00	7.4869E-12	2.75E+03	2.623E+05	1.382E+05	1.540E+11	5.888E+10	1.544E+02
9.9218E-01	9.7673E-01	9.7936E-01	6.0266E+00	7.4059E-12	3.00E+03	2.635E+05	1.386E+05	1.550E+11	5.922E+10	1.549E+02
9.9159E-01	9.7497E-01	9.7799E-01	6.0266E+00	7.3273E-12	3.25E+03	2.647E+05	1.390E+05	1.560E+11	5.956E+10	1.553E+02
9.9100E-01	9.7324E-01	9.7666E-01	6.0266E+00	7.2509E-12	3.50E+03	2.658E+05	1.394E+05	1.570E+11	5.990E+10	1.558E+02
9.9042E-01	9.7154E-01	9.7537E-01	6.0266E+00	7.1768E-12	3.75E+03	2.670E+05	1.398E+05	1.579E+11	6.023E+10	1.562E+02
9.8985E-01	9.6986E-01	9.7411E-01	6.0266E+00	7.1049E-12	4.00E+03	2.681E+05	1.402E+05	1.589E+11	6.055E+10	1.567E+02
9.8928E-01	9.6820E-01	9.7288E-01	6.0266E+00	7.0352E-12	4.25E+03	2.692E+05	1.405E+05	1.598E+11	6.088E+10	1.571E+02
9.8873E-01	9.6656E-01	9.7169E-01	6.0266E+00	6.9676E-12	4.50E+03	2.703E+05	1.409E+05	1.607E+11	6.119E+10	1.575E+02
9.8817E-01	9.6494E-01	9.7052E-01	6.0266E+00	6.9023E-12	4.75E+03	2.713E+05	1.413E+05	1.616E+11	6.151E+10	1.579E+02
9.8763E-01	9.6335E-01	9.6939E-01	6.0266E+00	6.8390E-12	5.00E+03	2.724E+05	1.416E+05	1.625E+11	6.181E+10	1.583E+02
9.8709E-01	9.6177E-01	9.6828E-01	6.0266E+00	6.7779E-12	5.25E+03	2.734E+05	1.420E+05	1.634E+11	6.211E+10	1.587E+02
9.8656E-01	9.6021E-01	9.6719E-01	6.0266E+00	6.7188E-12	5.50E+03	2.744E+05	1.423E+05	1.643E+11	6.241E+10	1.591E+02
9.8603E-01	9.5867E-01	9.6612E-01	6.0266E+00	6.6618E-12	5.75E+03	2.754E+05	1.426E+05	1.651E+11	6.270E+10	1.595E+02
9.8551E-01	9.5715E-01	9.6508E-01	6.0266E+00	6.6068E-12	6.00E+03	2.763E+05	1.430E+05	1.659E+11	6.298E+10	1.599E+02
9.8499E-01	9.5564E-01	9.6405E-01	6.0266E+00	6.5538E-12	6.25E+03	2.773E+05	1.433E+05	1.667E+11	6.326E+10	1.602E+02
9.8448E-01	9.5416E-01	9.6305E-01	6.0266E+00	6.5028E-12	6.50E+03	2.782E+05	1.436E+05	1.675E+11	6.353E+10	1.606E+02
9.8397E-01	9.5268E-01	9.6206E-01	6.0266E+00	6.4538E-12	6.75E+03	2.791E+05	1.439E+05	1.683E+11	6.380E+10	1.609E+02
9.8347E-01	9.5123E-01	9.6108E-01	6.0266E+00	6.4068E-12	7.00E+03	2.799E+05	1.442E+05	1.690E+11	6.406E+10	1.613E+02
9.8297E-01	9.4979E-01	9.6012E-01	6.0266E+00	6.3616E-12	7.25E+03	2.808E+05	1.444E+05	1.698E+11	6.431E+10	1.616E+02
9.8248E-01	9.4836E-01	9.5917E-01	6.0266E+00	6.3184E-12	7.50E+03	2.816E+05	1.447E+05	1.705E+11	6.455E+10	1.619E+02
9.8199E-01	9.4694E-01	9.5824E-01	6.0266E+00	6.2771E-12	7.75E+03	2.823E+05	1.450E+05	1.712E+11	6.479E+10	1.622E+02
9.8151E-01	9.4554E-01	9.5731E-01	6.0266E+00	6.2377E-12	8.00E+03	2.831E+05	1.452E+05	1.718E+11	6.502E+10	1.625E+02
9.8103E-01	9.4416E-01	9.5639E-01	6.0266E+00	6.2001E-12	8.25E+03	2.838E+05	1.455E+05	1.725E+11	6.524E+10	1.628E+02
9.8055E-01	9.4278E-01	9.5549E-01	6.0266E+00	6.1644E-12	8.50E+03	2.845E+05	1.457E+05	1.731E+11	6.545E+10	1.631E+02

Material: As_2S_3 Temperature: 78 °C Y =1

L/LO	V/VO	V/VOM	DBDP	KAPPA	PRESSURE	VL	VS	Y-MOD	SHEAR-MOD	THETA
1.0000E+00	1.0000E+00	1.0000E+00	1.0000E+00	8.6423E-12	0.	2.471E+05	1.328E+05	1.411E+11	5.438E+10	1.482E+02
9.9971E-01	9.9914E-01	9.9914E-01	6.0242E+00	8.5975E-12	1.00E+02	2.477E+05	1.330E+05	1.415E+11	5.454E+10	1.484E+02
9.9943E-01	9.9828E-01	9.9830E-01	6.0242E+00	8.5532E-12	2.00E+02	2.482E+05	1.332E+05	1.420E+11	5.470E+10	1.486E+02
9.9914E-01	9.9743E-01	9.9747E-01	6.0242E+00	8.5093E-12	3.00E+02	2.487E+05	1.334E+05	1.424E+11	5.486E+10	1.488E+02
9.9886E-01	9.9659E-01	9.9665E-01	6.0242E+00	8.4659E-12	4.00E+02	2.493E+05	1.336E+05	1.429E+11	5.501E+10	1.491E+02
9.9858E-01	9.9575E-01	9.9585E-01	6.0242E+00	8.4228E-12	5.00E+02	2.498E+05	1.338E+05	1.433E+11	5.517E+10	1.493E+02
9.9789E-01	9.9368E-01	9.9390E-01	6.0242E+00	8.3172E-12	7.50E+02	2.511E+05	1.343E+05	1.444E+11	5.556E+10	1.498E+02
9.9721E-01	9.9165E-01	9.9201E-01	6.0242E+00	8.2142E-12	1.00E+03	2.524E+05	1.347E+05	1.455E+11	5.595E+10	1.504E+02
9.9654E-01	9.8964E-01	9.9020E-01	6.0242E+00	8.1138E-12	1.25E+03	2.537E+05	1.352E+05	1.466E+11	5.633E+10	1.509E+02
9.9587E-01	9.8767E-01	9.8846E-01	6.0242E+00	8.0159E-12	1.50E+03	2.550E+05	1.357E+05	1.477E+11	5.671E+10	1.514E+02
9.9522E-01	9.8573E-01	9.8678E-01	6.0242E+00	7.9207E-12	1.75E+03	2.562E+05	1.361E+05	1.488E+11	5.709E+10	1.519E+02
9.9458E-01	9.8382E-01	9.8515E-01	6.0242E+00	7.8279E-12	2.00E+03	2.575E+05	1.366E+05	1.499E+11	5.747E+10	1.525E+02
9.9394E-01	9.8194E-01	9.8358E-01	6.0242E+00	7.7377E-12	2.25E+03	2.588E+05	1.370E+05	1.510E+11	5.784E+10	1.530E+02
9.9332E-01	9.8009E-01	9.8206E-01	6.0242E+00	7.6499E-12	2.50E+03	2.600E+05	1.374E+05	1.521E+11	5.821E+10	1.535E+02
9.9270E-01	9.7827E-01	9.8059E-01	6.0242E+00	7.5645E-12	2.75E+03	2.612E+05	1.379E+05	1.531E+11	5.858E+10	1.540E+02
9.9210E-01	9.7647E-01	9.7917E-01	6.0242E+00	7.4816E-12	3.00E+03	2.624E+05	1.383E+05	1.542E+11	5.894E+10	1.545E+02
9.9150E-01	9.7470E-01	9.7779E-01	6.0242E+00	7.4010E-12	3.25E+03	2.636E+05	1.387E+05	1.552E+11	5.930E+10	1.550E+02
9.9090E-01	9.7296E-01	9.7645E-01	6.0242E+00	7.3227E-12	3.50E+03	2.648E+05	1.391E+05	1.562E+11	5.965E+10	1.554E+02
9.9032E-01	9.7124E-01	9.7515E-01	6.0242E+00	7.2467E-12	3.75E+03	2.660E+05	1.395E+05	1.572E+11	6.000E+10	1.559E+02
9.8974E-01	9.6954E-01	9.7388E-01	6.0242E+00	7.1731E-12	4.00E+03	2.671E+05	1.399E+05	1.582E+11	6.035E+10	1.564E+02
9.8917E-01	9.6786E-01	9.7265E-01	6.0242E+00	7.1017E-12	4.25E+03	2.682E+05	1.403E+05	1.592E+11	6.069E+10	1.568E+02
9.8861E-01	9.6621E-01	9.7145E-01	6.0242E+00	7.0325E-12	4.50E+03	2.693E+05	1.407E+05	1.602E+11	6.103E+10	1.573E+02
9.8805E-01	9.6458E-01	9.7028E-01	6.0242E+00	6.9655E-12	4.75E+03	2.704E+05	1.411E+05	1.611E+11	6.136E+10	1.577E+02
9.8750E-01	9.6297E-01	9.6914E-01	6.0242E+00	6.9007E-12	5.00E+03	2.715E+05	1.415E+05	1.621E+11	6.168E+10	1.581E+02
9.8696E-01	9.6138E-01	9.6802E-01	6.0242E+00	6.8380E-12	5.25E+03	2.725E+05	1.418E+05	1.630E+11	6.200E+10	1.586E+02
9.8642E-01	9.5981E-01	9.6693E-01	6.0242E+00	6.7775E-12	5.50E+03	2.736E+05	1.422E+05	1.639E+11	6.232E+10	1.590E+02
9.8589E-01	9.5826E-01	9.6586E-01	6.0242E+00	6.7191E-12	5.75E+03	2.746E+05	1.425E+05	1.648E+11	6.262E+10	1.594E+02
9.8536E-01	9.5673E-01	9.6482E-01	6.0242E+00	6.6628E-12	6.00E+03	2.755E+05	1.429E+05	1.656E+11	6.292E+10	1.598E+02
9.8484E-01	9.5521E-01	9.6379E-01	6.0242E+00	6.6085E-12	6.25E+03	2.765E+05	1.432E+05	1.665E+11	6.322E+10	1.602E+02
9.8433E-01	9.5371E-01	9.6278E-01	6.0242E+00	6.5563E-12	6.50E+03	2.774E+05	1.435E+05	1.673E+11	6.351E+10	1.605E+02
9.8382E-01	9.5223E-01	9.6179E-01	6.0242E+00	6.5060E-12	6.75E+03	2.783E+05	1.439E+05	1.681E+11	6.379E+10	1.609E+02
9.8331E-01	9.5076E-01	9.6081E-01	6.0242E+00	6.4578E-12	7.00E+03	2.792E+05	1.442E+05	1.689E+11	6.406E+10	1.613E+02
9.8281E-01	9.4931E-01	9.5985E-01	6.0242E+00	6.4116E-12	7.25E+03	2.801E+05	1.445E+05	1.697E+11	6.433E+10	1.616E+02
9.8231E-01	9.4787E-01	9.5890E-01	6.0242E+00	6.3673E-12	7.50E+03	2.809E+05	1.448E+05	1.704E+11	6.459E+10	1.619E+02
9.8182E-01	9.4645E-01	9.5796E-01	6.0242E+00	6.3250E-12	7.75E+03	2.817E+05	1.450E+05	1.711E+11	6.484E+10	1.623E+02
9.8133E-01	9.4504E-01	9.5703E-01	6.0242E+00	6.2846E-12	8.00E+03	2.825E+05	1.453E+05	1.718E+11	6.508E+10	1.626E+02
9.8085E-01	9.4364E-01	9.5611E-01	6.0242E+00	6.2462E-12	8.25E+03	2.832E+05	1.456E+05	1.725E+11	6.532E+10	1.629E+02
9.8037E-01	9.4226E-01	9.5520E-01	6.0242E+00	6.2096E-12	8.50E+03	2.839E+05	1.458E+05	1.731E+11	6.554E+10	1.632E+02

Material: As_2S_3 Temperature: 100°C

L/LO	V/VO	V/VOM	DBDP	KAPPA	PRESSURE	VL	VS	Y-MOD	SHEAR-MOD	THETA
1.0000E+00	1.0000E+00	1.0000E+00	1.0000E+00	7.3690E-12	0.	2.194E+05	1.198E+05	1.732E+11	6.726E+10	1.320E+02
9.9976E-01	9.9927E-01	9.9927E-01	5.8358E+00	7.3375E-12	1.00E+02	2.197E+05	1.200E+05	1.736E+11	6.741E+10	1.322E+02
9.9951E-01	9.9853E-01	9.9865E-01	5.8358E+00	7.3062E-12	2.00E+02	2.201E+05	1.201E+05	1.740E+11	6.755E+10	1.323E+02
9.9927E-01	9.9781E-01	9.9793E-01	5.8358E+00	7.2752E-12	3.00E+02	2.205E+05	1.202E+05	1.745E+11	6.770E+10	1.325E+02
9.9903E-01	9.9709E-01	9.9713E-01	5.8358E+00	7.2445E-12	4.00E+02	2.209E+05	1.204E+05	1.749E+11	6.784E+10	1.326E+02
9.9879E-01	9.9637E-01	9.9644E-01	5.8358E+00	7.2140E-12	5.00E+02	2.212E+05	1.205E+05	1.753E+11	6.799E+10	1.328E+02
9.9819E-01	9.9459E-01	9.9474E-01	5.8358E+00	7.1391E-12	7.50E+02	2.222E+05	1.208E+05	1.764E+11	6.835E+10	1.331E+02
9.9761E-01	9.9284E-01	9.9310E-01	5.8358E+00	7.0659E-12	1.00E+03	2.231E+05	1.211E+05	1.774E+11	6.871E+10	1.335E+02
9.9703E-01	9.9111E-01	9.9151E-01	5.8358E+00	6.9943E-12	1.25E+03	2.240E+05	1.214E+05	1.785E+11	6.907E+10	1.339E+02
9.9645E-01	9.8940E-01	9.8997E-01	5.8358E+00	6.9243E-12	1.50E+03	2.249E+05	1.217E+05	1.795E+11	6.942E+10	1.342E+02
9.9589E-01	9.8772E-01	9.8847E-01	5.8358E+00	6.8560E-12	1.75E+03	2.258E+05	1.221E+05	1.805E+11	6.978E+10	1.346E+02
9.9533E-01	9.8606E-01	9.8702E-01	5.8358E+00	6.7893E-12	2.00E+03	2.267E+05	1.224E+05	1.816E+11	7.013E+10	1.349E+02
9.9478E-01	9.8442E-01	9.8561E-01	5.8358E+00	6.7242E-12	2.25E+03	2.276E+05	1.227E+05	1.826E+11	7.047E+10	1.353E+02
9.9423E-01	9.8280E-01	9.8423E-01	5.8358E+00	6.6606E-12	2.50E+03	2.285E+05	1.230E+05	1.836E+11	7.082E+10	1.356E+02
9.9369E-01	9.8120E-01	9.8290E-01	5.8358E+00	6.5987E-12	2.75E+03	2.294E+05	1.233E+05	1.846E+11	7.116E+10	1.359E+02
9.9316E-01	9.7962E-01	9.8160E-01	5.8358E+00	6.5382E-12	3.00E+03	2.302E+05	1.235E+05	1.856E+11	7.150E+10	1.363E+02
9.9263E-01	9.7806E-01	9.8034E-01	5.8358E+00	6.4793E-12	3.25E+03	2.311E+05	1.238E+05	1.866E+11	7.183E+10	1.366E+02
9.9211E-01	9.7652E-01	9.7910E-01	5.8358E+00	6.4218E-12	3.50E+03	2.319E+05	1.241E+05	1.875E+11	7.217E+10	1.369E+02
9.9160E-01	9.7500E-01	9.7790E-01	5.8358E+00	6.3659E-12	3.75E+03	2.328E+05	1.244E+05	1.885E+11	7.249E+10	1.373E+02
9.9109E-01	9.7350E-01	9.7672E-01	5.8358E+00	6.3114E-12	4.00E+03	2.336E+05	1.247E+05	1.894E+11	7.282E+10	1.376E+02
9.9058E-01	9.7201E-01	9.7558E-01	5.8358E+00	6.2584E-12	4.25E+03	2.344E+05	1.250E+05	1.904E+11	7.314E+10	1.379E+02
9.9008E-01	9.7054E-01	9.7446E-01	5.8358E+00	6.2068E-12	4.50E+03	2.352E+05	1.252E+05	1.913E+11	7.346E+10	1.382E+02
9.8959E-01	9.6909E-01	9.7336E-01	5.8358E+00	6.1566E-12	4.75E+03	2.360E+05	1.255E+05	1.922E+11	7.377E+10	1.385E+02
9.8910E-01	9.6765E-01	9.7229E-01	5.8358E+00	6.1079E-12	5.00E+03	2.367E+05	1.258E+05	1.931E+11	7.408E+10	1.388E+02
9.8861E-01	9.6623E-01	9.7124E-01	5.8358E+00	6.0605E-12	5.25E+03	2.375E+05	1.260E+05	1.940E+11	7.438E+10	1.391E+02
9.8813E-01	9.6482E-01	9.7021E-01	5.8358E+00	6.0145E-12	5.50E+03	2.382E+05	1.263E+05	1.949E+11	7.469E+10	1.394E+02
9.8766E-01	9.6343E-01	9.6920E-01	5.8358E+00	5.9699E-12	5.75E+03	2.390E+05	1.265E+05	1.957E+11	7.498E+10	1.397E+02
9.8719E-01	9.6205E-01	9.6820E-01	5.8358E+00	5.9267E-12	6.00E+03	2.397E+05	1.268E+05	1.966E+11	7.527E+10	1.400E+02
9.8672E-01	9.6068E-01	9.6723E-01	5.8358E+00	5.8847E-12	6.25E+03	2.404E+05	1.270E+05	1.974E+11	7.556E+10	1.403E+02
9.8626E-01	9.5933E-01	9.6627E-01	5.8358E+00	5.8441E-12	6.50E+03	2.411E+05	1.272E+05	1.982E+11	7.584E+10	1.405E+02
9.8580E-01	9.5799E-01	9.6533E-01	5.8358E+00	5.8049E-12	6.75E+03	2.418E+05	1.275E+05	1.990E+11	7.612E+10	1.408E+02
9.8534E-01	9.5667E-01	9.6440E-01	5.8358E+00	5.7669E-12	7.00E+03	2.424E+05	1.277E+05	1.998E+11	7.639E+10	1.411E+02
9.8489E-01	9.5536E-01	9.6349E-01	5.8358E+00	5.7302E-12	7.25E+03	2.431E+05	1.279E+05	2.006E+11	7.665E+10	1.413E+02
9.8444E-01	9.5405E-01	9.6258E-01	5.8358E+00	5.6948E-12	7.50E+03	2.437E+05	1.281E+05	2.013E+11	7.691E+10	1.416E+02
9.8400E-01	9.5276E-01	9.6169E-01	5.8358E+00	5.6607E-12	7.75E+03	2.443E+05	1.284E+05	2.021E+11	7.717E+10	1.418E+02
9.8356E-01	9.5148E-01	9.6081E-01	5.8358E+00	5.6279E-12	8.00E+03	2.449E+05	1.286E+05	2.028E+11	7.742E+10	1.420E+02
9.8312E-01	9.5022E-01	9.5994E-01	5.8358E+00	5.5963E-12	8.25E+03	2.455E+05	1.288E+05	2.035E+11	7.766E+10	1.423E+02
9.8269E-01	9.4896E-01	9.5908E-01	5.8358E+00	5.5659E-12	8.50E+03	2.460E+05	1.290E+05	2.042E+11	7.790E+10	1.425E+02

Material: As_2Se_3 Temperature: 25°C δ =1

L/LO	V/VO	V/VOM	DBDP	KAPPA	PRESSURE	VL	VS	Y-MOD	SHEAR-MOD	THETA
1.0000E+00	1.0000E+00	1.0000E+00	1.0000E+00	7.4368E-12	0.	2.182E+05	1.190E+05	1.710E+11	6.637E+10	1.311E+02
9.9975E-01	9.9926E-01	9.9926E-01	5.9617E+00	7.4039E-12	1.00E+02	2.186E+05	1.192E+05	1.714E+11	6.652E+10	1.313E+02
9.9951E-01	9.9852E-01	9.9853E-01	5.9617E+00	7.3714E-12	2.00E+02	2.190E+05	1.193E+05	1.719E+11	6.667E+10	1.315E+02
9.9926E-01	9.9779E-01	9.9781E-01	5.9617E+00	7.3392E-12	3.00E+02	2.193E+05	1.194E+05	1.723E+11	6.682E+10	1.316E+02
9.9902E-01	9.9706E-01	9.9711E-01	5.9617E+00	7.3072E-12	4.00E+02	2.197E+05	1.196E+05	1.727E+11	6.697E+10	1.318E+02
9.9878E-01	9.9634E-01	9.9641E-01	5.9617E+00	7.2756E-12	5.00E+02	2.201E+05	1.197E+05	1.732E+11	6.712E+10	1.319E+02
9.9818E-01	9.9454E-01	9.9470E-01	5.9617E+00	7.1977E-12	7.50E+02	2.211E+05	1.200E+05	1.743E+11	6.750E+10	1.323E+02
9.9759E-01	9.9278E-01	9.9305E-01	5.9617E+00	7.1216E-12	1.00E+03	2.220E+05	1.204E+05	1.754E+11	6.787E+10	1.327E+02
9.9700E-01	9.9103E-01	9.9145E-01	5.9617E+00	7.0473E-12	1.25E+03	2.230E+05	1.207E+05	1.764E+11	6.824E+10	1.331E+02
9.9643E-01	9.8931E-01	9.8990E-01	5.9617E+00	6.9747E-12	1.50E+03	2.239E+05	1.210E+05	1.775E+11	6.861E+10	1.334E+02
9.9586E-01	9.8762E-01	9.8840E-01	5.9617E+00	6.9039E-12	1.75E+03	2.248E+05	1.213E+05	1.786E+11	6.897E+10	1.338E+02
9.9529E-01	9.8595E-01	9.8694E-01	5.9617E+00	6.8348E-12	2.00E+03	2.258E+05	1.217E+05	1.796E+11	6.933E+10	1.342E+02
9.9474E-01	9.8430E-01	9.8553E-01	5.9617E+00	6.7673E-12	2.25E+03	2.267E+05	1.220E+05	1.807E+11	6.969E+10	1.345E+02
9.9419E-01	9.8267E-01	9.8416E-01	5.9617E+00	6.7015E-12	2.50E+03	2.276E+05	1.223E+05	1.817E+11	7.004E+10	1.349E+02
9.9365E-01	9.8106E-01	9.8282E-01	5.9617E+00	6.6374E-12	2.75E+03	2.285E+05	1.226E+05	1.827E+11	7.040E+10	1.352E+02
9.9311E-01	9.7947E-01	9.8152E-01	5.9617E+00	6.5749E-12	3.00E+03	2.294E+05	1.229E+05	1.837E+11	7.074E+10	1.356E+02
9.9258E-01	9.7791E-01	9.8026E-01	5.9617E+00	6.5140E-12	3.25E+03	2.302E+05	1.232E+05	1.847E+11	7.109E+10	1.359E+02
9.9206E-01	9.7636E-01	9.7903E-01	5.9617E+00	6.4547E-12	3.50E+03	2.311E+05	1.235E+05	1.857E+11	7.143E+10	1.363E+02
9.9154E-01	9.7483E-01	9.7783E-01	5.9617E+00	6.3969E-12	3.75E+03	2.320E+05	1.238E+05	1.867E+11	7.177E+10	1.366E+02
9.9103E-01	9.7332E-01	9.7666E-01	5.9617E+00	6.3408E-12	4.00E+03	2.328E+05	1.241E+05	1.877E+11	7.210E+10	1.369E+02
9.9052E-01	9.7183E-01	9.7551E-01	5.9617E+00	6.2861E-12	4.25E+03	2.336E+05	1.244E+05	1.887E+11	7.243E+10	1.372E+02
9.9002E-01	9.7035E-01	9.7440E-01	5.9617E+00	6.2330E-12	4.50E+03	2.344E+05	1.246E+05	1.896E+11	7.275E+10	1.376E+02
9.8952E-01	9.6889E-01	9.7331E-01	5.9617E+00	6.1814E-12	4.75E+03	2.352E+05	1.249E+05	1.905E+11	7.307E+10	1.379E+02
9.8903E-01	9.6745E-01	9.7224E-01	5.9617E+00	6.1313E-12	5.00E+03	2.360E+05	1.252E+05	1.915E+11	7.339E+10	1.382E+02
9.8854E-01	9.6602E-01	9.7119E-01	5.9617E+00	6.0826E-12	5.25E+03	2.368E+05	1.254E+05	1.924E+11	7.370E+10	1.385E+02
9.8806E-01	9.6461E-01	9.7017E-01	5.9617E+00	6.0354E-12	5.50E+03	2.376E+05	1.257E+05	1.932E+11	7.401E+10	1.388E+02
9.8758E-01	9.6322E-01	9.6916E-01	5.9617E+00	5.9897E-12	5.75E+03	2.383E+05	1.260E+05	1.941E+11	7.431E+10	1.391E+02
9.8711E-01	9.6183E-01	9.6817E-01	5.9617E+00	5.9454E-12	6.00E+03	2.391E+05	1.262E+05	1.950E+11	7.460E+10	1.394E+02
9.8664E-01	9.6046E-01	9.6720E-01	5.9617E+00	5.9025E-12	6.25E+03	2.398E+05	1.264E+05	1.958E+11	7.489E+10	1.397E+02
9.8618E-01	9.5911E-01	9.6625E-01	5.9617E+00	5.8610E-12	6.50E+03	2.405E+05	1.267E+05	1.967E+11	7.516E+10	1.399E+02
9.8572E-01	9.5777E-01	9.6531E-01	5.9617E+00	5.8209E-12	6.75E+03	2.412E+05	1.269E+05	1.975E+11	7.546E+10	1.402E+02
9.8526E-01	9.5644E-01	9.6439E-01	5.9617E+00	5.7822E-12	7.00E+03	2.418E+05	1.272E+05	1.983E+11	7.573E+10	1.405E+02
9.8481E-01	9.5512E-01	9.6348E-01	5.9617E+00	5.7449E-12	7.25E+03	2.425E+05	1.274E+05	1.990E+11	7.600E+10	1.407E+02
9.8436E-01	9.5382E-01	9.6258E-01	5.9617E+00	5.7089E-12	7.50E+03	2.431E+05	1.276E+05	1.998E+11	7.626E+10	1.410E+02
9.8392E-01	9.5253E-01	9.6170E-01	5.9617E+00	5.6742E-12	7.75E+03	2.437E+05	1.278E+05	2.005E+11	7.651E+10	1.412E+02
9.8348E-01	9.5125E-01	9.6082E-01	5.9617E+00	5.6409E-12	8.00E+03	2.443E+05	1.280E+05	2.012E+11	7.676E+10	1.414E+02
9.8304E-01	9.4997E-01	9.5996E-01	5.9617E+00	5.6089E-12	8.25E+03	2.449E+05	1.282E+05	2.019E+11	7.700E+10	1.417E+02
9.8260E-01	9.4871E-01	9.5910E-01	5.9617E+00	5.5782E-12	8.50E+03	2.455E+05	1.284E+05	2.026E+11	7.724E+10	1.419E+02

Material: As_2Se_3 Temperature: 50°C

3.1 g

L/L0	V/V0	V/V0M	DROP	KAPPA	PRESSURE	VL	VS	Y-MOD	SHEAR-MOD	THETA
1.0000E+00	1.0000E+00	1.0000E+00	1.0000E+00	7.4705E-12	0.	2.195E+05	1.250E+05	1.928E+11	7.653E+10	1.316E+02
9.9975E-01	9.9976E-01	9.9926E-01	5.601RE+00	7.4394E-12	1.00E+02	2.199E+05	1.251E+05	1.933E+11	7.669E+10	1.314E+02
9.995E-01	9.9951E-01	9.9853E-01	5.601RE+00	7.4085E-12	2.00E+02	2.202E+05	1.253E+05	1.937E+11	7.683E+10	1.319E+02
9.992RE-01	9.977RE-01	9.9780E-01	5.601RE+00	7.3779E-12	3.00E+02	2.206E+05	1.254E+05	1.942E+11	7.699E+10	1.320E+02
9.9902E-01	9.9705E-01	9.9704E-01	5.601RE+00	7.3475E-12	4.00E+02	2.209E+05	1.255E+05	1.946E+11	7.712E+10	1.322E+02
9.9877E-01	9.9632E-01	9.9630E-01	5.601RE+00	7.3174E-12	5.00E+02	2.213E+05	1.256E+05	1.950E+11	7.727E+10	1.323E+02
9.9817E-01	9.9451E-01	9.9406E-01	5.601RE+00	7.2433E-12	7.50E+02	2.221E+05	1.259E+05	1.961E+11	7.763E+10	1.326E+02
9.9757E-01	9.9273E-01	9.9299E-01	5.601RE+00	7.170RE-12	1.00E+03	2.230E+05	1.262E+05	1.972E+11	7.798E+10	1.329E+02
9.9698E-01	9.9096E-01	9.9194E-01	5.601RE+00	7.099RE-12	1.25E+03	2.239E+05	1.265E+05	1.983E+11	7.834E+10	1.333E+02
9.9640E-01	9.8921E-01	9.9089E-01	5.601RE+00	7.0304E-12	1.50E+03	2.247E+05	1.268E+05	1.993E+11	7.868E+10	1.336E+02
9.9583E-01	9.8748E-01	9.8984E-01	5.601RE+00	6.9625E-12	1.75E+03	2.255E+05	1.270E+05	2.003E+11	7.903E+10	1.339E+02
9.9526E-01	9.8575E-01	9.8880E-01	5.601RE+00	6.8962E-12	2.00E+03	2.263E+05	1.273E+05	2.014E+11	7.937E+10	1.342E+02
9.947QE-01	9.8419E-01	9.8776E-01	5.601RE+00	6.8313E-12	2.25E+03	2.272E+05	1.276E+05	2.024E+11	7.970E+10	1.345E+02
9.9415E-01	9.8254E-01	9.8672E-01	5.601RE+00	6.7680E-12	2.50E+03	2.280E+05	1.281E+05	2.034E+11	8.003E+10	1.348E+02
9.9360E-01	9.8092E-01	9.8568E-01	5.601RE+00	6.7061E-12	2.75E+03	2.288E+05	1.284E+05	2.044E+11	8.036E+10	1.351E+02
9.9306E-01	9.7932E-01	9.8464E-01	5.601RE+00	6.6456E-12	3.00E+03	2.296E+05	1.286E+05	2.053E+11	8.068E+10	1.354E+02
9.9252E-01	9.7773E-01	9.7999E-01	5.601RE+00	6.5866E-12	3.25E+03	2.304E+05	1.289E+05	2.063E+11	8.100E+10	1.356E+02
9.9199E-01	9.7617E-01	9.7873E-01	5.601RE+00	6.5290E-12	3.50E+03	2.311E+05	1.291E+05	2.072E+11	8.131E+10	1.359E+02
9.9147E-01	9.7462E-01	9.7750E-01	5.601RE+00	6.4728E-12	3.75E+03	2.319E+05	1.293E+05	2.081E+11	8.161E+10	1.362E+02
9.9095E-01	9.7310E-01	9.7630E-01	5.601RE+00	6.4180E-12	4.00E+03	2.327E+05	1.296E+05	2.090E+11	8.191E+10	1.364E+02
9.9044E-01	9.7159E-01	9.7513E-01	5.601RE+00	6.3646E-12	4.25E+03	2.334E+05	1.298E+05	2.100E+11	8.221E+10	1.367E+02
9.8993E-01	9.7009E-01	9.7398E-01	5.601RE+00	6.3126E-12	4.50E+03	2.341E+05	1.298E+05	2.109E+11	8.249E+10	1.370E+02
9.8943E-01	9.6861E-01	9.7286E-01	5.601RE+00	6.2619E-12	4.75E+03	2.349E+05	1.300E+05	2.117E+11	8.277E+10	1.372E+02
9.8893E-01	9.6715E-01	9.7177E-01	5.601RE+00	6.2125E-12	5.00E+03	2.356E+05	1.302E+05	2.126E+11	8.305E+10	1.375E+02
9.8844E-01	9.6571E-01	9.7070E-01	5.601RE+00	6.1645E-12	5.25E+03	2.363E+05	1.305E+05	2.134E+11	8.332E+10	1.377E+02
9.8795E-01	9.6428E-01	9.6964E-01	5.601RE+00	6.1177E-12	5.50E+03	2.370E+05	1.307E+05	2.142E+11	8.358E+10	1.379E+02
9.8746E-01	9.6286E-01	9.6861E-01	5.601RE+00	6.0723E-12	5.75E+03	2.376E+05	1.309E+05	2.150E+11	8.384E+10	1.381E+02
9.8699E-01	9.6146E-01	9.6760E-01	5.601RE+00	6.0281E-12	6.00E+03	2.383E+05	1.311E+05	2.158E+11	8.409E+10	1.384E+02
9.8651E-01	9.6008E-01	9.6661E-01	5.601RE+00	5.9852E-12	6.25E+03	2.389E+05	1.312E+05	2.166E+11	8.433E+10	1.386E+02
9.8604E-01	9.5871E-01	9.6563E-01	5.601RE+00	5.9436E-12	6.50E+03	2.396E+05	1.314E+05	2.173E+11	8.457E+10	1.388E+02
9.8557E-01	9.5735E-01	9.6467E-01	5.601RE+00	5.9032E-12	6.75E+03	2.402E+05	1.316E+05	2.180E+11	8.479E+10	1.390E+02
9.8511E-01	9.5600E-01	9.6373E-01	5.601RE+00	5.8640E-12	7.00E+03	2.408E+05	1.318E+05	2.187E+11	8.501E+10	1.392E+02
9.8465E-01	9.5467E-01	9.6280E-01	5.601RE+00	5.8261E-12	7.25E+03	2.414E+05	1.319E+05	2.194E+11	8.523E+10	1.394E+02
9.8420E-01	9.5334E-01	9.6188E-01	5.601RE+00	5.7894E-12	7.50E+03	2.420E+05	1.321E+05	2.200E+11	8.543E+10	1.396E+02
9.8375E-01	9.5204E-01	9.6098E-01	5.601RE+00	5.7539E-12	7.75E+03	2.425E+05	1.323E+05	2.207E+11	8.563E+10	1.397E+02
9.8330E-01	9.5074E-01	9.6008E-01	5.601RE+00	5.7195E-12	8.00E+03	2.431E+05	1.324E+05	2.213E+11	8.582E+10	1.399E+02
9.8286E-01	9.4945E-01	9.5920E-01	5.601RE+00	5.6864E-12	8.25E+03	2.436E+05	1.325E+05	2.219E+11	8.601E+10	1.400E+02
9.8242E-01	9.4817E-01	9.5833E-01	5.601RE+00	5.6544E-12	8.50E+03	2.441E+05	1.327E+05	2.224E+11	8.618E+10	1.402E+02

Material: AsGeTe **Temperature: 25 °C** **F =1**

3.1 h

L/LO	V/VO	V/VOM	DROP	KAPPA	PRESSURE	VL	VS	Y-MOD	SHEAR-MOD	THETA
1.0000E+00	1.0000E+00	1.0000E+00	1.0000E+00	7.5361E-12	0.	2.185E+05	1.245E+05	1.911E+11	7.554E+10	1.310E+02
9.9975E-01	9.9925E-01	9.9925E-01	6.4310E+00	7.4994E-12	1.00E+02	2.189E+05	1.246E+05	1.916E+11	7.598E+10	1.312E+02
9.9951E-01	9.9850E-01	9.9852E-01	6.4310E+00	7.4639E-12	2.00E+02	2.193E+05	1.247E+05	1.920E+11	7.612E+10	1.313E+02
9.9925E-01	9.9776E-01	9.9779E-01	6.4310E+00	7.4284E-12	3.00E+02	2.197E+05	1.248E+05	1.924E+11	7.625E+10	1.314E+02
9.9901E-01	9.9702E-01	9.9707E-01	6.4310E+00	7.3933E-12	4.00E+02	2.201E+05	1.249E+05	1.929E+11	7.641E+10	1.316E+02
9.9876E-01	9.9629E-01	9.9637E-01	6.4310E+00	7.3587E-12	5.00E+02	2.205E+05	1.250E+05	1.933E+11	7.655E+10	1.317E+02
9.9851E-01	9.9556E-01	9.9565E-01	6.4310E+00	7.3234E-12	6.50E+02	2.214E+05	1.253E+05	1.944E+11	7.690E+10	1.320E+02
9.9750E-01	9.9249E-01	9.9299E-01	6.4310E+00	7.1914E-12	1.00E+03	2.223E+05	1.256E+05	1.955E+11	7.724E+10	1.323E+02
9.9497E-01	9.9093E-01	9.9139E-01	6.4310E+00	7.1122E-12	1.25E+03	2.233E+05	1.259E+05	1.966E+11	7.759E+10	1.326E+02
9.9639E-01	9.8920E-01	9.8984E-01	6.4310E+00	7.0350E-12	1.50E+03	2.242E+05	1.262E+05	1.977E+11	7.793E+10	1.330E+02
9.9588E-01	9.8765E-01	9.8834E-01	6.4310E+00	6.9604E-12	1.75E+03	2.251E+05	1.264E+05	1.987E+11	7.822E+10	1.333E+02
9.9525E-01	9.8591E-01	9.8689E-01	6.4310E+00	6.8881E-12	2.00E+03	2.260E+05	1.267E+05	1.998E+11	7.856E+10	1.336E+02
9.9469E-01	9.8415E-01	9.8548E-01	6.4310E+00	6.8182E-12	2.25E+03	2.268E+05	1.270E+05	2.008E+11	7.893E+10	1.339E+02
9.9410E-01	9.8251E-01	9.8411E-01	6.4310E+00	6.7507E-12	2.50E+03	2.277E+05	1.272E+05	2.018E+11	7.926E+10	1.342E+02
9.9359E-01	9.8084E-01	9.8277E-01	6.4310E+00	6.6854E-12	2.75E+03	2.285E+05	1.275E+05	2.028E+11	7.958E+10	1.345E+02
9.9305E-01	9.7929E-01	9.8148E-01	6.4310E+00	6.6225E-12	3.00E+03	2.293E+05	1.277E+05	2.038E+11	7.990E+10	1.347E+02
9.9251E-01	9.7771E-01	9.8021E-01	6.4310E+00	6.5617E-12	3.25E+03	2.302E+05	1.280E+05	2.047E+11	8.021E+10	1.350E+02
9.9196E-01	9.7615E-01	9.7898E-01	6.4310E+00	6.5031E-12	3.50E+03	2.309E+05	1.282E+05	2.057E+11	8.052E+10	1.353E+02
9.9146E-01	9.7461E-01	9.7778E-01	6.4310E+00	6.4466E-12	3.75E+03	2.317E+05	1.285E+05	2.066E+11	8.083E+10	1.356E+02
9.9095E-01	9.7309E-01	9.7661E-01	6.4310E+00	6.3925E-12	4.00E+03	2.325E+05	1.287E+05	2.075E+11	8.113E+10	1.358E+02
9.9044E-01	9.7159E-01	9.7546E-01	6.4310E+00	6.3403E-12	4.25E+03	2.332E+05	1.290E+05	2.084E+11	8.143E+10	1.361E+02
9.8993E-01	9.7010E-01	9.7433E-01	6.4310E+00	6.2903E-12	4.50E+03	2.339E+05	1.292E+05	2.093E+11	8.172E+10	1.364E+02
9.8943E-01	9.6863E-01	9.7323E-01	6.4310E+00	6.2422E-12	4.75E+03	2.346E+05	1.294E+05	2.102E+11	8.201E+10	1.366E+02
9.8893E-01	9.6717E-01	9.7214E-01	6.4310E+00	6.1962E-12	5.00E+03	2.353E+05	1.296E+05	2.110E+11	8.229E+10	1.369E+02
9.8844E-01	9.6573E-01	9.7108E-01	6.4310E+00	6.1522E-12	5.25E+03	2.360E+05	1.299E+05	2.119E+11	8.257E+10	1.371E+02
9.8796E-01	9.6430E-01	9.7003E-01	6.4310E+00	6.1102E-12	5.50E+03	2.366E+05	1.301E+05	2.126E+11	8.284E+10	1.373E+02
9.8747E-01	9.6289E-01	9.6900E-01	6.4310E+00	6.0701E-12	5.75E+03	2.372E+05	1.303E+05	2.134E+11	8.310E+10	1.376E+02
9.8699E-01	9.6149E-01	9.6799E-01	6.4310E+00	6.0320E-12	6.00E+03	2.378E+05	1.305E+05	2.142E+11	8.336E+10	1.378E+02
9.8652E-01	9.6010E-01	9.6699E-01	6.4310E+00	5.9958E-12	6.25E+03	2.384E+05	1.307E+05	2.149E+11	8.362E+10	1.380E+02
9.8605E-01	9.5872E-01	9.6599E-01	6.4310E+00	5.9615E-12	6.50E+03	2.390E+05	1.309E+05	2.157E+11	8.386E+10	1.382E+02
9.8558E-01	9.5736E-01	9.6501E-01	6.4310E+00	5.9291E-12	6.75E+03	2.395E+05	1.311E+05	2.164E+11	8.411E+10	1.384E+02
9.8511E-01	9.5600E-01	9.6404E-01	6.4310E+00	5.8985E-12	7.00E+03	2.400E+05	1.313E+05	2.170E+11	8.434E+10	1.386E+02
9.8465E-01	9.5466E-01	9.6308E-01	6.4310E+00	5.8698E-12	7.25E+03	2.405E+05	1.314E+05	2.177E+11	8.457E+10	1.388E+02
9.8419E-01	9.5333E-01	9.6213E-01	6.4310E+00	5.8429E-12	7.50E+03	2.409E+05	1.316E+05	2.183E+11	8.479E+10	1.390E+02
9.8374E-01	9.5201E-01	9.6118E-01	6.4310E+00	5.8179E-12	7.75E+03	2.414E+05	1.318E+05	2.189E+11	8.501E+10	1.392E+02
9.8329E-01	9.5069E-01	9.6024E-01	6.4310E+00	5.7947E-12	8.00E+03	2.418E+05	1.319E+05	2.195E+11	8.522E+10	1.394E+02
9.8284E-01	9.4939E-01	9.5930E-01	6.4310E+00	5.7733E-12	8.25E+03	2.422E+05	1.321E+05	2.201E+11	8.542E+10	1.395E+02
9.8239E-01	9.4809E-01	9.5837E-01	6.4310E+00	5.7536E-12	8.50E+03	2.425E+05	1.322E+05	2.206E+11	8.562E+10	1.397E+02

Material: AsGeTe Temperature: 66°C =1

5.1.2

Z/L0	V/V0	V/V0M	DROP	KAPPA	PRESSURE	VL	VS	Y-MOD	SHEAR-MOD	THETA
1.0000E+00	1.0000E+00	1.0000E+00	1.0000E+00	7.5905E-12	0.	2.179E+05	1.242E+05	1.901E+11	7.548E+10	1.307E+02
9.9975E-01	9.9924E-01	9.9925E-01	5.9602E+00	7.5563E-12	1.00E+02	2.182E+05	1.243E+05	1.906E+11	7.562E+10	1.308E+02
9.9950E-01	9.9849E-01	9.9850E-01	5.9602E+00	7.5224E-12	2.00E+02	2.186E+05	1.244E+05	1.910E+11	7.576E+10	1.310E+02
9.9925E-01	9.9774E-01	9.9775E-01	5.9602E+00	7.4889E-12	3.00E+02	2.190E+05	1.245E+05	1.914E+11	7.590E+10	1.311E+02
9.9900E-01	9.9700E-01	9.9705E-01	5.9602E+00	7.4558E-12	4.00E+02	2.193E+05	1.246E+05	1.919E+11	7.604E+10	1.312E+02
9.9875E-01	9.9626E-01	9.9634E-01	5.9602E+00	7.4229E-12	5.00E+02	2.197E+05	1.247E+05	1.923E+11	7.618E+10	1.314E+02
9.9851E-01	9.9553E-01	9.9564E-01	5.9602E+00	7.3902E-12	6.00E+02	2.201E+05	1.248E+05	1.927E+11	7.632E+10	1.315E+02
9.9826E-01	9.9480E-01	9.9494E-01	5.9602E+00	7.3577E-12	7.00E+02	2.204E+05	1.250E+05	1.934E+11	7.653E+10	1.317E+02
9.9754E-01	9.9263E-01	9.9291E-01	5.9602E+00	7.2636E-12	1.00E+03	2.215E+05	1.253E+05	1.944E+11	7.688E+10	1.320E+02
9.9694E-01	9.9085E-01	9.9129E-01	5.9602E+00	7.1870E-12	1.25E+03	2.224E+05	1.256E+05	1.955E+11	7.722E+10	1.323E+02
9.9635E-01	9.8910E-01	9.8971E-01	5.9602E+00	7.1123E-12	1.50E+03	2.232E+05	1.259E+05	1.965E+11	7.756E+10	1.326E+02
9.9577E-01	9.8737E-01	9.8818E-01	5.9602E+00	7.0396E-12	1.75E+03	2.241E+05	1.261E+05	1.976E+11	7.790E+10	1.329E+02
9.9520E-01	9.8567E-01	9.8670E-01	5.9602E+00	6.9687E-12	2.00E+03	2.250E+05	1.264E+05	1.986E+11	7.824E+10	1.332E+02
9.9463E-01	9.8399E-01	9.8526E-01	5.9602E+00	6.8994E-12	2.25E+03	2.258E+05	1.267E+05	1.996E+11	7.857E+10	1.335E+02
9.9407E-01	9.8233E-01	9.8386E-01	5.9602E+00	6.8328E-12	2.50E+03	2.267E+05	1.269E+05	2.006E+11	7.890E+10	1.338E+02
9.9352E-01	9.8069E-01	9.8251E-01	5.9602E+00	6.7675E-12	2.75E+03	2.275E+05	1.272E+05	2.016E+11	7.923E+10	1.341E+02
9.9297E-01	9.7908E-01	9.8118E-01	5.9602E+00	6.7041E-12	3.00E+03	2.283E+05	1.275E+05	2.026E+11	7.955E+10	1.344E+02
9.9244E-01	9.7748E-01	9.7990E-01	5.9602E+00	6.6425E-12	3.25E+03	2.291E+05	1.277E+05	2.036E+11	7.987E+10	1.347E+02
9.9191E-01	9.7590E-01	9.7864E-01	5.9602E+00	6.5826E-12	3.50E+03	2.299E+05	1.280E+05	2.046E+11	8.018E+10	1.350E+02
9.9137E-01	9.7434E-01	9.7742E-01	5.9602E+00	6.5245E-12	3.75E+03	2.307E+05	1.282E+05	2.055E+11	8.050E+10	1.353E+02
9.9085E-01	9.7280E-01	9.7623E-01	5.9602E+00	6.4681E-12	4.00E+03	2.315E+05	1.285E+05	2.064E+11	8.081E+10	1.355E+02
9.9033E-01	9.7128E-01	9.7506E-01	5.9602E+00	6.4134E-12	4.25E+03	2.322E+05	1.287E+05	2.074E+11	8.111E+10	1.358E+02
9.8982E-01	9.6978E-01	9.7392E-01	5.9602E+00	6.3604E-12	4.50E+03	2.330E+05	1.289E+05	2.083E+11	8.141E+10	1.361E+02
9.8932E-01	9.6829E-01	9.7280E-01	5.9602E+00	6.3090E-12	4.75E+03	2.337E+05	1.292E+05	2.092E+11	8.171E+10	1.363E+02
9.8882E-01	9.6682E-01	9.7171E-01	5.9602E+00	6.2592E-12	5.00E+03	2.344E+05	1.294E+05	2.101E+11	8.200E+10	1.366E+02
9.8832E-01	9.6537E-01	9.7064E-01	5.9602E+00	6.2111E-12	5.25E+03	2.351E+05	1.296E+05	2.109E+11	8.229E+10	1.368E+02
9.8783E-01	9.6393E-01	9.6959E-01	5.9602E+00	6.1645E-12	5.50E+03	2.358E+05	1.299E+05	2.118E+11	8.257E+10	1.371E+02
9.8734E-01	9.6250E-01	9.6856E-01	5.9602E+00	6.1194E-12	5.75E+03	2.365E+05	1.301E+05	2.126E+11	8.285E+10	1.373E+02
9.8686E-01	9.6109E-01	9.6755E-01	5.9602E+00	6.0761E-12	6.00E+03	2.372E+05	1.303E+05	2.134E+11	8.312E+10	1.376E+02
9.8638E-01	9.5970E-01	9.6655E-01	5.9602E+00	6.0343E-12	6.25E+03	2.378E+05	1.305E+05	2.142E+11	8.339E+10	1.378E+02
9.8591E-01	9.5831E-01	9.6557E-01	5.9602E+00	5.9939E-12	6.50E+03	2.384E+05	1.307E+05	2.150E+11	8.365E+10	1.380E+02
9.8544E-01	9.5694E-01	9.6461E-01	5.9602E+00	5.9551E-12	6.75E+03	2.391E+05	1.309E+05	2.158E+11	8.391E+10	1.383E+02
9.8497E-01	9.5559E-01	9.6365E-01	5.9602E+00	5.9178E-12	7.00E+03	2.397E+05	1.311E+05	2.165E+11	8.417E+10	1.385E+02
9.8451E-01	9.5424E-01	9.6272E-01	5.9602E+00	5.8819E-12	7.25E+03	2.402E+05	1.313E+05	2.173E+11	8.441E+10	1.387E+02
9.8405E-01	9.5291E-01	9.6179E-01	5.9602E+00	5.8475E-12	7.50E+03	2.408E+05	1.315E+05	2.180E+11	8.466E+10	1.389E+02
9.8359E-01	9.5159E-01	9.6087E-01	5.9602E+00	5.8146E-12	7.75E+03	2.413E+05	1.317E+05	2.187E+11	8.489E+10	1.391E+02
9.8314E-01	9.5028E-01	9.5996E-01	5.9602E+00	5.7831E-12	8.00E+03	2.419E+05	1.319E+05	2.194E+11	8.512E+10	1.393E+02
9.8269E-01	9.4899E-01	9.5907E-01	5.9602E+00	5.7531E-12	8.25E+03	2.424E+05	1.320E+05	2.200E+11	8.535E+10	1.395E+02
9.8225E-01	9.4769E-01	9.5817E-01	5.9602E+00	5.7245E-12	8.50E+03	2.429E+05	1.322E+05	2.207E+11	8.557E+10	1.397E+02

Material: AsGeTe **Temperature: 92^{0}C** =1

L/L0	V/V0	V/V0A	ONDP	KAPPA	PRESSURE	VL	VS	Y-MOD	SHEAR-MOD	THETA
1.0000E+00	1.0000E+00	1.0000E+00	4.7803E+00	0.	0.	2.6946E+05	1.551E+05	3.001E+11	1.198E+11	1.592E+02
9.9994E-01	9.9991E-01	9.9991E-01	4.7803E+00	0.	1.00E+02	2.6949E+05	1.552E+05	3.004E+11	1.199E+11	1.593E+02
9.9987E-01	9.9981E-01	9.9981E-01	4.7803E+00	0.	2.00E+02	2.6955E+05	1.553E+05	3.008E+11	1.200E+11	1.594E+02
9.9981E-01	9.9972E-01	9.9972E-01	4.7803E+00	0.	3.00E+02	2.6963E+05	1.554E+05	3.012E+11	1.202E+11	1.595E+02
9.9974E-01	9.9963E-01	9.9963E-01	4.7803E+00	0.	4.00E+02	2.6966E+05	1.555E+05	3.014E+11	1.203E+11	1.596E+02
9.9968E-01	9.9955E-01	9.9955E-01	4.7803E+00	0.	5.00E+02	2.6968E+05	1.555E+05	3.015E+11	1.204E+11	1.597E+02
9.9961E-01	9.9946E-01	9.9946E-01	4.7803E+00	0.	6.00E+02	2.6971E+05	1.556E+05	3.016E+11	1.204E+11	1.597E+02
9.9954E-01	9.9937E-01	9.9937E-01	4.7803E+00	0.	7.00E+02	2.6974E+05	1.557E+05	3.018E+11	1.205E+11	1.598E+02
9.9948E-01	9.9928E-01	9.9928E-01	4.7803E+00	0.	8.00E+02	2.6977E+05	1.558E+05	3.020E+11	1.206E+11	1.599E+02
9.9941E-01	9.9919E-01	9.9919E-01	4.7803E+00	0.	9.00E+02	2.6980E+05	1.559E+05	3.022E+11	1.207E+11	1.600E+02
9.9934E-01	9.9910E-01	9.9910E-01	4.7803E+00	0.	1.00E+03	2.6983E+05	1.560E+05	3.024E+11	1.208E+11	1.601E+02
9.9927E-01	9.9901E-01	9.9901E-01	4.7803E+00	0.	1.10E+03	2.6986E+05	1.561E+05	3.026E+11	1.209E+11	1.602E+02
9.9921E-01	9.9892E-01	9.9892E-01	4.7803E+00	0.	1.20E+03	2.6989E+05	1.562E+05	3.028E+11	1.210E+11	1.603E+02
9.9914E-01	9.9883E-01	9.9883E-01	4.7803E+00	0.	1.30E+03	2.6992E+05	1.563E+05	3.030E+11	1.211E+11	1.604E+02
9.9907E-01	9.9874E-01	9.9874E-01	4.7803E+00	0.	1.40E+03	2.6995E+05	1.564E+05	3.032E+11	1.212E+11	1.605E+02
9.9901E-01	9.9865E-01	9.9865E-01	4.7803E+00	0.	1.50E+03	2.6998E+05	1.565E+05	3.034E+11	1.213E+11	1.606E+02
9.9894E-01	9.9856E-01	9.9856E-01	4.7803E+00	0.	1.60E+03	2.7001E+05	1.566E+05	3.036E+11	1.214E+11	1.607E+02
9.9887E-01	9.9847E-01	9.9847E-01	4.7803E+00	0.	1.70E+03	2.7004E+05	1.567E+05	3.038E+11	1.215E+11	1.608E+02
9.9881E-01	9.9838E-01	9.9838E-01	4.7803E+00	0.	1.80E+03	2.7007E+05	1.568E+05	3.040E+11	1.216E+11	1.609E+02
9.9874E-01	9.9829E-01	9.9829E-01	4.7803E+00	0.	1.90E+03	2.7010E+05	1.569E+05	3.042E+11	1.217E+11	1.610E+02
9.9867E-01	9.9820E-01	9.9820E-01	4.7803E+00	0.	2.00E+03	2.7013E+05	1.570E+05	3.044E+11	1.218E+11	1.611E+02
9.9861E-01	9.9811E-01	9.9811E-01	4.7803E+00	0.	2.10E+03	2.7016E+05	1.571E+05	3.046E+11	1.219E+11	1.612E+02
9.9854E-01	9.9802E-01	9.9802E-01	4.7803E+00	0.	2.20E+03	2.7019E+05	1.572E+05	3.048E+11	1.220E+11	1.613E+02
9.9847E-01	9.9793E-01	9.9793E-01	4.7803E+00	0.	2.30E+03	2.7022E+05	1.573E+05	3.050E+11	1.221E+11	1.614E+02
9.9841E-01	9.9784E-01	9.9784E-01	4.7803E+00	0.	2.40E+03	2.7025E+05	1.574E+05	3.052E+11	1.222E+11	1.615E+02
9.9834E-01	9.9775E-01	9.9775E-01	4.7803E+00	0.	2.50E+03	2.7028E+05	1.575E+05	3.054E+11	1.223E+11	1.616E+02
9.9827E-01	9.9766E-01	9.9766E-01	4.7803E+00	0.	2.60E+03	2.7031E+05	1.576E+05	3.056E+11	1.224E+11	1.617E+02
9.9821E-01	9.9757E-01	9.9757E-01	4.7803E+00	0.	2.70E+03	2.7034E+05	1.577E+05	3.058E+11	1.225E+11	1.618E+02
9.9814E-01	9.9748E-01	9.9748E-01	4.7803E+00	0.	2.80E+03	2.7037E+05	1.578E+05	3.060E+11	1.226E+11	1.619E+02
9.9807E-01	9.9739E-01	9.9739E-01	4.7803E+00	0.	2.90E+03	2.7040E+05	1.579E+05	3.062E+11	1.227E+11	1.620E+02
9.9801E-01	9.9730E-01	9.9730E-01	4.7803E+00	0.	3.00E+03	2.7043E+05	1.580E+05	3.064E+11	1.228E+11	1.621E+02
9.9794E-01	9.9721E-01	9.9721E-01	4.7803E+00	0.	3.10E+03	2.7046E+05	1.581E+05	3.066E+11	1.229E+11	1.622E+02
9.9787E-01	9.9712E-01	9.9712E-01	4.7803E+00	0.	3.20E+03	2.7049E+05	1.582E+05	3.068E+11	1.230E+11	1.623E+02
9.9781E-01	9.9703E-01	9.9703E-01	4.7803E+00	0.	3.30E+03	2.7052E+05	1.583E+05	3.070E+11	1.231E+11	1.624E+02
9.9774E-01	9.9694E-01	9.9694E-01	4.7803E+00	0.	3.40E+03	2.7055E+05	1.584E+05	3.072E+11	1.232E+11	1.625E+02
9.9767E-01	9.9685E-01	9.9685E-01	4.7803E+00	0.	3.50E+03	2.7058E+05	1.585E+05	3.074E+11	1.233E+11	1.626E+02
9.9761E-01	9.9676E-01	9.9676E-01	4.7803E+00	0.	3.60E+03	2.7061E+05	1.586E+05	3.076E+11	1.234E+11	1.627E+02
9.9754E-01	9.9667E-01	9.9667E-01	4.7803E+00	0.	3.70E+03	2.7064E+05	1.587E+05	3.078E+11	1.235E+11	1.628E+02
9.9747E-01	9.9658E-01	9.9658E-01	4.7803E+00	0.	3.80E+03	2.7067E+05	1.588E+05	3.080E+11	1.236E+11	1.629E+02
9.9741E-01	9.9649E-01	9.9649E-01	4.7803E+00	0.	3.90E+03	2.7070E+05	1.589E+05	3.082E+11	1.237E+11	1.630E+02
9.9734E-01	9.9640E-01	9.9640E-01	4.7803E+00	0.	4.00E+03	2.7073E+05	1.590E+05	3.084E+11	1.238E+11	1.631E+02
9.9727E-01	9.9631E-01	9.9631E-01	4.7803E+00	0.	4.10E+03	2.7076E+05	1.591E+05	3.086E+11	1.239E+11	1.632E+02
9.9721E-01	9.9622E-01	9.9622E-01	4.7803E+00	0.	4.20E+03	2.7079E+05	1.592E+05	3.088E+11	1.240E+11	1.633E+02
9.9714E-01	9.9613E-01	9.9613E-01	4.7803E+00	0.	4.30E+03	2.7082E+05	1.593E+05	3.090E+11	1.241E+11	1.634E+02
9.9707E-01	9.9604E-01	9.9604E-01	4.7803E+00	0.	4.40E+03	2.7085E+05	1.594E+05	3.092E+11	1.242E+11	1.635E+02
9.9701E-01	9.9595E-01	9.9595E-01	4.7803E+00	0.	4.50E+03	2.7088E+05	1.595E+05	3.094E+11	1.243E+11	1.636E+02
9.9694E-01	9.9586E-01	9.9586E-01	4.7803E+00	0.	4.60E+03	2.7091E+05	1.596E+05	3.096E+11	1.244E+11	1.637E+02
9.9687E-01	9.9577E-01	9.9577E-01	4.7803E+00	0.	4.70E+03	2.7094E+05	1.597E+05	3.098E+11	1.245E+11	1.638E+02
9.9681E-01	9.9568E-01	9.9568E-01	4.7803E+00	0.	4.80E+03	2.7097E+05	1.598E+05	3.100E+11	1.246E+11	1.639E+02
9.9674E-01	9.9559E-01	9.9559E-01	4.7803E+00	0.	4.90E+03	2.7100E+05	1.599E+05	3.102E+11	1.247E+11	1.640E+02
9.9667E-01	9.9550E-01	9.9550E-01	4.7803E+00	0.	5.00E+03	2.7103E+05	1.600E+05	3.104E+11	1.248E+11	1.641E+02
9.9661E-01	9.9541E-01	9.9541E-01	4.7803E+00	0.	5.10E+03	2.7106E+05	1.601E+05	3.106E+11	1.249E+11	1.642E+02
9.9654E-01	9.9532E-01	9.9532E-01	4.7803E+00	0.	5.20E+03	2.7109E+05	1.602E+05	3.108E+11	1.250E+11	1.643E+02
9.9647E-01	9.9523E-01	9.9523E-01	4.7803E+00	0.	5.30E+03	2.7112E+05	1.603E+05	3.110E+11	1.251E+11	1.644E+02
9.9641E-01	9.9514E-01	9.9514E-01	4.7803E+00	0.	5.40E+03	2.7115E+05	1.604E+05	3.112E+11	1.252E+11	1.645E+02

Material: As_2Ge_2SeTe Temperature: 25°C γ =1

3.1-2

L/LO	V/VO	V/VOM	DBDP	KAPPA	PRESSURE	VL	VS	Y-MOD	SHEAR-MOD	THETA
1.0000E+00	1.0000E+00	1.0000E+00	1.0000E+00	4.9636E-12	0.	2.6886E+05	1.541E+05	2.965E+11	1.181E+11	1.681E+02
9.9983E-01	9.9950E-01	9.9951E-01	4.7598E+00	4.9519E-12	1.00E+02	2.688E+05	1.541E+05	2.968E+11	1.182E+11	1.682E+02
9.9967E-01	9.9901E-01	9.9901E-01	4.7598E+00	4.9402E-12	2.00E+02	2.690E+05	1.542E+05	2.971E+11	1.184E+11	1.683E+02
9.9951E-01	9.9852E-01	9.9853E-01	4.7598E+00	4.9286E-12	3.00E+02	2.693E+05	1.543E+05	2.975E+11	1.185E+11	1.683E+02
9.9934E-01	9.9803E-01	9.9804E-01	4.7598E+00	4.9171E-12	4.00E+02	2.695E+05	1.543E+05	2.978E+11	1.186E+11	1.684E+02
9.9918E-01	9.9754E-01	9.9756E-01	4.7598E+00	4.9056E-12	5.00E+02	2.697E+05	1.544E+05	2.982E+11	1.187E+11	1.685E+02
9.9877E-01	9.9632E-01	9.9638E-01	4.7598E+00	4.8771E-12	7.50E+02	2.703E+05	1.546E+05	2.990E+11	1.189E+11	1.687E+02
9.9837E-01	9.9512E-01	9.9522E-01	4.7598E+00	4.8489E-12	1.00E+03	2.709E+05	1.548E+05	2.998E+11	1.192E+11	1.689E+02
9.9797E-01	9.9392E-01	9.9408E-01	4.7598E+00	4.8211E-12	1.25E+03	2.714E+05	1.549E+05	3.007E+11	1.195E+11	1.691E+02
9.9757E-01	9.9274E-01	9.9295E-01	4.7598E+00	4.7935E-12	1.50E+03	2.720E+05	1.551E+05	3.015E+11	1.197E+11	1.693E+02
9.9718E-01	9.9156E-01	9.9185E-01	4.7598E+00	4.7663E-12	1.75E+03	2.726E+05	1.553E+05	3.023E+11	1.200E+11	1.695E+02
9.9679E-01	9.9039E-01	9.9077E-01	4.7598E+00	4.7394E-12	2.00E+03	2.731E+05	1.554E+05	3.031E+11	1.202E+11	1.697E+02
9.9640E-01	9.8924E-01	9.8971E-01	4.7598E+00	4.7128E-12	2.25E+03	2.737E+05	1.556E+05	3.039E+11	1.205E+11	1.699E+02
9.9601E-01	9.8809E-01	9.8866E-01	4.7598E+00	4.6866E-12	2.50E+03	2.743E+05	1.558E+05	3.047E+11	1.207E+11	1.701E+02
9.9563E-01	9.8695E-01	9.8764E-01	4.7598E+00	4.6606E-12	2.75E+03	2.748E+05	1.559E+05	3.055E+11	1.210E+11	1.703E+02
9.9525E-01	9.8582E-01	9.8663E-01	4.7598E+00	4.6349E-12	3.00E+03	2.754E+05	1.561E+05	3.063E+11	1.212E+11	1.705E+02
9.9487E-01	9.8470E-01	9.8563E-01	4.7598E+00	4.6096E-12	3.25E+03	2.759E+05	1.562E+05	3.071E+11	1.215E+11	1.706E+02
9.9450E-01	9.8358E-01	9.8466E-01	4.7598E+00	4.5845E-12	3.50E+03	2.765E+05	1.564E+05	3.079E+11	1.217E+11	1.708E+02
9.9412E-01	9.8248E-01	9.8370E-01	4.7598E+00	4.5598E-12	3.75E+03	2.770E+05	1.565E+05	3.087E+11	1.220E+11	1.710E+02
9.9376E-01	9.8138E-01	9.8275E-01	4.7598E+00	4.5354E-12	4.00E+03	2.776E+05	1.567E+05	3.094E+11	1.222E+11	1.712E+02
9.9339E-01	9.8029E-01	9.8182E-01	4.7598E+00	4.5112E-12	4.25E+03	2.781E+05	1.568E+05	3.102E+11	1.224E+11	1.714E+02
9.9302E-01	9.7921E-01	9.8090E-01	4.7598E+00	4.4874E-12	4.50E+03	2.786E+05	1.570E+05	3.110E+11	1.227E+11	1.716E+02
9.9266E-01	9.7814E-01	9.8000E-01	4.7598E+00	4.4638E-12	4.75E+03	2.792E+05	1.571E+05	3.117E+11	1.229E+11	1.717E+02
9.9230E-01	9.7706E-01	9.7911E-01	4.7598E+00	4.4406E-12	5.00E+03	2.797E+05	1.573E+05	3.125E+11	1.231E+11	1.719E+02
9.9194E-01	9.7602E-01	9.7824E-01	4.7598E+00	4.4176E-12	5.25E+03	2.802E+05	1.574E+05	3.132E+11	1.234E+11	1.721E+02
9.9159E-01	9.7497E-01	9.7738E-01	4.7598E+00	4.3949E-12	5.50E+03	2.808E+05	1.576E+05	3.139E+11	1.236E+11	1.722E+02
9.9123E-01	9.7393E-01	9.7653E-01	4.7598E+00	4.3724E-12	5.75E+03	2.813E+05	1.577E+05	3.147E+11	1.238E+11	1.724E+02
9.9088E-01	9.7290E-01	9.7570E-01	4.7598E+00	4.3505E-12	6.00E+03	2.818E+05	1.579E+05	3.154E+11	1.240E+11	1.726E+02
9.9054E-01	9.7188E-01	9.7487E-01	4.7598E+00	4.3288E-12	6.25E+03	2.823E+05	1.580E+05	3.161E+11	1.243E+11	1.727E+02
9.9019E-01	9.7086E-01	9.7406E-01	4.7598E+00	4.3071E-12	6.50E+03	2.828E+05	1.581E+05	3.168E+11	1.245E+11	1.729E+02
9.8985E-01	9.6985E-01	9.7326E-01	4.7598E+00	4.2859E-12	6.75E+03	2.833E+05	1.583E+05	3.175E+11	1.247E+11	1.731E+02
9.8950E-01	9.6884E-01	9.7247E-01	4.7598E+00	4.2649E-12	7.00E+03	2.838E+05	1.584E+05	3.182E+11	1.249E+11	1.732E+02
9.8916E-01	9.6784E-01	9.7169E-01	4.7598E+00	4.2442E-12	7.25E+03	2.843E+05	1.585E+05	3.189E+11	1.251E+11	1.734E+02
9.8883E-01	9.6685E-01	9.7093E-01	4.7598E+00	4.2238E-12	7.50E+03	2.848E+05	1.587E+05	3.195E+11	1.253E+11	1.735E+02
9.8849E-01	9.6587E-01	9.7017E-01	4.7598E+00	4.2036E-12	7.75E+03	2.853E+05	1.588E+05	3.202E+11	1.255E+11	1.737E+02
9.8816E-01	9.6489E-01	9.6942E-01	4.7598E+00	4.1838E-12	8.00E+03	2.858E+05	1.589E+05	3.209E+11	1.257E+11	1.738E+02
9.8783E-01	9.6392E-01	9.6868E-01	4.7598E+00	4.1642E-12	8.25E+03	2.863E+05	1.590E+05	3.215E+11	1.259E+11	1.740E+02
9.8750E-01	9.6296E-01	9.6795E-01	4.7598E+00	4.1449E-12	8.50E+03	2.868E+05	1.592E+05	3.222E+11	1.261E+11	1.741E+02

Material: As_2Ge_2SeTe **Temperature:** 82^0C =1

L/LO	V/VO	V/VOM	DRDP	KAPPA	PRESSURE	VL	VS	Y-MOD	SHEAR-MOD	THETA
1.0000E+00	1.0000E+00	1.0000E+00	1.0000E+00	4.9782E-12	0.	2.6808E+05	1.536E+05	2.949E+11	1.174E+11	1.676E+02
9.9983E-01	9.9950E-01	9.9950E-01	4.9597E+00	4.9459E-12	1.00E+02	2.682E+05	1.537E+05	2.952E+11	1.176E+11	1.677E+02
9.9967E-01	9.9901E-01	9.9901E-01	4.9597E+00	4.9537E-12	2.00E+02	2.685E+05	1.538E+05	2.956E+11	1.177E+11	1.678E+02
9.9950E-01	9.9851E-01	9.9852E-01	4.9597E+00	4.9416E-12	3.00E+02	2.687E+05	1.538E+05	2.959E+11	1.178E+11	1.679E+02
9.9934E-01	9.9802E-01	9.9804E-01	4.9597E+00	4.9296E-12	4.00E+02	2.690E+05	1.539E+05	2.963E+11	1.179E+11	1.680E+02
9.9918E-01	9.9753E-01	9.9756E-01	4.9597E+00	4.9176E-12	5.00E+02	2.692E+05	1.540E+05	2.966E+11	1.180E+11	1.680E+02
9.9877E-01	9.9631E-01	9.9637E-01	4.9597E+00	4.8879E-12	7.50E+02	2.698E+05	1.541E+05	2.975E+11	1.183E+11	1.682E+02
9.9837E-01	9.9511E-01	9.9521E-01	4.9597E+00	4.8588E-12	1.00E+03	2.704E+05	1.543E+05	2.983E+11	1.185E+11	1.684E+02
9.9797E-01	9.9391E-01	9.9407E-01	4.9597E+00	4.8300E-12	1.25E+03	2.710E+05	1.545E+05	2.992E+11	1.188E+11	1.687E+02
9.9757E-01	9.9272E-01	9.9295E-01	4.9597E+00	4.8017E-12	1.50E+03	2.716E+05	1.547E+05	3.000E+11	1.191E+11	1.689E+02
9.9717E-01	9.9154E-01	9.9185E-01	4.9597E+00	4.7738E-12	1.75E+03	2.721E+05	1.548E+05	3.009E+11	1.193E+11	1.691E+02
9.9678E-01	9.9037E-01	9.9077E-01	4.9597E+00	4.7463E-12	2.00E+03	2.727E+05	1.550E+05	3.017E+11	1.196E+11	1.693E+02
9.9639E-01	9.8921E-01	9.8971E-01	4.9597E+00	4.7192E-12	2.25E+03	2.733E+05	1.552E+05	3.025E+11	1.198E+11	1.695E+02
9.9601E-01	9.8806E-01	9.8866E-01	4.9597E+00	4.6926E-12	2.50E+03	2.738E+05	1.553E+05	3.033E+11	1.201E+11	1.696E+02
9.9562E-01	9.8692E-01	9.8764E-01	4.9597E+00	4.6664E-12	2.75E+03	2.744E+05	1.555E+05	3.041E+11	1.204E+11	1.698E+02
9.9524E-01	9.8579E-01	9.8663E-01	4.9597E+00	4.6406E-12	3.00E+03	2.750E+05	1.557E+05	3.049E+11	1.206E+11	1.700E+02
9.9486E-01	9.8467E-01	9.8564E-01	4.9597E+00	4.6152E-12	3.25E+03	2.755E+05	1.558E+05	3.057E+11	1.209E+11	1.702E+02
9.9449E-01	9.8355E-01	9.8466E-01	4.9597E+00	4.5902E-12	3.50E+03	2.761E+05	1.560E+05	3.065E+11	1.211E+11	1.704E+02
9.9412E-01	9.8245E-01	9.8370E-01	4.9597E+00	4.5656E-12	3.75E+03	2.766E+05	1.561E+05	3.073E+11	1.214E+11	1.706E+02
9.9374E-01	9.8135E-01	9.8276E-01	4.9597E+00	4.5414E-12	4.00E+03	2.772E+05	1.563E+05	3.081E+11	1.216E+11	1.708E+02
9.9338E-01	9.8026E-01	9.8183E-01	4.9597E+00	4.5176E-12	4.25E+03	2.777E+05	1.565E+05	3.088E+11	1.218E+11	1.710E+02
9.9301E-01	9.7918E-01	9.8091E-01	4.9597E+00	4.4942E-12	4.50E+03	2.782E+05	1.566E+05	3.096E+11	1.221E+11	1.711E+02
9.9265E-01	9.7811E-01	9.8001E-01	4.9597E+00	4.4711E-12	4.75E+03	2.788E+05	1.568E+05	3.104E+11	1.223E+11	1.713E+02
9.9229E-01	9.7704E-01	9.7912E-01	4.9597E+00	4.4485E-12	5.00E+03	2.793E+05	1.569E+05	3.111E+11	1.225E+11	1.715E+02
9.9193E-01	9.7598E-01	9.7825E-01	4.9597E+00	4.4263E-12	5.25E+03	2.798E+05	1.571E+05	3.118E+11	1.228E+11	1.717E+02
9.9157E-01	9.7493E-01	9.7738E-01	4.9597E+00	4.4044E-12	5.50E+03	2.803E+05	1.572E+05	3.126E+11	1.230E+11	1.718E+02
9.9122E-01	9.7389E-01	9.7653E-01	4.9597E+00	4.3829E-12	5.75E+03	2.808E+05	1.574E+05	3.133E+11	1.232E+11	1.720E+02
9.9087E-01	9.7286E-01	9.7569E-01	4.9597E+00	4.3618E-12	6.00E+03	2.813E+05	1.575E+05	3.140E+11	1.235E+11	1.722E+02
9.9052E-01	9.7183E-01	9.7487E-01	4.9597E+00	4.3411E-12	6.25E+03	2.818E+05	1.576E+05	3.147E+11	1.237E+11	1.724E+02
9.9017E-01	9.7081E-01	9.7405E-01	4.9597E+00	4.3207E-12	6.50E+03	2.823E+05	1.578E+05	3.154E+11	1.239E+11	1.725E+02
9.8983E-01	9.6979E-01	9.7324E-01	4.9597E+00	4.3007E-12	6.75E+03	2.828E+05	1.579E+05	3.161E+11	1.241E+11	1.727E+02
9.8948E-01	9.6878E-01	9.7245E-01	4.9597E+00	4.2811E-12	7.00E+03	2.833E+05	1.580E+05	3.168E+11	1.243E+11	1.728E+02
9.8914E-01	9.6778E-01	9.7166E-01	4.9597E+00	4.2618E-12	7.25E+03	2.837E+05	1.582E+05	3.174E+11	1.245E+11	1.730E+02
9.8880E-01	9.6679E-01	9.7089E-01	4.9597E+00	4.2429E-12	7.50E+03	2.842E+05	1.583E+05	3.181E+11	1.247E+11	1.731E+02
9.8847E-01	9.6580E-01	9.7012E-01	4.9597E+00	4.2244E-12	7.75E+03	2.847E+05	1.584E+05	3.187E+11	1.249E+11	1.733E+02
9.8813E-01	9.6482E-01	9.6936E-01	4.9597E+00	4.2062E-12	8.00E+03	2.851E+05	1.586E+05	3.194E+11	1.251E+11	1.735E+02
9.8780E-01	9.6384E-01	9.6861E-01	4.9597E+00	4.1883E-12	8.25E+03	2.856E+05	1.587E+05	3.200E+11	1.253E+11	1.736E+02
9.8747E-01	9.6287E-01	9.6787E-01	4.9597E+00	4.1709E-12	8.50E+03	2.860E+05	1.588E+05	3.206E+11	1.255E+11	1.737E+02

Material: As_2Ge_2SeTe Temperature: 107°C =1

3.1 m

L/L0	V/V0	V/V0M	DBDP	KAPPA	PRESSURE	VL	VS	Y-MOD	SHEAR-MOD	THETA
1.0000E+00	1.0000E+00	1.0000E+00	1.0000E+00	5.7626E-12	0.	2.290E+05	1.295E+05	2.446E+11	9.66AE+10	1.340E+02
9.9981E-01	9.9943E-01	9.9943E-01	7.0437E+00	5.7393E-12	1.00E+02	2.294E+05	1.296E+05	2.453E+11	9.691E+10	1.341E+02
9.9962E-01	9.9885E-01	9.9886E-01	7.0437E+00	5.7162E-12	2.00E+02	2.298E+05	1.298E+05	2.459E+11	9.714E+10	1.343E+02
9.9943E-01	9.9828E-01	9.9830E-01	7.0437E+00	5.6931E-12	3.00E+02	2.302E+05	1.300E+05	2.466E+11	9.737E+10	1.344E+02
9.9924E-01	9.9772E-01	9.9775E-01	7.0437E+00	5.6702E-12	4.00E+02	2.306E+05	1.301E+05	2.472E+11	9.760E+10	1.346E+02
9.9905E-01	9.9716E-01	9.9721E-01	7.0437E+00	5.6475E-12	5.00E+02	2.309E+05	1.303E+05	2.478E+11	9.783E+10	1.348E+02
9.9858E-01	9.9576E-01	9.9588E-01	7.0437E+00	5.5912E-12	7.50E+02	2.319E+05	1.306E+05	2.494E+11	9.840E+10	1.352E+02
9.9812E-01	9.9438E-01	9.9458E-01	7.0437E+00	5.5358E-12	1.00E+03	2.328E+05	1.310E+05	2.510E+11	9.895E+10	1.356E+02
9.9767E-01	9.9302E-01	9.9333E-01	7.0437E+00	5.4811E-12	1.25E+03	2.338E+05	1.314E+05	2.526E+11	9.951E+10	1.360E+02
9.9722E-01	9.9168E-01	9.9212E-01	7.0437E+00	5.4274E-12	1.50E+03	2.347E+05	1.317E+05	2.542E+11	1.001E+11	1.364E+02
9.9677E-01	9.9036E-01	9.9093E-01	7.0437E+00	5.3744E-12	1.75E+03	2.356E+05	1.321E+05	2.557E+11	1.006E+11	1.367E+02
9.9634E-01	9.8905E-01	9.8979E-01	7.0437E+00	5.3223E-12	2.00E+03	2.366E+05	1.324E+05	2.572E+11	1.011E+11	1.371E+02
9.9590E-01	9.8775E-01	9.8867E-01	7.0437E+00	5.2710E-12	2.25E+03	2.375E+05	1.328E+05	2.587E+11	1.016E+11	1.375E+02
9.9547E-01	9.8647E-01	9.8759E-01	7.0437E+00	5.2204E-12	2.50E+03	2.384E+05	1.331E+05	2.602E+11	1.022E+11	1.378E+02
9.9505E-01	9.8521E-01	9.8654E-01	7.0437E+00	5.1707E-12	2.75E+03	2.393E+05	1.334E+05	2.617E+11	1.027E+11	1.382E+02
9.9463E-01	9.8396E-01	9.8552E-01	7.0437E+00	5.1219E-12	3.00E+03	2.402E+05	1.338E+05	2.632E+11	1.032E+11	1.386E+02
9.9421E-01	9.8273E-01	9.8452E-01	7.0437E+00	5.0738E-12	3.25E+03	2.412E+05	1.341E+05	2.646E+11	1.037E+11	1.389E+02
9.9380E-01	9.8151E-01	9.8355E-01	7.0437E+00	5.0265E-12	3.50E+03	2.420E+05	1.344E+05	2.660E+11	1.042E+11	1.392E+02
9.9339E-01	9.8031E-01	9.8261E-01	7.0437E+00	4.9799E-12	3.75E+03	2.429E+05	1.347E+05	2.674E+11	1.046E+11	1.396E+02
9.9299E-01	9.7912E-01	9.8169E-01	7.0437E+00	4.9342E-12	4.00E+03	2.438E+05	1.350E+05	2.688E+11	1.051E+11	1.399E+02
9.9259E-01	9.7795E-01	9.8079E-01	7.0437E+00	4.8892E-12	4.25E+03	2.447E+05	1.353E+05	2.702E+11	1.056E+11	1.402E+02
9.9220E-01	9.7678E-01	9.7992E-01	7.0437E+00	4.8451E-12	4.50E+03	2.456E+05	1.356E+05	2.715E+11	1.060E+11	1.405E+02
9.9181E-01	9.7563E-01	9.7907E-01	7.0437E+00	4.8016E-12	4.75E+03	2.464E+05	1.359E+05	2.728E+11	1.064E+11	1.408E+02
9.9143E-01	9.7450E-01	9.7824E-01	7.0437E+00	4.7590E-12	5.00E+03	2.473E+05	1.361E+05	2.741E+11	1.069E+11	1.411E+02
9.9104E-01	9.7337E-01	9.7743E-01	7.0437E+00	4.7171E-12	5.25E+03	2.481E+05	1.364E+05	2.754E+11	1.073E+11	1.414E+02
9.9067E-01	9.7226E-01	9.7664E-01	7.0437E+00	4.6759E-12	5.50E+03	2.490E+05	1.367E+05	2.766E+11	1.077E+11	1.417E+02
9.9029E-01	9.7116E-01	9.7587E-01	7.0437E+00	4.6355E-12	5.75E+03	2.498E+05	1.369E+05	2.778E+11	1.081E+11	1.420E+02
9.8992E-01	9.7008E-01	9.7511E-01	7.0437E+00	4.5959E-12	6.00E+03	2.506E+05	1.372E+05	2.790E+11	1.085E+11	1.422E+02
9.8956E-01	9.6900E-01	9.7438E-01	7.0437E+00	4.5570E-12	6.25E+03	2.514E+05	1.374E+05	2.802E+11	1.088E+11	1.425E+02
9.8920E-01	9.6794E-01	9.7366E-01	7.0437E+00	4.5188E-12	6.50E+03	2.522E+05	1.376E+05	2.813E+11	1.092E+11	1.428E+02
9.8884E-01	9.6688E-01	9.7295E-01	7.0437E+00	4.4813E-12	6.75E+03	2.530E+05	1.378E+05	2.824E+11	1.095E+11	1.430E+02
9.8848E-01	9.6584E-01	9.7226E-01	7.0437E+00	4.4446E-12	7.00E+03	2.538E+05	1.380E+05	2.835E+11	1.099E+11	1.432E+02
9.8813E-01	9.6481E-01	9.7158E-01	7.0437E+00	4.4086E-12	7.25E+03	2.546E+05	1.382E+05	2.845E+11	1.102E+11	1.435E+02
9.8778E-01	9.6379E-01	9.7092E-01	7.0437E+00	4.3733E-12	7.50E+03	2.554E+05	1.384E+05	2.855E+11	1.105E+11	1.437E+02
9.8744E-01	9.6278E-01	9.7027E-01	7.0437E+00	4.3387E-12	7.75E+03	2.561E+05	1.386E+05	2.865E+11	1.108E+11	1.439E+02
9.8709E-01	9.6178E-01	9.6964E-01	7.0437E+00	4.3048E-12	8.00E+03	2.569E+05	1.388E+05	2.875E+11	1.111E+11	1.441E+02
9.8676E-01	9.6079E-01	9.6901E-01	7.0437E+00	4.2716E-12	8.25E+03	2.576E+05	1.390E+05	2.884E+11	1.114E+11	1.443E+02
9.8642E-01	9.5981E-01	9.6840E-01	7.0437E+00	4.2390E-12	8.50E+03	2.583E+05	1.391E+05	2.892E+11	1.116E+11	1.445E+02

Material: $As_2Ge_3Te_{15}$ Temperature: 25°C γ =1

3-1 IR

L/LO	V/VO	V/VOM	DRDP	KAPPA	PRESSURE	VL	VS	Y-MOD	SHEAR-MOD	THETA
1.0000E+00	1.0000E+00	1.0000E+00	1.0000E+00	2.6627E-12	0.	3.254E+05	1.769E+05	4.724E+11	1.830E+11	2.028E+02
9.9991E-01	9.9973E-01	9.9973E-01	2.9491E+00	2.6606E-12	1.00E+02	3.255E+05	1.769E+05	4.724E+11	1.830E+11	2.028E+02
9.9982E-01	9.9947E-01	9.9947E-01	2.9491E+00	2.6585E-12	2.00E+02	3.255E+05	1.769E+05	4.725E+11	1.830E+11	2.028E+02
9.9973E-01	9.9920E-01	9.9920E-01	2.9491E+00	2.6565E-12	3.00E+02	3.256E+05	1.769E+05	4.726E+11	1.831E+11	2.028E+02
9.9965E-01	9.9894E-01	9.9894E-01	2.9491E+00	2.6544E-12	4.00E+02	3.257E+05	1.769E+05	4.726E+11	1.831E+11	2.028E+02
9.9956E-01	9.9867E-01	9.9868E-01	2.9491E+00	2.6524E-12	5.00E+02	3.258E+05	1.769E+05	4.727E+11	1.831E+11	2.028E+02
9.9934E-01	9.9801E-01	9.9802E-01	2.9491E+00	2.6473E-12	7.50E+02	3.260E+05	1.769E+05	4.728E+11	1.831E+11	2.028E+02
9.9912E-01	9.9735E-01	9.9737E-01	2.9491E+00	2.6423E-12	1.00E+03	3.262E+05	1.769E+05	4.730E+11	1.831E+11	2.028E+02
9.9890E-01	9.9670E-01	9.9672E-01	2.9491E+00	2.6373E-12	1.25E+03	3.264E+05	1.769E+05	4.731E+11	1.831E+11	2.029E+02
9.9868E-01	9.9604E-01	9.9608E-01	2.9491E+00	2.6324E-12	1.50E+03	3.266E+05	1.769E+05	4.733E+11	1.831E+11	2.029E+02
9.9846E-01	9.9539E-01	9.9544E-01	2.9491E+00	2.6275E-12	1.75E+03	3.267E+05	1.769E+05	4.734E+11	1.831E+11	2.029E+02
9.9824E-01	9.9474E-01	9.9481E-01	2.9491E+00	2.6227E-12	2.00E+03	3.269E+05	1.769E+05	4.735E+11	1.831E+11	2.029E+02
9.9803E-01	9.9410E-01	9.9418E-01	2.9491E+00	2.6180E-12	2.25E+03	3.271E+05	1.769E+05	4.737E+11	1.831E+11	2.029E+02
9.9781E-01	9.9345E-01	9.9355E-01	2.9491E+00	2.6133E-12	2.50E+03	3.273E+05	1.769E+05	4.738E+11	1.831E+11	2.029E+02
9.9760E-01	9.9281E-01	9.9293E-01	2.9491E+00	2.6087E-12	2.75E+03	3.275E+05	1.769E+05	4.739E+11	1.831E+11	2.029E+02
9.9738E-01	9.9216E-01	9.9231E-01	2.9491E+00	2.6042E-12	3.00E+03	3.276E+05	1.769E+05	4.740E+11	1.831E+11	2.029E+02
9.9717E-01	9.9152E-01	9.9169E-01	2.9491E+00	2.5997E-12	3.25E+03	3.278E+05	1.769E+05	4.741E+11	1.831E+11	2.029E+02
9.9695E-01	9.9089E-01	9.9108E-01	2.9491E+00	2.5953E-12	3.50E+03	3.280E+05	1.769E+05	4.742E+11	1.831E+11	2.029E+02
9.9674E-01	9.9025E-01	9.9047E-01	2.9491E+00	2.5909E-12	3.75E+03	3.281E+05	1.769E+05	4.743E+11	1.831E+11	2.029E+02
9.9653E-01	9.8962E-01	9.8986E-01	2.9491E+00	2.5866E-12	4.00E+03	3.283E+05	1.769E+05	4.743E+11	1.831E+11	2.029E+02
9.9631E-01	9.8899E-01	9.8926E-01	2.9491E+00	2.5823E-12	4.25E+03	3.285E+05	1.769E+05	4.744E+11	1.831E+11	2.029E+02
9.9610E-01	9.8835E-01	9.8866E-01	2.9491E+00	2.5781E-12	4.50E+03	3.286E+05	1.769E+05	4.745E+11	1.830E+11	2.029E+02
9.9589E-01	9.8772E-01	9.8806E-01	2.9491E+00	2.5739E-12	4.75E+03	3.288E+05	1.768E+05	4.745E+11	1.830E+11	2.029E+02
9.9568E-01	9.8710E-01	9.8747E-01	2.9491E+00	2.5699E-12	5.00E+03	3.289E+05	1.768E+05	4.746E+11	1.830E+11	2.029E+02
9.9547E-01	9.8647E-01	9.8688E-01	2.9491E+00	2.5658E-12	5.25E+03	3.291E+05	1.768E+05	4.746E+11	1.830E+11	2.029E+02
9.9526E-01	9.8585E-01	9.8629E-01	2.9491E+00	2.5619E-12	5.50E+03	3.292E+05	1.768E+05	4.747E+11	1.829E+11	2.029E+02
9.9505E-01	9.8523E-01	9.8571E-01	2.9491E+00	2.5579E-12	5.75E+03	3.294E+05	1.768E+05	4.747E+11	1.829E+11	2.029E+02
9.9484E-01	9.8461E-01	9.8512E-01	2.9491E+00	2.5541E-12	6.00E+03	3.295E+05	1.768E+05	4.747E+11	1.829E+11	2.029E+02
9.9463E-01	9.8399E-01	9.8454E-01	2.9491E+00	2.5503E-12	6.25E+03	3.296E+05	1.768E+05	4.747E+11	1.828E+11	2.029E+02
9.9443E-01	9.8337E-01	9.8397E-01	2.9491E+00	2.5465E-12	6.50E+03	3.298E+05	1.767E+05	4.748E+11	1.828E+11	2.029E+02
9.9422E-01	9.8276E-01	9.8340E-01	2.9491E+00	2.5428E-12	6.75E+03	3.299E+05	1.767E+05	4.748E+11	1.828E+11	2.028E+02
9.9401E-01	9.8214E-01	9.8282E-01	2.9491E+00	2.5392E-12	7.00E+03	3.300E+05	1.767E+05	4.748E+11	1.827E+11	2.028E+02
9.9381E-01	9.8153E-01	9.8226E-01	2.9491E+00	2.5356E-12	7.25E+03	3.302E+05	1.767E+05	4.747E+11	1.827E+11	2.028E+02
9.9360E-01	9.8092E-01	9.8169E-01	2.9491E+00	2.5321E-12	7.50E+03	3.303E+05	1.767E+05	4.747E+11	1.826E+11	2.028E+02
9.9339E-01	9.8031E-01	9.8113E-01	2.9491E+00	2.5286E-12	7.75E+03	3.304E+05	1.766E+05	4.747E+11	1.826E+11	2.028E+02
9.9319E-01	9.7971E-01	9.8057E-01	2.9491E+00	2.5252E-12	8.00E+03	3.305E+05	1.766E+05	4.747E+11	1.825E+11	2.028E+02
9.9299E-01	9.7910E-01	9.8001E-01	2.9491E+00	2.5219E-12	8.25E+03	3.307E+05	1.766E+05	4.747E+11	1.825E+11	2.027E+02
9.9278E-01	9.7850E-01	9.7945E-01	2.9491E+00	2.5186E-12	8.50E+03	3.308E+05	1.766E+05	4.746E+11	1.824E+11	2.027E+02

Material: $Cd_6 Ge_3 As_{11}$ Temperature: 25 ^{0}C γ = 1

L/LO	V/VO	V/VOM	DBDP	KAPPA	PRESSURE	VL	VS	Y-MOD	SHEAR-MOD	THETA
1.0000E+00	1.0000E+00	1.0000E+00	1.0000E+00	2.6756E-12	0.	3.241E+05	1.757E+05	4.669E+11	1.807E+11	2.015E+02
9.9991E-01	9.9973E-01	9.9973E-01	3.0580E+00	2.6734E-12	1.00E+02	3.242E+05	1.757E+05	4.670E+11	1.807E+11	2.015E+02
9.9982E-01	9.9947E-01	9.9947E-01	3.0580E+00	2.6712E-12	2.00E+02	3.243E+05	1.757E+05	4.671E+11	1.807E+11	2.015E+02
9.9973E-01	9.9920E-01	9.9920E-01	3.0580E+00	2.6691E-12	3.00E+02	3.244E+05	1.757E+05	4.671E+11	1.808E+11	2.016E+02
9.9964E-01	9.9893E-01	9.9894E-01	3.0580E+00	2.6669E-12	4.00E+02	3.244E+05	1.758E+05	4.672E+11	1.808E+11	2.016E+02
9.9956E-01	9.9867E-01	9.9867E-01	3.0580E+00	2.6648E-12	5.00E+02	3.245E+05	1.758E+05	4.673E+11	1.808E+11	2.016E+02
9.9933E-01	9.9800E-01	9.9801E-01	3.0580E+00	2.6595E-12	7.50E+02	3.247E+05	1.758E+05	4.675E+11	1.808E+11	2.016E+02
9.9911E-01	9.9734E-01	9.9736E-01	3.0580E+00	2.6542E-12	1.00E+03	3.249E+05	1.758E+05	4.676E+11	1.808E+11	2.016E+02
9.9889E-01	9.9668E-01	9.9671E-01	3.0580E+00	2.6490E-12	1.25E+03	3.251E+05	1.758E+05	4.678E+11	1.808E+11	2.016E+02
9.9867E-01	9.9603E-01	9.9607E-01	3.0580E+00	2.6439E-12	1.50E+03	3.253E+05	1.758E+05	4.680E+11	1.809E+11	2.017E+02
9.9845E-01	9.9537E-01	9.9542E-01	3.0580E+00	2.6389E-12	1.75E+03	3.255E+05	1.758E+05	4.681E+11	1.809E+11	2.017E+02
9.9824E-01	9.9472E-01	9.9479E-01	3.0580E+00	2.6339E-12	2.00E+03	3.257E+05	1.758E+05	4.683E+11	1.809E+11	2.017E+02
9.9802E-01	9.9407E-01	9.9415E-01	3.0580E+00	2.6290E-12	2.25E+03	3.259E+05	1.758E+05	4.684E+11	1.809E+11	2.017E+02
9.9780E-01	9.9342E-01	9.9353E-01	3.0580E+00	2.6242E-12	2.50E+03	3.261E+05	1.758E+05	4.685E+11	1.809E+11	2.017E+02
9.9759E-01	9.9277E-01	9.9290E-01	3.0580E+00	2.6194E-12	2.75E+03	3.263E+05	1.758E+05	4.687E+11	1.809E+11	2.017E+02
9.9737E-01	9.9213E-01	9.9228E-01	3.0580E+00	2.6147E-12	3.00E+03	3.264E+05	1.758E+05	4.688E+11	1.809E+11	2.017E+02
9.9715E-01	9.9149E-01	9.9166E-01	3.0580E+00	2.6100E-12	3.25E+03	3.266E+05	1.758E+05	4.689E+11	1.809E+11	2.017E+02
9.9694E-01	9.9085E-01	9.9105E-01	3.0580E+00	2.6054E-12	3.50E+03	3.268E+05	1.758E+05	4.690E+11	1.809E+11	2.017E+02
9.9673E-01	9.9021E-01	9.9044E-01	3.0580E+00	2.6009E-12	3.75E+03	3.270E+05	1.758E+05	4.691E+11	1.809E+11	2.017E+02
9.9651E-01	9.8957E-01	9.8983E-01	3.0580E+00	2.5965E-12	4.00E+03	3.271E+05	1.758E+05	4.691E+11	1.809E+11	2.017E+02
9.9630E-01	9.8894E-01	9.8922E-01	3.0580E+00	2.5921E-12	4.25E+03	3.273E+05	1.758E+05	4.692E+11	1.808E+11	2.017E+02
9.9609E-01	9.8830E-01	9.8862E-01	3.0580E+00	2.5878E-12	4.50E+03	3.275E+05	1.758E+05	4.693E+11	1.808E+11	2.017E+02
9.9587E-01	9.8767E-01	9.8803E-01	3.0580E+00	2.5835E-12	4.75E+03	3.276E+05	1.758E+05	4.693E+11	1.808E+11	2.017E+02
9.9566E-01	9.8704E-01	9.8743E-01	3.0580E+00	2.5794E-12	5.00E+03	3.278E+05	1.758E+05	4.694E+11	1.808E+11	2.017E+02
9.9545E-01	9.8642E-01	9.8684E-01	3.0580E+00	2.5752E-12	5.25E+03	3.279E+05	1.757E+05	4.694E+11	1.808E+11	2.017E+02
9.9524E-01	9.8579E-01	9.8625E-01	3.0580E+00	2.5712E-12	5.50E+03	3.281E+05	1.757E+05	4.695E+11	1.807E+11	2.017E+02
9.9503E-01	9.8517E-01	9.8567E-01	3.0580E+00	2.5672E-12	5.75E+03	3.282E+05	1.757E+05	4.695E+11	1.807E+11	2.017E+02
9.9482E-01	9.8455E-01	9.8508E-01	3.0580E+00	2.5633E-12	6.00E+03	3.284E+05	1.757E+05	4.695E+11	1.807E+11	2.017E+02
9.9461E-01	9.8392E-01	9.8450E-01	3.0580E+00	2.5594E-12	6.25E+03	3.285E+05	1.757E+05	4.695E+11	1.806E+11	2.017E+02
9.9440E-01	9.8331E-01	9.8393E-01	3.0580E+00	2.5556E-12	6.50E+03	3.286E+05	1.757E+05	4.695E+11	1.806E+11	2.017E+02
9.9420E-01	9.8269E-01	9.8335E-01	3.0580E+00	2.5519E-12	6.75E+03	3.288E+05	1.756E+05	4.695E+11	1.805E+11	2.016E+02
9.9399E-01	9.8207E-01	9.8278E-01	3.0580E+00	2.5482E-12	7.00E+03	3.289E+05	1.756E+05	4.695E+11	1.805E+11	2.016E+02
9.9378E-01	9.8146E-01	9.8221E-01	3.0580E+00	2.5446E-12	7.25E+03	3.290E+05	1.756E+05	4.695E+11	1.804E+11	2.016E+02
9.9357E-01	9.8085E-01	9.8165E-01	3.0580E+00	2.5411E-12	7.50E+03	3.292E+05	1.756E+05	4.694E+11	1.804E+11	2.016E+02
9.9337E-01	9.8024E-01	9.8108E-01	3.0580E+00	2.5376E-12	7.75E+03	3.293E+05	1.755E+05	4.694E+11	1.803E+11	2.016E+02
9.9316E-01	9.7963E-01	9.8052E-01	3.0580E+00	2.5342E-12	8.00E+03	3.294E+05	1.755E+05	4.693E+11	1.803E+11	2.015E+02
9.9296E-01	9.7902E-01	9.7996E-01	3.0580E+00	2.5309E-12	8.25E+03	3.295E+05	1.755E+05	4.693E+11	1.802E+11	2.015E+02
9.9275E-01	9.7842E-01	9.7941E-01	3.0580E+00	2.5276E-12	8.50E+03	3.296E+05	1.755E+05	4.692E+11	1.801E+11	2.015E+02

Material: $Cd_6Ge_3As_{11}$ Temperature: 58°C

5-1 P

L/LO	V/VO	V/VOM	DADP	KAPPA	PRESSURE	VL	VS	Y-MOD	SHEAR-MOD	THETA
1.0000E+00	1.0000E+00	1.0000E+00	1.0000E+00	2.6696E-12	0.	3.235E+05	1.746E+05	4.618E+11	1.783E+11	2.003E+02
9.9991E-01	9.9973E-01	9.9973E-01	2.6847E+00	2.6677E-12	1.00E+02	3.236E+05	1.746E+05	4.618E+11	1.784E+11	2.003E+02
9.9982E-01	9.9947E-01	9.9947E-01	2.6847E+00	2.6658E-12	2.00E+02	3.236E+05	1.746E+05	4.619E+11	1.784E+11	2.003E+02
9.9973E-01	9.9920E-01	9.9920E-01	2.6847E+00	2.6639E-12	3.00E+02	3.237E+05	1.746E+05	4.620E+11	1.784E+11	2.003E+02
9.9964E-01	9.9893E-01	9.9894E-01	2.6847E+00	2.6620E-12	4.00E+02	3.238E+05	1.746E+05	4.621E+11	1.784E+11	2.003E+02
9.9956E-01	9.9867E-01	9.9867E-01	2.6847E+00	2.6601E-12	5.00E+02	3.239E+05	1.746E+05	4.622E+11	1.784E+11	2.003E+02
9.9934E-01	9.9801E-01	9.9802E-01	2.6847E+00	2.6554E-12	7.50E+02	3.241E+05	1.746E+05	4.624E+11	1.785E+11	2.004E+02
9.9911E-01	9.9735E-01	9.9736E-01	2.6847E+00	2.6507E-12	1.00E+03	3.242E+05	1.746E+05	4.625E+11	1.785E+11	2.004E+02
9.9890E-01	9.9669E-01	9.9671E-01	2.6847E+00	2.6460E-12	1.25E+03	3.244E+05	1.747E+05	4.627E+11	1.785E+11	2.004E+02
9.9868E-01	9.9603E-01	9.9607E-01	2.6847E+00	2.6413E-12	1.50E+03	3.246E+05	1.747E+05	4.629E+11	1.786E+11	2.004E+02
9.9846E-01	9.9538E-01	9.9542E-01	2.6847E+00	2.6367E-12	1.75E+03	3.248E+05	1.747E+05	4.631E+11	1.786E+11	2.004E+02
9.9824E-01	9.9473E-01	9.9479E-01	2.6847E+00	2.6321E-12	2.00E+03	3.250E+05	1.747E+05	4.632E+11	1.786E+11	2.005E+02
9.9802E-01	9.9408E-01	9.9415E-01	2.6847E+00	2.6276E-12	2.25E+03	3.252E+05	1.747E+05	4.634E+11	1.786E+11	2.005E+02
9.9780E-01	9.9343E-01	9.9352E-01	2.6847E+00	2.6230E-12	2.50E+03	3.253E+05	1.747E+05	4.635E+11	1.786E+11	2.005E+02
9.9759E-01	9.9278E-01	9.9289E-01	2.6847E+00	2.6185E-12	2.75E+03	3.255E+05	1.747E+05	4.636E+11	1.786E+11	2.005E+02
9.9737E-01	9.9214E-01	9.9227E-01	2.6847E+00	2.6140E-12	3.00E+03	3.257E+05	1.747E+05	4.638E+11	1.786E+11	2.005E+02
9.9716E-01	9.9150E-01	9.9165E-01	2.6847E+00	2.6096E-12	3.25E+03	3.259E+05	1.747E+05	4.639E+11	1.787E+11	2.005E+02
9.9694E-01	9.9086E-01	9.9103E-01	2.6847E+00	2.6051E-12	3.50E+03	3.260E+05	1.747E+05	4.640E+11	1.787E+11	2.005E+02
9.9673E-01	9.9022E-01	9.9042E-01	2.6847E+00	2.6007E-12	3.75E+03	3.262E+05	1.747E+05	4.641E+11	1.787E+11	2.006E+02
9.9651E-01	9.8958E-01	9.8981E-01	2.6847E+00	2.5963E-12	4.00E+03	3.264E+05	1.747E+05	4.642E+11	1.786E+11	2.006E+02
9.9630E-01	9.8895E-01	9.8920E-01	2.6847E+00	2.5920E-12	4.25E+03	3.265E+05	1.747E+05	4.643E+11	1.786E+11	2.006E+02
9.9609E-01	9.8831E-01	9.8860E-01	2.6847E+00	2.5877E-12	4.50E+03	3.267E+05	1.747E+05	4.643E+11	1.786E+11	2.006E+02
9.9588E-01	9.8768E-01	9.8800E-01	2.6847E+00	2.5834E-12	4.75E+03	3.269E+05	1.747E+05	4.644E+11	1.786E+11	2.006E+02
9.9567E-01	9.8705E-01	9.8740E-01	2.6847E+00	2.5791E-12	5.00E+03	3.270E+05	1.747E+05	4.645E+11	1.786E+11	2.006E+02
9.9545E-01	9.8643E-01	9.8681E-01	2.6847E+00	2.5748E-12	5.25E+03	3.272E+05	1.747E+05	4.645E+11	1.786E+11	2.006E+02
9.9524E-01	9.8580E-01	9.8622E-01	2.6847E+00	2.5706E-12	5.50E+03	3.273E+05	1.747E+05	4.646E+11	1.786E+11	2.005E+02
9.9503E-01	9.8518E-01	9.8563E-01	2.6847E+00	2.5664E-12	5.75E+03	3.275E+05	1.747E+05	4.646E+11	1.785E+11	2.005E+02
9.9482E-01	9.8455E-01	9.8505E-01	2.6847E+00	2.5622E-12	6.00E+03	3.277E+05	1.746E+05	4.646E+11	1.785E+11	2.005E+02
9.9462E-01	9.8393E-01	9.8447E-01	2.6847E+00	2.5581E-12	6.25E+03	3.278E+05	1.746E+05	4.647E+11	1.785E+11	2.005E+02
9.9441E-01	9.8332E-01	9.8389E-01	2.6847E+00	2.5540E-12	6.50E+03	3.280E+05	1.746E+05	4.647E+11	1.784E+11	2.005E+02
9.9420E-01	9.8270E-01	9.8331E-01	2.6847E+00	2.5499E-12	6.75E+03	3.281E+05	1.746E+05	4.647E+11	1.784E+11	2.005E+02
9.9399E-01	9.8208E-01	9.8274E-01	2.6847E+00	2.5458E-12	7.00E+03	3.283E+05	1.746E+05	4.647E+11	1.783E+11	2.005E+02
9.9379E-01	9.8147E-01	9.8217E-01	2.6847E+00	2.5418E-12	7.25E+03	3.284E+05	1.745E+05	4.647E+11	1.783E+11	2.005E+02
9.9358E-01	9.8086E-01	9.8161E-01	2.6847E+00	2.5378E-12	7.50E+03	3.286E+05	1.745E+05	4.647E+11	1.782E+11	2.004E+02
9.9337E-01	9.8025E-01	9.8104E-01	2.6847E+00	2.5338E-12	7.75E+03	3.287E+05	1.745E+05	4.646E+11	1.782E+11	2.004E+02
9.9317E-01	9.7964E-01	9.8048E-01	2.6847E+00	2.5299E-12	8.00E+03	3.288E+05	1.745E+05	4.646E+11	1.781E+11	2.004E+02
9.9296E-01	9.7904E-01	9.7993E-01	2.6847E+00	2.5259E-12	8.25E+03	3.290E+05	1.744E+05	4.646E+11	1.781E+11	2.004E+02
9.9276E-01	9.7843E-01	9.7937E-01	2.6847E+00	2.5220E-12	8.50E+03	3.291E+05	1.744E+05	4.645E+11	1.780E+11	2.003E+02

Material: $Cd_6Ge_3As_{11}$ Temperature: 73°C -1

L/LO	V/VO	V/VOM	DADP	KAPPA	PRESSURE	VL	VS	Y-MOD	SHEAR-MOD	THETA
1.0000E+00	1.0000E+00	1.0000E+00	1.0000E+00	2.[illegible]97E-12	0.	3.224E+05	1.746E+05	4.610E+11	1.783E+11	2.002E+02
9.9991E-01	9.9973E-01	9.9973E-01	3.3942E+00	[illegible]73E-12	1.00E+02	3.225E+05	1.746E+05	4.611E+11	1.784E+11	2.002E+02
9.9982E-01	9.9946E-01	9.9946E-01	3.3942E+00	[illegible]94BE-12	2.00E+02	3.226E+05	1.746E+05	4.612E+11	1.784E+11	2.002E+02
9.9973E-01	9.9919E-01	9.9919E-01	3.3942E+00	[illegible]924E-12	3.00E+02	3.227E+05	1.746E+05	4.613E+11	1.784E+11	2.003E+02
9.9964E-01	9.9892E-01	9.9893E-01	3.3942E+00	[illegible]900E-12	4.00E+02	3.228E+05	1.746E+05	4.614E+11	1.784E+11	2.003E+02
9.9955E-01	9.9866E-01	9.9866E-01	3.3942E+00	2.6876E-12	5.00E+02	3.229E+05	1.746E+05	4.615E+11	1.784E+11	2.003E+02
9.9933E-01	9.9799E-01	9.9800E-01	3.3942E+00	2.6816E-12	7.50E+02	3.231E+05	1.746E+05	4.617E+11	1.785E+11	2.003E+02
9.9911E-01	9.9732E-01	9.9734E-01	3.3942E+00	2.6758E-12	1.00E+03	3.233E+05	1.747E+05	4.620E+11	1.785E+11	2.003E+02
9.9888E-01	9.9666E-01	9.9669E-01	3.3942E+00	2.6701E-12	1.25E+03	3.235E+05	1.747E+05	4.622E+11	1.785E+11	2.004E+02
9.9866E-01	9.9599E-01	9.9604E-01	3.3942E+00	2.6645E-12	1.50E+03	3.238E+05	1.747E+05	4.624E+11	1.786E+11	2.004E+02
9.9844E-01	9.9533E-01	9.9539E-01	3.3942E+00	2.6590E-12	1.75E+03	3.240E+05	1.747E+05	4.626E+11	1.786E+11	2.004E+02
9.9822E-01	9.9468E-01	9.9475E-01	3.3942E+00	2.6536E-12	2.00E+03	3.242E+05	1.747E+05	4.628E+11	1.786E+11	2.004E+02
9.9800E-01	9.9402E-01	9.9412E-01	3.3942E+00	2.6483E-12	2.25E+03	3.244E+05	1.747E+05	4.629E+11	1.787E+11	2.005E+02
9.9778E-01	9.9337E-01	9.9349E-01	3.3942E+00	2.6431E-12	2.50E+03	3.246E+05	1.747E+05	4.631E+11	1.787E+11	2.005E+02
9.9757E-01	9.9272E-01	9.9286E-01	3.3942E+00	2.6380E-12	2.75E+03	3.248E+05	1.747E+05	4.633E+11	1.787E+11	2.005E+02
9.9735E-01	9.9207E-01	9.9224E-01	3.3942E+00	2.6330E-12	3.00E+03	3.250E+05	1.748E+05	4.634E+11	1.787E+11	2.005E+02
9.9713E-01	9.9142E-01	9.9162E-01	3.3942E+00	2.6282E-12	3.25E+03	3.252E+05	1.748E+05	4.636E+11	1.787E+11	2.005E+02
9.9692E-01	9.9078E-01	9.9100E-01	3.3942E+00	2.6234E-12	3.50E+03	3.254E+05	1.748E+05	4.638E+11	1.787E+11	2.006E+02
9.9670E-01	9.9013E-01	9.9039E-01	3.3942E+00	2.6187E-12	3.75E+03	3.255E+05	1.748E+05	4.639E+11	1.788E+11	2.006E+02
9.9649E-01	9.8949E-01	9.8978E-01	3.3942E+00	2.6142E-12	4.00E+03	3.257E+05	1.748E+05	4.640E+11	1.788E+11	2.006E+02
9.9627E-01	9.8885E-01	9.8917E-01	3.3942E+00	2.6097E-12	4.25E+03	3.259E+05	1.748E+05	4.641E+11	1.788E+11	2.006E+02
9.9606E-01	9.8822E-01	9.8857E-01	3.3942E+00	2.6053E-12	4.50E+03	3.261E+05	1.748E+05	4.643E+11	1.788E+11	2.006E+02
9.9584E-01	9.8758E-01	9.8797E-01	3.3942E+00	2.6011E-12	4.75E+03	3.262E+05	1.748E+05	4.644E+11	1.788E+11	2.006E+02
9.9563E-01	9.8695E-01	9.8737E-01	3.3942E+00	2.5969E-12	5.00E+03	3.264E+05	1.748E+05	4.645E+11	1.789E+11	2.006E+02
9.9542E-01	9.8632E-01	9.8678E-01	3.3942E+00	2.5929E-12	5.25E+03	3.266E+05	1.748E+05	4.646E+11	1.788E+11	2.006E+02
9.9521E-01	9.8569E-01	9.8619E-01	3.3942E+00	2.5889E-12	5.50E+03	3.267E+05	1.748E+05	4.647E+11	1.788E+11	2.006E+02
9.9499E-01	9.8506E-01	9.8560E-01	3.3942E+00	2.5850E-12	5.75E+03	3.269E+05	1.748E+05	4.647E+11	1.788E+11	2.006E+02
9.9478E-01	9.8443E-01	9.8502E-01	3.3942E+00	2.5813E-12	6.00E+03	3.270E+05	1.748E+05	4.648E+11	1.788E+11	2.006E+02
9.9457E-01	9.8381E-01	9.8444E-01	3.3942E+00	2.5776E-12	6.25E+03	3.271E+05	1.748E+05	4.649E+11	1.788E+11	2.006E+02
9.9436E-01	9.8319E-01	9.8386E-01	3.3942E+00	2.5741E-12	6.50E+03	3.273E+05	1.748E+05	4.649E+11	1.787E+11	2.006E+02
9.9415E-01	9.8256E-01	9.8328E-01	3.3942E+00	2.5706E-12	6.75E+03	3.274E+05	1.748E+05	4.650E+11	1.787E+11	2.006E+02
9.9394E-01	9.8194E-01	9.8271E-01	3.3942E+00	2.5673E-12	7.00E+03	3.275E+05	1.748E+05	4.650E+11	1.787E+11	2.006E+02
9.9374E-01	9.8133E-01	9.8214E-01	3.3942E+00	2.5640E-12	7.25E+03	3.277E+05	1.747E+05	4.651E+11	1.787E+11	2.006E+02
9.9353E-01	9.8071E-01	9.8157E-01	3.3942E+00	2.5609E-12	7.50E+03	3.278E+05	1.747E+05	4.651E+11	1.787E+11	2.006E+02
9.9332E-01	9.8010E-01	9.8100E-01	3.3942E+00	2.5578E-12	7.75E+03	3.279E+05	1.747E+05	4.651E+11	1.787E+11	2.006E+02
9.9311E-01	9.7948E-01	9.8043E-01	3.3942E+00	2.5548E-12	8.00E+03	3.280E+05	1.747E+05	4.651E+11	1.786E+11	2.006E+02
9.9291E-01	9.7887E-01	9.7987E-01	3.3942E+00	2.5520E-12	8.25E+03	3.281E+05	1.747E+05	4.651E+11	1.786E+11	2.006E+02
9.9270E-01	9.7826E-01	9.7931E-01	3.3942E+00	2.5492E-12	8.50E+03	3.282E+05	1.747E+05	4.651E+11	1.786E+11	2.006E+02

Material: $Cd_6Ge_3As_{11}$ Temperature: 100°C =1

wt., v_{ave} = average velocity

$$= \left[\frac{1}{3}\left(\frac{2}{v_s^3} + \frac{1}{v_e^3}\right)\right]^{-1/3} .$$

These data are presented, in part, on the following graphs. Though data were taken from 25 to 100°C, the present analysis only covers the room temperature results.

Fig. 12 shows the ratio V/V_o for 5 alloys calculated from Cooks analysis (solid line) and from the Murnaghan equation (dotted line) as a function of pressure from 0 - 8 kbar with temperature held constant at 25°. The heat capacity ratio γ is taken as unity.

Fig. 13 shows the values of the isothermal compressibility of five chalcogenide alloys, calculated using Cook's analysis, over the range of pressure from 0 - 8 kbar with the temperature held at 25°C.

The shear modulus is shown in Fig. 14 for 5 alloys. The curves shown are calculated using Cook's analysis over the pressure range 0 - 8 kbar with temperature held at 25°C.

Young's modulus is plotted in Fig. 15 from calculations based on Cook's analysis for 5 alloys over the pressure range 0 - 8 kbar with the temperature held at 25°C.

In each case one notes remarkably different behavior as the connectivity[5] is changed. Further remarks will be delayed until after the isothermal data is presented.

The apparatus described in Sec. 2.D for measurement of isothermal compressibility was calibrated by measuring the linear dilation of NaCl, KCl, KBr, and KI single crystals obtained from Harshaw Chemical Company. The change in length under pressure ($\Delta\ell$), as well as the

length at atmospheric pressure (ℓ_o), were measured for the alkali halide single crystals and for the glasses at room temperature of 23°C. Some of the measured quantities are shown in Fig. 16. The data shown terminates at 5 kbar though on some occasions data were taken to 10 kbar. Noting that the ratio of volume change under pressure (ΔV) to the atmospheric volume (V_o) can be approximated by $3\Delta\ell/\ell_o$, $\Delta V/V_o$ was calculated for the glasses by an interpolation process using the data of Vaidya and Kennedy[38], as shown in Table 4, for the alkali halides.

The compressibility of Vaidya and Kennedy was chosen because their measurement is the most recent direct measurement of the compressibilities of all four alkali halides chosen for calibration. Unfortunately their data was taken in a piston cylinder apparatus to 45 kbar so its accuracy is questionable in the pressure range considered in our experiments. Nevertheless it seems advantageous to use data taken by one set of investigators using a single technique. We have reproduced our measurements on KBr within 2% in two independent runs.

Values of the accumulated change in length for the calibrant were calculated from the data of Vaidya and Kennedy and compared with the measured accumulated change in length of the calibrant, as expressed in mV output from the LVDT, at every 0.25 kbar between 1 and 5 kbar. Fig. 17 shows a typical display of calibration cata showing the scatter in the alkali halide data points. A linear interpolation formula was fitted to the four points by a least squares technique[39]. The calibration was then used to convert measured instrument output to the

change in length of sample. The arrow shows the measured data point for $Te_{15}Ge_3As_2$, corresponding to a compressibility of 5.8×10^{-12} cm^2/dyne at 3 kbar.

The 2% reproducibility of the KBr data together with the internal consistency of a given run would indicate an accuracy of near 2% for the chalcogenide data. However, the inconsistencies within the alkali halides force the assignment of an overall accuracy of only 5%. The calculated values of $\Delta V/V_o$ for the amorphous chalcogenides were fitted to a quadratic equation by a least squares technique. The constant term of the quadratic fit is due to experimental error in determining the zero point in the measurement of the change of length. The accuracy of the data did not warrant fitting to a third order or higher equation. The data for the glasses is in Table 5.

The isothermal compressibilities were then calculated from the expression

$$\kappa_T = \frac{1}{V}\frac{\partial V}{\partial P}\Big]_T = -\frac{1}{(1 + \Delta V/V_o)}\ \frac{\partial}{\partial P}\left(\frac{\Delta V}{V_o}\right)\Big]_T$$

since $V = V_o + \Delta V$. The results are also shown in Table 2. The error in the compressibility is about 5%. The present data are some 5% lower than the adiabatic compressibility quoted by Chernov, Dembovskii and Chistov[40] and 14% lower than the adiabatic compressibility measured in this lab for As_2Se_3 at atmospheric pressure. The numbers which are calculated both for $\Delta V/V_o$ and for κ_T are very sensitive to the fitting equation chosen. A third order fit would change the extrapolated atmospheric pressure compressibility by about 2%. The compressibilities are shown as changing linearly with pressure because of the quadratic fit chosen for $\Delta V/V_o$. The coefficient of

P in the compressibility indicates that the compressibility decreases with pressure for $Te_{15}Ge_3As_2$ and As_2Se_3 and is essentially flat for $Te_{15}Ge_2As_3$. In glasses, both increasing and decreasing compressibilities have been observed in this pressure range. SiO_2, for example, shows an increasing compressibility below 31 kbar[16,41]. The work of Weir and Shartis [42] on the compressibilities of alkali borate and silicate glasses demonstrates the more common decrease of compressibility with increasing pressure. For the chalcogenide glasses considered here, the compressibilities are 2-3 times greater than those of the silicate glasses and about the same as those of the borate glasses[42].

There was no permanent densification observed at room temperature within 0.04% in the chalcogenide glasses to 8 kbar when the samples were returned to atmospheric pressure. The atmospheric-pressure adiabatic compressibility[35] of $Te_{15}Ge_3As_2$ leads to a value of the ratio of κ_T/κ_S of 1.04 which is also the heat capacity ratio C_P/C_V. Table 6 gives some values for a variety of other substances for comparison purposes[43]. Though the 5% error in κ_T causes the last digit shown for the semiconducting glass to be suspect, there is no apparent trend which sets this material apart from the others insofar as the compressibility is concerned. The fact that the measured κ_T is 5% less than the quoted κ_S for As_2Se_3 is indicative of the lack of accuracy in the measurement.

TABLE 4

$\Delta V/V_o$ for alkali halides due to Vaidya and Kennedy. Pressure (P) in kbar.

	$\Delta V/V_o \times 10^3$
NaCl	$-4.273\ P + .0466\ P^2$
KCl	$-5.4906\ P + .0580\ P^2$
KBr	$-6.0351\ P + .0536\ P^2$
KI	$-7.886\ P + .1129\ P^2$

Table 5

Measured values of $\Delta V/V_o$ and κ_T for amorphous glasses at 23° C

	$\Delta V/V_o \times 10^3$ P in kbar	κ_T P in dynes/cm^2
$Te_{15}Ge_3As_2$	$-0.271 - (6.00 \pm 0.3)P + (0.05 \pm 0.05)P^2$	$(6.00 \pm 0.3) \times 10^{-12} - (0.7 \pm 1.0) \times 10^{-22}P$
$Te_{15}Ge_2As_3$	$-.377 - (5.58 \pm 0.3)P + (0.0 \pm 0.05)P^2$	$(5.58 \pm 0.3) \times 10^{-12} + (0.3 \pm 1.0) \times 10^{-22}P$
As_2Se_3	$-.196 - (6.30 \pm 0.3)P + (0.06 \pm 0.05)P^2$	$(6.30 \pm 0.3) \times 10^{-12} - (0.8 \pm 1.0) \times 10^{-22}P$

The constant term in $\Delta V/V_o$ is due to experimental error in determining the zero in the measurement.

TABLE 6

κ_T/κ_S for a variety of materials

$Te_{15}Ge_3As_2$	1.04	Semiconducting glass
Ge	1.04	Semiconducting crystal
Si	1.01	Semiconducting crystal
SiO_2	1.001	Insulating glass
KCl	1.05	Ionic crystal
K	1.08	Metallic crystal

The differences between acoustic determinations of κ_T and those based on direct measurement of volume changes under pressure are displayed most clearly in Fig. 18. One sees there distinct differences in magnitude and slope which cannot be resolved by altering the value of γ used in Cook's analysis. Such differences also occur in data reported for the better known alkali halide crystals[38,44], (including those we have used) as may be seen in Fig. 19. It is not clear which experiment is in error. The only systematic observation is that agreement is better when compressibilities are lower. As our acoustic experiments are far more extensive than the other, the acoustic data will form the basis of all further analysis. One must be aware, nevertheless, of the problems susggested by this comparison.

We now turn to an attempt to understand the trends of, say, compressibility as revealed by Fig. 13. This requires a brief aside on the bonding of the alloys we have been considering, and on the relationship of bonding to structure and other properties.

The recent restatement by J. C. Phillips[45] of the chemical bond approach to solids has led to new and significant insight into the relationship between structure and a variety of properties in alloys of the type $A^N B^{8-N}$. Using Phillip's spectroscopic definition of ionicity one is able to understand the variation of, say, compressibility, in certain alloy series as arising from the variation of ionicity, i.e. from the replacement of covalent bonds with (less directional) ionic bonding. Harrison[46] has made the same sort of correlation using a bond-orbital model.

The value of schemes such as this lies in the predictive value they have insofar as alloying trends are concerned. Even when the ionicity scale lacks the precision it has in the $A^N B^{8-N}$ series, one is still able to organize and understand variations in alloy behavior.

Emphasis on chemical bonds is also valuable in disordered systems such as amorphous semiconductors[47]. One of the fundamental cornerstones[48] of current amorphous semiconductor theory is (Mott's rule) that: the material arranges itself such that valence bond requirements are satisfied locally. Impurity effects are therefore much weaker (with a few exceptions) than in crystalline semiconductors.

Kastner[49] has introduced the term "lone pair" semiconductor and used the concept to correlate the properties of alloys such as $GeTe_2$ and As_2Se_3. He observes that in Se the uppermost filled band is not a valence band composed of bonding wavefunctions rather a band formed from lone-pair electrons in non-bonding states. Carriers excited into the conduction band do not vacate bonding states as they do in conventional semiconductors such as Ge. Structural consequences of this difference will be discussed below. At the same time there are important alloying effects. Kastner therefore introduces the concept of Bond Free Solid Angle (BFSA) to account for the variations along an alloy sequence. In materials with lone pairs, such as Se, the bonding is two-fold with a bond angle near 100°. There is thus a substantial solid angle in which no bonding charge is to be found. This is the bond free solid angle (BFSA), and it is large in Se. In contrast, the tetrahedral bonding of Ge leaves little BFSA. As Kastner points out, the application of stress requires atoms to move together compressing

bonds in the case of Ge but merely moving into the BFSA in the case of Se. Only when the compression is sufficient to cause overlap of the core electrons does strong repulsion occur.

Clearly there will be significant differences in mechanical properties and atomic mobilities in the two situations.

Kastner considers a series of amorphous and crystalline compounds and elements varying from diamond to Se and shows the varying effect of pressure on the optical absorption edge may be interpreted in terms of varying bond free solid angle. He also considers the correlation of band gap Eg and melting point T_M. Whenever the melting process involves the breaking of covalent bonds, Eg and T_M increase together so long as the BFSA is constant but as the BFSA increases T_M decreases.

The present author[50] and de Neufville and Rockstad[51] (see also Munoshita and Arai[15]) have used somewhat similar arguments to develop relations between Eg and Tg in various glasses. Considering the number of near neighbors ("Connectedness" C) or the average number of valence electrons $\bar{N}$ instead of the similar quantity BFSA, relations were demonstrated between Tg and Eg for a wide variety of glasses. Fig. 19 shows some data from Krebs and Fischer[52] in the Ge-Te-As ternary. When one considers the uncertainties in Eg (computed from $d\sigma/dT$) arising from temperature dependence of the gap as well as even greater uncertainties intrinsic to Tg the clustering of the data is striking indeed, but interpretation is difficult. Fig. 20

shows a less confusing plot[53] of T_g vs. Eg for the pseudobinary $As_2 Se_3$ - $As_2 Te_3$.

de Neufville and Rockstad[51] have covered a smaller number of materials but have done so systematically. They also determined E_g from optical absorption and thereby somewhat reduced the ambiguities. Their results are shown in Fig. 21. There the role of connectedness is clearly displayed.

When C = 2, as in Se or Te, the glass transition is independent of E_g, the decrease of viscosity does not involve the breakup of the molecular units (chains or rings) rather the disruption of van der Waals forces holding one chain to another. When C = 2.4, as in $As_2 Se_3$, one has puckered layers of the $As_2 Se_3$ molecules with primarily van der Waals bands between layers. The effect of band gap on Tg is weak, but certainly present. One might guess that geometrical constraints preclude effective motion of the layers as units and some covalent bonds must be broken before sufficient mobility for the glass transition is attained. But there are other data which reveal that the situation is much more complex. NMR data from the Naval Research Lab[54] fail to observe the motional narrowing of the NMR line of Se in molten $As_2 Se_3$ which would be expected if correlation times of 10^{-4} sec occurred for that nucleus. The viscosity does, contrastingly, suggest such jump frequencies[55] just above T_g In pure Se the material narrowing is observed. The layer structure must therefore have much slower motion within the layer, for a given viscosity, than in ring or chain materials such as Se. T_g in layered materials must be related more to van der Waals forces between layers and it is the polarization of lone pair states which are altered by the thermal excitation of carriers from

covalent bands within the layers. In glasses such $As_2 Se_3$ the layered structure persists in the melt perhaps as high as 725K. IR data show the peak attributed to in-plane vibration well above T_g ~ 450K. Even at 725K (300K above T_g and 100K above T_M the viscosity is only 4 Stokes--compared to 10^{-2} Stokes for H_2O and 8 Stokes for glycerol, both at room temperature only 100K above tg for the latter. $As_2 Se_3$ is a remarkable fluid indeed.

The bond breaking process is simply thermal excitation of electrons from bonding to antibonding states. At any given temperature a certain fraction of the bonding states will be so emptied. When sufficient bonds are broken (emptied) for the atoms of the glass to move with a jump frequency of 10^{-5} sec^{-1} the glass transition, as it is conventionally defined, occurs. The temperature at which the "sufficient" number of broken bonds occurs is T_g. Interpretation is simplest when a single bond, e.g. Ge-Te, dominates. When lone pair electrons exist the process is somewhat different. Electronic excitation does not break bonds but it does lead to change in antibonding states and therefore still weakens the glass. When C = 3.0 this difference is clearly displayed as in Fig. 21 curves d and e. The alloys Ge Se and Ge_2 Se Te are more like alloys with C =2.66 than the other materials with C = 3, wuch as Ge Te As. The latter materials are apparently characterized by 3-fold coordination as in pure amorphous As or graphite with itinerant π-bands and no lone pairs while the former (C = 2.66: Ge Se ; Ge_2 Se Te) contain primarily bonds such as Ge:Se, there is complete cross linking and the influence of lone-pairs can still be felt. One thus has two separate branches of the

$T_g = f(P)$ relation when C = 3. This interpretation is somewhat controversial as yet and further study is required.

The roles of ionicity and of d-bands have not been elucidated.

de Neufville and Rockstad further observe that for zero gap the glass transition in all cases occur near 325K. They associate this temperature with the T_o appearing in the Fulcher viscosity[55] or fluidity ϕ equation:

$$\phi = \phi_o \exp [-A/(T-T_o)] \tag{1}$$

while A is related to E_g by $A = \alpha E_g/k$ and assemble all of their results into a viscosity equation

$$\phi = \phi_o \exp [-\delta (C-2) E_g/k (T-T_o)] \tag{2}$$

where $\phi_o = 10^2$ poise $^{-1}$, $\delta = 0.55$ and $T_o \sim 325$K. This relation needs extensive verification. In the case of $As_2 Se_3$, where extensive data is available, there is order-of-magnitude agreement over 15 decades of fluidity. They assume the two-fold coordination dominates in these materials because the fumdamental diffusing element is chain-like. The jumprate of this unit then increases with temperature.

It thus appears that a beginning for understanding atomic motion in these semiconducting glasses exists. The glasses studied or yet to be studied are shown in Fig. 22, where T_g is plotted against the energy gap as in Fig. 21. The connectedness is also shown. Consistent with the arguments above, we expect 1) if C is low, the compressibility is high and 2) since T_g varies with ΔE, and ΔE decreases with applied pressure, T_g should decrease with applied pressure (most strongly for C = 4).

The results of Fig. 12 - 15 confirm the first of these expectations. Se is soft indeed and $Cd_6 Ge_3 As_{11}$ is not only relatively incompressible but is less influenced by pressure. While no quantitative prediction is yet possible, the trends are clear. It is only recently that shear moduli have been computed from Harrison's bond-orbital model[56] for tetrahedral crystals, the glasses require more time.

4. The Glass Transition

Turning now to Tg determinations, we face the problem of separating artifacts of the experimental procedure from the atomic relaxation processes which are responsible for the glass transition.

In using the reflection technique described in Section 2.E, initial tests have been directed to those glasses for which previous acoustic data have been published:[29] pentachlorinated-biphenyl (PCB) and glycerol. Fig. 23 shows data at 10 MHz for PCB. The upper dashed curve is the expected reflectance computed from Ref. 28; though the units of the ordinate are indicated to be arbitrary the deviation from per cent reflectance is small. The solid curve is our data as traced from a chart; the arrow near -40C marks the conventional, dc glass transition. We believe the agreement is quite satisfactory. Even the small break in slope near -40C is reproduced. The dot-dash curve is the derivative of the data, taken graphically. There is a shift in slope at the dc T_g, a shoulder near -10C and a peak near +20C. The peak is to be associated with the glass transition characteristic of the 10 MHz frequency.

Fig. 24 shows similar data for glycerol taken at 10 and 30 MHz. As expected[29] T_g (ac) shifts to higher temperatures as the frequency increases; the shoulder does not and we do not know its origin at present. The fact that the high frequency glass transition correlates with the relaxation times of experiment is indicated in Fig. 25.

The two circles represent the peaks in the derivative curve of our measurement plotted as the appropriate relaxation times such that $\omega\tau = 1$. The two curves are the average relaxation times for shear and compressional processes obtained by Piccirelli and Litovitz[45a]. Piccirelli and Litovitz calculated the distribution of relaxation times necessary to fit their data on the viscosity and the complex moduli of glycerol measured for both shear and longitudinal waves at frequencies from 15 to 85 MHz. As can be seen, quite good agreement is observed between our experiment and the data of Piccirelli and Litovitz.

We wished to apply this technique to determine glass transition points in amorphous semiconductors. We were unsuccessful in polishing the surfaces of the delay line and the sample sufficiently flat and smooth that the two materials could be wrung together. It was necessary to use a viscous material between the delay line and the sample that can transmit the ultrasonic waves between the two solids. Such a viscous material can be Dow Corning 200 fluid, a diffusion pump oil Santovac 5, or something similar.

The reflection coefficient at the interface between the delay line and the sample depends on the impedances of the two materials and also on the characteristics of the bond between the materials. For instance, if the experiment is run inside the high pressure vessel, the hydrostatic pressure will increase the viscosity of the bonding fluid, resulting in a considerable change in the efficiency with which

the bonding agent acts as an acoustic coupling agent. The changes in the quality of the coupling invalidates the simple theory relating the reflection coefficient to the acoustical impedances of the two solids. As an example of other complications, in the data taken on $Te_{15}Ge_2As_3$, surface crystallization occured above 200°C. The surface crystallization disrupted the surface sufficiently to destroy the acoustical bond, resulting in a sharp increase in the reflected signal.

The reflected acoustical signal was used to determine glass transition temperature of $Te_{15}Ge_2As_3$ under pressure. An example of the data is shown in Fig. 26. The arrow points to the rapid drop in the amplitude of the reflected wave. We attribute this to the glass transition. The sample has softened and flowed into better contact with the delay line. More of the acoustical energy is transmitted through the better bond into the sample and scattered; less is reflected.

Fig. 27 shows the glass transition temperature for $Te_{15}Ge_2As_3$ determined by this technique as a function of pressure at heating rates of approximately 15°/min. There is an initial increase in the glass transition and then an apparent drop off. We have less confidence in the higher pressure data because the pressure effects on the bonding agent become more important and renders interpretation of the data more questionable. When the pressure was increased, the viscosity of the bonding agent increased tremendously. The thermal expansion coefficient of the chalcogenide is in the neighborhood of 1-2 x 10^{-5} $^{o}C^{-1}$ as compared to 0.6 x 10^{-6} $^{o}C^{-1}$ for quartz. As the temperature is

increased at the higher pressures, the bonding agent is too stiff to relieve the stress caused by relative thermal expansion. Thus the stress is built up and relieved in a non-uniform manner with respect to temperature. This process leads to sudden decreases in the reflected signal which tend to obscure the glass transition.

Further measurements were therefore taken simply by measuring transit time as in Section 2.C. and looking for a change in slope. As expected from the Litovitz work[29], there is a clear change at the dc glass transition temperature. An example of the data is shown in Fig. 28. The transit time is plotted as a function of temperature for the glass $Te_{15}Ge_2As_3$ at atmospheric pressure. The sample was heated at about $1^{o}C$/min. The dip slightly above $100^{o}C$ occurs because the sample has not been annealed since quenching. The fact that the cooling rate during preparation is much faster than the present heat rate will cause this type of deviation from straight line behavior[27]. At the glass transition, the transit time breaks upward. The transit time breaks upward at the glass transition for the following reason. In the neighborhood at the glass transition, the viscosity of the material is reduced until atomic rearrangements are possible within the time scale of the experiment: a few minutes or a few seconds. Above the glass transiton, the compressibility of the substance increases and the sound speed decreases.

The glass transition temperature is obtained by straight line approximation to the regions above and below the glass transition.

The glass transition temperature so obtained (113 ^{o}C) is less than that obtained by the reflection method discussed above, in part because of the slower heating rate.

Slightly above 130 ^{o}C, the sagging of the sample becomes observable in the shorting of the transit time as at point S. The sample is then cooled at about 2^{o}C/min. While the break at the glass transition is not as evident upon cooling, the glass transition can be determined by examining the derivative curve (Fig. 29). There is a fairly obvious break in the derivative curve at about 103^{o}C. Although this determination of the glass transition temperature is lower than that based on the heating curve, this difference is not indicative of a measurement error. Rather, the difference arises from the difference in the thermal and pressure history and the rates of change of temperature. Furthermore, on the heating curve the transition temperature is defined in the middle of the transition; on the cooling curve the transition is defined at the low temperature end of the transition. The procedure of defining the glass transition through the use of the derivative curve was chosen to make the change in slope of the transit time at the glass transition more evident. Whether the transition in a series of measurements is defined at the initiation of the transition or at the middle is of little importance. Obviously when comparing data, the definition of the transition temperature must be consistent.

As an example of the effect of pressure, Fig. 30 shows the transit time plotted as a function of temperature at 3.4 kbar for another

sample of the same chalcogenide. The change in slope at 75° indicates that the sample is being densified by the high pressure. As the sample is densified, the sound velocity changes due to the resultant change in compressibility and density. The transit time breaks upward at the glass transition at 124°C. The sample is then cooled at pressure. If the sample is then reheated at atmospheric pressure, the sample will return to its original density. The behavior of the transit time vs.temperatureis shown in Fig. 31. Above 75°C, the sample expands on heating rather than contracts since the density exceeds the equilibrium valve of the density at atmospheric pressure. The sample was earlier quenched at high pressure yielding a glass with a density greater than the same material quenched at atmospheric pressure. This greater density is stable at atmospheric pressure because of rigidity of the material but near the glass transition, the material softens and relaxes toward the normal volume of the glass. Of course, the transit time would have shown sample sag if the heating had been continued to higher temperatures. On cooling, the sample exhibited similar behavior to other cooling curves.

As a more complete example of the thermal and pressure cycling effects when one of the glasses passes through the glass transition, consider Fig. 32. That figure shows As_2S_3 taken through the glass transition first at atmospheric pressure, then at 2 kbar, next at 4 kbar, and finally at atmospheric pressure again. The path labeled (1) shows the acoustic transit time in the sample increasing as the

temperature is raised; the break upward is at the glass transition (point x) and the return to room temperature is at point y. Path (2) starts at a shorter transit time due to the application of 2 kbar pressure. At about 150°C, the sample begins to densify as evidenced by the shortening of the transit time. Again the sample is carried through the glass transition (point z) and cooled. Path (3) is the same procedure carried out at 4 kbar with Tg at point W. Next the sample is returned to atmospheric pressure and the heating cycle started again (path (4)). At about 150°C (point u) the sample has become soft enough to start relaxing rapidly back to an equilibrium volume, thereby removing the effects of the densification which occured near the glass transition at high pressures. When the sample is cooled, the transit time returns close to the original transit time of the sample. If the sample had been retained near the glass transition at atmospheric pressure longer, the transit time would have returned to its initial value.

The glass transition of the chalcogenides $Te_{15}Ge_2As_3$, $Cd_6Ge_3As_{11}$ and As_2S_3 have been found as described above. The glass transition temperature as a function of pressure for $Te_{15}Ge_2As_3$ is shown in Fig. 33. Fig. 34 and Fig. 35 give the same information for $Cd_6Ge_3As_{11}$ and As_2Se_3.

To allow easier comparison of the effect of pressure on the glass transition, the data of Figs. 33, 34, and 35 are shown in Fig. 36 as Tg(P)/tg(0). $Te_{15}G_2As_3$ shows an asymptotic approach to a constant value as pressure increases. The slope of dTg/dP is much

lower than the other materials. As_2Se_3 shows a near straight line behavior. Its glass transition has not been measured above 4kbar. $Cd_6Ge_3As_{11}$ shows the most remarkable behavior. The glass transition initially increases with pressure; but above 2 kbar, the glass transition decreases with pressure. The initial increase of Tg with pressure is very similar to a variety of different glasses[46a] as shown in Fig. 37. The derivatives of $Tg(P)/Tg(0)$ near atmospheric pressure are nearly identical for these glasses with the exception of the network glass $Te_{15}Ge_2As_3$. Similarity between dTg/dP for such a wide variety of glasses is remarkable. There has been a lot of interest in the investigation of dTg/dP because it is looked upon as a means of deciding between two competing theories of the glass transition: free volume theory (WLF) or configurational entropy (Gibbs) theory[47a].

There have been a very great number of publications on the development of these two theories of the glass transition and the behavior of the material in the region of the glass transition. There is considerable controversy over which treatment of the problem is correct. The calculations give rise to the following equations[47a]:

$$\frac{dTg}{dP} = \frac{\Delta\beta}{\Delta\alpha} \qquad (1)$$

$$\frac{\Delta\beta}{\Delta\alpha} \geq TV \frac{\Delta\alpha}{\Delta C_P} \qquad (2)$$

where $\Delta\beta$ is the difference between the compressibility in the liquid and glassy states $\Delta\beta = \beta_\ell - \beta_g$; $\Delta\alpha$ is the difference in

thermal expansion $\Delta\alpha = \alpha_\ell - \alpha_g$; V is the volume; ΔC_p is the change in heat capacity at constant pressure in going through the glass transition. The free volume theory requires that $\frac{dTy}{dP} = \frac{\Delta\beta}{\Delta\alpha} = TV \frac{\Delta\alpha}{\Delta C_p}$. Most of the experimental data on polymers has satisfied the relation $\frac{dt_g}{dP} \sim \frac{TV\Delta\alpha}{\Delta C_p} < \frac{\Delta\beta}{\Delta\alpha}$. We do not have $\Delta\alpha$, $\Delta\beta$, ΔC_p data to allow comparison of the theory with the chalcogenide glasses we have studied. The controversy has pointed out the need for precise definitions of the experimental parameters and the need to define the preparation procedures of the glass. Bianchi[48a] has studied polyvinyl acetate over three different temperature-pressure cycles with radically different dTg/dP. Assume that it is possible to introduce a parameter z which will define the configurational state of the glass as determined for instance by the rate of quench of the glass at the pressure under which the glass was formed. Then it can be noted that

$$dTg/dP = \left(\frac{\partial Tg}{\partial P}\right)_z + \left(\frac{\partial Tg}{\partial z}\right)_p \left(\frac{dz}{dP}\right) .$$

It is crucially important that the experiment to measure dTg/dP attempt to do so with glasses of the same configurational state z. Bianchi proposes the cycle illustrated in Fig. 38. Line ABC is an isobar at one atmosphere. GFD or HED are isobars at some higher pressure P. All data is taken at the same cooling rate. On Polyvinyl acetate, the pressure used was 300 atmospheres. For a cycle CDEH where the pressure is applied to the liquid, dTg/dP = 0.015°C/atm. For the cycle AGFD where the pressure is applied to the glass, dTg/dP = 0.037°C/atm. This difference between the

two experimental results demonstrates difference between the glass prepared from the melt and then compressed with a glass quenched under pressure for this material. The volumes of the two glasses are different as are the internal configurations of the atoms or molecules.

All the theories concerned with the comparison of dTg/dP with $\Delta\theta/\Delta\alpha$ are for vanishing small changes in pressure. Our experiments with the chalcogenide glasses were pointed at much higher pressures. As explained earlier, our data was taken with a cycle AGFD then DEH yielding two glass transitions. The two glass transition temperatures found had the same behavior under pressure within the experimental error. The glass transitions determined upon heating are presented in Figs. 33, 34, and 35 noted earlier.

The low pressure $\frac{1}{Tg(0)} \frac{dTg}{dP}$ of As_2S_3 and $Cd_6Ge_3As_{11}$ are very similar to various polymers also shown in Fig. 37. $Te_{15}Ge_2As_3$ has considerably different behavior. The initial rise in Tg is at a much smaller $\frac{1}{Tg(0)} \frac{dTg}{dP}$; Tg then increases to what appears to be an asymptotic value. The pressure range is not sufficient to determine its further behavior. As_2S_3 appears roughly linear; higher pressure data has not been taken as yet. The behavior of $Cd_6Ge_3As_{11}$ is most interesting. After the initial increase in the glass transition, the glass transition starts to decrease. This behavior may be explained in terms of the concepts of bond free solid angle (BFSA) or in terms of correctness as presented in section 3 of this report.

The organic polymers listed above are large molecules with primarily van der Waals forces between the molecules. The major

restraint to structural relaxation of the molecules is the large size and the complexity of the molecule. Se with a connectedness C = 2 is very similar. Se consists of chains and rings with van der Waals forces between the chain segments. In such materials, the application of pressure greatly reduces the "free volume" hindering structural relaxation. It thus takes a higher temperature to activate molecular motion.

The situation is more complicated in glasses with increasing amounts of cross linking. B_2O_3 (C = 4.0) consists of planar BO_3 units which are randomly arranged in a three dimensional network[49a] with all three oxygen atoms shared with adjacent BO_3 units. Although B_2O_3 is a network glass with a great deal of cross linking, it is dangerous to compare it with other glasses of the same structure. For instance, B_2O_3 can be compacted at pressures of a few kbar at room temperature (some 200°C below its glass transition). This compaction occurs for the chalcogenide glasses only near their glass transition. Any densification at room temperature points toward the existence of structural relaxation processes which do not exist for the chalcogenide glasses far from the glass transition.

As_2S_3 (C = 2.4) is composed of puckered layers of As_2S_3 molecules with van der Waals bonds between layers. One might guess that some of the covalent bonds holding the layers together must be broken to permit the glass transition to take place. Yet much of the structural relaxation only involves van der Waals bonds.

Probably the necessary structural changes are produced primarily by rearrangement of sections of layers so that the low pressure behavior is like that of the other glasses discussed above. The data on dTg/dP has not yet been taken to higher pressures. Thermal excitation of electrons from lone pair states weakens the polarizabilities responsible for the van der Waals bonding between layers. The behavior of $Te_{15}Ge_2As_3$ and $Cd_6Ge_3As_{11}$ are the most interesting. There are probably several competing processes. For instance a free volume argument given by Sanchez[50a] predicts that the glass transition temperature should rise with pressure to an asymptotic value.

The material above the glass transition consists of occupied volume (the atoms) and holes (free volume). For the purposes of this argument, consider the viscosity to be infinite or at least very large below the glass transition and that there are no holes present below the glass transition. As the temperature of the material increases above the glass transition, the number and size of the holes increase. The thermal expansion can be broken into two components: a thermal expansion due to the occupied volume and a thermal expansion associated with the liquid due to the holes. Similarily the compressibility can be divided into the compressibilities of the holes.

As the pressure is increased, the number and/or size of the holes decrease. Hence the glass transition temperature is increased since more thermal energy is required to produce sufficient free volume to enable structural rearrangements to take place. The glass transition temperature will increase to a limiting value as the pressure is increased. The volume of the holes will vanish as the

pressure is increased, but the material will still have a finite glass transition temperature even with a minimal number of holes.

Since the chalcogenide glasses are semiconductors with primarily covalent bonding, there is a direct relationship between the electrons which provide the electronic behavior and the atomic bonding. This relationship is clearer for $Cd_6Ge_3As_{11}$. The average coordination is 4.0 (C = 4.0) so each atom has its valence requirements satisfied with a full complement of valence electrons. Of course, the bonds are hydridized to the appropriate geometrical distributions. A direct relationship between the electronic properties and the atomic bonding is thus expected.

The case for $Te_{15}Ge_2As_3$ (C = 2.4) is more complicated. $Te_{15}Ge_2As_3$ is a network glass, but the valence band is probably formed by lone pair electrons from the Te atoms. The excitation of electrons from the valence into the conduction band will effect the antibonding states and thus weaken the bonding. While the excitation of the lone pair electrons will weaken the bonding of the glass, there is no direct relationship between the electronic properties and the physical characteristics of the glass.

Since the conductivity of the semiconducting glasses are related to its mechanical characteristics and hence the glass transition, the band gap of the glass becomes important. For $Te_{15}Ge_2A_3$ the band gap closes slightly with pressure[1]. At a given temperature, the number of electrons excited to antibonding states band increases as the band gap decreases. The material should weaken rapidly if

the electrons which are excited participate in the covalent bonding and hence the glass transition should decrease. This effect is probably not observed for $Te_{15}Ge_2As_3$ because the valence electrons are the lone pair electrons, and only interlayer forces are weakened.

Unfortunately the effect of pressure on the band gap of $Cd_6Ge_3As_{11}$ has not been determined. We hope to do so in the near future.

There are therefore two competing processes influencing the effect of pressure on the glass transition. The free volume arguments would suggest that the glass transition should increase asymptotically under pressure. The fact that these glasses are semiconducting should provide a relationship between the electronic excitation of the valence electrons and the atomic bonding. The effect of pressure on the band gap of the material would then be important. It is not possible <u>a priori</u> to separate the influence of these two processes in deciding what the glass transition would do under pressure.

5. Electrical Measurements

Measurements of the electrical conductivity have been made as a function of pressure, temperature, and frequency for a number of samples. In order to test a cryostat system, the d.c. conductivity as a function of temperature was measured on a sample of $Ge_{16}As_{35}Te_{28}S_{21}$. These results merely verified results previously reported by Fagen et al[1]. Measurements of the effect of pressure on the d.c. conductivity of $Ge_{16}As_{35}Te_{28}S_{21}$ extended the pressure range of Fagen et al. to 10 kbar. The results did not show any change in the pressure coefficient of the d.c. conductivity at the higher pressures.

After these preliminary measurements, work was initiated on samples from the tellurium rich glass forming region of the Te-As-Ge system. The first a.c. measurements indicated that any frequency dependent component of the conductivity was much smaller than the frequency independent component since the conductivities at even the highest frequencies of the Wayne-Kerr bridge were always the same as the d.c. conductivities within experimental error although several different samples were measured.

Since the change in the frequency dependent conductivity with pressure was, at that time, believed to be much larger than the change in the frequency independent conductivity, measurements of the a.c. conductivity were made on two samples up to approximately

6 kbar. Even at this pressure, no frequency dependence was observed.

As the frequency dependent conductivity is much less temperature dependent than the frequency independent component, measurements were made of the a.c. conductivity as a function of temperature below room temperature. Although the temperature was taken as low as 140 K for one sample, no frequency dependence was observed for any of the samples measured in the Te-As-Ge system within the accuracy of the measurements made at that time.

Some of these a.c. conductivity measurements at low temperatures were made while the data was being corrected by computer calculated corrections. The cooling of the samples inadvertently took them into the range of conductance and capacitance values where the correction program was no longer valid. The improperly corrected data appeared to show a frequency dependence which has since been found to be spurious. These data were, however, unfortunately published[57] before this error was discovered.

Although the measurements of a.c. conductivity as a function of pressure and temperature failed to yield any results, the associated d.c. measurements which were made at the same time are of some interest. The pressure dependence of the d.c. conductivity for two amorphous semiconducting compounds, $Te_{72}As_{19}Ge_9$ and $Te_{72}As_{17}Ge_{11}$ are plotted in Fig. 39. The data points falling below the lines are points taken for increasing pressure where insufficient time has been allowed for a return to thermal equilibrium after the temperature rise due to compressive heating. A striking ovservation is that if the slopes of these lines are compared to that for the

room temperature data of $Ge_{16}As_{35}Te_{28}S_{21}$ as reported by Fagen, et al[1], the effect of pressure on the conductivity is found to be, within experimental error, exactly the same. As data have only been taken at one temperature, the pressure dependence of the activation energy cannot be calculated.

The temperature dependence of the d.c. conductivity has been obtained for four amorphous semiconducting compounds. This data is plotted as log resistivity vs. reciprocal temperature in Figs. 40 and 41. The resistivity is expressed by the equation:

$$\rho = \rho_o \exp.^{-(\Delta E_o/2kT)} ,$$

and ρ_o and ΔE_o for each sample as determined from the lines approximating the data are given in the table

Sample	ρ_o	ΔE_o	
$Te_{72}Sd_{19}Ge_9$	$9.2 \cdot 10^{-4}$ Ωcm	.86 eV	1.01
$Te_{72}As_{15}Ge_{13}$	$9.7 \cdot 10^{-4}$ Ωcm	.88 eV	1.06
$Te_{75}As_{10}Ge_{15}$	$1.07 \cdot 10^{-3}$ Ωcm	.89 eV	1.08
$Te_{78}As_{13}Ge_9$	$3.3 \cdot 10^{-3}$ Ωcm	.79 eV	1.01

It should be noted in looking at Fig. 40 that the curvature indicated at the highest temperatures is believed to be due to surface crystallization and sample deformation. Further measurements were made at low temperatures on the samples of $Te_{72}As_{19}Ge_9$ and $Te_{75}As_{10}Ge_{15}$. In these measurements it was found that the conductivity had increased a great deal and showed only a slightly

activated behavior as if the sample resistances were being shorted by a parallel resistance with a metallic behavior. The resistances are nevertheless quite high for a very good metallic path. It is believed that the samples started to crystallize from the surface and that the bulk conduction of the interior is being shunted by a higher (at low temperatures) metallic type conductivity of a surface layer.

As one may see from the table both ρ_o and ΔE_o have similar values for all of the samples except for $Te_{78}As_{13}Ge_9$. As data for $Te_{78}As_{13}Ge_9$ has been taken only below 200K whereas data for the other samples have been taken only at higher temperatures, the two cannot be directly compared. It is believed, however, that the anomalous σ_o and ΔE_o values for $Te_{78}As_{13}Ge_9$ are due to the increase in relative importance of surface conductivity at the low temperatures.

Measurements of d.c. conductivity in the Te-As-Ge ternary system have also been made by Krebs anf Fischer[52] and by Panus and Borisova[58]. The values for σ_o presented here agree fairly well with the results of Krebs and Fischer; however, the activation energies reported here are about 20% lower than Krebs and Fischer. The samples studied by Panus and Borisova all contain much more arsenic than any reported here; however, their reported activation energies also lie approximately 20% below the results of Krebs and Fischer. It should be noted that the data taken in the present investigations spanned a much wider temperature range for conductivity

measurements than in either of the earlier investigations.

With the failure to find any frequency dependent conductivity in any of the samples in the tellurium rich region of the Te-As-Ge system, we decided to make measurements of the a.c. conductivity of some other materials which have previously been reported to display a frequency dependent conductivity. To this end, measurements were made on a sample of Te_2AsSi to try to duplicate the observations of Rockstad[59]. This sample was chosen because the absolute conductivity values were among the highest reported and the compound displayed a large frequency dependence from 10^6 to 10^7 Hz. Our measurements showed a frequency independent conductivity at all frequencies up to 10^7 Hz with a value approximately three orders of magnitude below the frequency independent component observed by Rockstad for this compound. It is believed that this discrepancy is due to basic differences in the bulk samples measured in this lab and the thin film flash evaporated samples measured by Rockstad.

Attempts have also been made to produce a bulk glass sample of As_2Te_3 glass since Rockstad reported extremely high levels of frequency dependent conductivity at room temperature in this sample which should also be well within the measurement capabilities of the Wayne-Kerr bridge. In a private communication Rod Quinn of Sandia has reported the production of this compound as a bulk glass in very small samples using quartz compounds with very thin walls. Attempts to produce a glassy sample of As_2Te_3 included

the use of 3 mm I.D. quartz tubing with 0.4 mm wall thickness for making the ampoules. As_2Te_3 melts in these ampoules were quenched in both cold iced brine (~ $-7^{o}C$) and in liquid nitrogen; however, neither attempt produced a non-crystalline sample.

It was then decided to look at materials which had been easily made in bulk glass and also reported to have shown frequency dependent conductivity. The most readily available of these are As_2S_3 and As_2Se_3. Ivkin and Kolomiets[60] reported a frequency dependent conductivity for As_2Se_3 which should be measurable at frequencies above 10^6 Hz with the Wayne-Kerr bridge. Crevecoeur and de Wit[61] however report loss tangents at or below 10^{-4} which would be measurable only at 10^7 Hz with the Wayne-Kerr bridge. Crevecoeur and de Wit ascribe the larger losses observed by Ivkin and Kolomiets and also Kitao, Araki, and Yamada [62] to poor contacts or sample quality. Measurements at this lab have shown no measurable conductivity even at 10^7 Hz. We verify the results of Crevecoeur and de Wit.

Measurements of As_2S_3 show a very small conductance only at the highest frequency measured (10^7 Hz) and therefore the exact frequency dependence of conductivity cannot be determined for this sample. It appears that the absolute value of conductivity is about $2 \times 10^{-8} (\Omega\ cm)^{-1}$, somewhat below the value reported by Owen and Robertson[63] at 10^7 Hz for this compound. This value would fall close to an extension of the lower frequency linear portion

of the curve reported by Owen and Robertson.

Owen and Robertson[63] also reported measurements of the a.c. conductivity of silver doped As_2Se_3. With a doping level of 0.2 atomic per cent silver, they obtained a frequency dependent conductivity approximately two orders of magnitude higher than the results obtained by Crevecoeur and de Wit[61]. A number of samples have been made here with high doping levels of metallic elements. Samples of As_2S_3 have been made with silver doping levels ranging from 0.1 to 4 at. per cent, and with copper doping levels ranging from 0.5 to 2 at. per cent; As_2Se_3 has been made with silver doping levels from 0.1 to 2 at. per cent. Several attempts were made to dope As_2S_3 samples with comparable levels of gold; however, it was found that gold tends to separate and condense separately from the As_2S_3.

Measurements are presently under way on these samples and have been completed for $As_{40}S_{60}Ag$, $As_{40}S_{60}Ag_2$, and $As_{40}S_{60}Ag_4$ at pressures from atmospheric pressure to 7 kbar at room temperature and recently for $As_{40}S_{60}Ag_4$ at 80°C and over the same pressure range. This last data have not been completely corrected because measurements have not been completed yet to determine the exact bridge corrections necessary for these experimental conditions. The most recent measurements have been made at atmospheric pressure and room temperature with very short leads. These measurements have been made on $As_{40}S_{60}Ag_{0.5}$ in addition to the other three compounds previously measured in the pressure vessel and with

somewhat longer leads. The accuracy of these measurements is better than for those taken in the pressure vessel, especially for $As_{40}S_{60}Ag$.

Owen and Robertson observed that the a.c. conductivity of As_2Se_3 (+ 0.2 at.% Ag) was monotonically increasing with frequency and if the conductivity is expressed as:

$$\sigma(w) = \sigma_0 w^S ,$$

S varied between 1 and 2 for frequencies between 10^5 and 10^7 Hz, falling off to values of about 0.5 at lower frequencies. We observe that within the accuracy of the data S is frequency independent in the range 10^5 to 10^7 Hz, although S is a function of sample composition and probably pressure and temperature. The results for the three samples on which data have been taken are shown for several different pressures in Fig. 42-45. Fig. 46 also shows preliminary atmospheric pressure data for $As_{40}S_{60}Ag_4$ at 80°C. The table contains a tabulation of the values of S for the different and samples and experimental conditions. The room temperature atmospheric pressure data taken with the pressure vessel and longer leads is given for comparison with the higher pressure data, although the short lead data are much more accurate. The divergence between these two sets of data for room temperature and atmospheric pressure data are not as great as the values for S given in the table indicate. A comparison of the results in Figs. 42 and 43 shows that the agreement for the two methods is

indeed very good except for the lowest frequencies for $As_{40}S_{60}Ag$.

Temperature	Pressure	$As_{40}S_{60}Ag_{0.5}$	$As_{40}S_{60}Ag_{1}$	$As_{40}S_{60}Ag_{2}$	$As_{40}S_{60}Ag_{4}$
~22°C	Atmospheric		0.74	0.60	0.60
~22°C	4 Kbar		0.73	0.62	0.61
~22°C	7 Kbar		0.80	0.66	0.62
~80°C	Atmospheric				0.49
*~22°C	Atmospheric	0.91	0.86	0.64	0.58

It should be noted that the high temperature results are highly tentative and the data above 10^6 Hz is somewhat questionable.

No d.c. conductivity measurements have yet been made on these materials.

The d.c. conductivities for the samples on which measurements have been made behave in the same manner as most other amorphous semiconductor compounds do. All show an activated behavior with all but one having a pre-exponential factor, ρ_o, in or very near the 10^{-3} - 10^{-4} (Ωcm) range which Stuke[64] noted appeared to be universal for amorphous semiconductors. As noted earlier, the anomalous behavior of the one exception is quite possibly due to an artifact of the experimental technique.

*Short leads.

The extremely low values of d.c. conductivity which both doped and undoped samples of As_2S_3 and As_2Se_3 display at room temperature creates extreme difficulties in making accurate measurements for bulk glass samples of these compounds. No d.c. conductivity measurements have therefore been attempted yet. A number of conductivity measurements on silver and copper doped As_2S_3 and As_2Se_3 samples have been reported by several other investigators[63-69]. There is, however, a great deal of variance in the results reported in these papers. This variance is possibly due to contact problems. Kolomiets et al[2] used colloidal graphite electrodes with which we have experienced difficulties. Arai et al[68,69] and Edmund[67] used gold electrodes although Edmund noted the possibility of gold diffusion into the sample.

The conductivity observed in the a.c. conductivity measurements indicates that a hopping process is occuring in the samples. The variation of the frequency dependence with silver concentration suggests the possibility of multiple hopping. The theory for multiple hopping has been developed by Pollak for crystalline semiconductors[70,71]. Although this treatment needs at least some modification to be applicable to amorphous semiconductors, the basic predictions seem to have a strong correlation with the experimental results presented earlier in this report. There should be a decreased frequency dependence with increased concentration of impurity states and at the same time the temperature dependence should increase. The frequency dependence does, on

the average, indeed decrease with increasing silver concentration. The increase in the a.c. conductivity of $As_{40}S_{60}Ag_4$ at 10^5Hz between 295K and 353K was by a factor of 6. The increase for As_2S_3 at 10^5Hz between 360K and 420K as reported by Owen[66] was only by a factor of 1.5. At lower temperatures, the temperature dependence of the a.c. conductivity usually tends to be smaller rather than larger. Thus, the temperature dependence of the a.c. conductivity increases with concentration as predicted by Pollak[71].

The absence of frequency dependent conductivity in bulk glass samples where it is present in this film samples of nominally the same compounds is an important observation. It indicates that the thin films have a high concentration of energy states which are not characteristic of the solid compound, but are quite probably associated with microscopic voids or impurities in the films.

A continuation of measurements of the electrical properties of the heavily doped As_2S_3 and As_2Se_3 should lead to information concerning the effect of impurities on the distribution of energy states in amorphous semiconductors. It may also help to clarify the effect of preparation methods on the properties of amorphous semiconductors.

References

1. E. A. Fagen, S. H. Hohenberg, R. W. Seguin, J. C. Thompson, and H. Fritzsche, Proc. 10th Int'l, Conf. Semicond. (US AEC, Oak Ridge, 1970), p. 672.
2. M. Kastner, Phys. Rev. Lett. 28, 355 (1972).
   M. Kastner, Phys. Rev. B 6, 2273 (1972).
3. J. C. Thompson, ARO Technical Report, Grant DA-ARO-D-31-124-71-G102, 31 March 1972.
4. J. P. de Neufville, ARO Technical Report, Contract DAHC 15-70-C-0187, 18 May 1973.
5. J. P. de Neufville and H. Rockstad, in Amorphous and Liquid Semiconductors edited by H. Stuke and W. Brenig (Taylor and Francis, London, 1973), p. 419.
6. D. S. Hughes and F.C. Sawin, Phys. Rev. 161, 861 (1967).
7. E. C. Robertson, F. Birch, and G. J. F. MacDonald, Am. J. Sci. 255, 115 (1957).
   F. P. Bundy, J. App. Phys. 32, 483, (1961).
8. R. H. Cornish and A. L. Ruoff, Rev. Sci. Instru. 32, 483 (1961).
9. M. Whitfield, Rev. Sci. Instru. 39, 1053 (1968).
10. P. L. M. Heydemann, Rev. Sci. Instru. 41, 1896 (1970).
11. J. F. Schirber and P. W. Shanfellt, Rev. Sci. Instru. 39, 270 (1968).
12. D. Yoon, Rev. Sci. Instru. 37, 1611 (1966).
13. R. Cook, J. Acoust. Soc. Am. 29, 445 (1957).
14. P. W. Bridgman, Physics of High Pressure (G. Bell and Sons, London (1952).

15. E. Tatsumoto, T. Okamoto, and H. Fujii, Jap. J. Appl. Phys. 7, 939 (1968).

16. J. Reitzel, I. Simon, and J. A. Walker, Rev. Sci. Instru. 28, 828 (1957).

17. D. Carpentier and M. Contre, Rev. Sci. Instru. 41, 189 (1970).

18. P. Heydemann and H. D. Gulcking, Kolloid-Zeitschrift und Zeitschrift fur Polymere 193, 16 (1963).

19. S. H. Gelles, Rev. Sci. Instr. 39, 1814 (1968).

20. R. J. Charles, J. Am. Ceram. Soc. 45, 105 (1962).

21. N. Mizouchi, Rev. Sci. Instru. 44, 28 (1973).

22. Model 100 ML LVDT manufactured with minimum potting. Schaevitz Engineering, Pennsauken, New Jersey.

23. S. F. Chistov, A. P. Chernov, and S. A. Dembouskil, Inorganic Materials, 4, 1814 (1968).

24. V. D. Frechette (ed.), Non-Crystalline Solids (John Wiley & Sons, Inc., New York, 1960).

25. J. A. Prins (ed.) Physics of Non Crystalline Solids (North-Holland Publishing Company, Amsterdam, 1965).

26. R. W. Douglas and B. Ellis (eds.), Amorphous Materials (Wiley--Interscience, London, 1972).

27. G. O. Jones, Glass (Chapman and Hall Ltd., London, 1971).

28. M. R. Carpenter, D. B. Davies, and A. J. Matheson, J. Chem. Phys. 46, 2451 (1967).

29. T. A. Litovitz, T. Lyon, and L. Peselnick, J. Acoust. Soc. Am. 26, 566 (1954).

T. A. Litovitz and T. Lyon, J. Acoust. Soc. Am. 30, 856 (1958); T. A. Litovitz, in Non-Crystalline Solids, ed. by V. D. Frechette (John Wiley & Sons, Inc., New York, 1960), p. 252.

30. J. M. O'Reilly, J. Polym. Sci. 57, 429 (1962).

31. K. P. Singh and J. G. Mullen, Phys. Rev. A 6, 2354 (1972).

32. G. Allen, In Amorphous Materials, ed. by R. W. Douglas and B. Ellis (Wiley--Interscience, London, 1972), p. 361.

33. P.L.M. Heydemann and J. C. Houck, in Accurate Characterization of the High-Pressure Environment, ed. by E. C. Lloyd (U. S. Government Printing Office, Washington, 1971), p. 11.

34. M. Goldstein, Mod. Asp. Vit. St. 3, 90 (1964).

35. K. E. Bailey and J. C. Thompson, Mat. Res. Bull. 7, 363 (1972).

36. O. L. Anderson, J. Phys. Chem. Solids 27, 547 (1966).

37. C. Kittel, Intro. Sol. St. Phys. (Wiley, New York, 1971).

38. S. N. Vaidya and G. C. Kennedy, J. Phys. Chem. Solids 31, 2329, (1970).

39. The output of the LVDT was determined to be 35 mV/10^{-3} inch in the press at 3 kbar, for instance, as compared to 32 mV/10^{-3} inch at atmospheric pressure. The pressure dependence is to be expected because of compression of the LVDT secondary coils.

40. A.P. Chernov, S. A. Dembovskii, and S. F. Chistov, Inorganic Mat. (USSR) 4, 1449 (1969).

41. P. W. Bridgman, Proc. Am Acad. Arts Sci. 76, 71 (1948).

42. C. E. Weir and L. Shartis, J. Am Ceram. Soc. 38, 299 (1955).

43. O. L. Anderson, J. Phys. Chem. Solids 27, 547 (1966).

44. G. R. Barsch and H. Shull, Phys. Stat. Sol. B43, 637 (1971).

45. J. C. Phillips, Rev. Mod. Phys. 49, 317 (1970).

J. A. Van Vechten, Phys. Rev. 182, 891 (1969).

J. C. Phillips, in "Proc. R. A. Welch Found. Conf. on Chem. Res. XIV Solid State Chem," edited by W. O. Milligan (Welch, Houston, 1971), P. 17; "Bands and Bonds in Semiconductors" (Academic Press, New York, 1973).

45a. R. Piccirelli and T. A. Litovitz, J. Acoust. Soc. An. 29, 1009 (1957).

46. W. A. Harrison, Phys. Rev. B 8, 4487 (1973).

46a. A. Eisenberg, J. Phys. Chem. 67, 1333 (1963).

47. D. Adler, Amorphous Semiconductors, (CRC Press, Cleveland, 1971).

47a. M. Goldstein, J. Phy. Chem. 77, 667 (1973).

48. N. F. Mott and E. A. Davis, Electronic Processes in Non-Crystalline Materials,(Clarendon Press, Oxford, 1971).

48a. U. Bianchi, A. Turturro, and G. Basile, J. Phys. Chem. 71, 3555 (1967).

49. M. Kastner, Phys. Rev. B 7, 5237 (1973).

50. J. C. Thompson, ARO Technical Report, Grant DA-ARO-D-31-124-71-G102, 31 March 1972.

50a. I. C. Sanchez, J. Appl. Phys. 45, 4204 (1974).

51. J. P. de Neufville and H. Rockstad, in Amorphous and Liquid Semiconductors edited by H. Stuke and W. Brenig (Taylor and Francis, London, 1973), p. 419.

52. H. Krebs and P. Fischer, Faraday Soc. Disc., 50, 35 (1970).

53. As_2Se-Te data: T. N. Vergel and B. T. Kolomiets, Soviet Phys.-Tech. Phys. 2, 2318 (1957); H. L. Uphoff and J. H. Healy, J. Appl. Phys. 32, 950 (1961); J. T. Edmond, Brit. J. Appl. Phys. 17, 979 (1966).

54. S. G. Bishop andP. C. Taylor, Phys. Rev. B 7, 5177 (1973).

55. D. Turnbull, Contemp. Phys. 10,473 (1969).

56. W. A. Harrison, Phys. Rev. Lett. 33, 410 (1974).

57. K. E. Bailey, B. A. Joiner, P. L. Sherrell and J. C. Thompson, "Effects of Pressure on Amorphous Semiconductors," in Amorphous and Liquid Semiconductors edited by J. Stuke and W. Brenig (Taylor and Francis, Ltd. London, 1974), pp. 767-770.

58. V. R. Panus and Z. U. Borisova, J. Appl. Chem., USSR 40, 964 (1970).

59. H. K. Rockstad, J. Non-Cryst. Sol. 2, 192 (1970).

60. E. B. Irvkin and B. T. Kolomiets, J. Non-Cryst. Sol. 3, 41 (1970).

61. C. Crevecoeur and J. H. de Wit, Solid State Comm. 9, 445 (1971).

62. M. Kitao, F. Araki, and S. Yamada, Phys. Stat. Solidi 37, K119 (1970).

63. A. E. Owen and J. M. Robertson, J. Non-Cryst. Sol. 2, 40 (1970).

64. J. Stuke, J. Non-Cryst. Sol. 4, 1 (1970).

65. B. T. Kolomiets, Yu V. Rukhlyadev, and V. P. Shilo, J. Non-Cryst. Sol. 5, 389 (1971).

66. A. E. Owen, Glass Industry 48, 637, 695 (1967).

67. J. T. Edmund, J. Non-Cryst. Sol. 1, 39 (1968).

68. K. Arai, T. Kuwahata, H. Namiskawa, and S. Saito, Japanese J. App. Phys. 11, 1080 (1972).

69. K. Arai, K. Kumata, K. Kadota, K. Yamamoto, H. Namikawa, and S. Saito, J. Non-Cryst. Sol. 13, 131 (1973).

70. M. Pollak, Phys. Rev. 133, A 564, (1964).

71. M. Pollak, Phys. Rev., 138, A 1822 (1965).

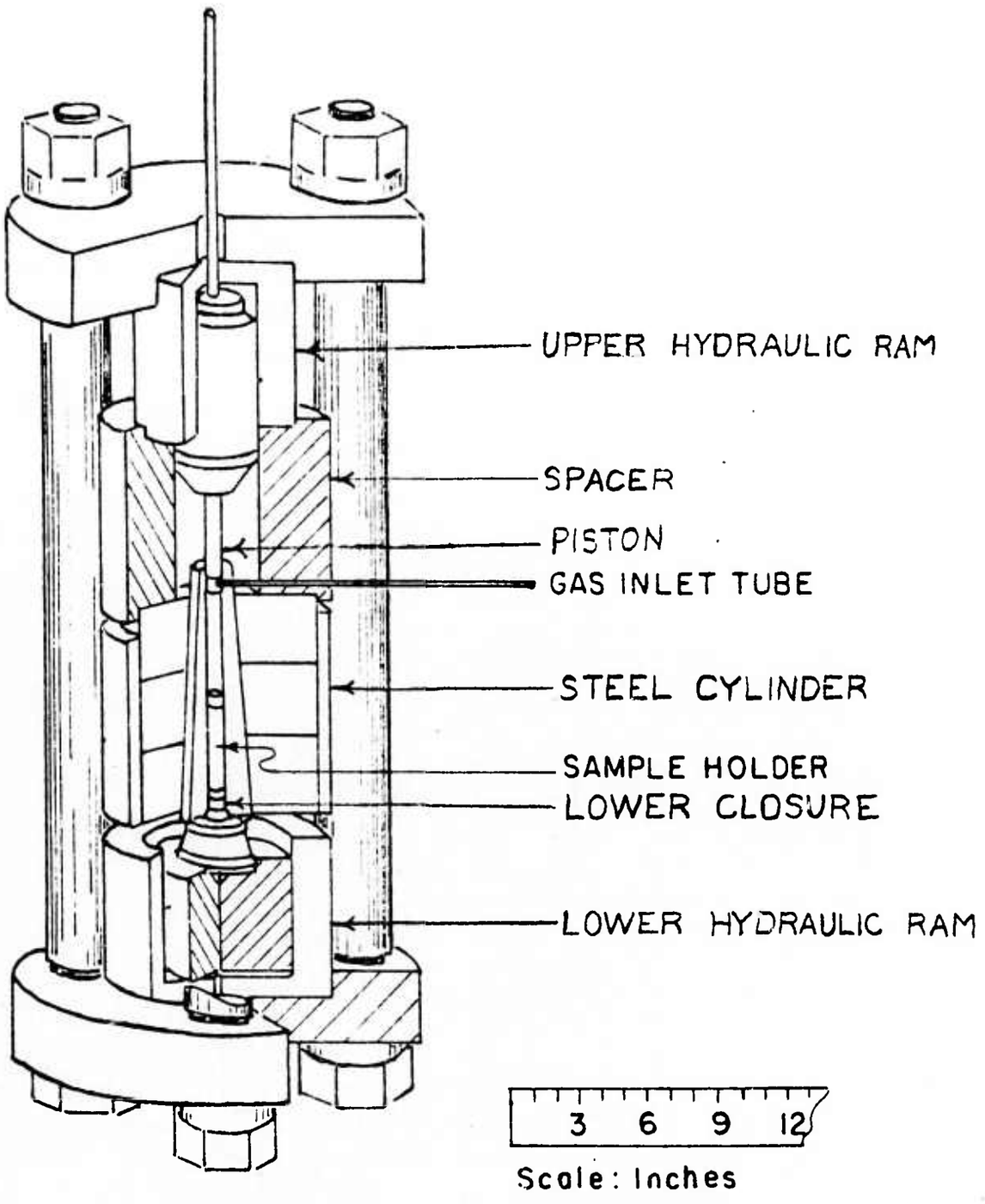
UPPER HYDRAULIC RAM
SPACER
PISTON
GAS INLET TUBE
STEEL CYLINDER
SAMPLE HOLDER
LOWER CLOSURE
LOWER HYDRAULIC RAM
3 6 9 12
Scale: Inches

Figure 1

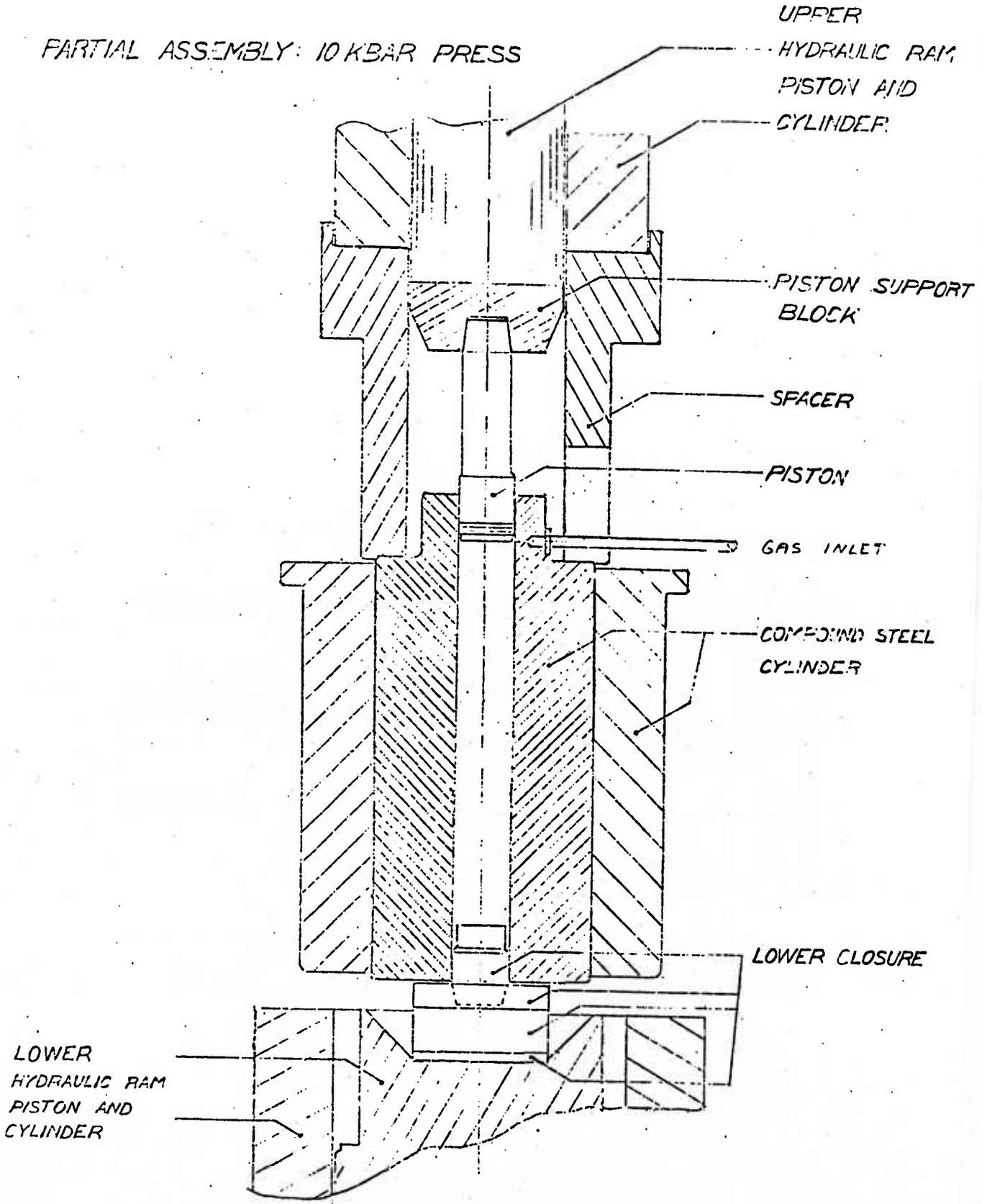
PARTIAL ASSEMBLY: 10 KBAR PRESS
UPPER HYDRAULIC RAM PISTON AND CYLINDER
PISTON SUPPORT BLOCK
SPACER
PISTON
GAS INLET
COMPOUND STEEL CYLINDER
LOWER CLOSURE
LOWER HYDRAULIC RAM PISTON AND CYLINDER

Figure 2

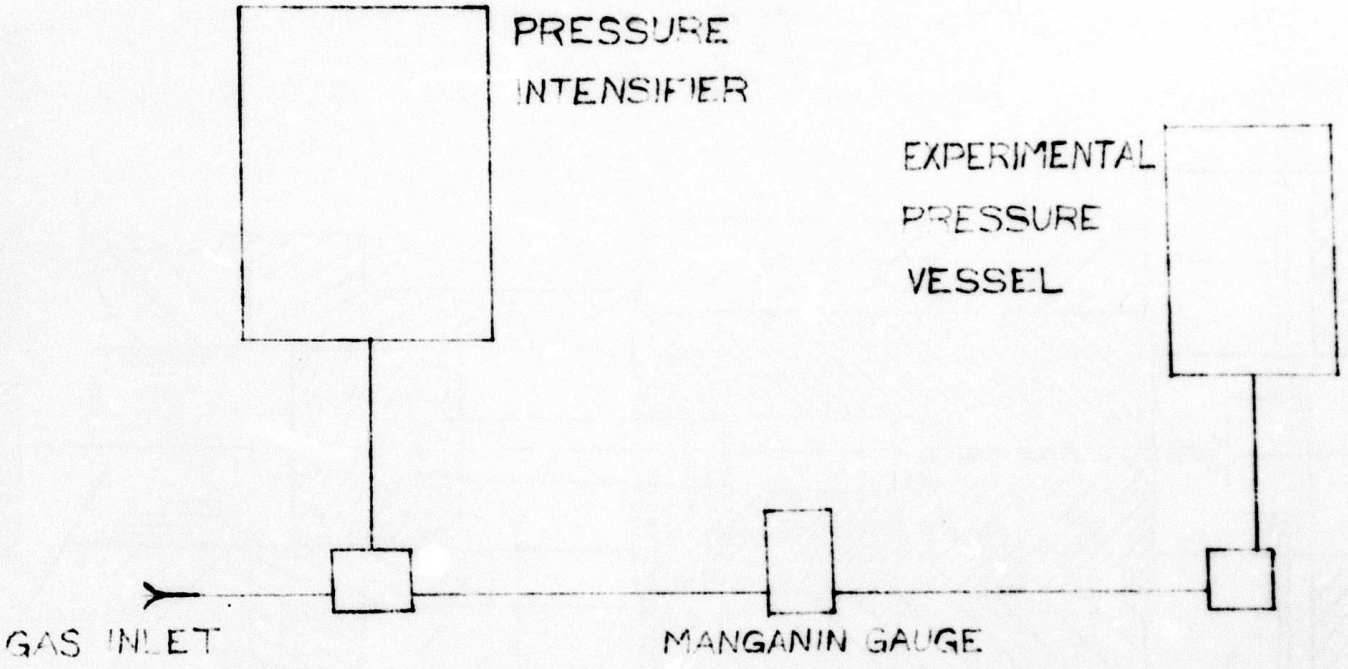
PRESSURE
INTENSIFIER
EXPERIMENTAL
PRESSURE
VESSEL
GAS INLET
MANGANIN GAUGE

Figure 3

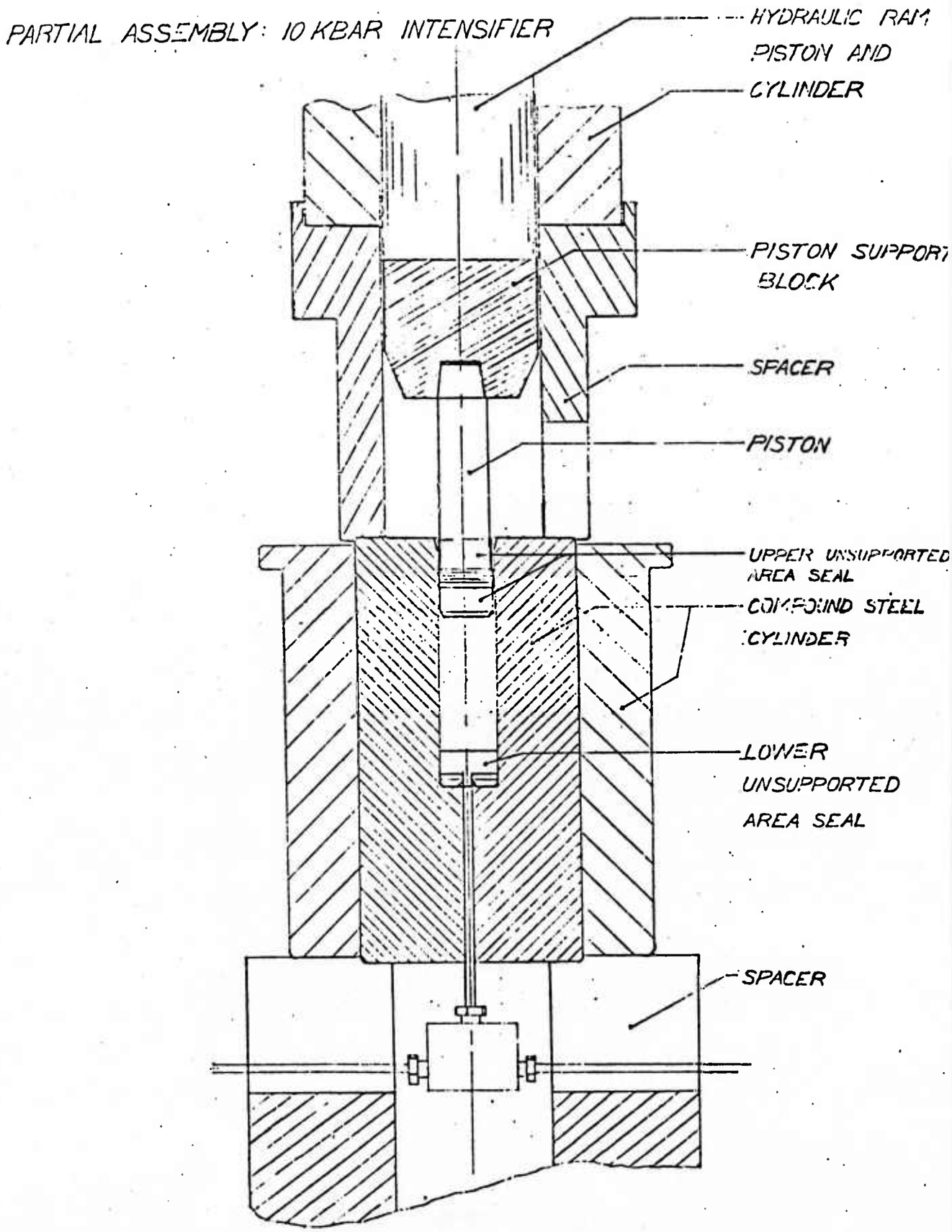
PARTIAL ASSEMBLY: 10 KBAR INTENSIFIER
HYDRAULIC RAM
PISTON AND
CYLINDER
PISTON SUPPORT
BLOCK
SPACER
PISTON
UPPER UNSUPPORTED
AREA SEAL
COMPOUND STEEL
CYLINDER
LOWER
UNSUPPORTED
AREA SEAL
SPACER

Figure 4

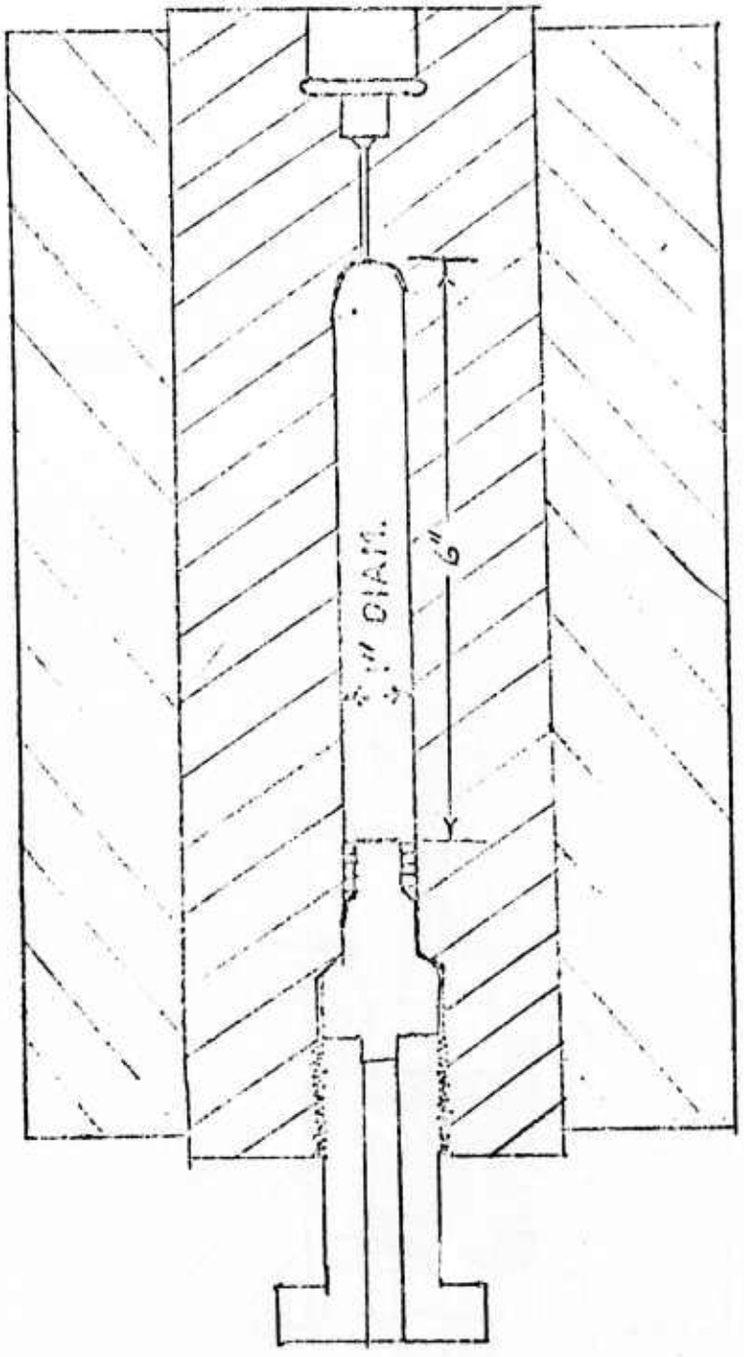

Figure 5

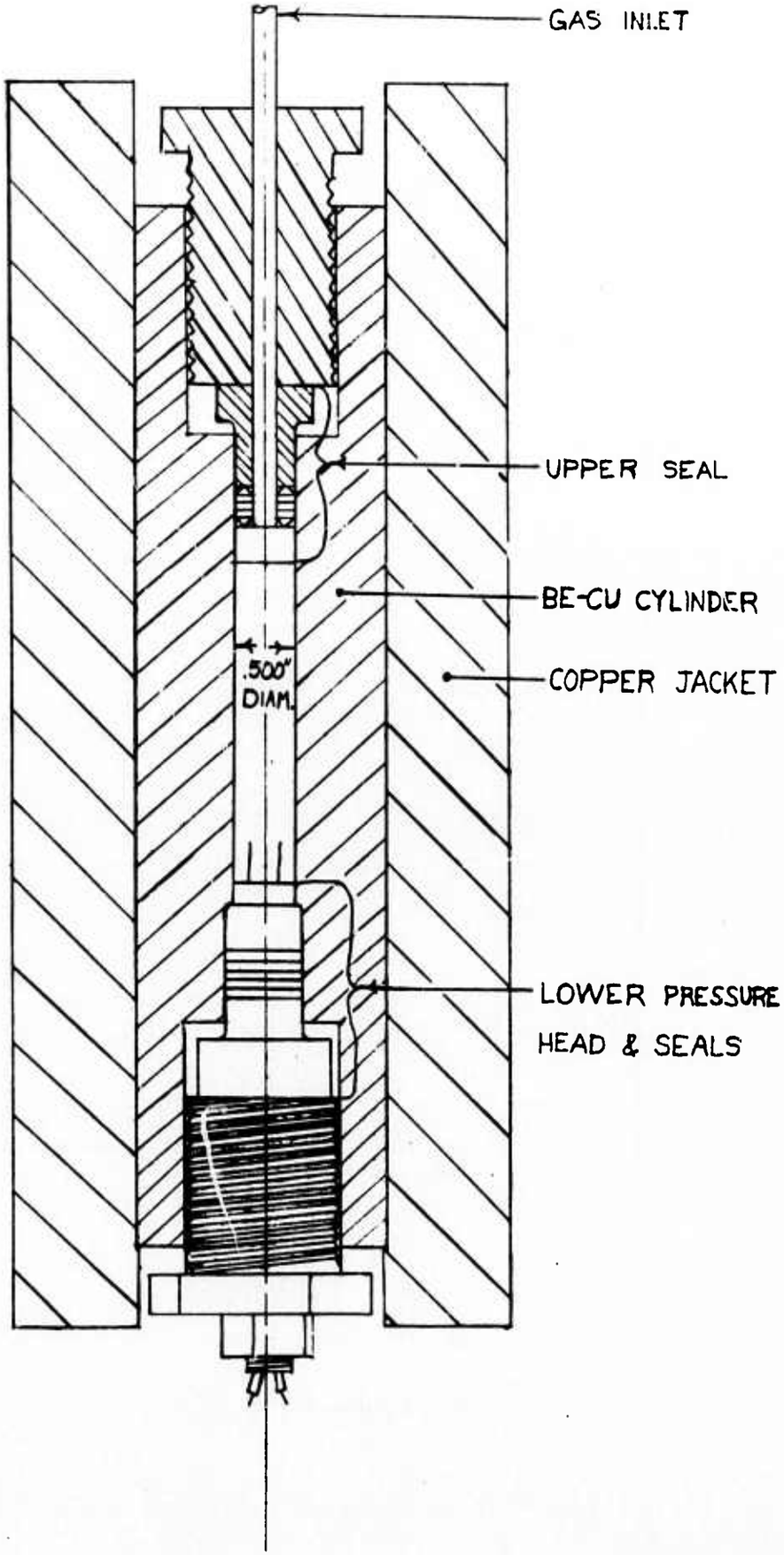
GAS INLET
UPPER SEAL
BE-CU CYLINDER
.500"
DIAM.
COPPER JACKET
LOWER PRESSURE
HEAD & SEALS

Figure 6

Figure 6a

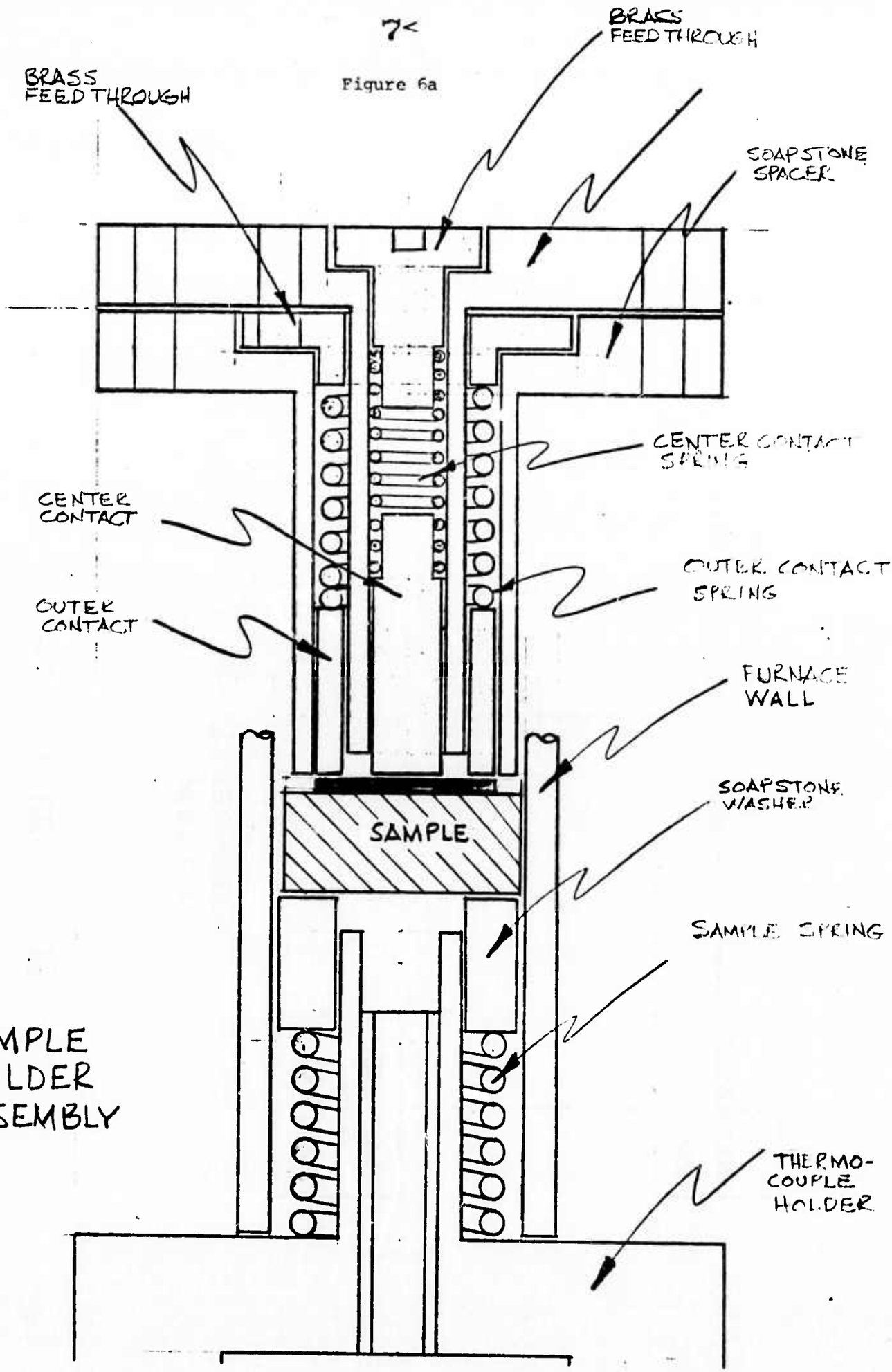

SAMPLE HOLDER ASSEMBLY

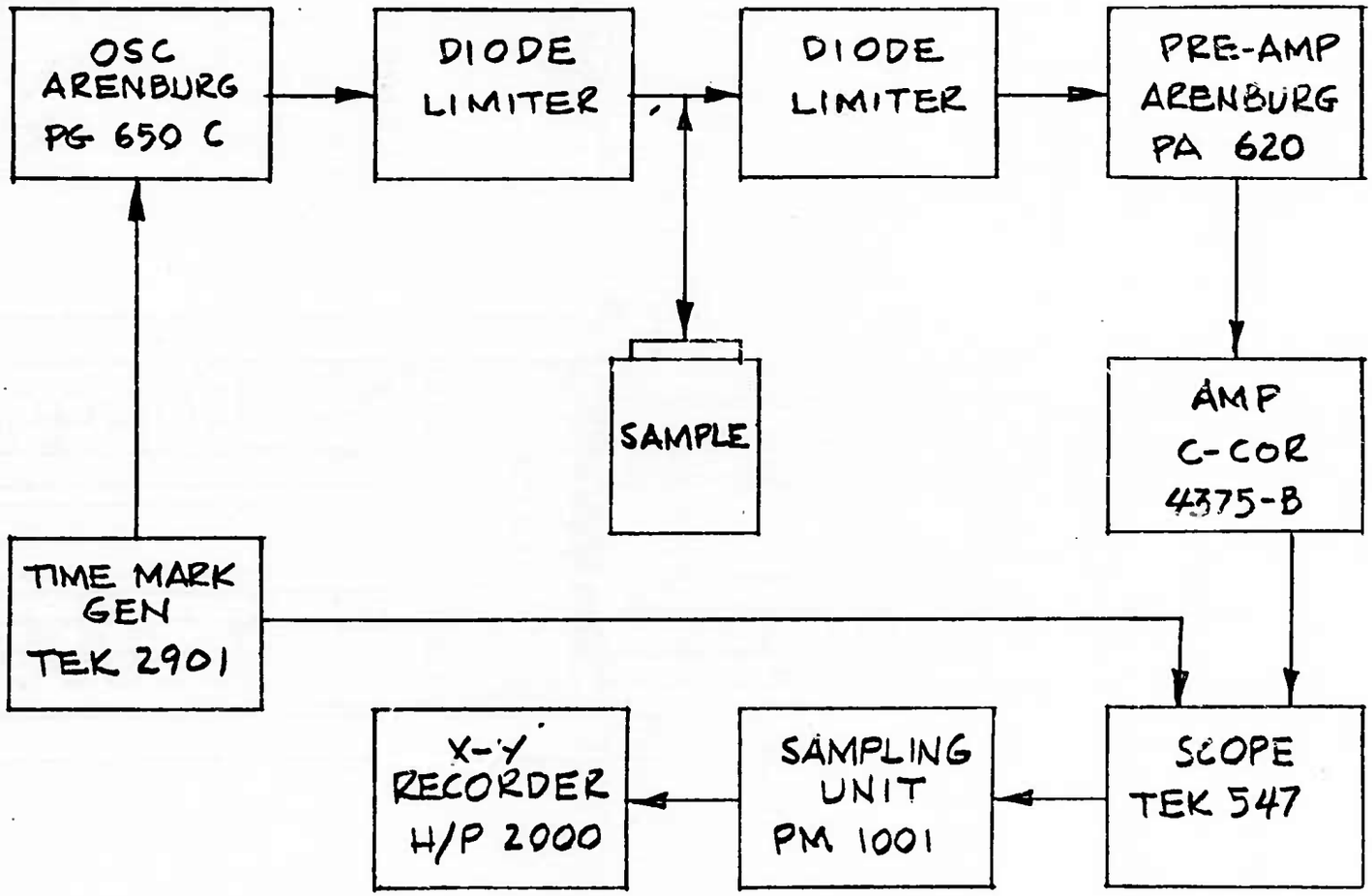

Figure 6b

SCHEMATIC OF
TRANSIT-TIME MEASUREMENT SYSTEM

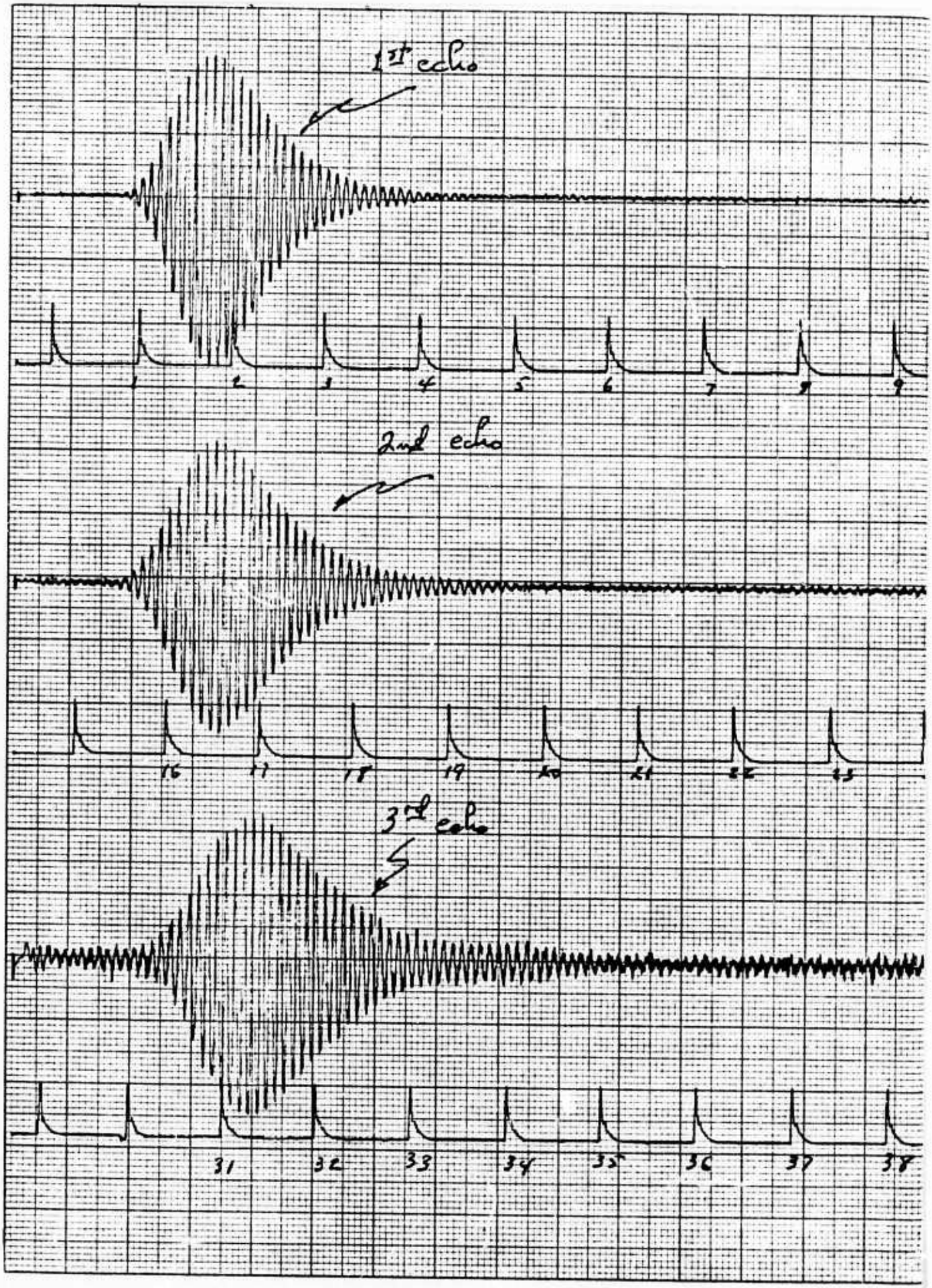
1st echo
1
2
3
4
5
6
7
8
9
2nd echo
16
17
18
19
20
21
22
23
3rd echo
31
32
33
34
35
36
37
38

Figure 7a

As_2S_3 (5CA-2) 12-28-73

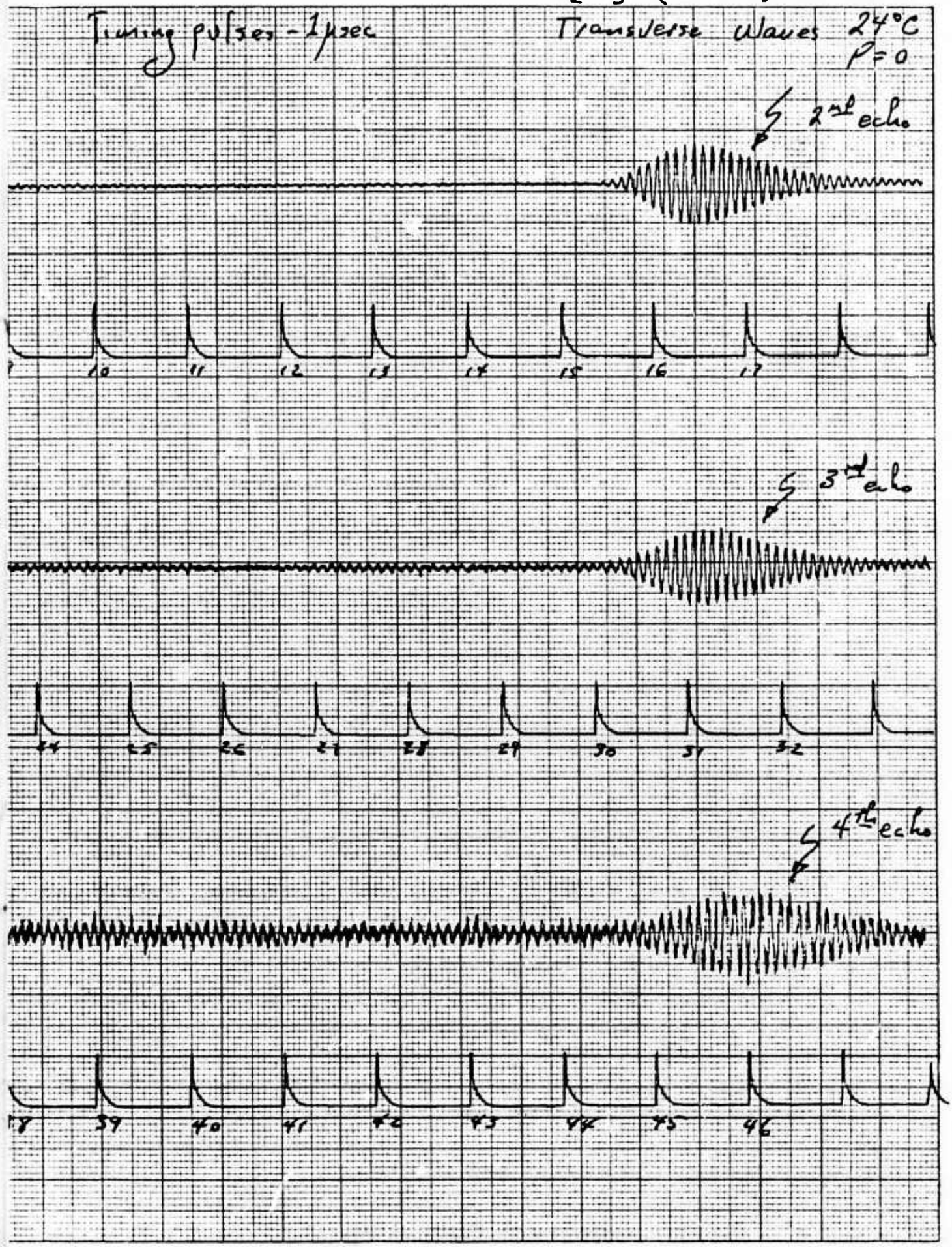

Figure 7a

Figure 7b

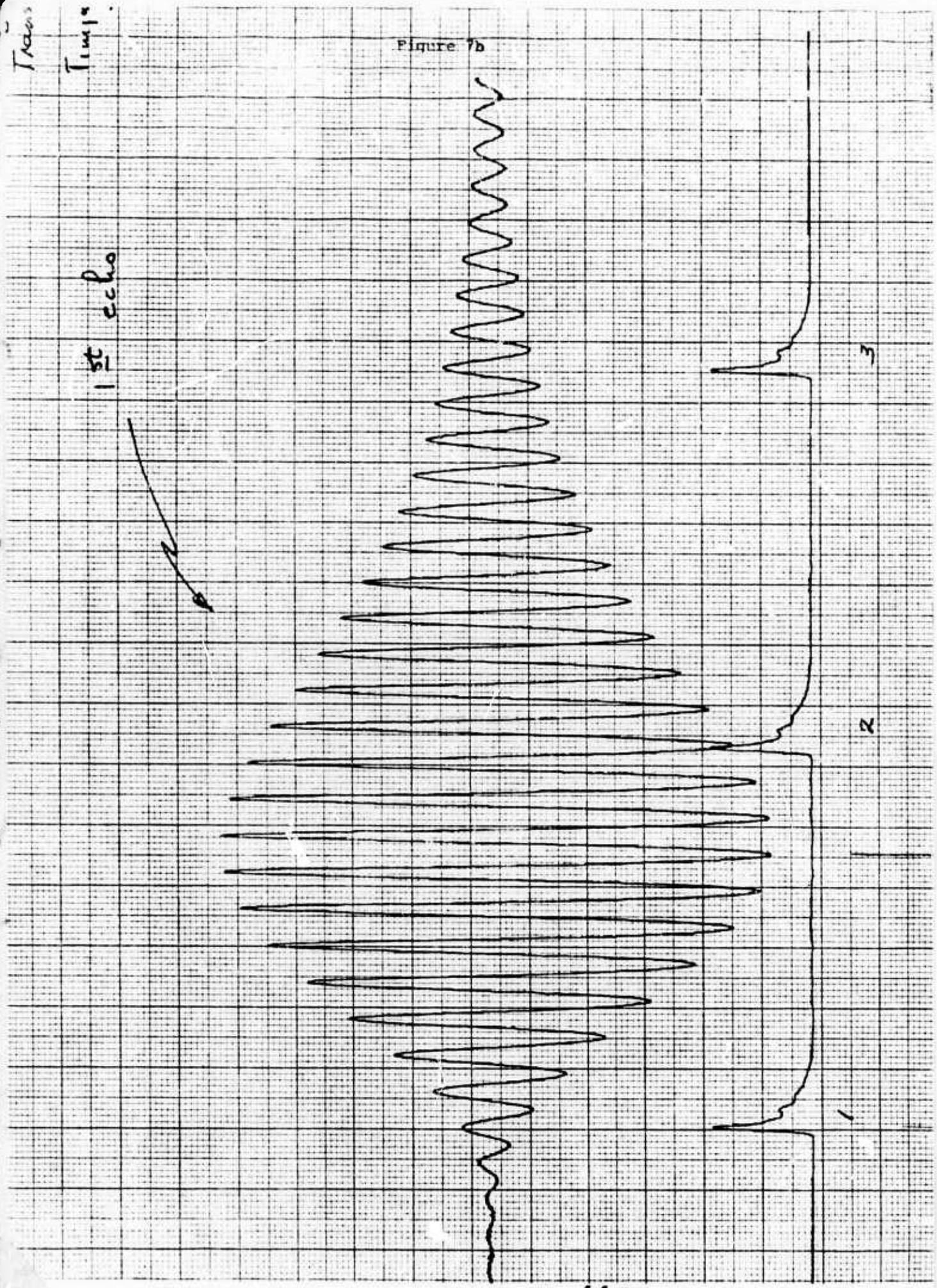

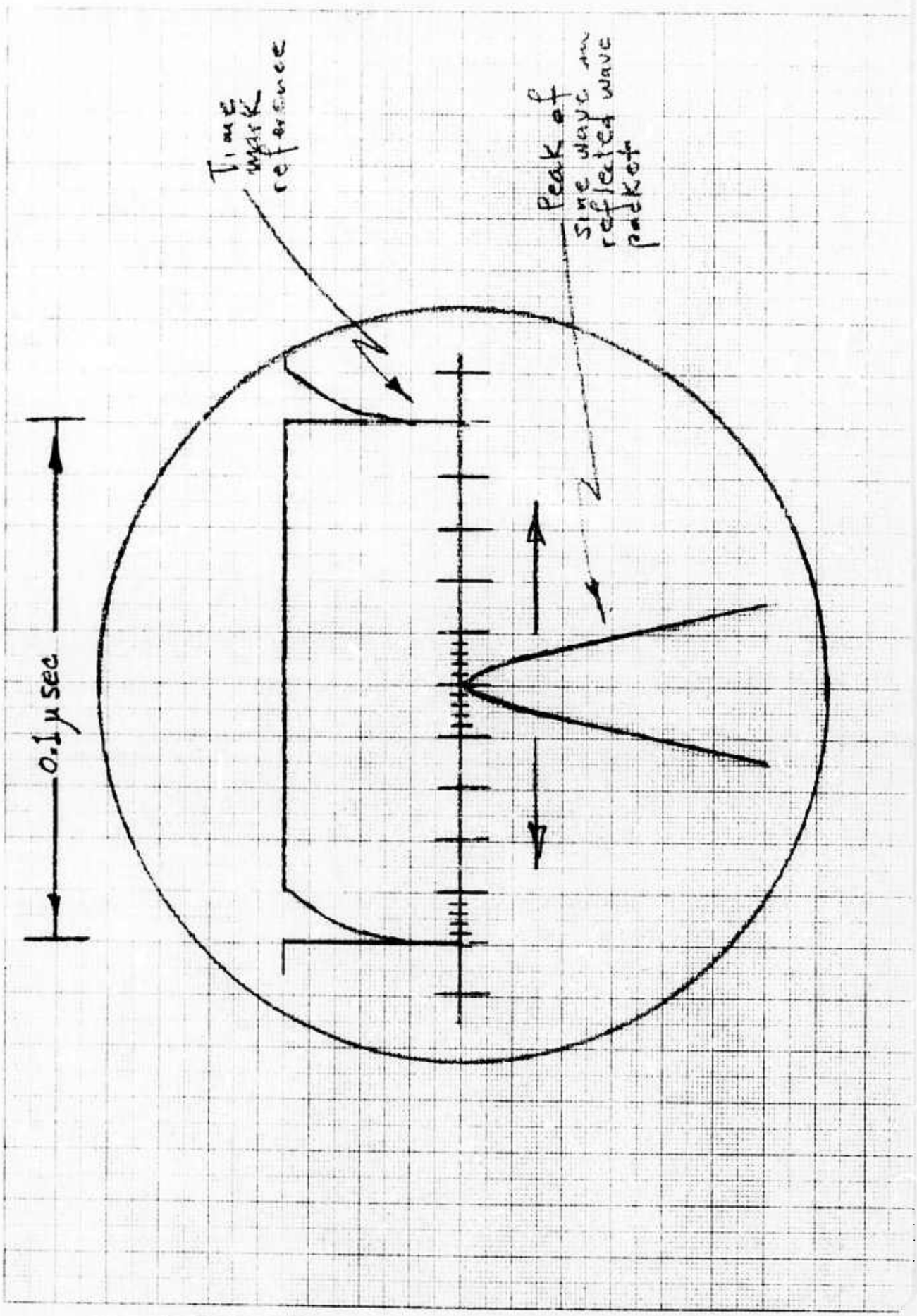

Figure 8

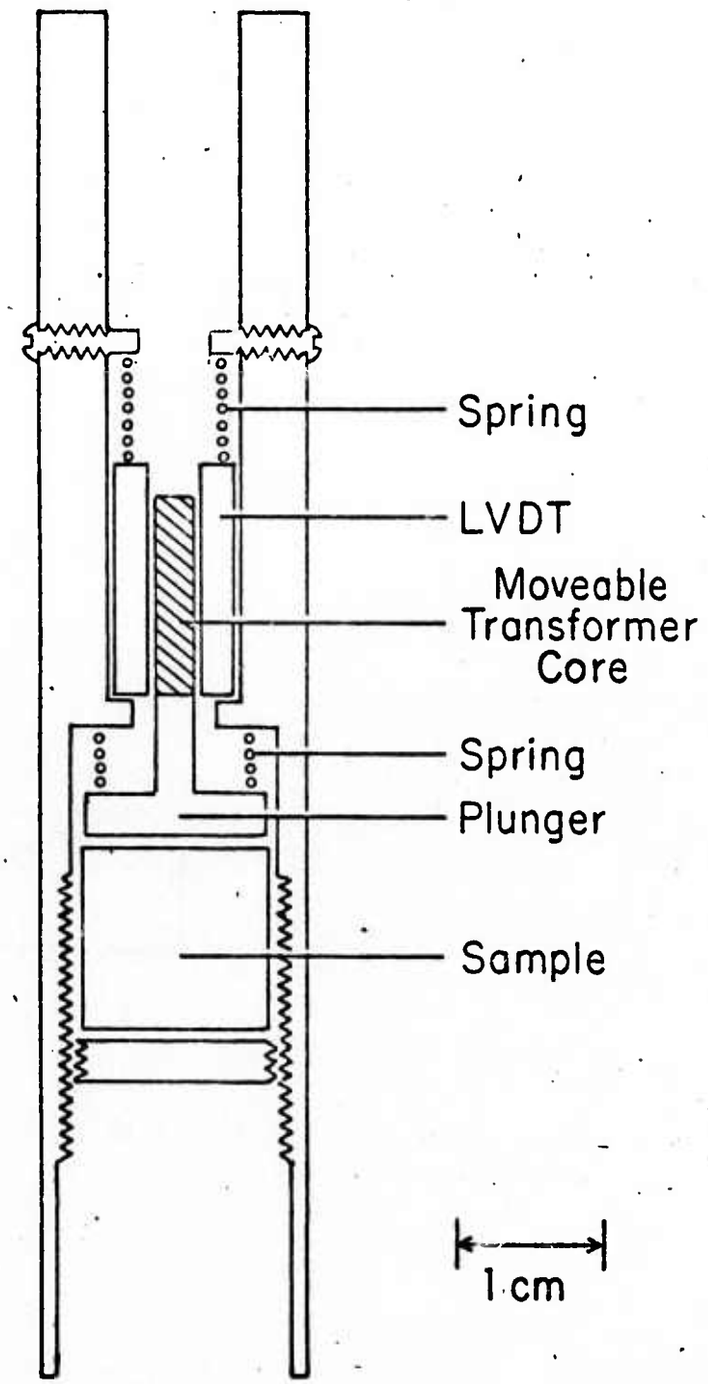
Spring
LVDT
Moveable
Transformer
Core
Spring
Plunger
Sample
1 cm

Figure 9

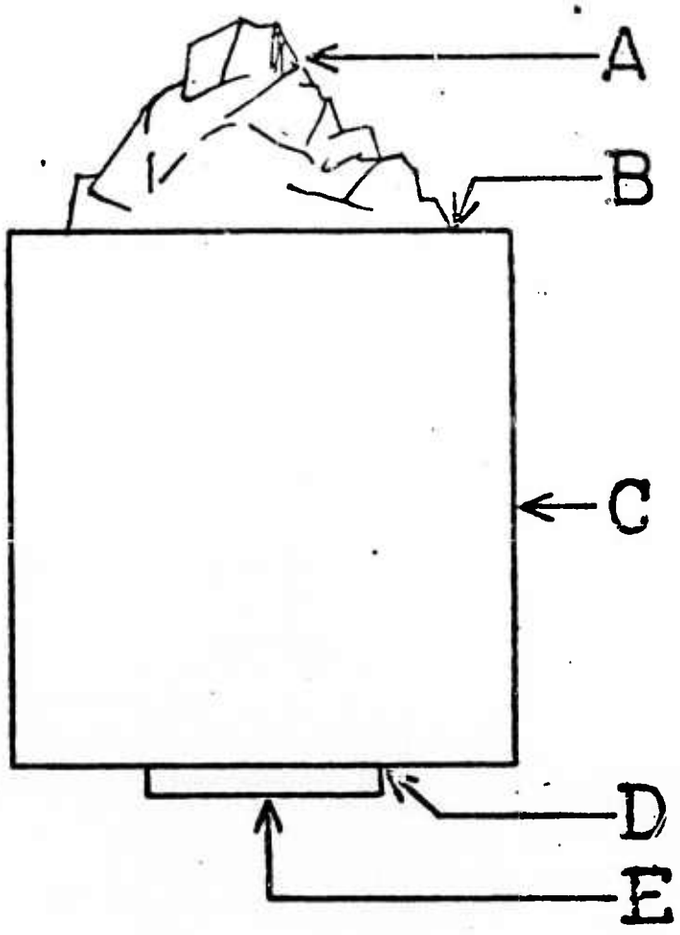

Figure 10

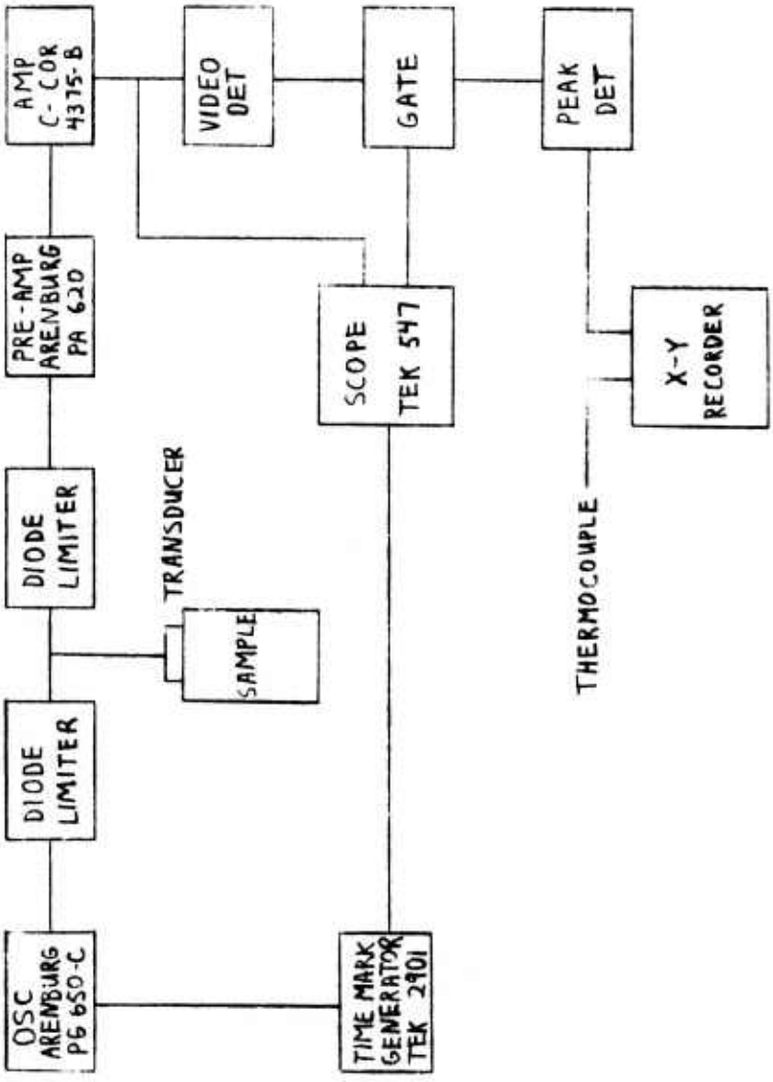
AMP
C-COR
4375-B
VIDEO
DET
GATE
PEAK
DET
PRE-AMP
ARENBURG
PA 620
SCOPE
TEK 547
X-Y
RECORDER
DIODE
LIMITER
TRANSDUCER
SAMPLE
THERMOCOUPLE
DIODE
LIMITER
OSC
ARENBURG
PG 650-C
TIME MARK
GENERATOR
TEK 2901

Figure 11a

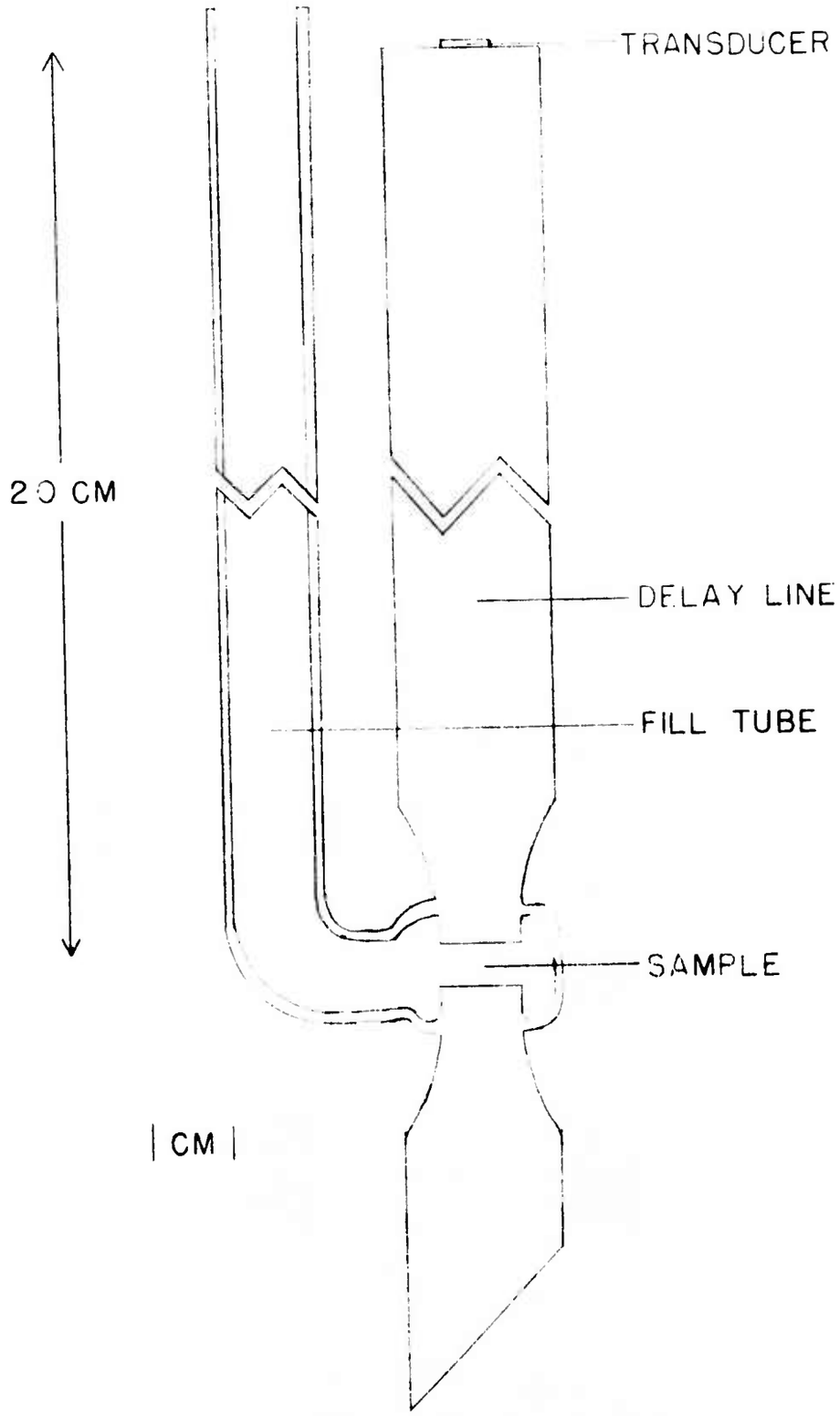

Figure 11b

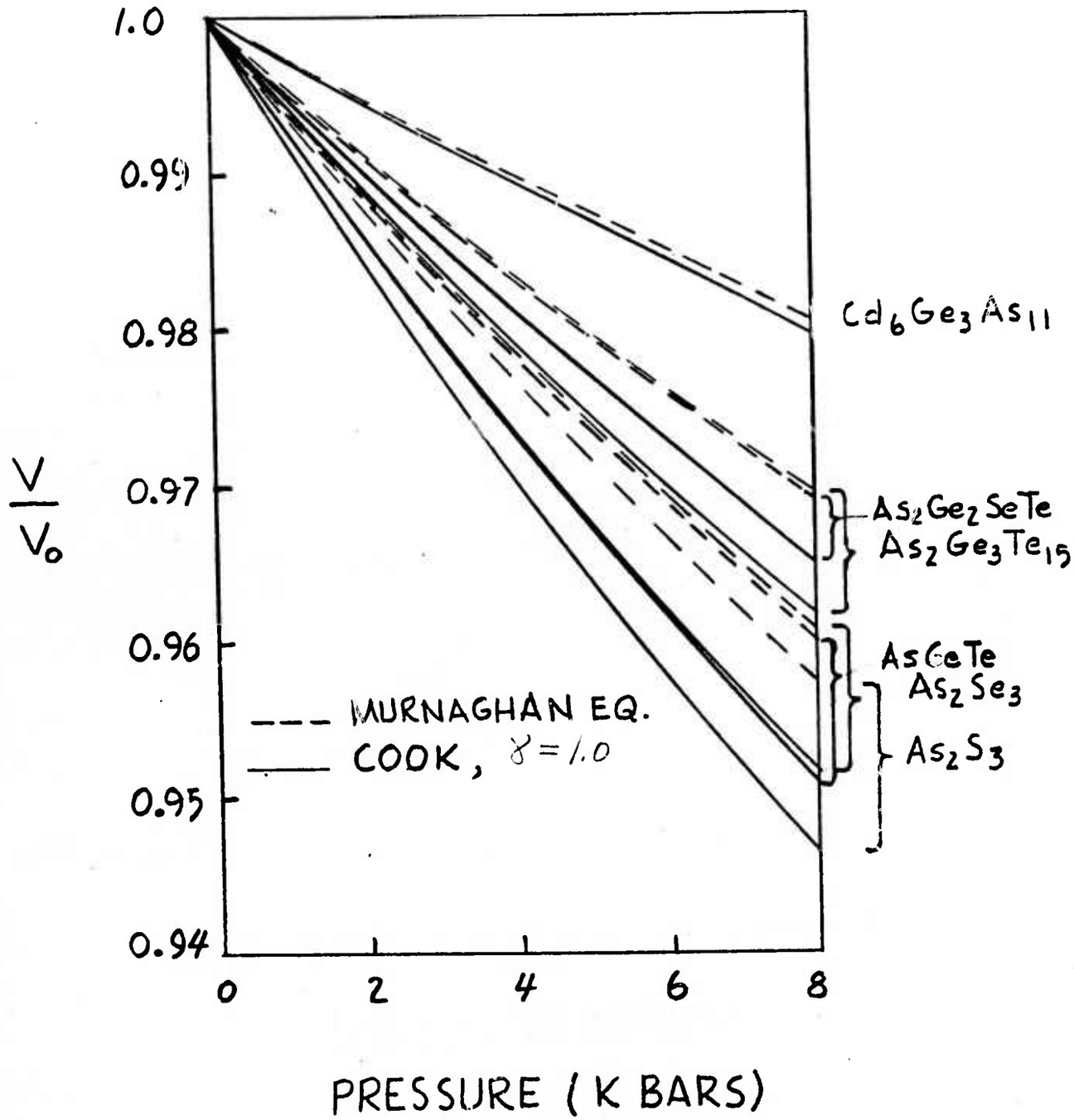
1.0
0.99
0.98
0.97
0.96
0.95
0.94
V/Vo
0
2
4
6
8
PRESSURE (K BARS)
--- MURNAGHAN EQ.
—— COOK, γ=1.0
Cd6Ge3As11
As2Ge2SeTe
As2Ge3Te15
AsGeTe
As2Se3
As2S3

Figure 12

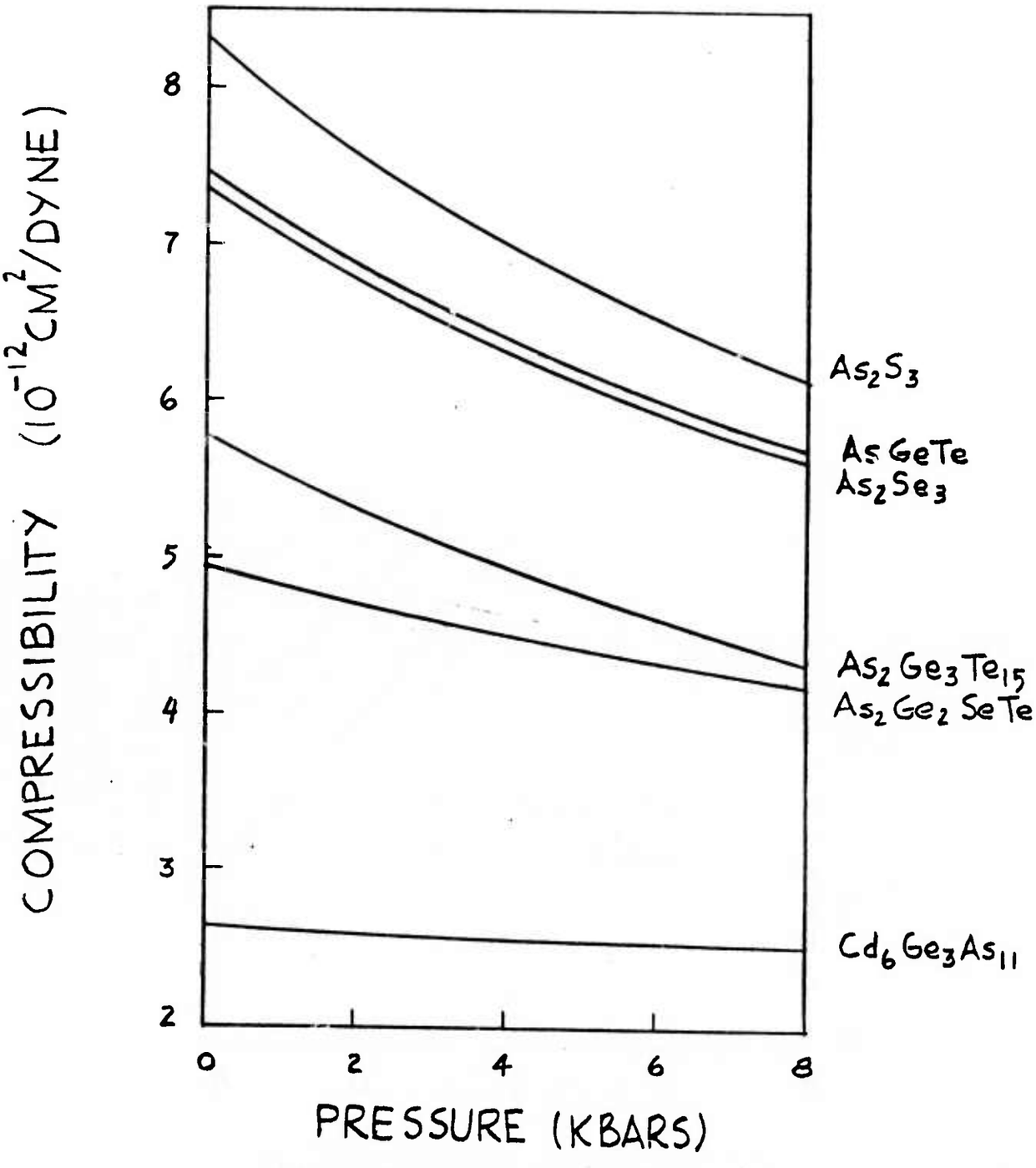
COMPRESSIBILITY (10⁻¹² CM²/DYNE)
8
7
6
5
4
3
2
0
2
4
6
8
PRESSURE (KBARS)
As₂S₃
As GeTe
As₂Se₃
As₂Ge₃Te₁₅
As₂Ge₂SeTe
Cd₆Ge₃As₁₁

Figure 13

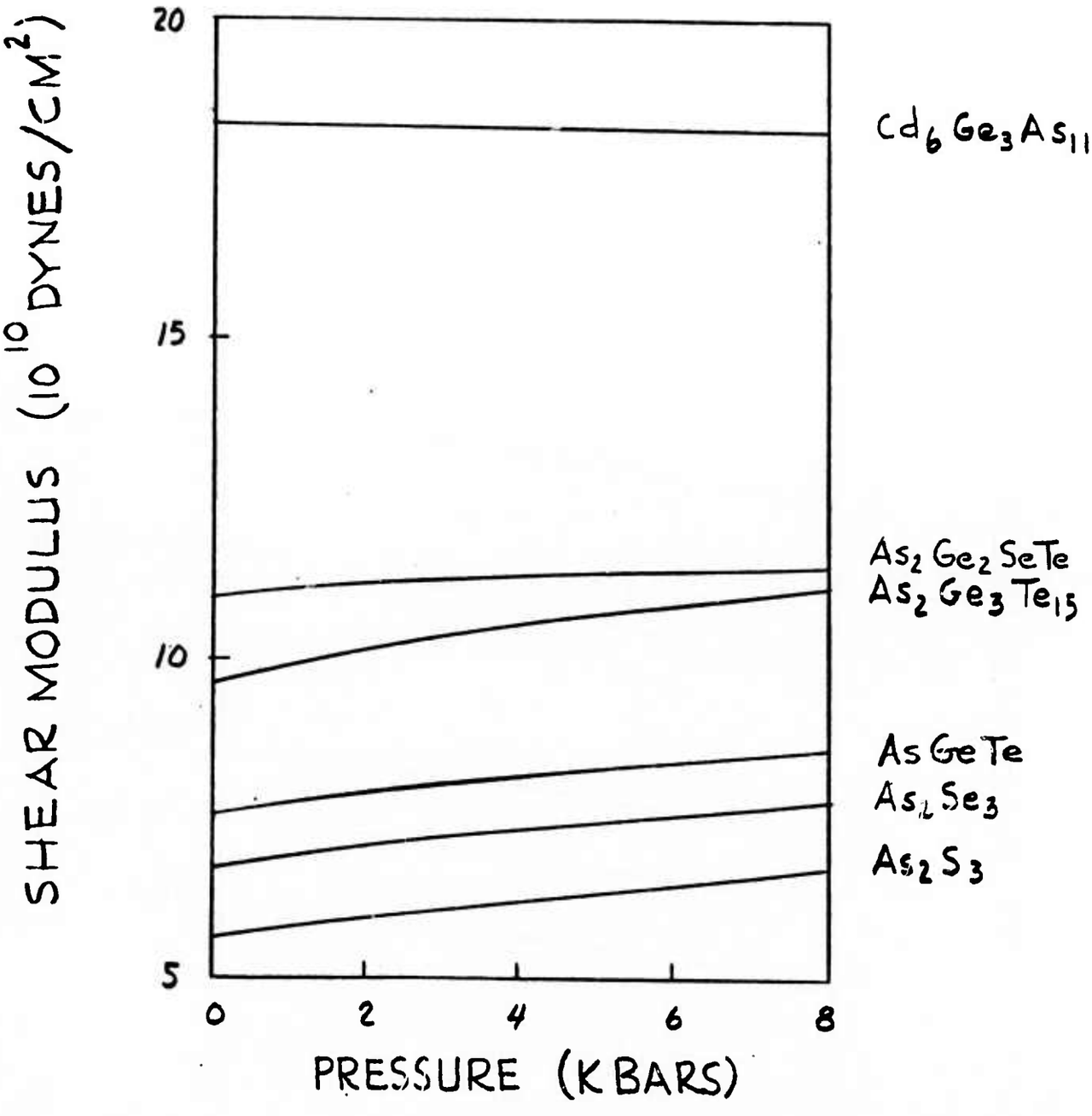
SHEAR MODULUS (10^{10} DYNES/CM^2)
20
15
10
5
0
2
4
6
8
PRESSURE (K BARS)
$Cd_6 Ge_3 As_{11}$
$As_2 Ge_2 SeTe$
$As_2 Ge_3 Te_{15}$
AsGeTe
$As_2 Se_3$
$As_2 S_3$

Figure 14

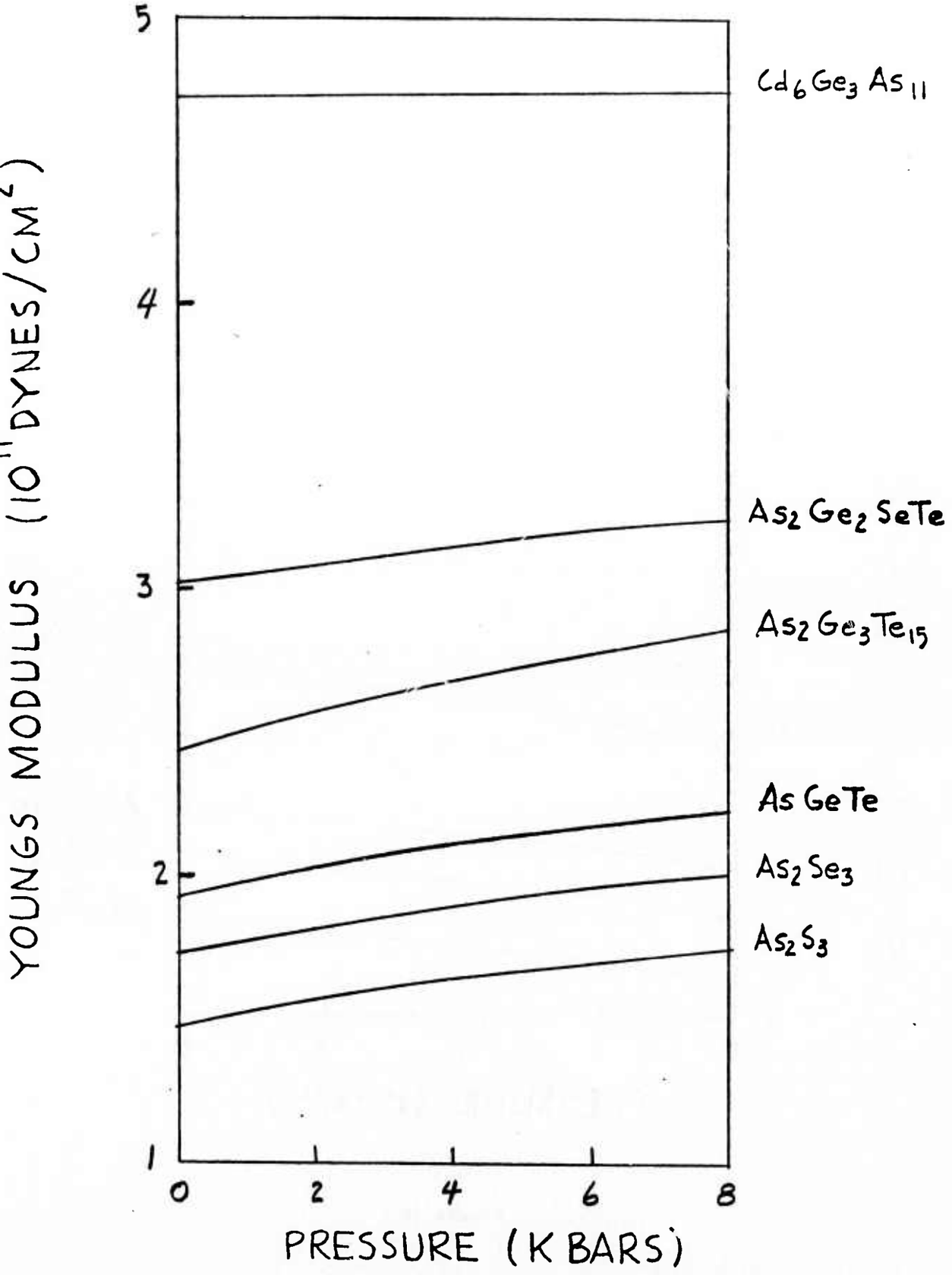
YOUNGS MODULUS (10^{11} DYNES/CM^2)
5
4
3
2
1
0
2
4
6
8
PRESSURE (K BARS)
$Cd_6Ge_3As_{11}$
As_2Ge_2SeTe
$As_2Ge_3Te_{15}$
AsGeTe
As_2Se_3
As_2S_3

Figure 15

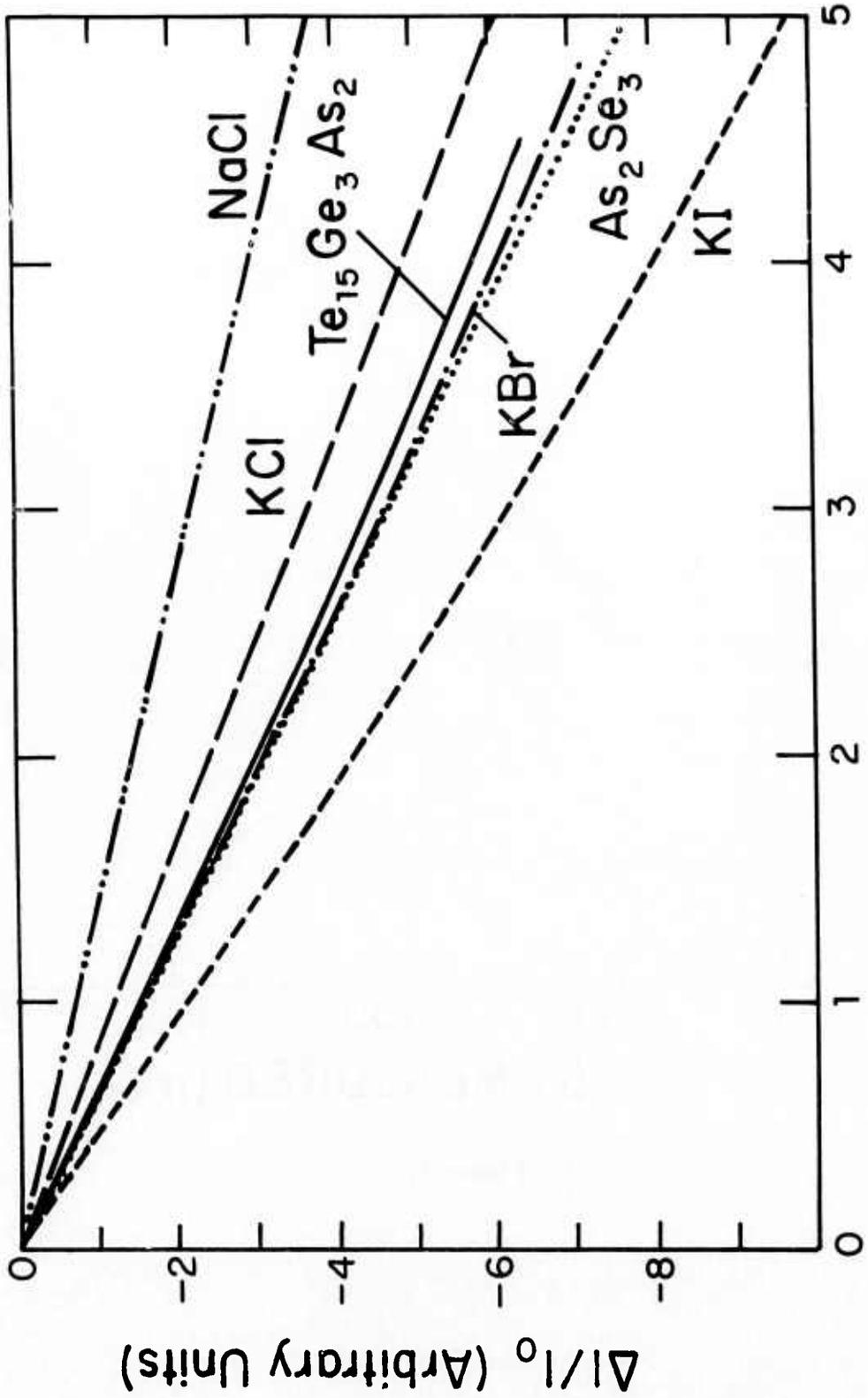
NaCl
KCl
$Te_{15}Ge_3As_2$
KBr
As_2Se_3
KI
0
-2
-4
-6
-8
$\Delta I/I_o$ (Arbitrary Units)
0
1
2
3
4
5
PRESSURE (K Bar)

Figure 16

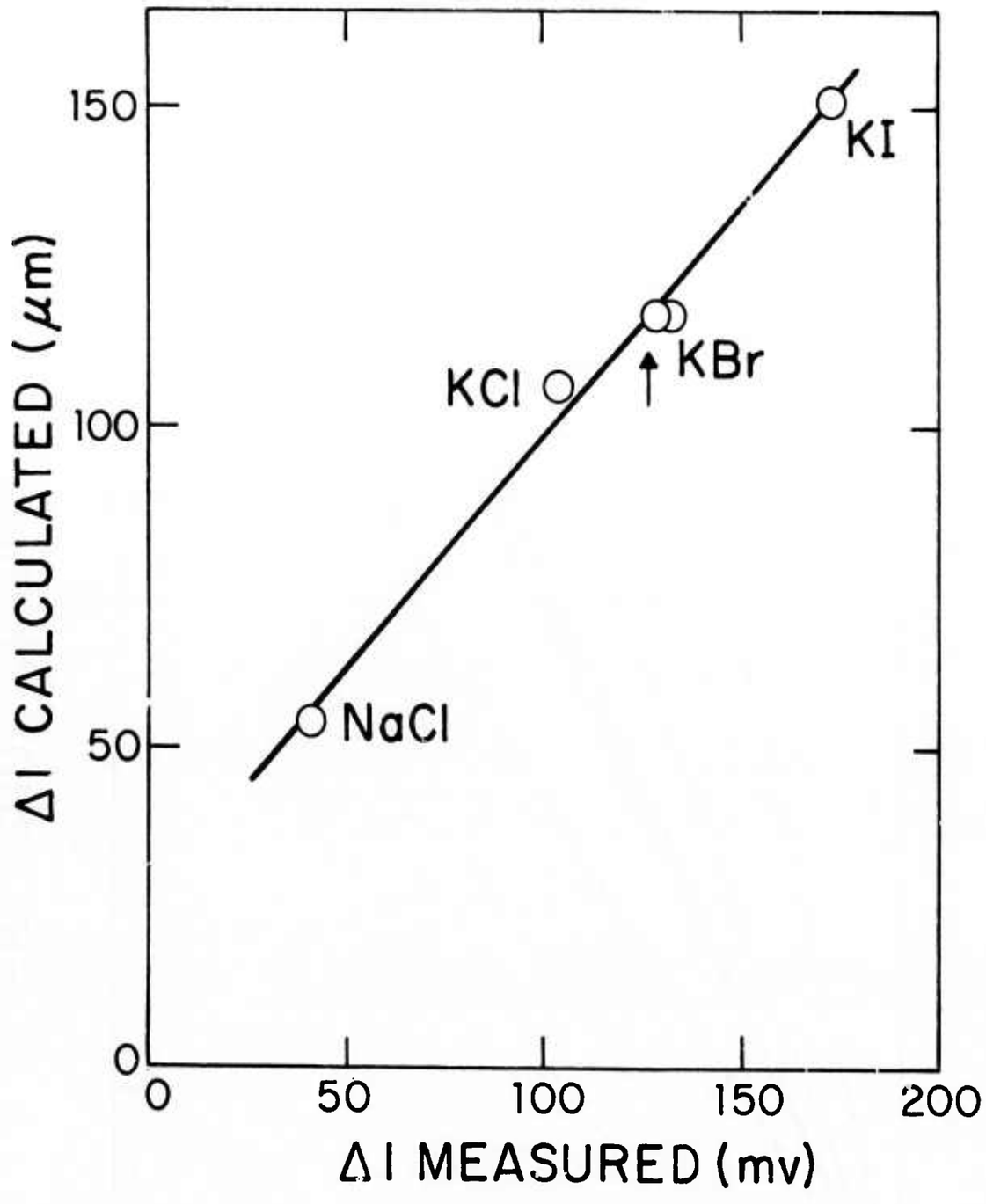
150
100
50
0
ΔI CALCULATED (μm)
KI
KBr
KCl
NaCl
0
50
100
150
200
ΔI MEASURED (mv)

Figure 17

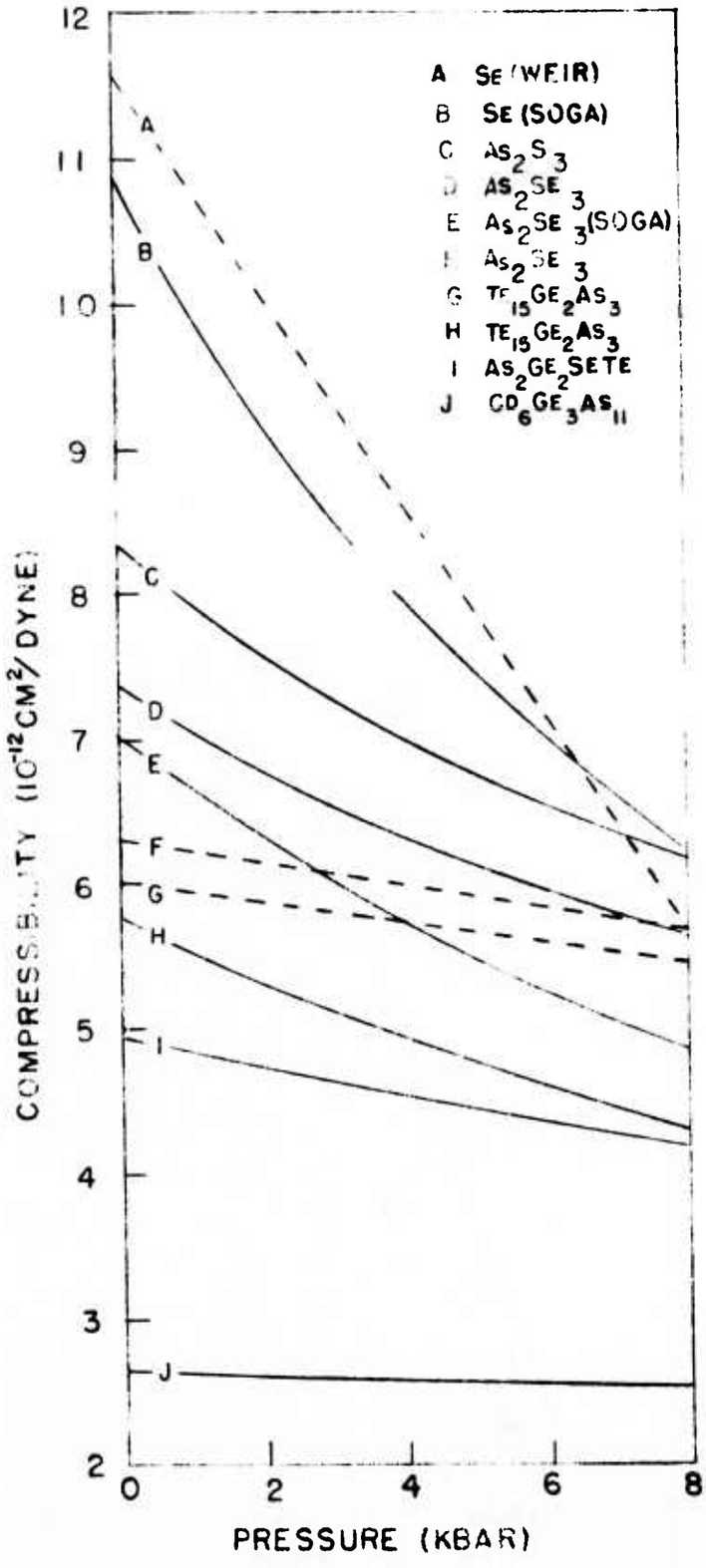
A SE (WEIR)
B SE (SOGA)
C AS_2S_3
D AS_2SE_3
E AS_2SE_3 (SOGA)
F AS_2SE_3
G $TE_{15}GE_2AS_3$
H $TE_{15}GE_2AS_3$
I AS_2GE_2SETE
J $CD_6GE_3AS_{11}$
COMPRESSIBILITY (10^{-12} CM²/DYNE)
PRESSURE (KBAR)
12
11
10
9
8
7
6
5
4
3
2
0
2
4
6
8

Figure 18

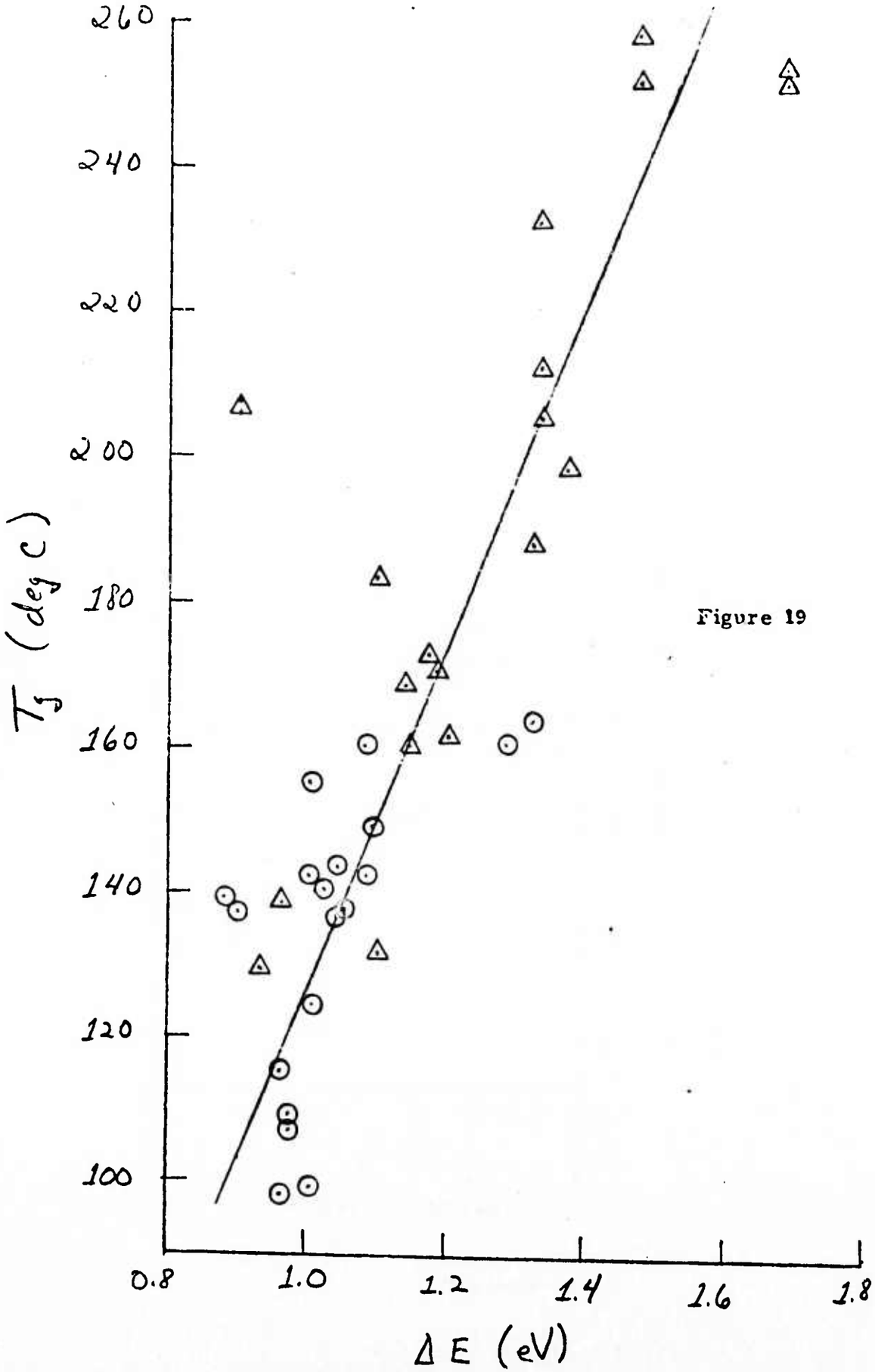
260
240
220
200
180
160
140
120
100
T_j (deg C)
0.8
1.0
1.2
1.4
1.6
1.8
ΔE (eV)

Figure 19

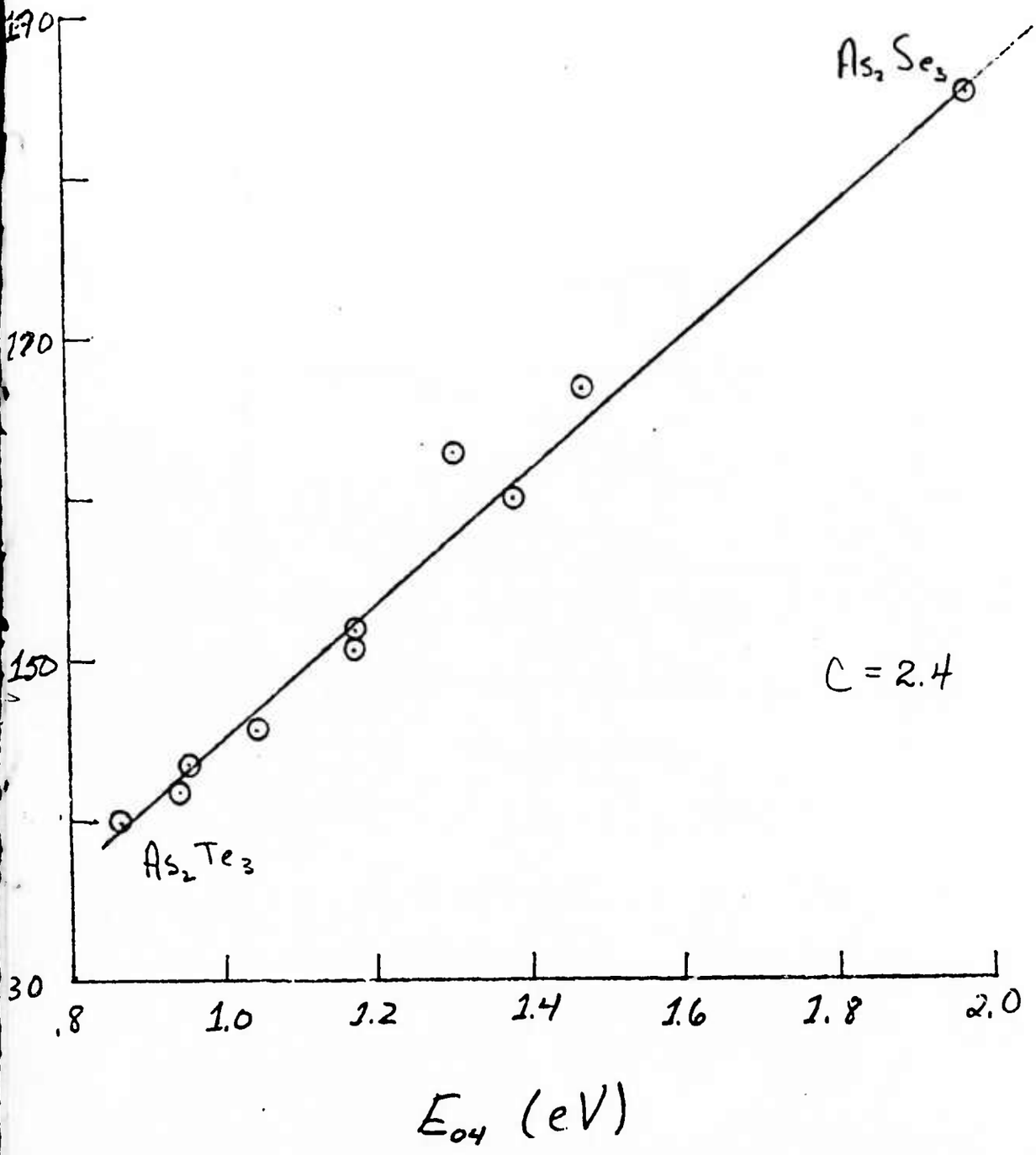

Figure 20

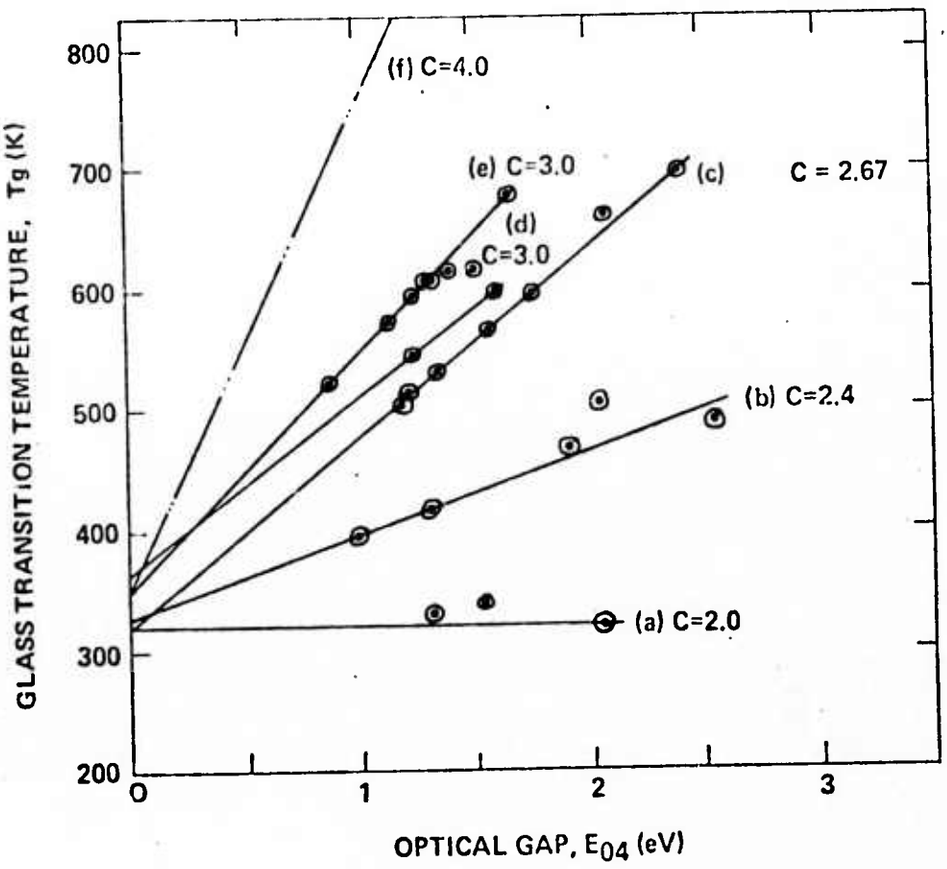
800
700
600
500
400
300
200
0
1
2
3
GLASS TRANSITION TEMPERATURE, Tg (K)
OPTICAL GAP, E_{04} (eV)
(f) C=4.0
(e) C=3.0
(d)
C=3.0
(c)
C = 2.67
(b) C=2.4
(a) C=2.0

Figure 21

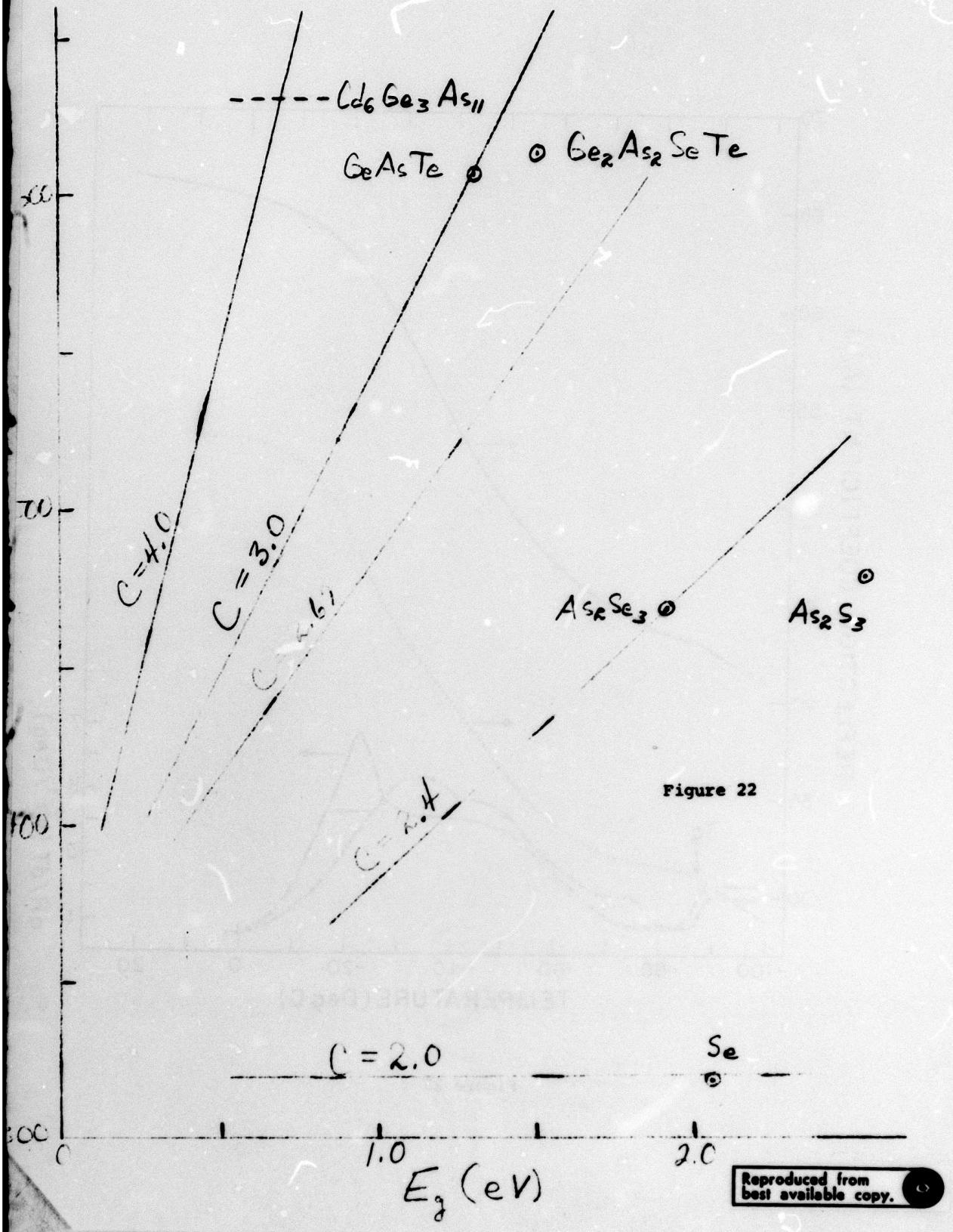

Figure 22

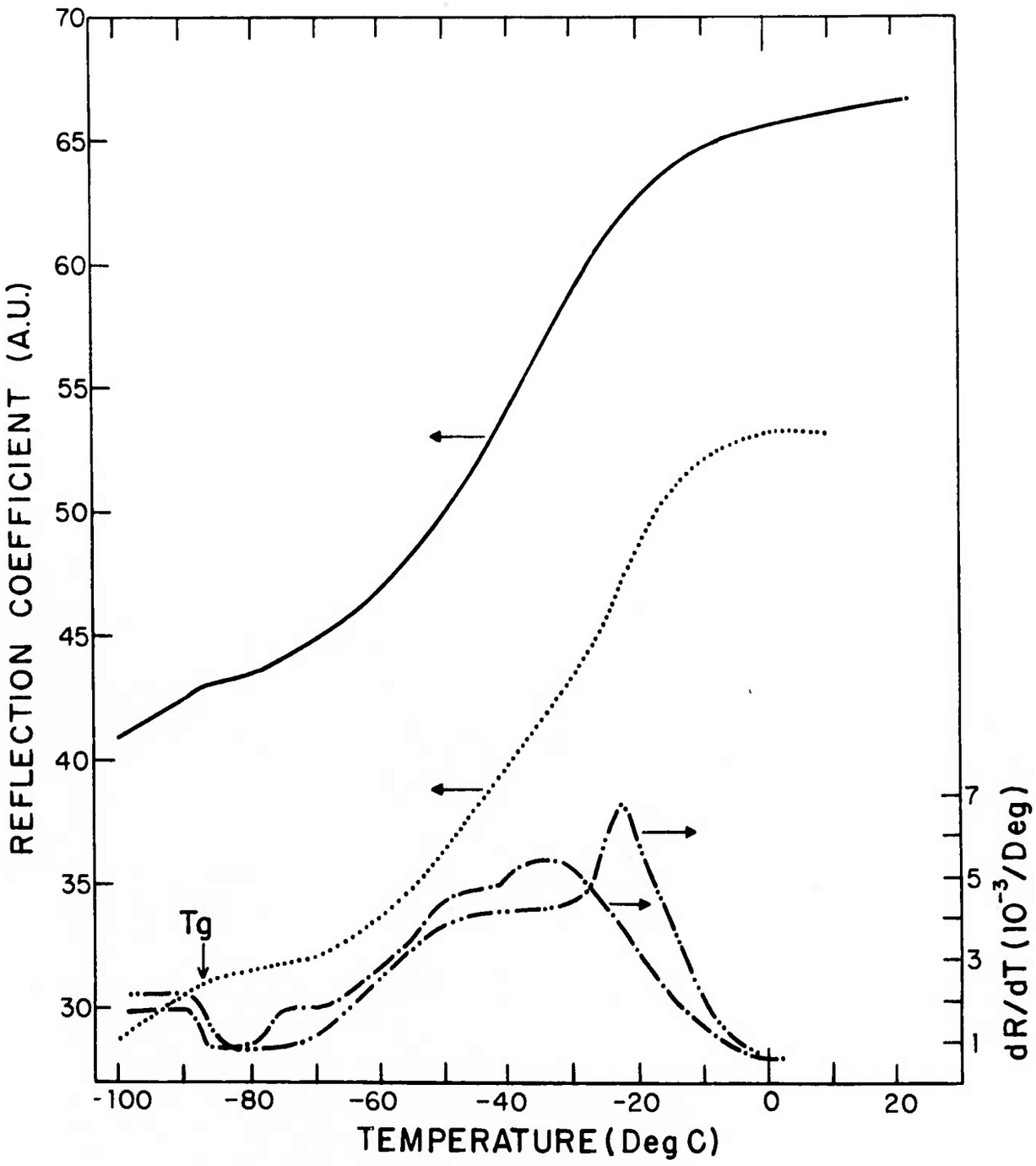
70
65
60
55
50
45
40
35
30
REFLECTION COEFFICIENT (A.U.)
Tg
-100
-80
-60
-40
-20
0
20
TEMPERATURE (Deg C)
7
5
3
1
dR/dT (10⁻³/Deg)

Figure 23

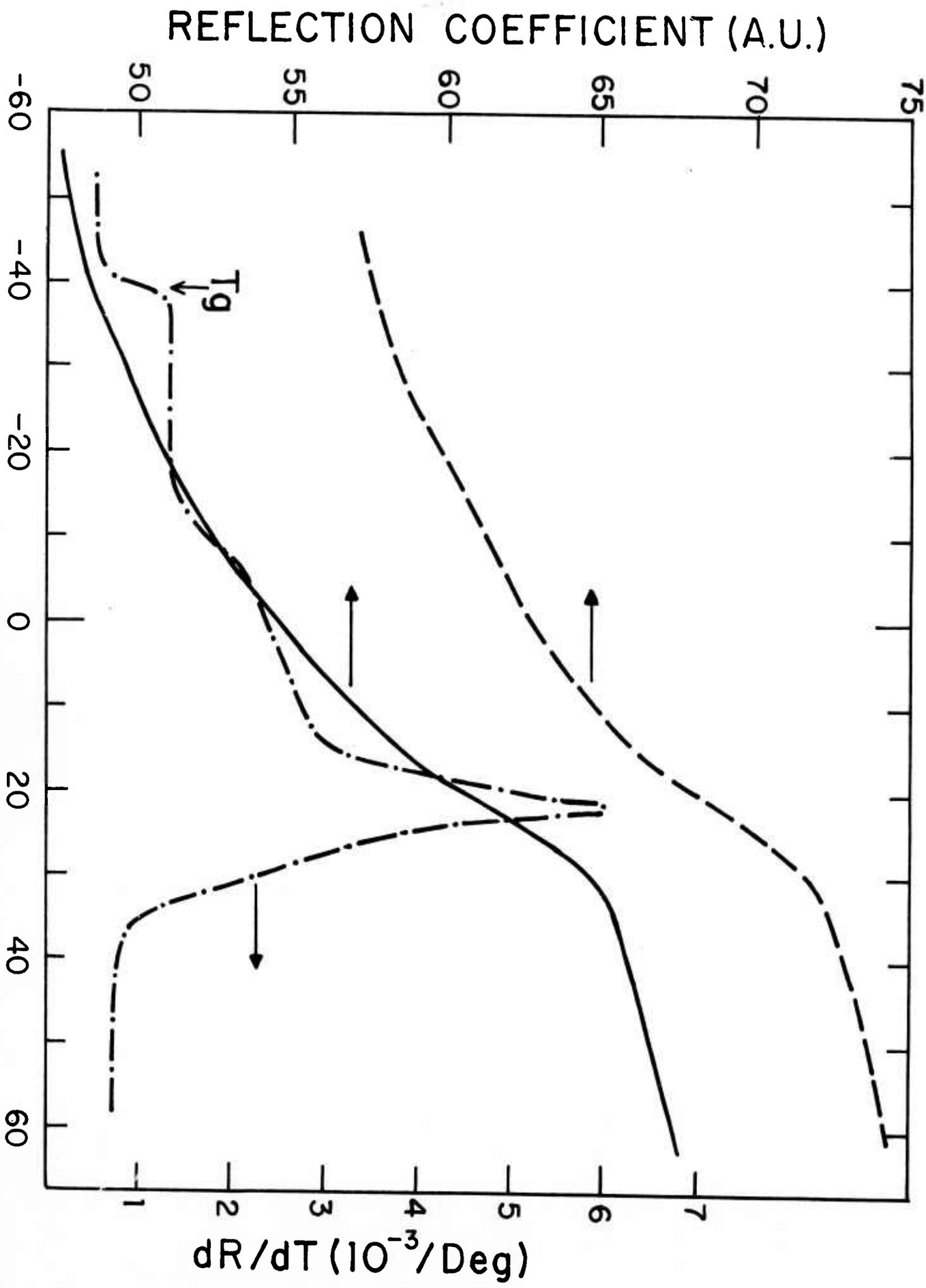
REFLECTION COEFFICIENT (A.U.)
50
55
60
65
70
75
-60
-40
-20
0
20
40
60
T_g
1
2
3
4
5
6
7
dR/dT (10^{-3}/Deg)

Figure 24

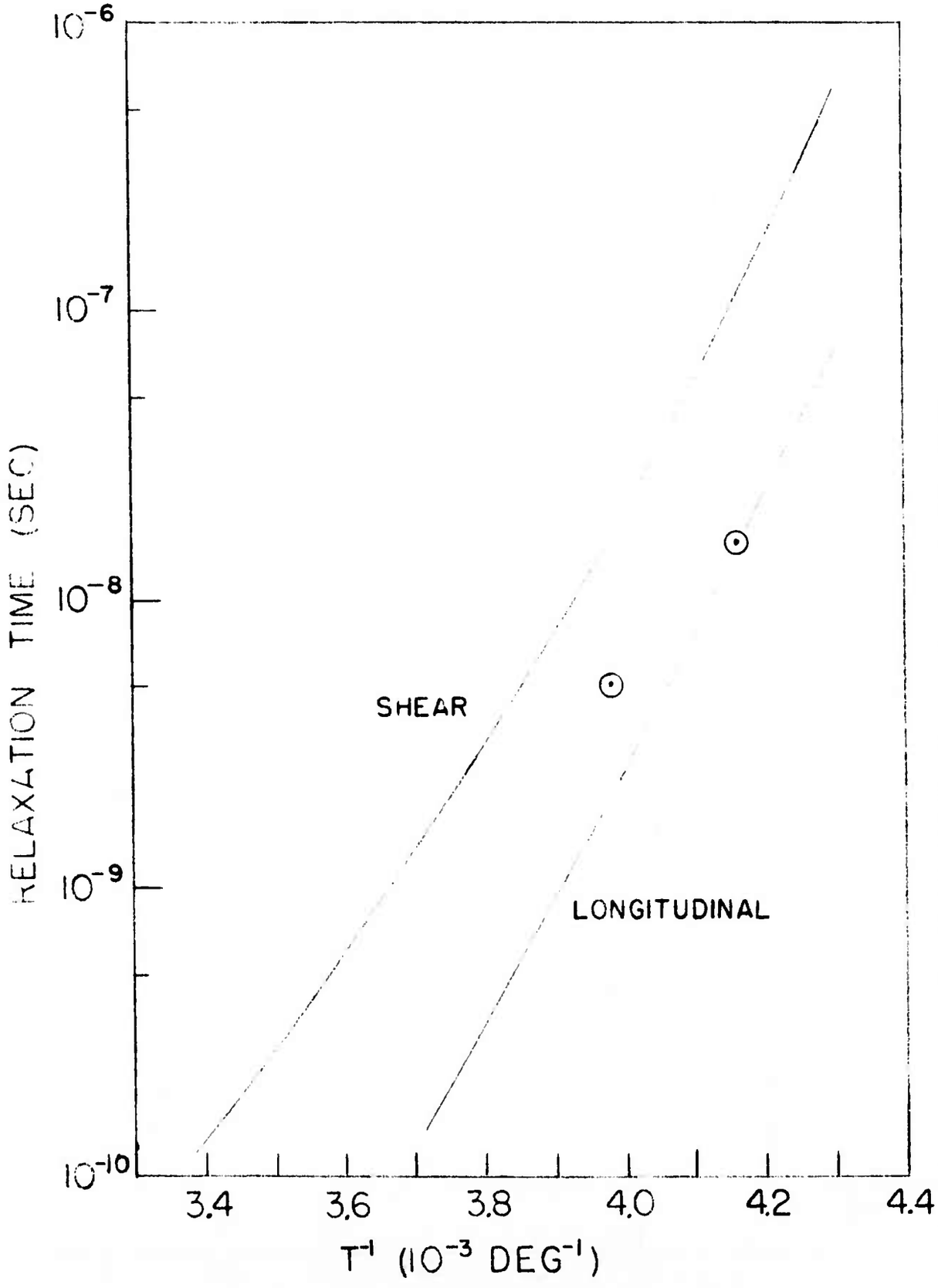
10^{-6}
10^{-7}
10^{-8}
10^{-9}
10^{-10}
RELAXATION TIME (SEC)
SHEAR
LONGITUDINAL
3.4
3.6
3.8
4.0
4.2
4.4
T^{-1} (10^{-3} DEG^{-1})

Figure 25

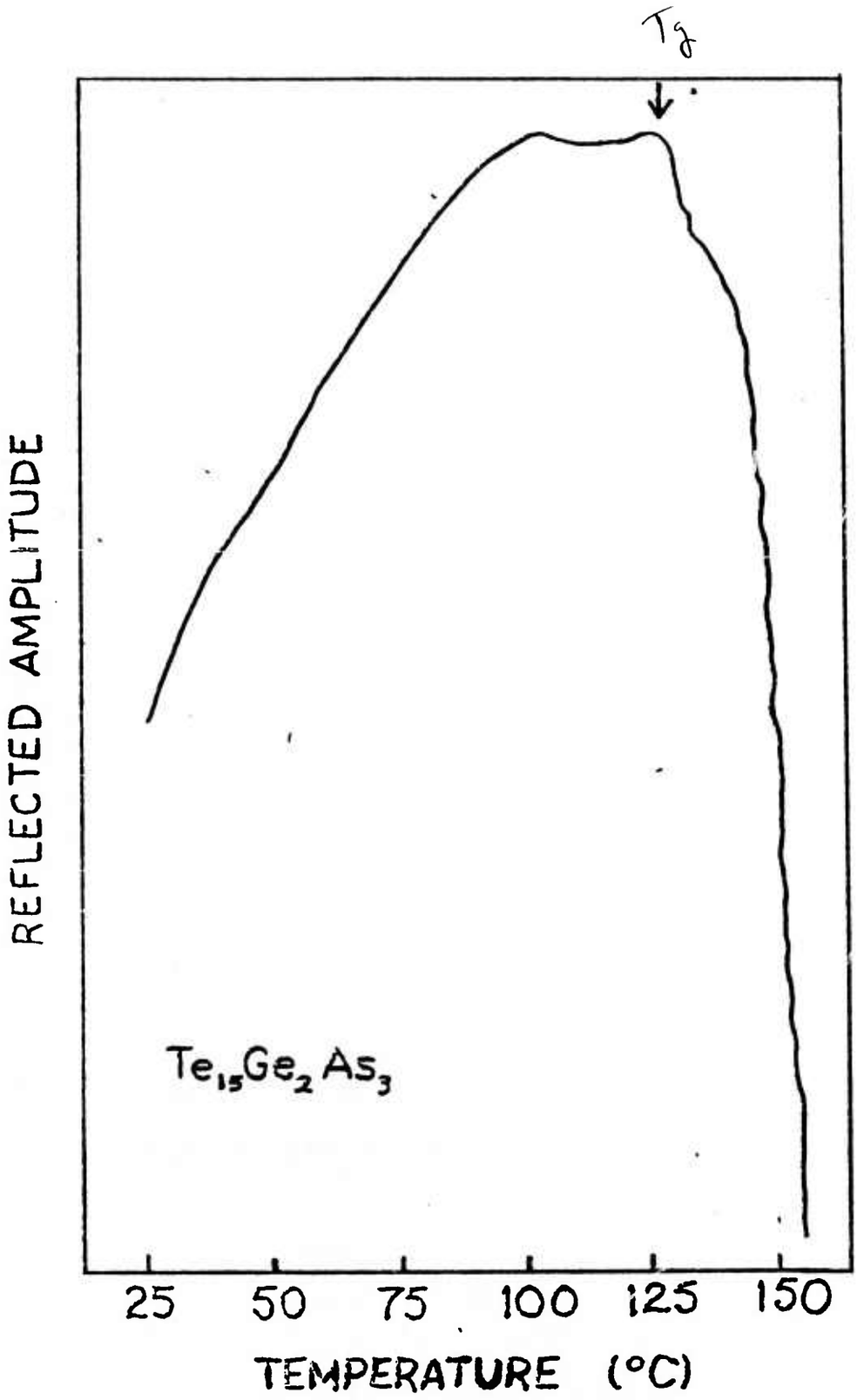
Tg
REFLECTED AMPLITUDE
$Te_{15}Ge_2As_3$
25
50
75
100
125
150
TEMPERATURE (°C)

Figure 26

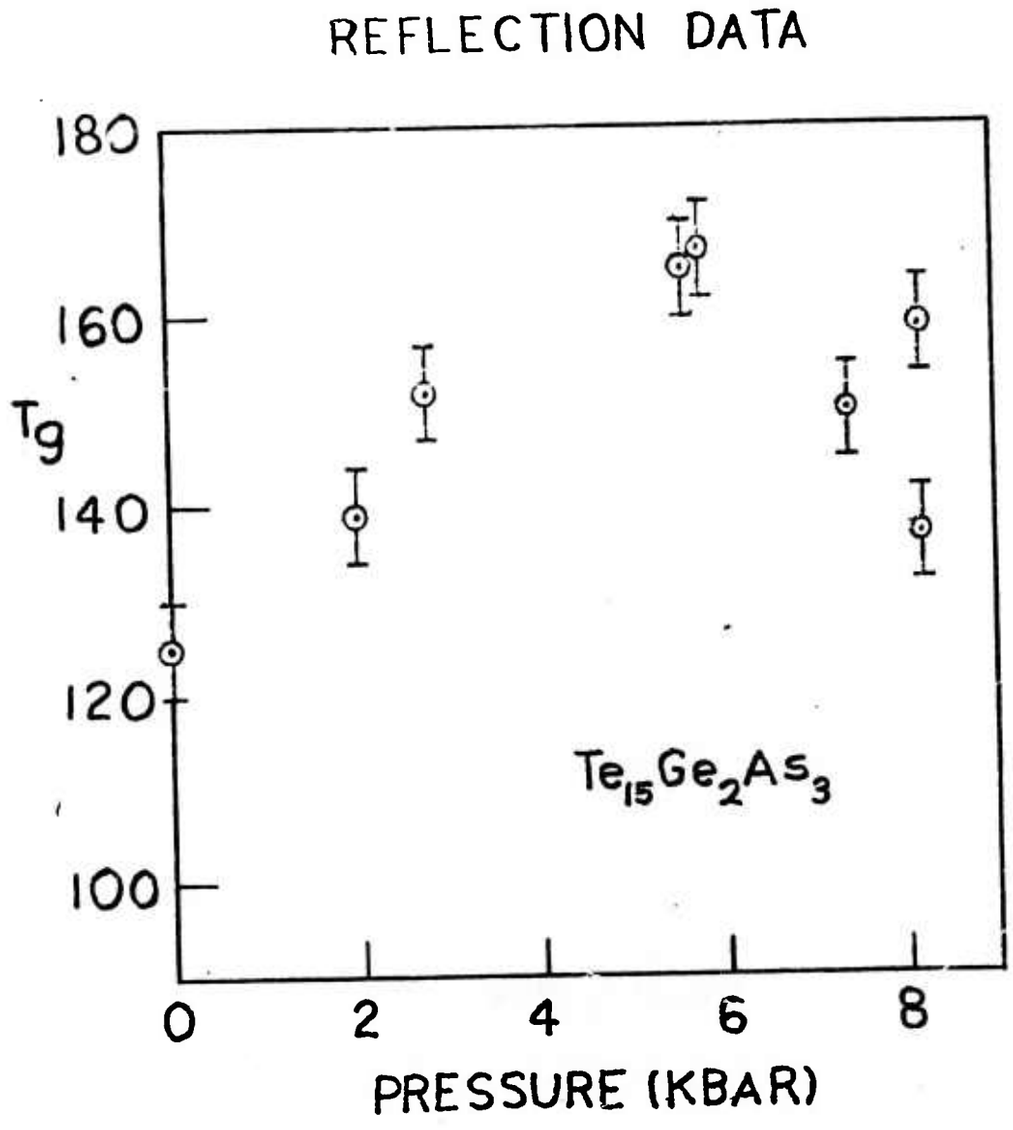
REFLECTION DATA
180
160
140
120
100
T_g
$Te_{15}Ge_2As_3$
0
2
4
6
8
PRESSURE (KBAR)

Figure 27

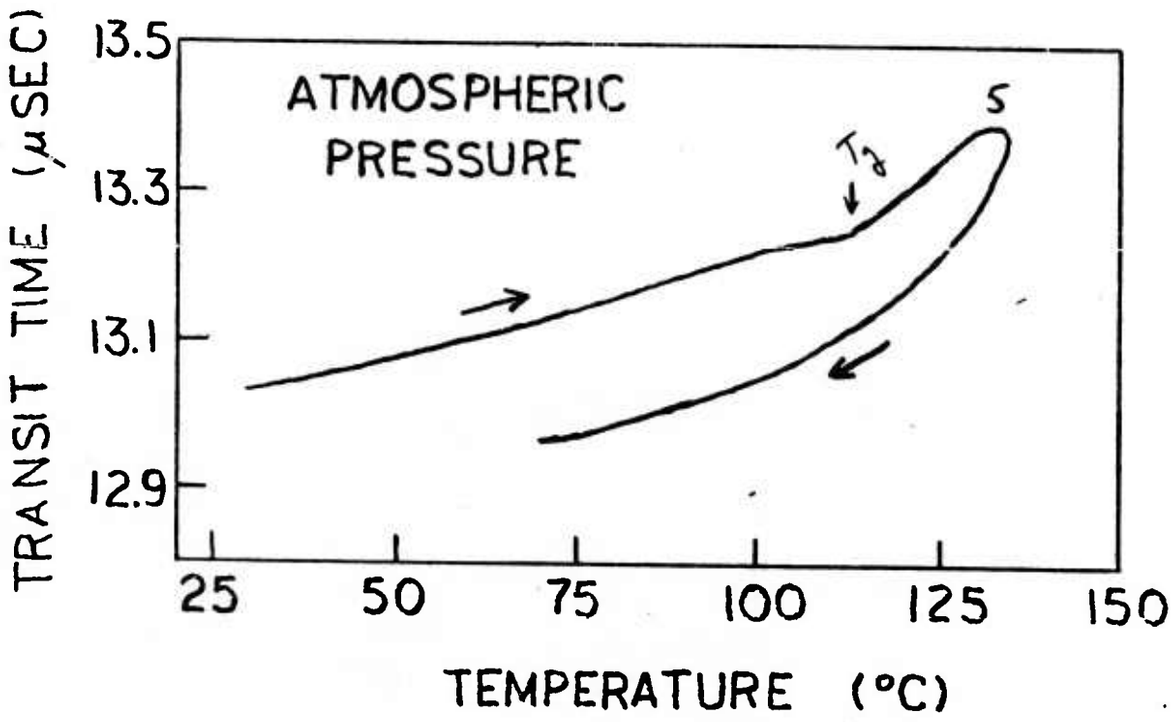
TRANSIT TIME (μSEC)
13.5
13.3
13.1
12.9
ATMOSPHERIC
PRESSURE
S
T_g
25
50
75
100
125
150
TEMPERATURE (°C)

Figure 28

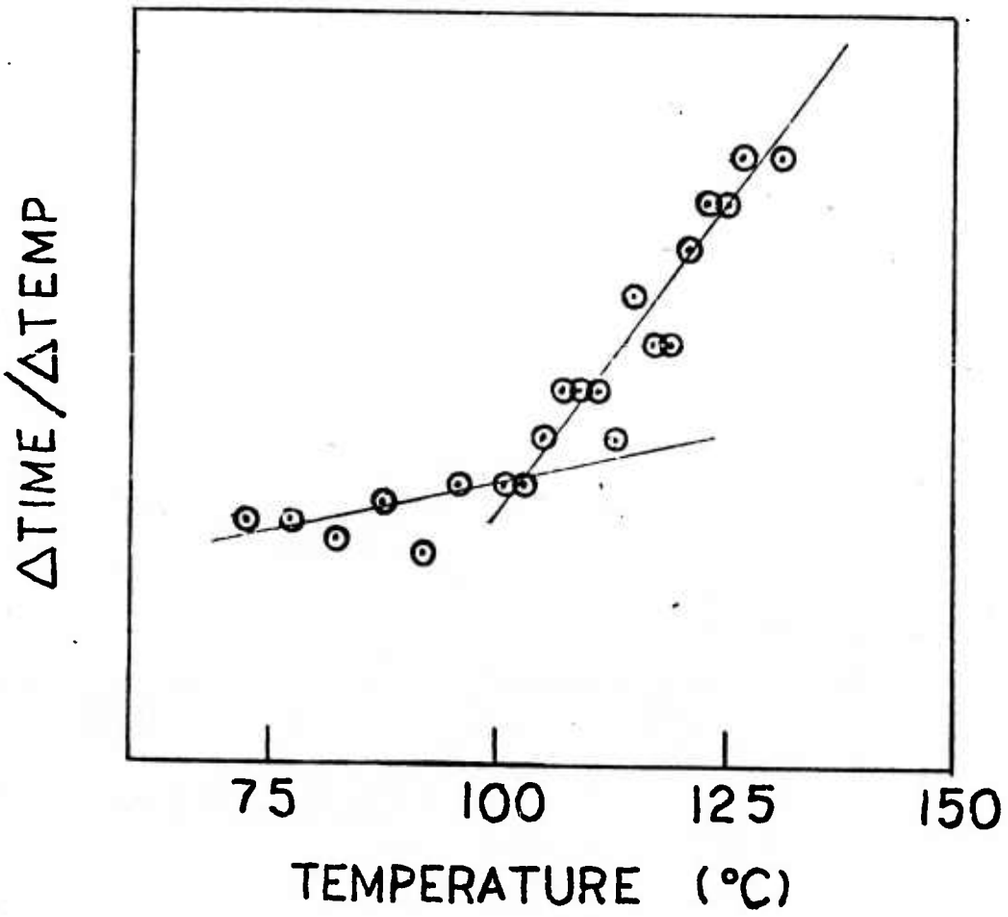

Figure 29

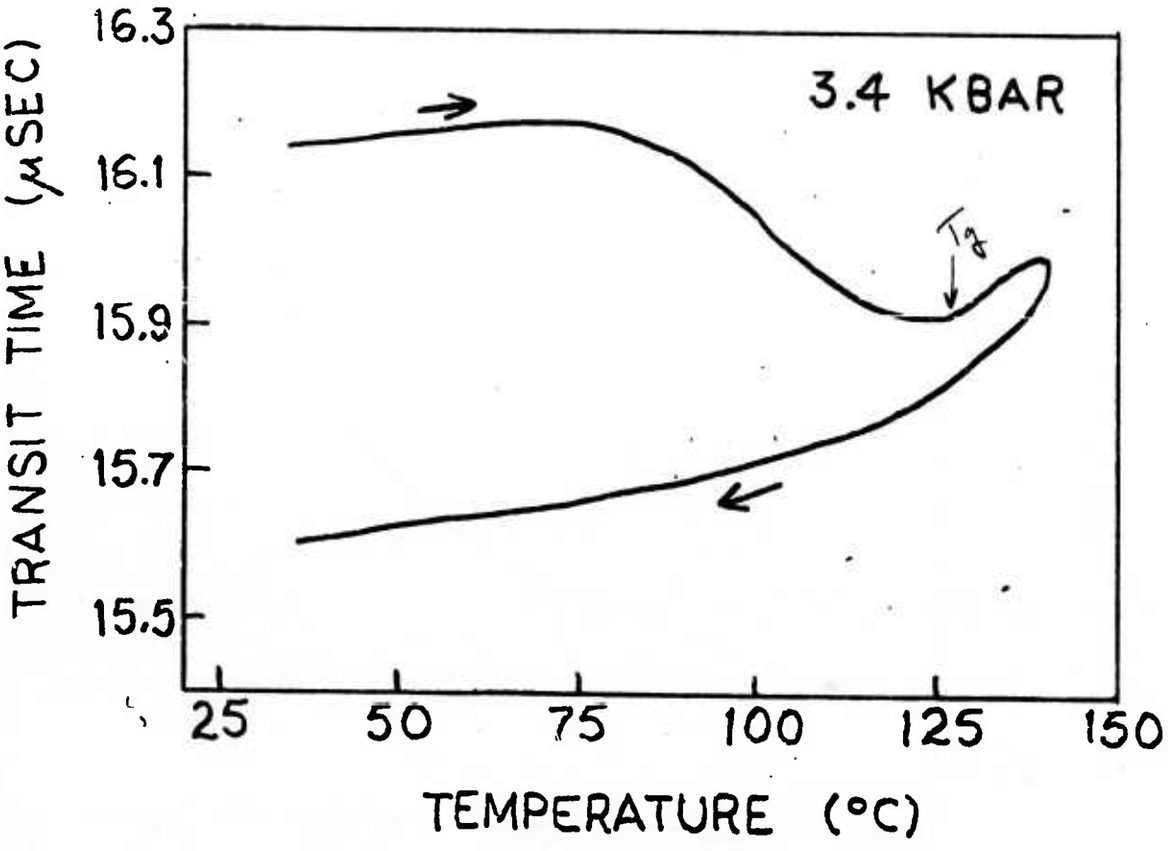
16.3
16.1
15.9
15.7
15.5
TRANSIT TIME (μSEC)
3.4 KBAR
T_g
25
50
75
100
125
150
TEMPERATURE (°C)

Figure 30

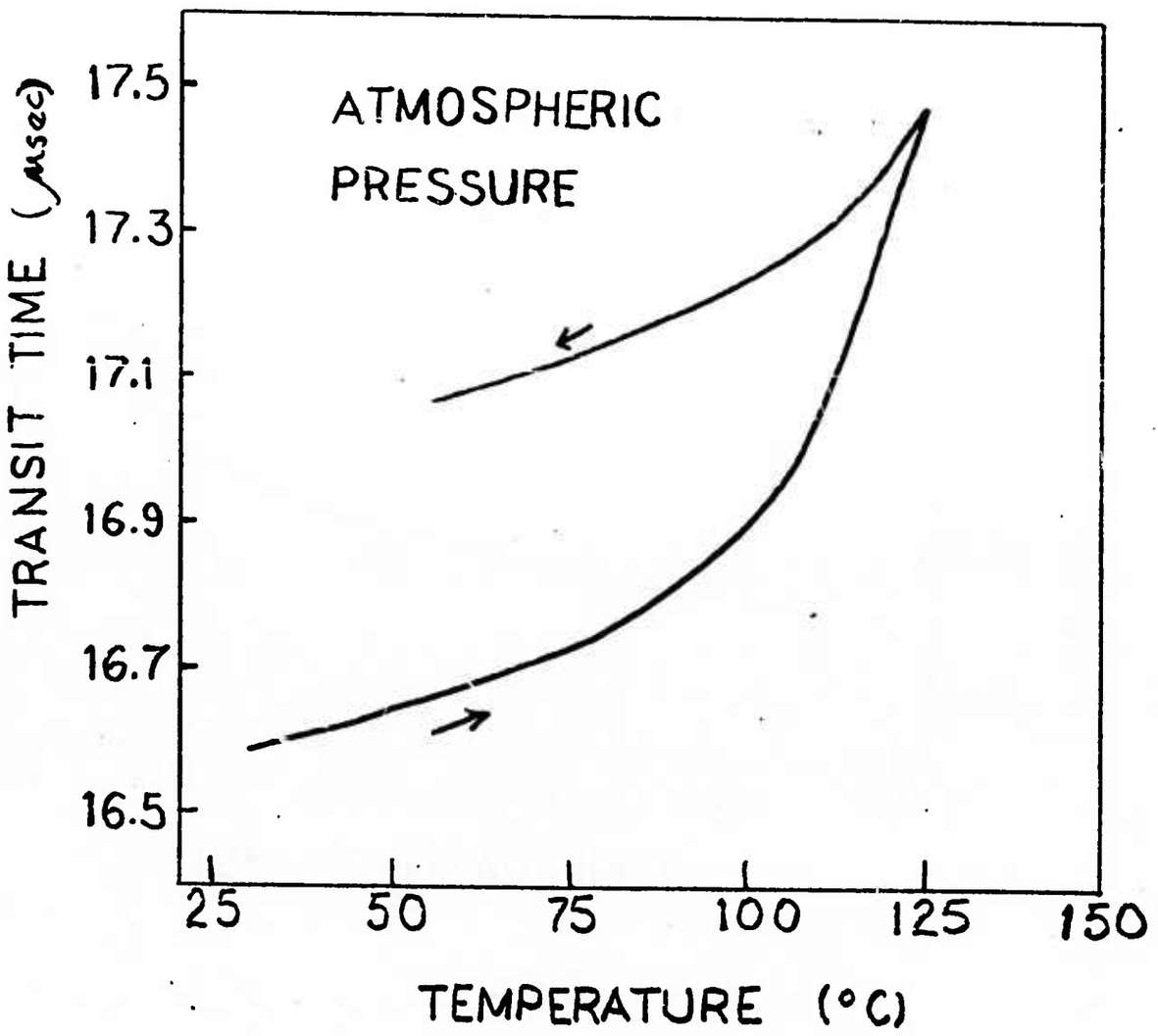
ATMOSPHERIC
PRESSURE
TRANSIT TIME (μsec)
17.5
17.3
17.1
16.9
16.7
16.5
25
50
75
100
125
150
TEMPERATURE (°C)

Figure 31

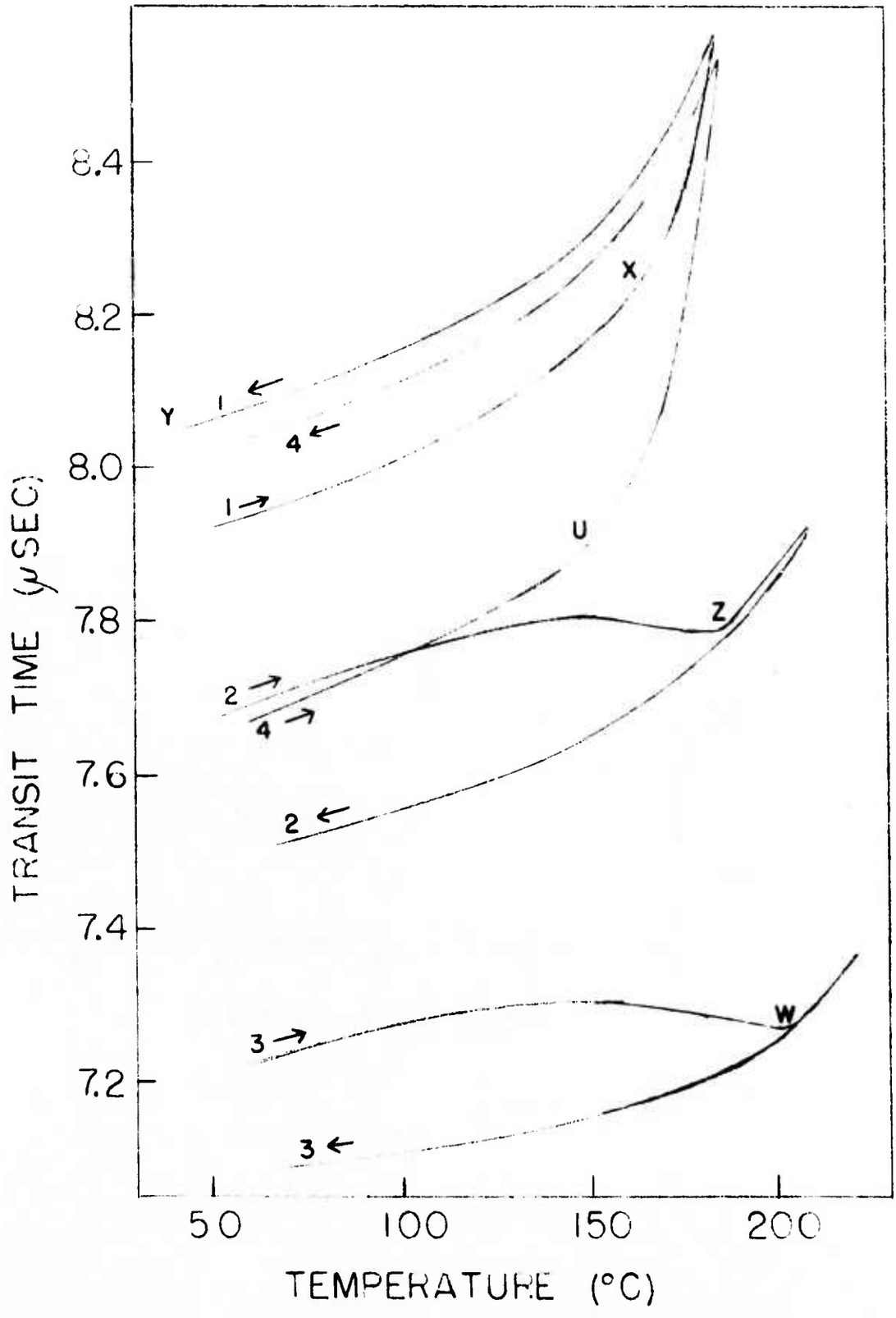
8.4
8.2
8.0
7.8
7.6
7.4
7.2
TRANSIT TIME (μSEC)
50
100
150
200
TEMPERATURE (°C)
X
Y
1
4
1
U
Z
2
4
2
3
W
3

Figure 32

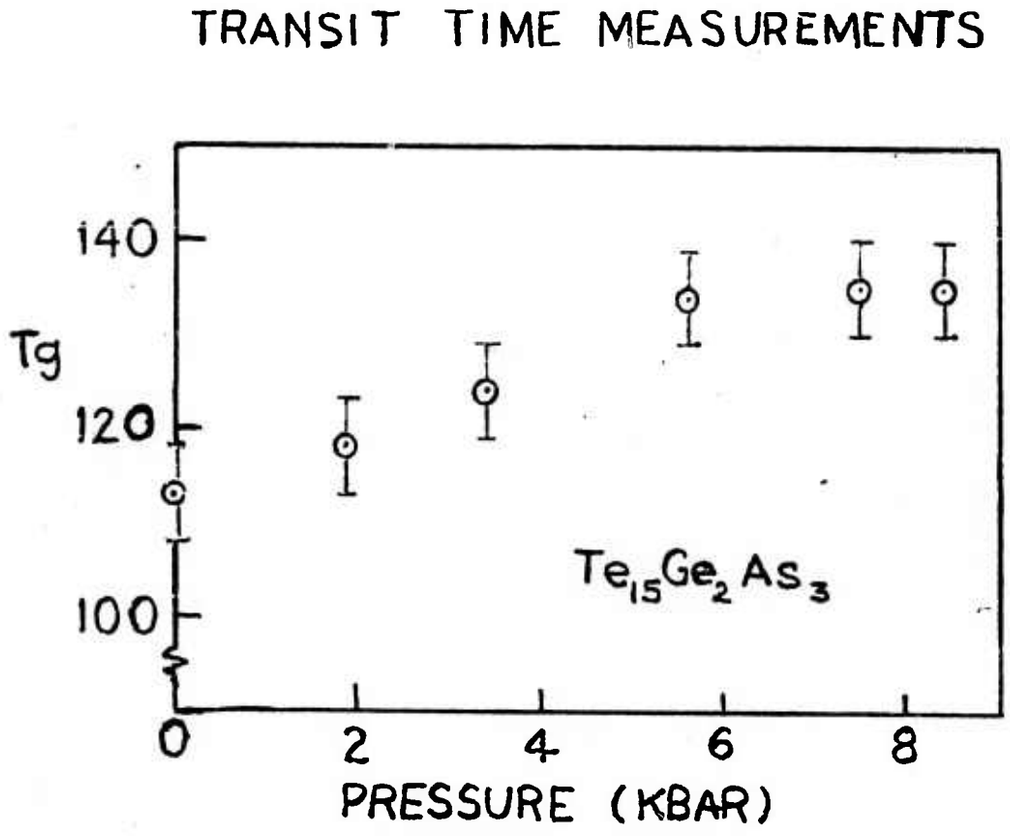
TRANSIT TIME MEASUREMENTS
140
120
100
Tg
0
2
4
6
8
PRESSURE (KBAR)
Te15Ge2As3

Figure 33

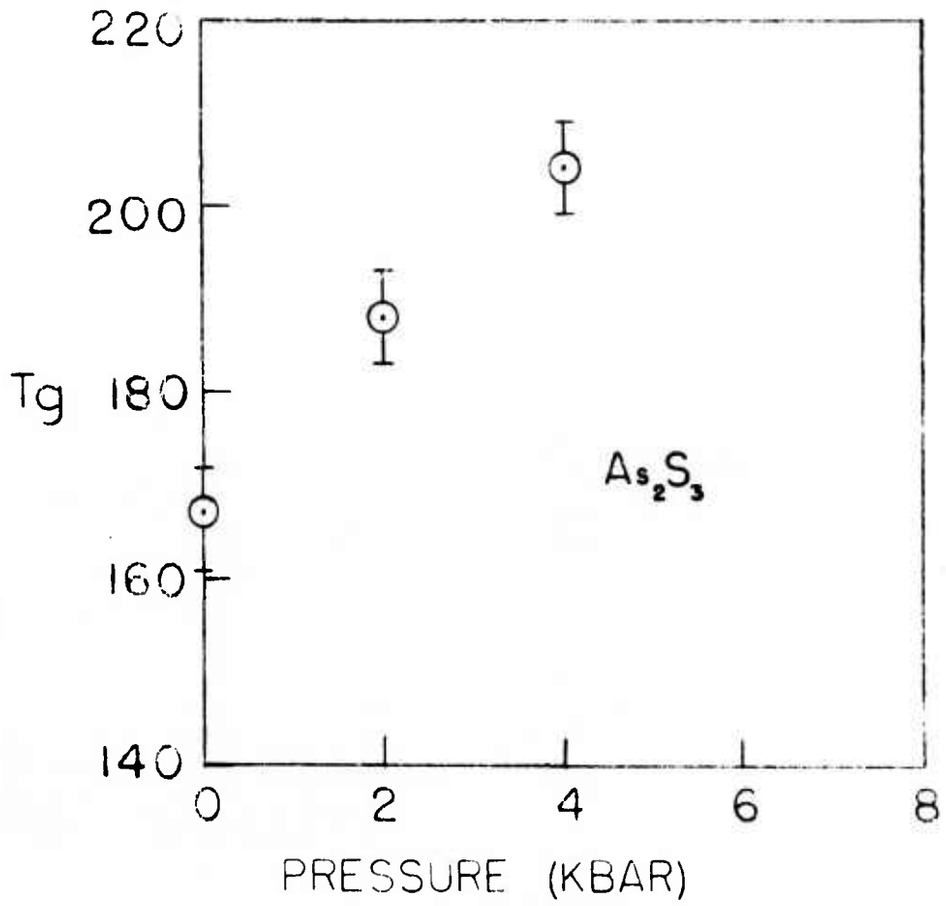

Figure 34

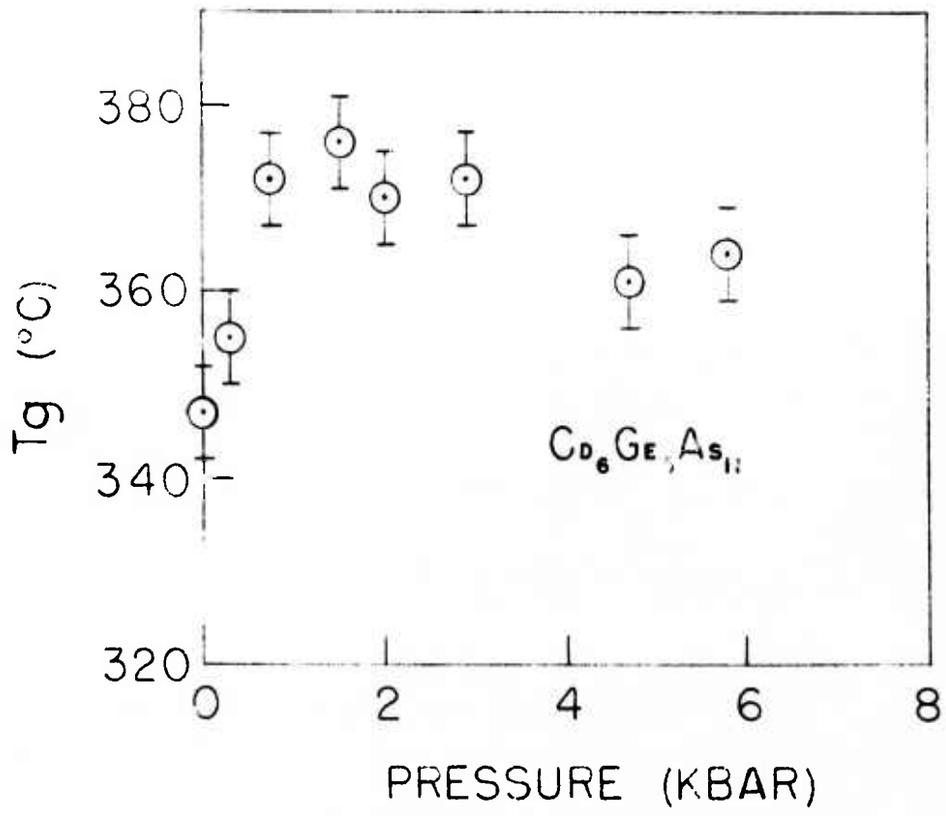

Figure 35

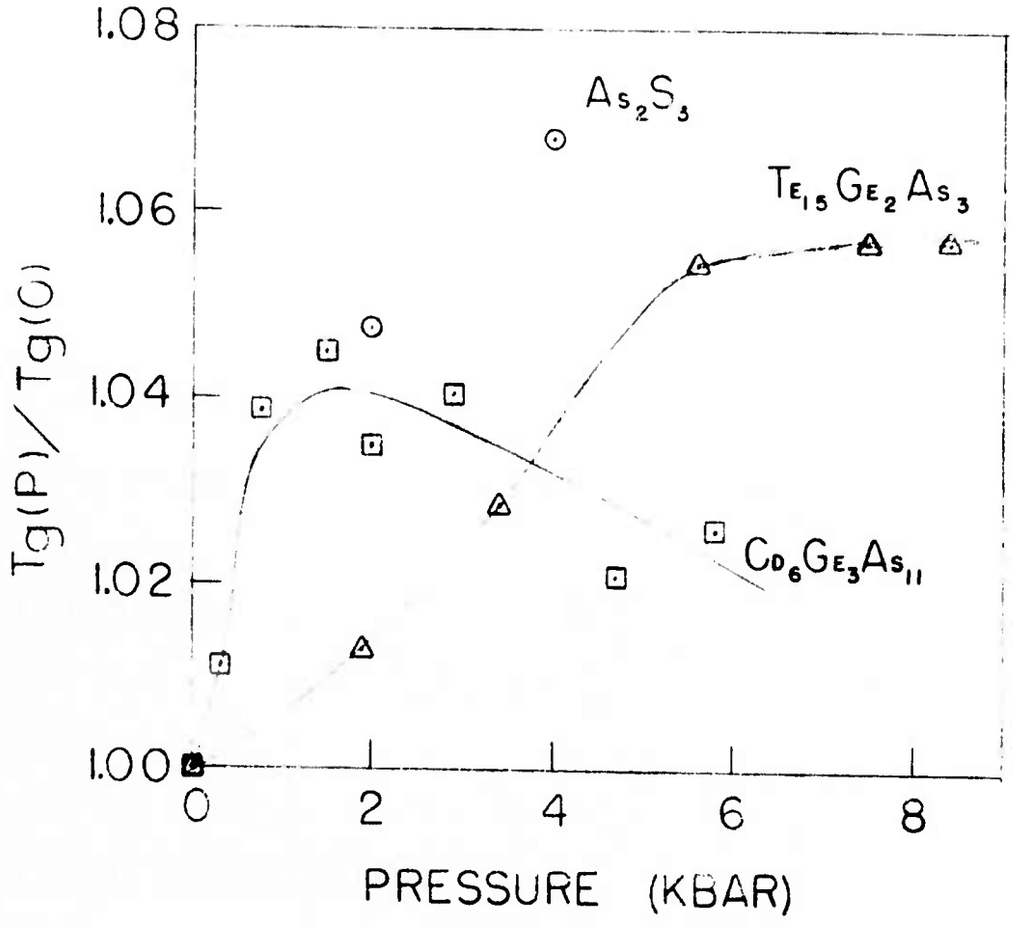
1.08
1.06
1.04
1.02
1.00
Tg(P)/ Tg(0)
As_2S_3
$Te_{15}Ge_2As_3$
$Cd_6Ge_3As_{11}$
0
2
4
6
8
PRESSURE (KBAR)

Figure 36

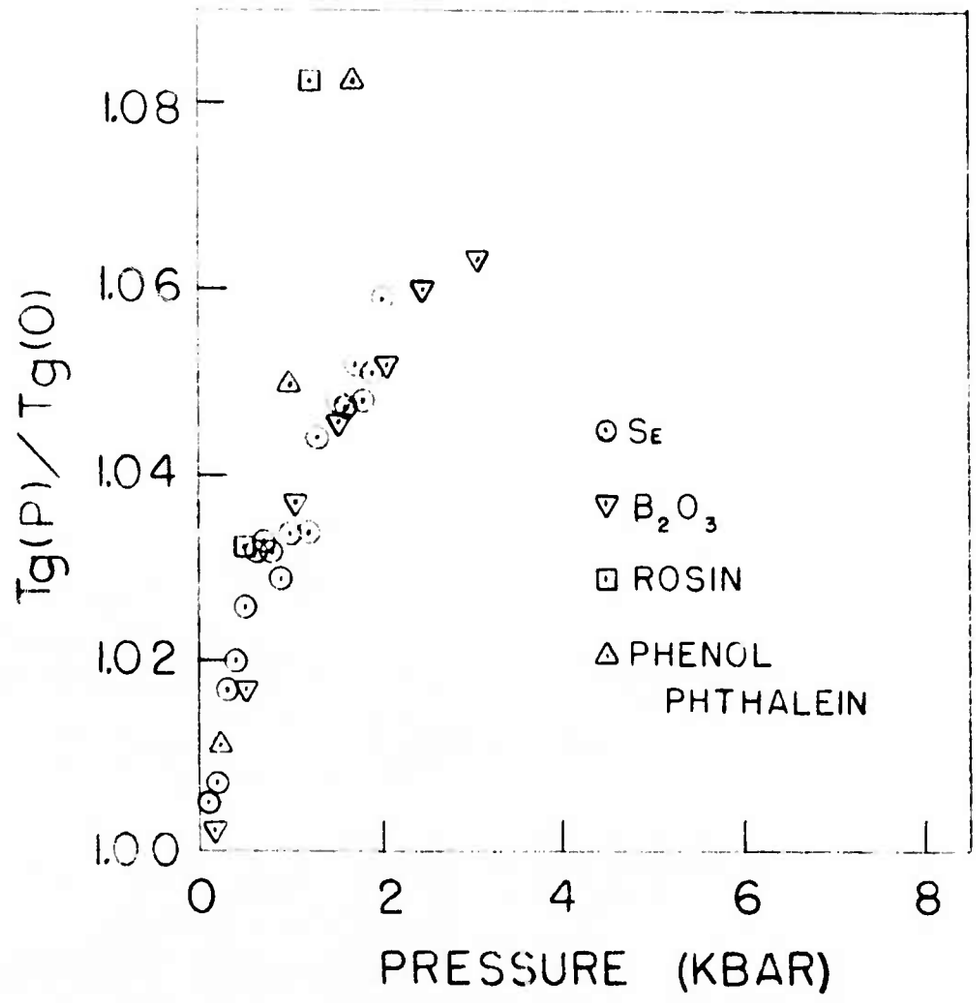
1.08
1.06
1.04
1.02
1.00
Tg(P)/Tg(0)
0
2
4
6
8
PRESSURE (KBAR)
Se
B2O3
ROSIN
PHENOL PHTHALEIN

Figure 37

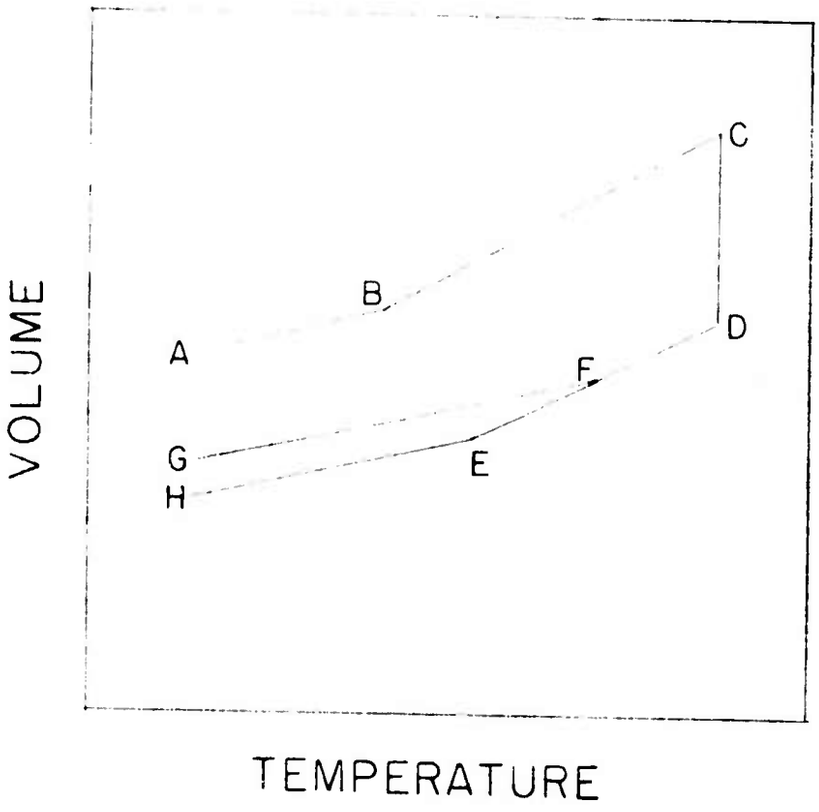

Figure 38

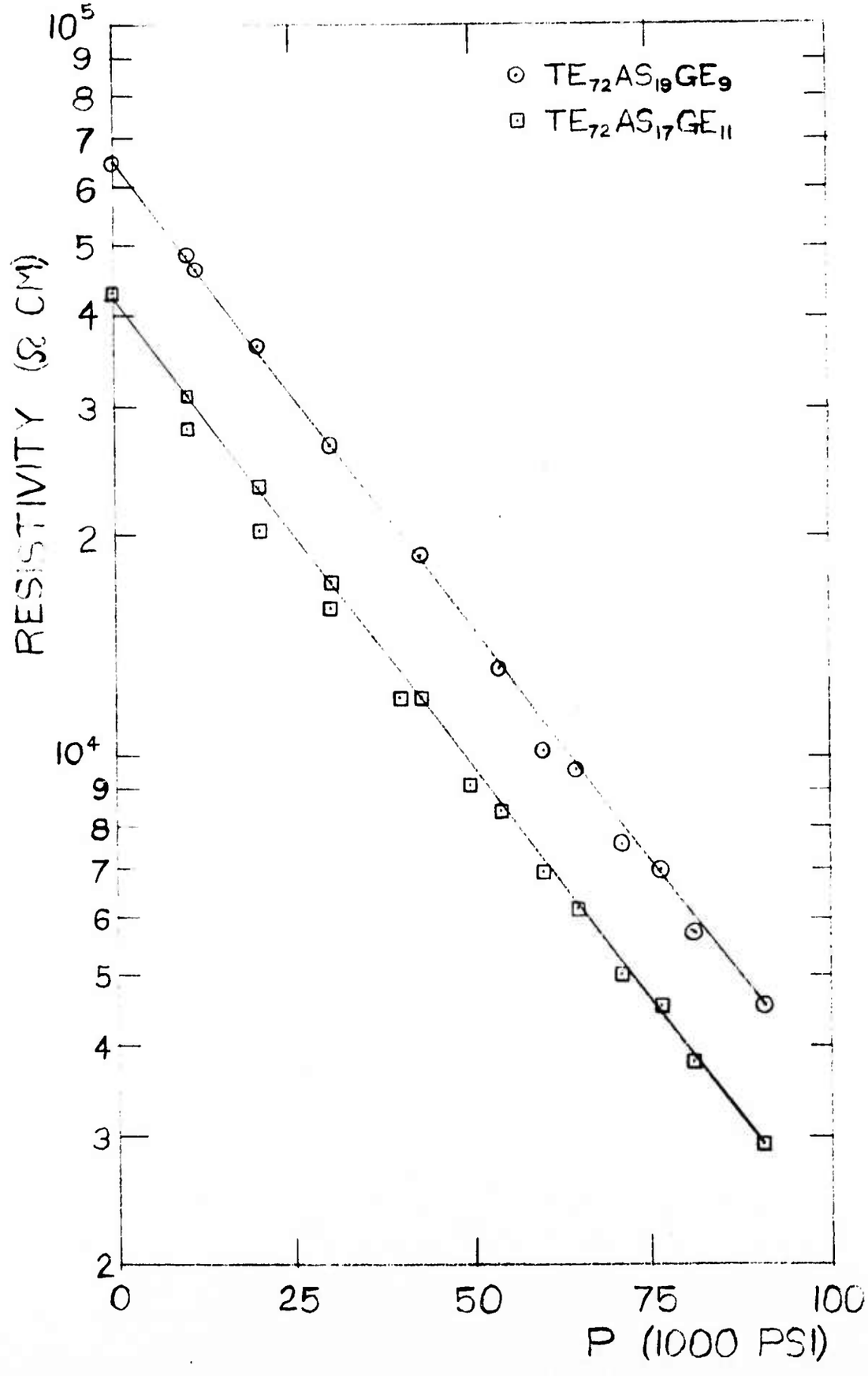
$TE_{72}AS_{19}GE_9$
$TE_{72}AS_{17}GE_{11}$
RESISTIVITY (Ω CM)
10^5
9
8
7
6
5
4
3
2
10^4
9
8
7
6
5
4
3
2
0
25
50
75
100
P (1000 PSI)

Figure 39

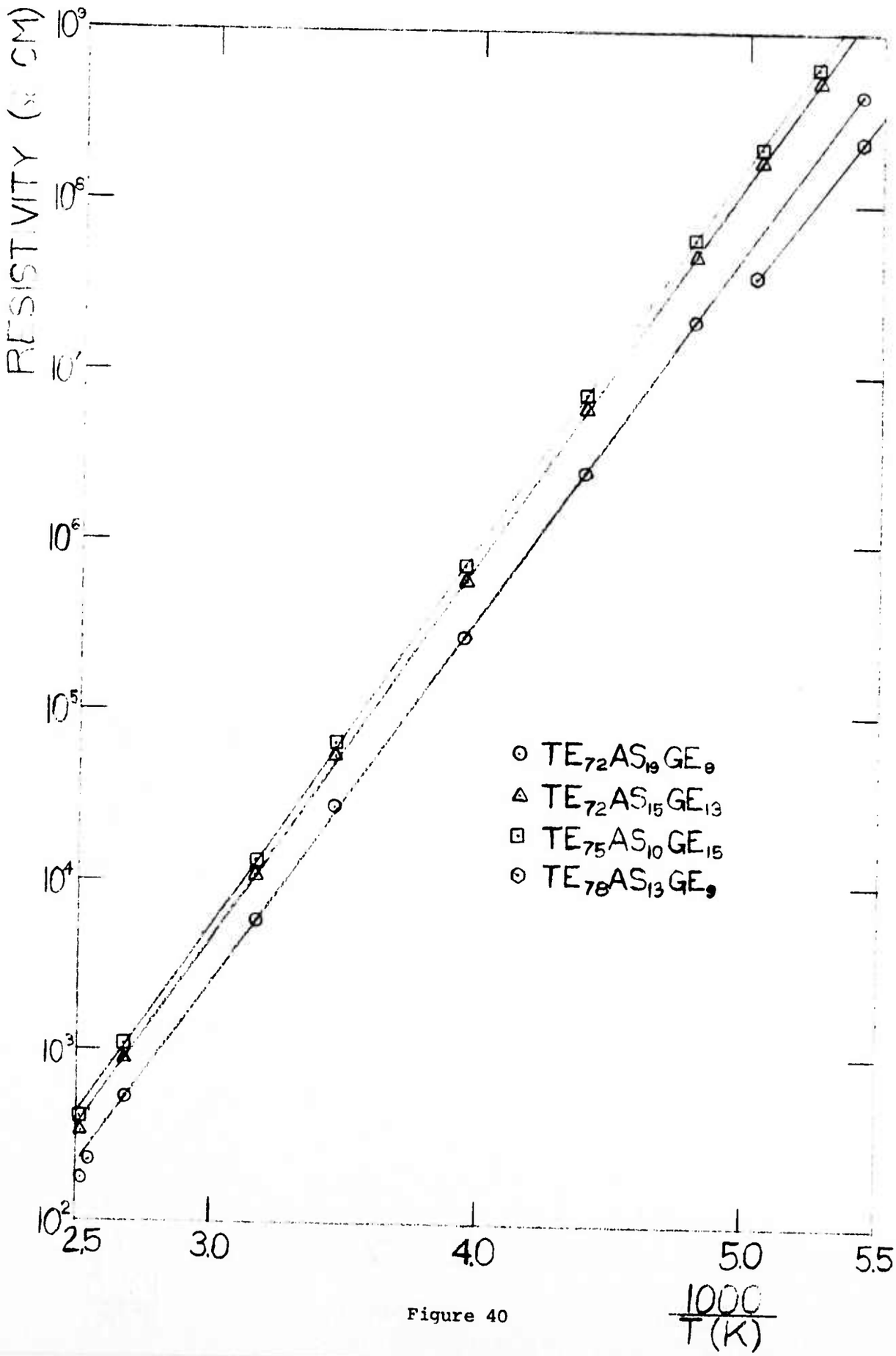
RESISTIVITY (Ω CM)
10³
10⁶
10⁵
10⁴
10³
10²
2.5
3.0
4.0
5.0
5.5
1000/T(K)
TE72AS19GE9
TE72AS15GE13
TE75AS10GE15
TE78AS13GE9

Figure 40

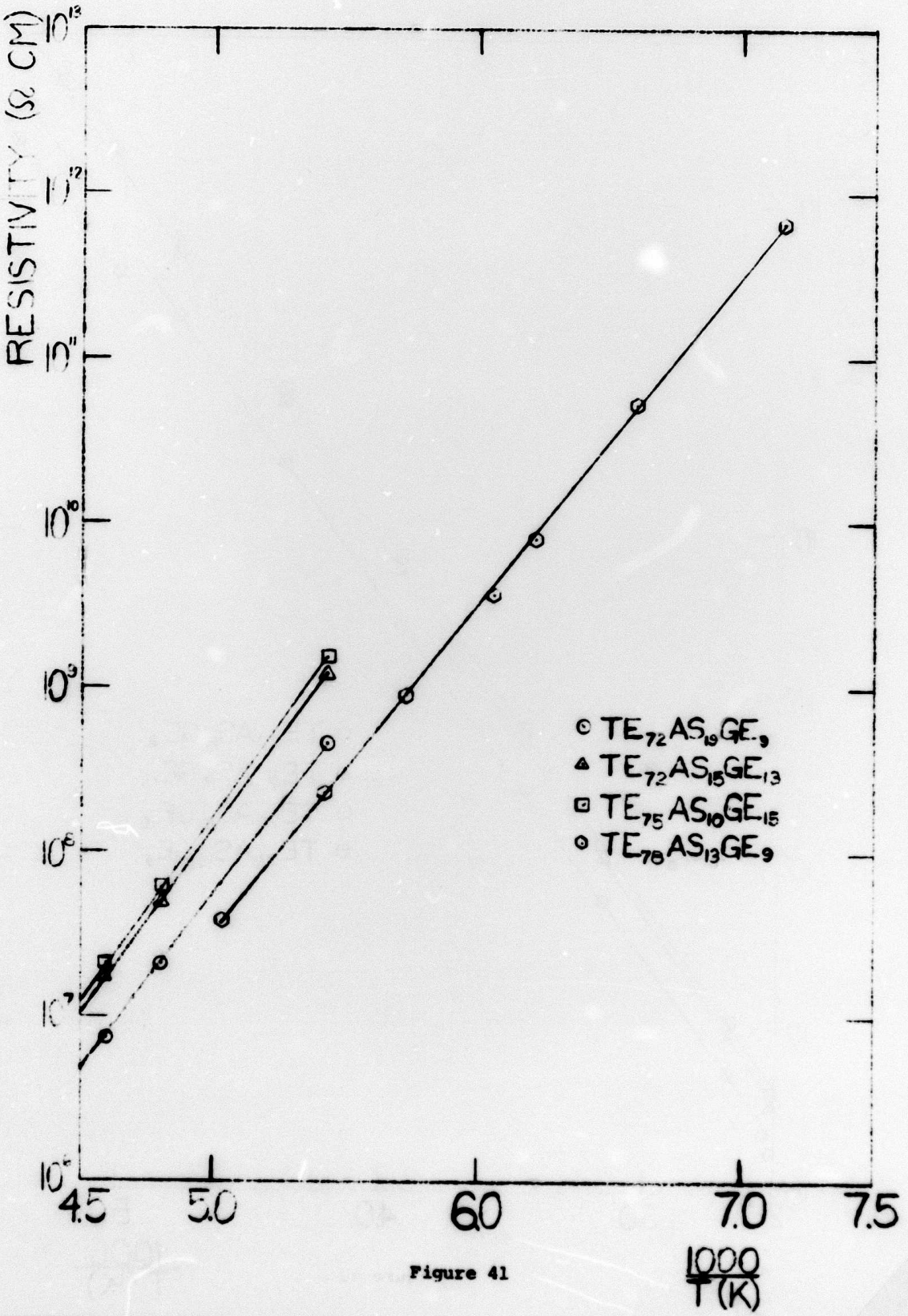
RESISTIVITY (Ω CM)
10^13
10^12
10^11
10^10
10^9
10^8
10^7
10^6
4.5
5.0
6.0
7.0
7.5
1000/T(K)
TE72AS19GE9
TE72AS15GE13
TE75AS10GE15
TE78AS13GE9

Figure 41

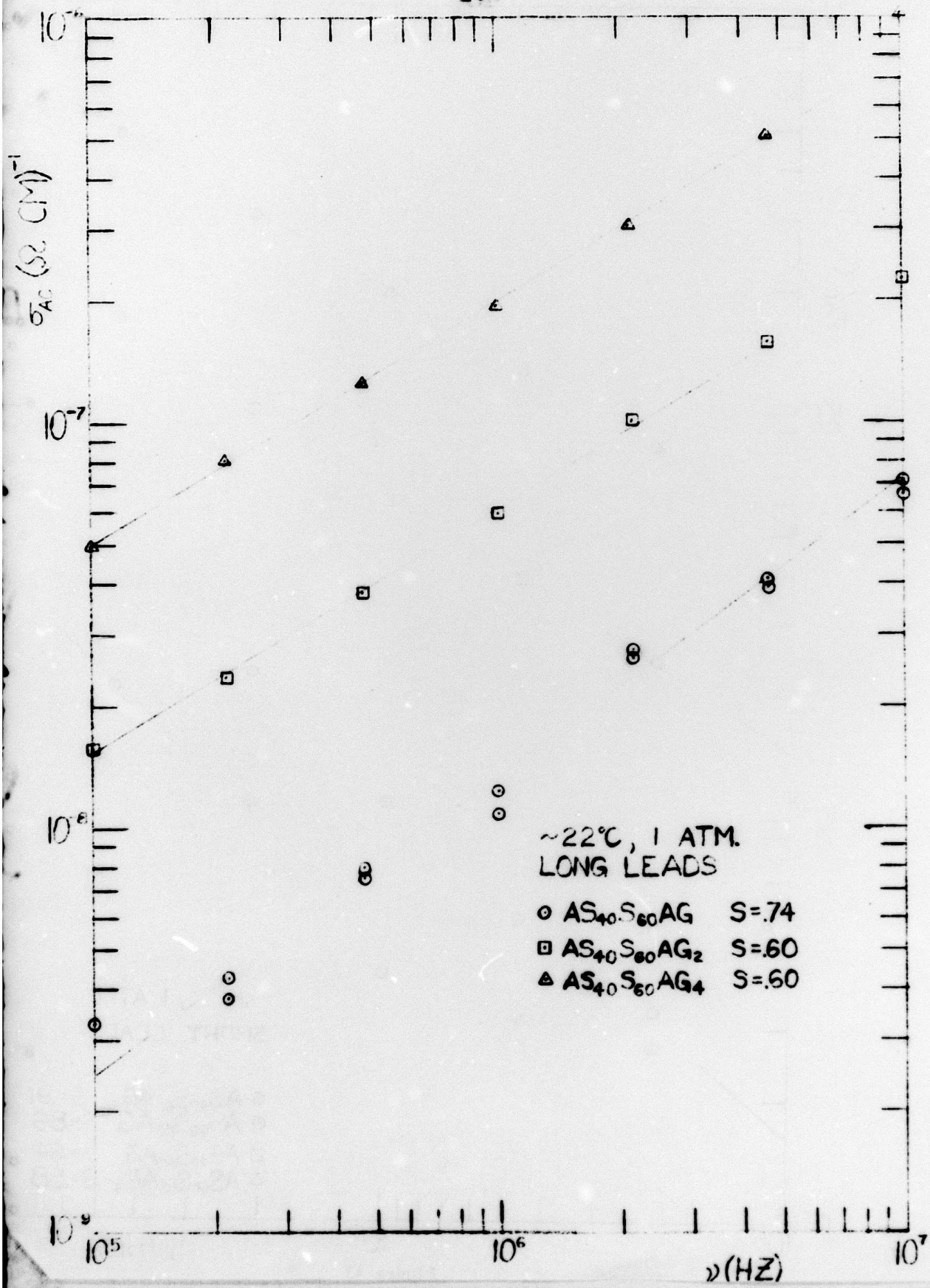
10^{-6}
10^{-7}
10^{-8}
10^{-9}
σ_{AC} (Ω CM)$^{-1}$
10^{5}
10^{6}
10^{7}
ν (HZ)
~22°C, 1 ATM.
LONG LEADS
$AS_{40}S_{60}AG$ S=.74
$AS_{40}S_{60}AG_2$ S=.60
$AS_{40}S_{60}AG_4$ S=.60

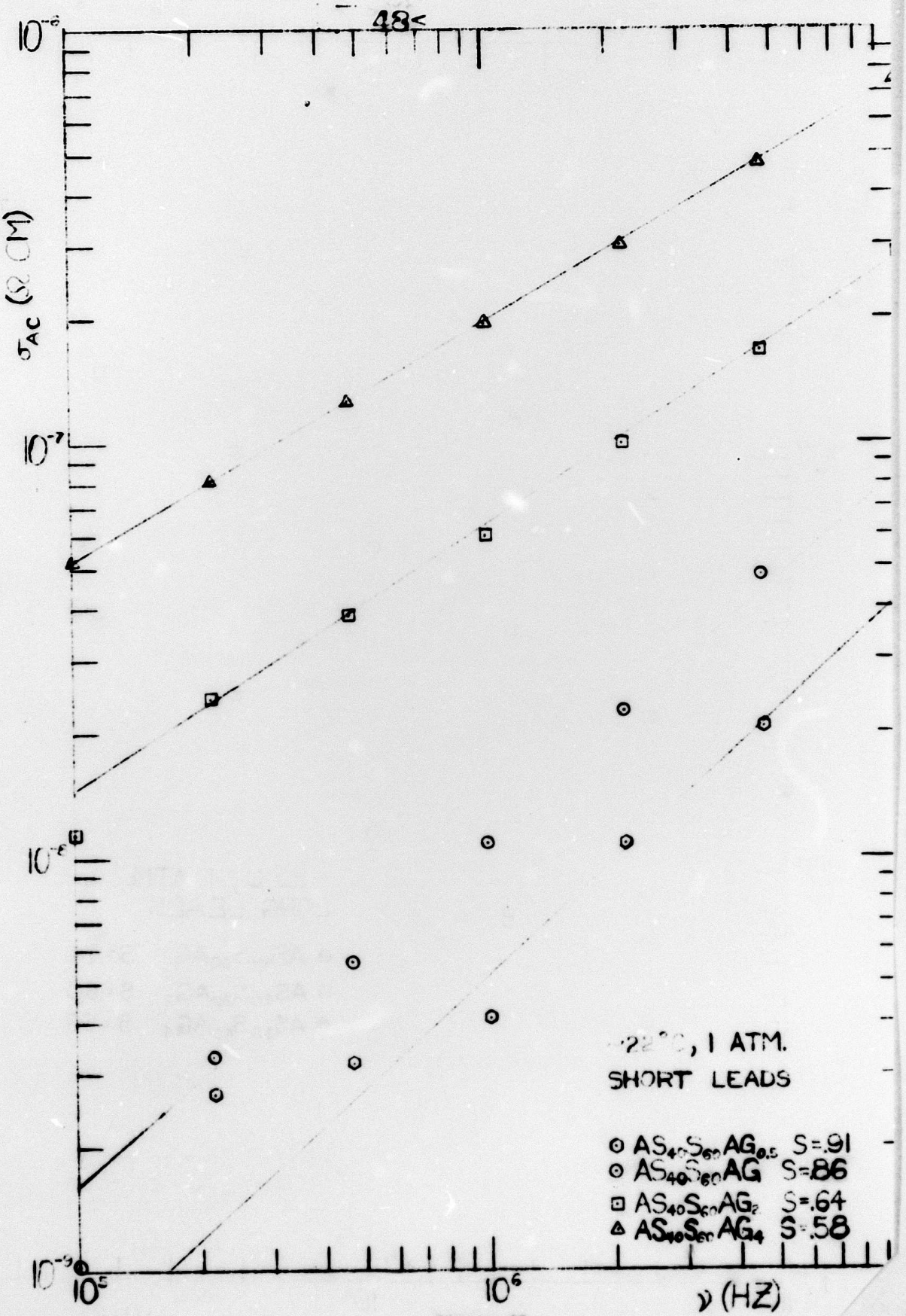
10^{-6}
10^{-7}
10^{-8}
10^{-9}
σ_{AC} (Ω CM)
10^5
10^6
ν (HZ)
, 1 ATM.
SHORT LEADS
$AS_{40}S_{60}AG_{0.5}$ S=.91
$AS_{40}S_{60}AG$ S=.86
$AS_{40}S_{60}AG_2$ S=.64
$AS_{40}S_{60}AG_4$ S=.58

Figure 43

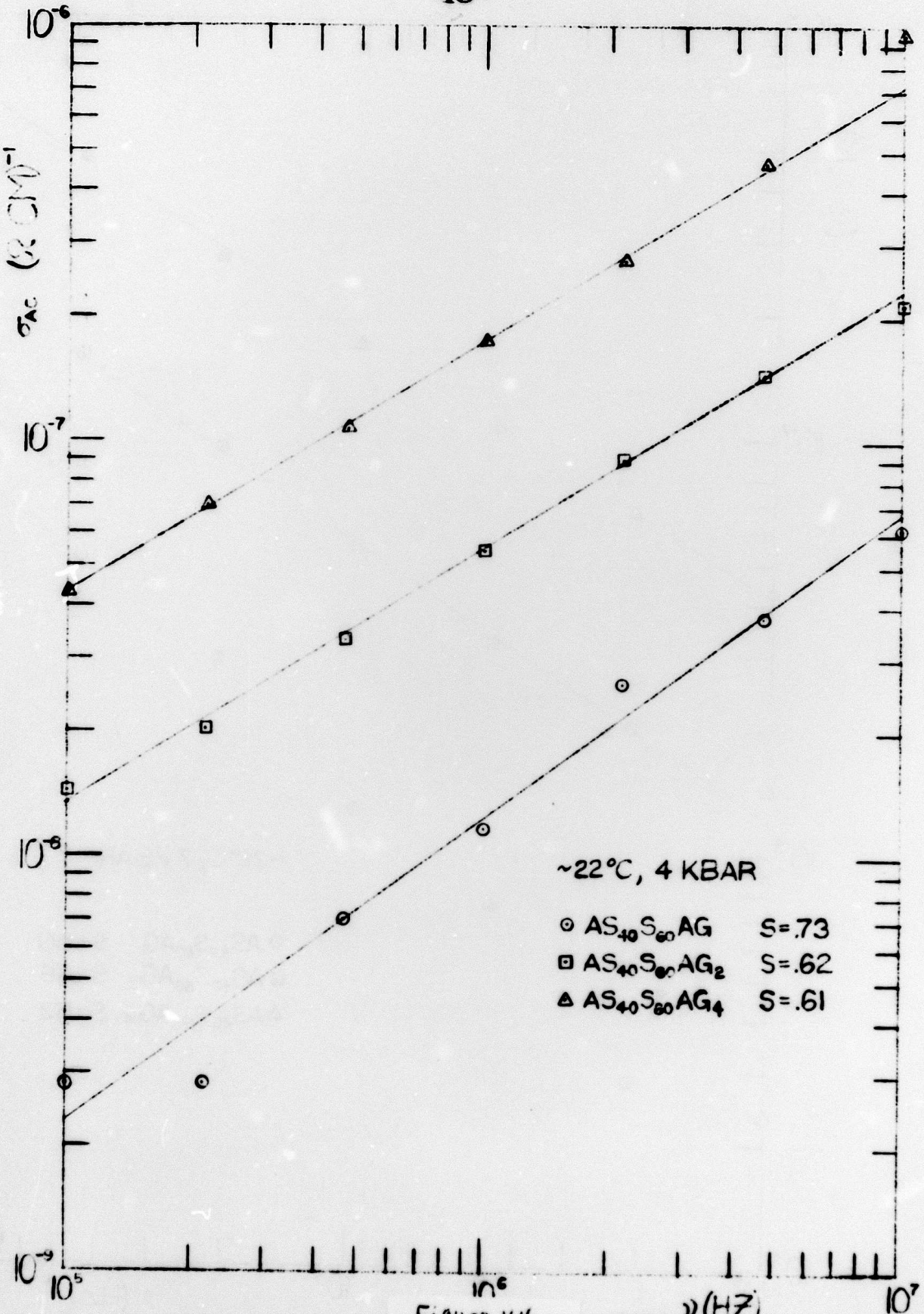
10^{-6}
10^{-7}
10^{-8}
10^{-9}
σ_{AC} (Ω CM)$^{-1}$
~22°C, 4 KBAR
⊙ $AS_{40}S_{60}AG$ S=.73
⊡ $AS_{40}S_{60}AG_2$ S=.62
△ $AS_{40}S_{60}AG_4$ S=.61
10^5
10^6
10^7
ν(HZ)

Figure 44

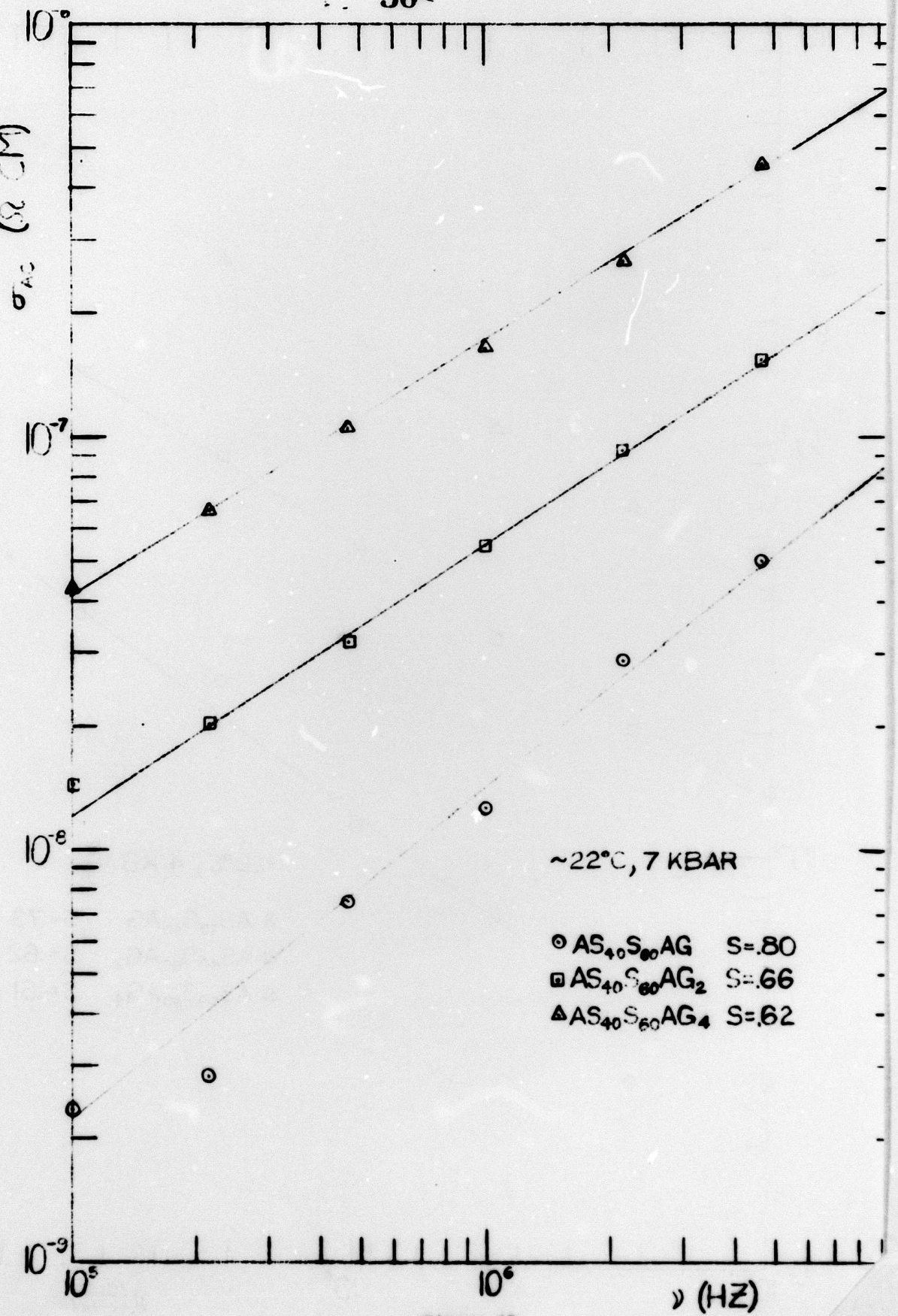
10^{-6}
10^{-7}
10^{-8}
10^{-9}
σ_{AC} $(\Omega\ CM)^{-1}$
10^{5}
10^{6}
ν (HZ)
~22°C, 7 KBAR
$AS_{40}S_{60}AG$ S=.80
$AS_{40}S_{60}AG_2$ S=.66
$AS_{40}S_{60}AG_4$ S=.62

Figure 45

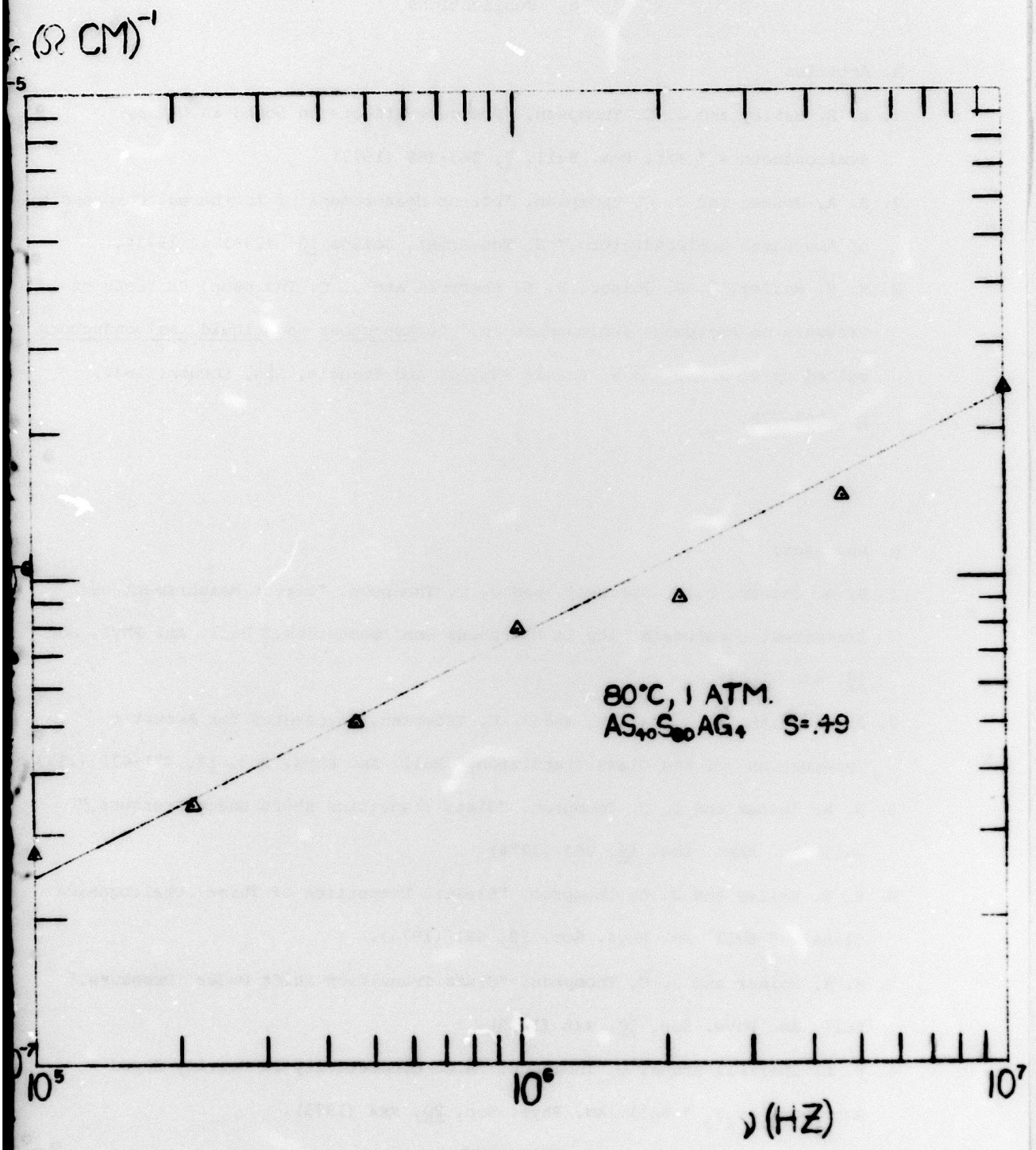

Figure 46

6. Publications

A. Articles

1. K. E. Bailey and J. C. Thompson, "Pressure Effects on Sound in Glassy Semiconductors," Mat. Res. Bull. 7, 363-368 (1972).

2. B. A. Joiner and J. C. Thompson, "Direct Measurement of Isothermal Compressibilit of Amorphous Semiconductors," J. Non-Cryst. Solids 13, 179-184 (1973).

3. K. E. Bailey, B. A. Joiner, P. L. Sherrell and J. C. Thompson, "Effects of Pressure on Amorphous Semiconductors," in Amorphous and Liquid Semiconductors edited by J. Stuke and W. Brenig (Taylor and Francis, Ltd, London, 1974), pp. 767-770.

B. Abstracts

1. B. A. Joiner, P. L. Sherrell, and J. C. Thompson, "Direct Measurement of Isothermal Compressibility in Amorphous Semiconductors," Bull. Am. Phys. Soc. 18, 436 (1973).

2. J. L. Smith, K. E. Bailey, and J. C. Thompson, "Apparatus for Acoustic Observation of the Glass Transition," Bull. Am. Phys. Soc. 18, 471-472 (1973).

3. B. A. Joiner and J. C. Thompson, "Glass Transition Shift Under Pressure," Bull. Am. Phys. Soc. 19, 661 (1974).

4. K. E. Bailey and J. C. Thompson, "Elastic Properties of Three Chalcogenide Glasses," Bull. Am. Phys. Soc. 19, 661 (1974).

5. B. A. Joiner and J. C. Thompson, "Glass Transition Shift Under Pressure," Bull. Am. Phys. Soc. 20, xxx (1975).

6. P. L. Sherrell and J. C. Thompson, "A.C. Conductivity in Heavily Doped Amorphous As_2S_3," Bull. Am. Phys. Soc. 20, xxx (1975).

7. Personnel

1. James C. Thompson	Principal Investigator
2. K. E. Bailey	Graduate Research Assistant; Ph.D. scheduled June 1975; employment accepted at Lockheed Aerospace
3. B. A. Joiner	Graduate Research Assistant; Ph.D. scheduled June 1975; postdoctoral expected at University of Marburg
4. P. L. Sherrell	NDEA Title IV, University, and Welch Foundation Fellow; Ph.D. scheduled June 1975; postdoctoral expected at University of St. Andrews.
5. J. D. Black	Laboratory Assistant
6. W. C. Shockley	Laboratory Assistant
7. J. D. Spillar	Machinist
8. C. R. Skipping	Laboratory Assistant
9. N. L. Frost	Secretary
10. S. D. M. Gibson	Secretary
11. R. A. Lopez	Secretary
12. M. P. O'Connor	Secretary
13. P. L. Thomas	Secretary